

Interfacial properties of saponins from *Quillaja saponaria* Molina and their functionality in dispersed systems

vorgelegt von
Sandra Böttcher, M.Sc.
geb. in Karl-Marx-Stadt

von der Fakultät III – Prozesswissenschaften
der Technischen Universität Berlin
zur Erlangung des akademischen Grades

Doktor der Ingenieurwissenschaften
- Dr.-Ing –
genehmigte Dissertation

Promotionsausschuss:

Vorsitzender: Prof. Dr. Lothar W. Kroh

Gutachter: Prof. Dr. Stephan Drusch

Gutachterin: Prof. Dr. Cornelia Rauh

Gutachter: Kamil Wojciechowski, PhD DSc

Tag der wissenschaftlichen Aussprache: 28. April 2017

Berlin, 2017

Acknowledgments

So this is it: I finished my thesis! You may not anticipate how much work this was, but that's ok. It was all worth it and I would certainly do it again! This section will give you a small hint how many people were involved in it and to whom I am deeply thankful to.

Let's start with the department *Food Technology and Food Material Science* at Technische Universität Berlin, Germany where I performed most of my research. I want to thank the Friedrich-Naumann-Foundation for Freedom and the Bundesministerium für Bildung und Forschung for the financial support of this thesis. Besides the financial support, I am very grateful for my time as a scholar because I met amazing people, went abroad for conferences and research stays and had the opportunity to actively participate and educate myself and let others benefit from my knowledge. Being a scholar in the FNF is more than money, once you are a scholar you become part of the Naumann family. I made so many great friends, participated in awesome events, broadened my perspective and learned so many new things.

I want to especially thank my supervisor Prof. Dr. Stephan Drusch for his guidance and his support throughout the time of my thesis. I know I have been a challenging PhD student but it's fair to say the same about you as a supervisor and I am very thankful to you that you pushed me to my personal limits. I grew with every heated discussion and tried every day to become a better researcher. Thanks for giving me the chance to make my PhD. It is not easy for graduates from a University of Applied Sciences to get the chance for starting a PhD. Also I want to thank Prof. Dr. Cornelia Rauh and Prof. Dr. Kamil Wojciechowski for agreeing to examine my thesis.

I want to thank Ingredion, especially Ines Fuhlrott for supplying the Quillaja saponin and for fruitful discussions and cooperation. And thanks to Scott Osborne and Procter & Gamble for offering a position in research as a scientist. This prospective helped me through the last weeks and I am looking forward to start a new chapter after the end of my thesis.

During my PhD, I had the honor to collaborate with other scientific research groups and want to thank Prof. Dr. Matteo Scampicchio and his group for a great research stay in Bolzano trying to get reasonable ITC measurement. Although it did not work out, we had a great time! I also like to thank Dr. Julia K. Keppler for the generous supply of the β -LG and her scientific help on the fluorescence experiments. I also want to thank Prof. Dr.

Sascha Rohn and Dr. Valeria Reim for teaching me the extraction of saponins and HPTLC at their department at Universität Hamburg.

My PhD would have been less fun and enjoyable without the people of the department *Food Technology and Food Material Science*. Thanks to all of my co-workers and especially to Kenneth. What's better than working with friends? Sharing an office with them. You were the best office buddy and I will miss our laughs. Laughing about all the cruel stuff the lab did to us, made it far easier to cope with it. Anja, why didn't you join us earlier? You will be such an amazing professor one day! Rocio, my crazy Spanish girl. Thank you for bringing so much sunshine to Berlin. With you I always had humongous laughs. Helena, we had so little time together and I wished it would have been more. You are such a great person with a caring and passionate soul and you will rock your PhD. Janine, Addi and Freddi thank you for establishing so many methods I was able to use and your welcoming arms when I arrived.

It was a pleasure having Ariane Muth, Hanna von Heymann and Irina Reifschneider as my students but the greatest was reserved for the end: Marina Eichhorn. You were absolutely amazing and I really loved working with you! Keep on going, there is so much you can achieve.

Sport ist Mord und Knieverletzungen sind ätzend. Danke an alle meine Taekwondoinn, die mich immer wieder aufgebaut haben! Der schwarze Gürtel wird kommen, auch wenn es noch etwas dauern wird.

Während meiner Doktorarbeit hatte ich die besten Freunde, die man sich wünschen kann. Ihr wart immer für mich da, besonders in den letzten Wochen vor der Abgabe haben mich eure Nachrichten, Treffen und Anrufe wiederaufgebaut und mir geholfen fertig zu werden. Julian, sei il migliore. Ohne dich wäre das Phdlife nicht halb so großartig gewesen. Danke für tausende lustige Bilder, Chats, Ablenkungen, wenn ich eigentlich hätte schreiben müssen, die unzähligen Besuche in Berlin und Treffen anderswo in der Welt. Frie, mein partner in crime, wenn es mal wieder ums „recherchieren“ ging. Mo, ich möchte dir sagen (3 Tage später) du bist großartig und ich freue mich wirklich, dass wir so nah beieinander wohnen. Marlene, ich bin immer noch so dankbar, dass du mich als Drill Instructor marathontfit gemacht hast und die letzten Jahre so viel Sonnenschein in mein Leben gebracht hast. Kenneth und Christoph, wenn's mit der Diss doch nicht klappt, könnt ihr als Comedy Duo auf jeden Fall den ganz großen Durchbruch schaffen! Sandra, mit dir habe ich so viele tolle Locations kennengelernt und Events erlebt. Wenn's mir mal reicht, komme ich vorbei zum Schaukeln.

Die wichtigsten Menschen aber nun zum Schluss: meine Familie. Mama, Papa, Omi, Opi, Conny und Lutz. Ich liebe euch und bin euch unendlich dankbar für eure konstante und bedingungslose Unterstützung in jeder Situation. Danke Mama, für deine unglaublich klugen Weisheiten. Danke Papa, dass du mich zu einer Kämpferin gemacht hast. Hinter jedem starken Kind stehen unglaubliche Eltern, ich kann euch nicht genug danken, dass ihr mich zu der erzogen habt, die ich nun bin. Danke Omi und Opi, ihr habt mich seit meiner Kindheit jederzeit unterstützt und wer hat schon so coole Großeltern wie euch?!

Steffen – du bist der Wichtigste von allen. Ohne dich und deine unendliche Liebe wäre meine Welt einfach nur grau und langweilig. Wir sind diesen Weg von Anfang an gemeinsam gegangen. Jetzt beginnt ein neues Kapitel, möge es eins von Hunderten weiteren sein.

Abstract

The aim of the present thesis was to connect interfacial properties of saponins at aqueous interfaces with their behavior in dispersed systems. Thereby the influence of changes in pH and ionic strength and interactions with β -lactoglobulin were discussed using spectroscopic equipment and knowledge on molecular structure.

Saponins are phytochemicals that can be found in numerous plant species in low concentrations. Due to their amphiphilic structure, saponins are surface active and may be used in dispersed systems like emulsions and foams. Molecular structure of saponins is highly variable as different aglycone types exist to which a varying quantity and type of sugar residues may be linked. Although it is known that saponins with a triterpenoid aglycone form viscoelastic films, knowledge on corresponding foam properties is scarce.

In the present thesis six saponins, which differed in molecular structure, were analyzed with respect to interfacial and foam properties. It was shown that high complex dilational and shear moduli were a requirement for stable foams but not a guarantee for high stability. However, it was also shown that the type of aglycone and length of the sugar chains had the highest impact on foam stability.

A saponin extract from *Quillaja saponaria* Molina (QS) is already approved for application in food products in the EU and US. But until now only little is known about interactions between QS and food-relevant ingredients like proteins. There has been evidences that QS and β -lactoglobulin (β -LG) form complexes, which affected interfacial properties. In the present thesis fluorescence experiments showed complex formation in the bulk and interfacial rheology indicated strong interactions at the air/water-interface. The interactions between QS and β -LG tremendously increased foam stability. In contrast mixtures of QS and β -LG negatively affected emulsion stability by inducing aggregation of oil droplets. Food systems may not only contain proteins but may also be a mixture of multiple dispersed phases. It was shown that oil droplet size of the emulsion and pH are key factors in controlling stability of foamed emulsions. Stability may further be enhanced by sequentially adding QS to a β -LG-emulsion.

Summarizing the results, experimental data showed that molecular structure of saponins distinctly affects foam stability. In addition, it was shown that mixing QS with β -LG may lead to synergistic or antagonistic effects in dispersed systems. However, it is necessary to perform experiments, which further deepen our understanding on the relationship of molecular structure and interfacial properties as well as behavior in dispersed systems. Furthermore, future research should focus on the underlying intermolecular interactions between proteins and QS to explain interfacial properties of mixtures of both.

Zusammenfassung

Ziel dieser Dissertation war es grundlegende Zusammenhänge zwischen Grenzflächen-eigenschaften von Saponinen und deren Verhalten in dispersen Systemen zu verstehen. Zusätzlich wurde auf Grundlage des molekularen Aufbaus der Saponine und mithilfe von spektroskopischen Verfahren der Einfluss von pH und Ionenstärke sowie die Interaktionen mit β -Laktoglobulin (β -LG) auf die Eigenschaften von dispersen Systemen diskutiert.

Saponine sind sekundäre Pflanzenstoffe, die in geringen Konzentrationen in einer Vielzahl von botanischen Quellen vorkommen. Durch ihre amphiphile Struktur sind Saponine grenzflächenaktiv und können demnach in dispersen Systemen, wie Schäumen und Emulsionen zur Stabilisierung eingesetzt werden. Es gibt zahlreiche Saponinderivate, die sich in der Art des Aglykongerüsts sowie der Anzahl und Länge der verknüpften Zuckerketten unterscheiden. Der Zusammenhang zwischen molekularer Struktur und Grenzflächeneigenschaften sowie Schaumeigenschaften ist bisher nur wenig erforscht.

Es wurden die Grenzflächen- und Schaumeigenschaften von sechs Saponinen aus unterschiedlichen botanischen Quellen untersucht, die sich in der Art des Aglykons und der Länge sowie Anzahl der Zuckerreste unterscheiden. Es wurde gezeigt, dass die Ausbildung eines stark viskoelastischen Films eine notwendige Bedingung aber keine Garantie für eine hohe Schaumstabilität ist. Die Art des Aglykons und die Länge der Zuckerketten waren dabei die strukturellen Merkmale, die den größten Einfluss auf die Schaumstabilität hatten. Im Gegensatz dazu hatte die Anzahl der verknüpften Zuckerketten (Mono- oder Bidesmosidisch) nur einen geringen Einfluss.

Bisher ist nur ein saponinreicher Extrakt aus *Quillaja saponaria* Molina (QS) für den Einsatz in Lebensmitteln zugelassen. Die Wechselwirkungen von QS mit Proteinen sind bisher nur wenig erforscht. Es gab in der Vergangenheit Hinweise auf eine Komplexbildung zwischen QS und β -LG. Fluoreszenzexperimente bestätigten eine Komplexbildung im Bulk und grenzflächenrheologische Untersuchungen zeigten intermolekulare Wechselwirkung an der Luft/Wasser-Grenzfläche. Die Wechselwirkungen zwischen QS und β -LG führten zu einer deutlich erhöhten Schaumstabilität. Im Gegensatz dazu führten Mischungen aus QS und β -LG in Emulsionen zur Aggregation von Öltröpfchen, welche die Stabilität der Emulsionen deutlich erniedrigte. Einige Lebensmittel sind Mehrphasengemische, wie z.B. aufgeschäumte Emulsionen. Es wurden zum ersten Mal Schlüsselfaktoren zur Kontrolle der Stabilität von aufgeschäumten QS-Emulsionen definiert. Dazu zählen die Öltröpfchengröße der Emulsion und der pH-Wert. Die Stabilität kann außerdem durch die sequentielle Zusage von QS zu einer β -LG Emulsion erhöht werden.

Es wurde in dieser Dissertation gezeigt, dass die molekulare Struktur von Saponinen einen signifikanten Einfluss auf die Schaumstabilität hat und dass Mischungen mit β -Laktoglobulin zu synergistischen und antagonistischen Effekten in dispersen Systemen führen können. Es wird mehr Forschung benötigt um den Zusammenhang zwischen molekularer Struktur von Saponinen und deren Grenzflächeneigenschaften sowie Eigenschaften in dispersen Systemen zu verstehen. Des Weiteren werden Untersuchungen benötigt um die Interaktionen mit Proteinen auf molekularer Ebene zu erklären.

Table of contents

List of tables.....	XIV
List of figures.....	XV
List of abbreviations.....	XIX
Publications.....	23
Conference contributions	25
1. Introduction	27
2. Literature review	33
2.1. Composition and characterization of saponin extracts.....	33
2.2. Self-assembly and micellar structure	36
2.3. Linking molecular structure and behavior at aqueous interfaces	37
2.3.1. Interfacial configuration of saponins at the air/water-interface.....	38
2.3.2. Supramolecular interfacial configuration of Quillaja saponins at the air/water-interface	41
2.3.3. Impact of the hydrophobic phase on interfacial properties of various saponins	43
2.4. Interactions of saponins with other (food) components	44
Manuscript I.....	47
I-1 Abstract	48
I-2 Introduction	49
I-3 Materials and Methods	51
I-3.1 Fourier transform infrared spectroscopy (FTIR)	52
I-3.2 Conductivity measurements.....	53
I-3.3 Interfacial tension measurements using Wilhelmy plate	53
I-3.4 Short-term adsorption of saponin extracts on the air-water interface.....	54
I-3.5 Foaming and foam stability	56
I-3.6 Determination of foam structure with analysis of brightness profiles and foam pictures	57
I-4 Results and discussion.....	57
I-4.1 CMC determination and fitting of interfacial tension isotherms using the modified Frumkin model	57
I-4.2 Short-term adsorption using two-fluid needle experiments.....	58
I-4.3 Foaming, foam stability and foam structure	61
I-4.4 Influence of pH and salt on interfacial tension and foam properties	63
I-5 Conclusions	68

Manuscript II	69
II-1 Abstract	70
II-2 Introduction	71
II-3 Material and methods	73
II-3.1 Purification of saponin extract	73
II-3.2 Fluorescence quenching of β -LG by the presence of QS	74
II-3.3 Dynamic interfacial tension measurements, dilational rheology, short-term adsorption and sequential two-fluid needle experiments	75
II-3.4 Shear rheology	76
II-3.5 Foaming, foam stability and foam structure	76
II-4 Results	77
II-4.1 Interactions in the bulk determined by fluorescence quenching	77
II-4.2 Interactions of QS and β -LG at the interface	78
II-4.3 Short- and midterm adsorption of mixtures of QS and β -LG	79
II-4.4 Dilational rheology of mixtures of β -LG/QS	80
II-4.5 Shear rheology	81
II-4.6 Foam properties	82
II-5 Discussion	83
II-6 Conclusion	89
Manuscript III	91
III-1 Abstract	92
III-2 Introduction	93
III-3 Material and methods	96
III-3.1 Materials	96
III-3.2 Drop shape analysis of adsorption, dynamic interfacial tension and dilational rheology	96
III-3.3 Interfacial shear rheology at the oil/water-interface	98
III-3.4 Emulsification and emulsion stability	98
III-3.5 Determination of oil droplet size distribution and ζ -potential	98
III-4 Results	99
III-4.1 Adsorption and dynamic interfacial tension at the oil/water-interface as determined by drop shape analysis	99
III-4.2 Dilational rheology determined by droplet oscillation and analysis of non-linear phenomena of interfacial layers	101
III-4.3 Shear rheology of interfacial layers	105
III-4.4 Oil droplet size distribution of emulsions as determined by static light scattering	106
III-4.5 ζ -potential of the emulsion droplets	107
III-4.6 Visual analysis of emulsion stability after a storage time of 7 days	108
III-5 Discussion	109
III-6 Conclusions	117

Manuscript IV	119
IV-1 Abstract	120
IV-2 Introduction	121
IV-3 Material and methods	125
IV-3.1 Preparation of emulsions	125
IV-3.2 Oil droplet size distribution, ζ -potential and interfacial tension of the emulsions	126
IV-3.3 Preparation and characterization of foamed emulsions	127
IV-4 Results and discussion	128
IV-4.1 Impact of homogenization parameters on oil droplet size distribution of emulsions	128
IV-4.2 Emulsion properties and stability of foamed QS-emulsions affected by the oil droplet size	130
IV-4.3 Influence of pH on ζ -potential and stability of foamed QS-emulsions	135
IV-4.4 Emulsification of a binary mix of QS and β -lactoglobulin and the influence on the stability of foamed emulsions	138
IV-5 Conclusion	144
6. General discussion	145
6.1. The impact of structural features on interfacial properties of saponins from different botanical sources	146
6.2. Synergistic and antagonistic effects of QS/ β -LG-mixtures on stability of dispersed systems	149
6.2.1. Synergistic effect of QS/ β -LG-mixtures on foam properties	150
6.2.2. Antagonistic effect of QS/ β -LG-mixtures on emulsion stability	153
6.2.3. Maximizing stability of foamed emulsions	156
7. Concluding remarks and outlook	161
References	165
Annex 179	
A-I Materials and devices	179
A-II Characterizing foaming, foam stability and foam structure	181
A-III Validation of foam analysis	184
Curriculum Vitae	187

List of tables

Table I-1 Origin, purity and general chemical properties of the six saponin extracts	51
Table I-2 Fitting parameters of the experimental data using the Frumkin model	58
Table I-3 Short- and midterm adsorption parameters of six saponin extracts at twofold CMC pH 5.....	59
Table I-4 Results from foam experiments of QS, GYP, TS, ESC and GA at twofold CMC, pH 5.....	62
Table I-5 CMC _{cond} , CMC _{SFT} , slope below (k_{below}), slope above (k_{above}) the CMC and ratio of both ($k_{\text{below}}/k_{\text{above}}$) for QS, GYP, ESC and GA; for TS and TT no breaking point was detected	64
Table II-1 Dynamic interfacial tension σ of β -LG-solutions and β -LG/QS-mixtures measured for 20 min with pendant drop analysis.....	79
Table III-1 Dynamic interfacial tension (IFT) of β -LG-solutions and β -LG/QS-mixtures measured for 20 min with pendant drop analysis at the oil/water-interface.....	100
Table IV-1 d_{50} of 0.3 % QS-emulsions (5 % MCT-oil) in relation to number of passes and homogenization pressure; bold numbers refer to chosen parameters for experiment on foaming of emulsions.....	126
Table A-1 Origin, purity and general chemical properties of the used saponin extracts.....	179
Table A-2 Devices.....	180
Table A-3 Parameters to characterize foaming, foam stability and foam structure; n - time point during the analysis; / - none	183
Table A-4 Variation of parameters to characterize foaming, foam stability and foam structure depending on QS concentration; n - time point during the analysis	185

List of figures

Figure I-1 Surface pressure Π versus square root of the drop age $t^{1/2}$ at the air/water interface of QS (◆), GYP (▲), TS (×), ESC (●), GA (■) and TT (+) from different botanical origins at pH 5, twofold CMC	60
Figure I-2 Foam characterization with the parameters a) foaming speed (k_f) and b) foam density at f-max ($f_{\text{Den},f\text{-max}}$) and (c) foaming pictures after 80 and 1800 s of foaming of QS, GYP, TS, ESC and GA at twofold CMC	61
Figure I-3 FTIR spectra of C=O binding region (1718-1731 cm^{-1}) of QS (◆), GYP (■), TS (▲), ESC (●), GA (+) and TT (x)	64
Figure I-4 Influence of pH and ionic strength on interfacial tension σ at 0.5-fold CMC	65
Figure I-5 Influence of decreased pH and increased ionic strength by the addition of NaCl on foaming speed (k_f), foam decay after 3600s (f_{3600s}) and foam structure ($BD_{m,600s}$, $BD_{w,600s}$ and $f_{\text{den},f\text{-max}}$) of A) QS, B) GYP, C) TS and D) ESC at 0.5-fold CMC; pH 5 - black solid line (reference values set as 1), pH 3 – gray solid line, 100 mM – gray dotted line, 500 mM – gray dashed line.....	66
Figure I-6 Foam pictures of GA at 0.5-fold CMC after 80s of start of foaming at pH 5 (upper left) and pH 3 (upper right) and TS at 0.5-fold after 600 s of start of foaming at 0 mM (lower left) and 500 mM (lower right)	67
Figure II-1 Fluorescence measurements on the interactions of β -LG and QS, A) absorption spectra between 250-300 nm of pure β -LG (solid line), pure QS (dashed line) and mixture of β -LG+QS, which was corrected for QS adsorption (dotted line), B) Cogan-Plot of quenching of β -LG by QS with $P=\beta$ -LG-concentration, α =fraction of free binding sites and L_t =QS-concentration.....	77
Figure II-2 Interfacial tension σ in relation to the drop age t for the injection of 0.15 % QS into a droplet of 10 mM phosphate buffer (◆) and sequential adsorption of 1 % β -LG at the air water interface with injection indicated by the arrow of 0.15 % QS (●) and injection of 10 mM phosphate buffer (○)	78
Figure II-3 Surface pressure Π versus square root of the drop age $t^{1/2}$ at the air/water interface of 0.005 % QS (+), 0.005 % β -LG (◇), 0.01 % β -LG (Δ), 0.05 % β -LG (○), 0.1 % β -LG (□); filled symbols indicate β -LG is mixed with 0.005 % QS	79
Figure II-4 Interfacial dilational modulus E^* in relation A) the drop age t and B) to the surface pressure Π of 0.005 % QS (+), 0.005 % β -LG (◇), 0.01 % β -LG (Δ), 0.05 % β -LG (○), 0.1 % β -LG (□); filled symbols indicate β -LG is mixed with 0.005 % QS	80
Figure II-5 Complex shear modulus G^* in relation the interface age t for of 0.005 % QS (+), 0.005 % β -LG (◇), 0.01 % β -LG (Δ), 0.05 % β -LG (○), 0.1 % β -LG (□); filled symbols indicate β -LG is mixed with 0.005 % QS	81
Figure II-6 Foam results of QS (red), β -LG (blue) and mixtures of QS and β -LG (violet) for A) remaining foam height after 3600 s and B) foam density at f_{max} in relation to β -LG concentration	82

- Figure III-1** Results of A) lag-time and B) surface pressure after 2 s of adsorption (Π_{2s}) in relation to the β -LG concentration of 0.005 % QS (\diamond), β -LG (\circ) and mixtures of 0.005 % QS and β -LG (\square) at the MCT-oil/water-interface 99
- Figure III-2** Interfacial dilational modulus E^* in relation to β -LG-concentration determined by dilational oscillation at $f=0.1$ Hz, 2.8 % amplitude of 0.005 % QS (\diamond), β -LG (\circ) and mixtures of 0.005 % QS and β -LG (\bullet) at the MCT-oil/water interface. Error bars represent 10 % deviation, which was determined in previous experiments.. 101
- Figure III-3** Phase angle Φ in relation to area change $\Delta A/A_0$ determined by dilational oscillation at $f=0.1$ Hz at the MCT-oil/water interface of 0.005 % QS (+), 0.005 % β -LG (\diamond), 0.01 % β -LG (Δ), 0.05 % β -LG (\circ), 0.1 % β -LG (\square); filled symbols indicate β -LG is mixed with 0.005 % QS 102
- Figure III-4** Interfacial tension σ versus area change $\Delta A/A_0$ (Lissajous-plots) determined by dilational oscillation at $f=0.1$ Hz at different amplitudes 1.4, 2.8, 4.2 and 7.0 % at the MCT-oil/water interface of a) 0.005 % QS (+), b) 0.01 % β -LG (Δ), c) 0.005 % QS+0.005 % β -LG (\blacklozenge), d) 0.005 % QS+0.05 % β -LG (Δ), e) 0.005 % QS+0.05 % β -LG (\bullet), f) 0.005 % QS+0.1 % β -LG (\square) 103
- Figure III-5** S-factor versus amplitude during expansion (left panel) and compression (right panel) of a droplet at the oil/water-interface determined by dilational oscillation at $f=0.1$ Hz of 0.005 % QS (+), 0.005 % β -LG (\diamond), 0.01 % β -LG (Δ), 0.05 % β -LG (\circ), 0.1 % β -LG (\square); filled symbols indicate β -LG is mixed with 0.005 % QS 104
- Figure III-6** Complex (G^*), elastic (G') and viscous (G'') shear moduli for 0.005 % QS; 0.005, 0.01, 0.05 & 0.1 % β -LG and 0.005 % QS mixed with 0.005, 0.01, 0.05 & 0.1 % β -LG (from left to right) at the MCT-oil/water-interface measured with $f=1$ Hz, deformation=0.1% after 9 h of film formation..... 105
- Figure III-7** Oil droplet size of emulsions prepared with 0.005 % QS (1st boxplot), 0.005...0.1 % β -LG (2nd to 5th boxplot) and mixtures of 0.005 % QS and 0.005...0.1 % β -LG (6th to 9th boxplot) with upper whisker representing d_{90} , upper box end d_{75} , dash in the box d_{50} , lower box end d_{25} and lower whisker d_{10} 106
- Figure III-8** ζ -potential in relation to the β -LG concentration of emulsions (600 bar, 4 passes, 5 % MCT-oil) with 0.005 % QS (\diamond), β -LG (\circ) and mixtures of 0.005 % QS and β -LG (\bullet)..... 107
- Figure III-9** Photographic images of emulsions prepared with 0.005 % QS; 0.005, 0.01, 0.05 & 0.1 % β -LG and 0.005 % QS mixed with 0.005, 0.01, 0.05 & 0.1 % β -LG (from left to right) after 7 days of storage 108
- Figure III-10** Fluorescence measurements on the interactions of β -LG and QS showing results of the Cogan-Plot with $P=\beta$ -LG-concentration, α =fraction of free binding sites and L_t =QS-concentration. Adapted from Böttcher *et al.* (2015) with permission from Elsevier. 110
- Figure III-11** Microscopic images of emulsions after 7 days of storage prepared with 0.005 % QS and A) 0.005 % β -LG, B) 0.01 % β -LG, C) 0.05 % β -LG and D) 0.1 % β -LG the black bar on the lower right represents 25 μm 115

Figure IV-1 Schematic illustration of the relationship between the stability of foamed emulsions and their oil droplet size. Please refer to the text for appropriate explanation of the different ranges.....	123
Figure IV-2 Influence of (A) number of on the oil droplet size distribution of 0.3 % QS-emulsion (200 bar, 5 % MCT-oil) with upper whisker representing d_{90} , upper box end d_{75} , dash in the box d_{50} , lower box end d_{25} and lower whisker d_{10} and (B) influence of homogenization pressure on the oil droplet size distribution of 0.3 % QS-emulsion (2 passes, 5 % MCT-oil).....	128
Figure IV-3 Double logarithmic plot of the relationship between d_{50} and homogenization pressure of a 0.3% QS-emulsion (5 % MCT-oil) for 1 pass (■), 2 (▲), 3 (●) and 4 passes (◆)	129
Figure IV-4 Emulsion properties with respect to (A) interfacial tension σ (□) and foaming speed v (◇) and (B) properties of the foamed emulsions described by the median of the brightness distribution BD_m after 1 h measurement (Δ) in relation to the median (d_{50}) of 0.3 % QS-emulsions with range 1, 2 and 3. Lines are only guide to the eye. Please refer to the text for appropriate explanation of the different ranges.	132
Figure IV-5 Brightness profiles of foamed emulsions of 0.3 % QS with d_{50} of A) 0.2 μm , 600 bar, 3 passes; B) 0.3 μm , 500 bar, 2 passes; C) 0.4 μm , 300 bar, 2 passes; D) 0.5 μm , 100 bar, 3 passes; E) 0.6 μm , 200 bar, 2 passes; F) 0.8 μm , 100 bar, 4 passes; G) 1 μm , 100 bar, 3 passes; H) 1.2 μm , 100 bar, 2 passes; I) 2.1 μm , 50 bar, 3 passes.....	133
Figure IV-6 Specific interfacial area A_{spec} In relation to d_{50} of 0.3% QS-emulsions.....	134
Figure IV-7 Foam profile showing total height in relation to measuring time for foamed emulsions (5 % MCT-oil, $d_{50}=0.5 \mu\text{m}$) prepared at A) pH 3 B) pH 5 and C) pH 7. A was analyzed for 1800 s, B and C for 3600 s	135
Figure IV-8 ζ -potential in relation to pH of 0.3 % QS-emulsions (5 % MCT-oil, $d_{50}=0.5 \mu\text{m}$) .	136
Figure IV-9 Foamed emulsion of 0.3 % QS (5 % MCT-Oil, $d_{50}=0.5 \mu\text{m}$) after 1800 s with macroscopic aggregation of oil droplets.....	137
Figure IV-10 ζ -potential (A) and interfacial tension after 150 s (B) of emulsions (0.3 % QS, 5 % MCT-oil, $d_{50}=0.5 \mu\text{m}$) in relation to β -LG-concentration for QS (○), β -LG (◇), Mix_{pre} (Δ) and Mix_{post} (□)	139
Figure IV-11 Schematic illustration of location of QS (green) and β -LG (violet) in emulsions (A+C) and foamed emulsions (B+D) whereas Mix_{pre} is illustrated in A+B and Mix_{post} in C+D	140
Figure IV-12 Foaming speed of emulsions (0.3 % QS, 5 % MCT-oil, $d_{50}=0.5 \mu\text{m}$) in relation to β -LG-concentration for QS (○), β -LG (◇), Mix_{pre} (Δ) and Mix_{post} (□).....	141
Figure IV-13 Foam profiles showing total height in relation to measuring time for a foamed emulsion ($d_{50}=0.5 \mu\text{m}$) prepared with 5 % MCT-oil and (A) 0.3 % QS; (B) 0.1 % β -LG; (C) 0.2 % β -LG; (D) 0.3 % β -LG; (E) 0.3 % QS+0.1% β -LG (Mix_{pre}); (F) 0.3 % QS+0.2 % β -LG (Mix_{pre}); (G) 0.3 % QS+0.3% β -LG (Mix_{pre}); (H) 0.3 % QS+0.1% β -LG (Mix_{post}); (I) 0.3 % QS+0.2 % β -LG (Mix_{post}); (J) 0.3 % QS+0.3% β -LG (Mix_{post})	142

Figure A-1 Foam profile of a foam made from a (A) 0.003 % and (B) 0.01 % QS solution..... 181

Figure A-2 Derived parameters from foam profile 1 - Time to maximum foaming level – t_{fmax} [s], 2 - Maximum foaming level – f_{max} [mm], 3 - Slope of foaming – k_f [mm/s], 4 – Relative remaining foam height– $f_n\%$ [%], 5 - Foam half-life time – $t_{f1/2}$ [s], 6 - Stability of maximum foam height – $t_{fmax-5\%}$ [s], 7 – relative drainage – $d_n\%$ [%], 8 - Foam density – $f_{den,n}$ [%], 9 - Foam density at f-max – $f_{den,fmax\%}$ [%], 10 - Analysis of image brightness distribution – median $BD_{m,n}$ and width $BD_{w,n}$... 182

Figure A-3 Example for histogram of brightness distribution at a specific time point (rectangle of 1 px width) of a foam made from 0.01 % QS solution after 1800 s... 184

List of abbreviations

%wt	Weight percent
A/W	Air/water-interface
ATR	Attenuated total reflection
BSC	Saponin-rich extract from <i>Sapindus mukurossi</i>
CCD	Charge-coupled device
CMC	Critical micelle concentration
CMC _{cond}	Critical micelle concentration determined with conductivity
C _n DMPO	Alkyldimethylphosphine oxide with alkyl chain (non-ionic surfactant)
Cryo-TEM	Cryo-transmission electron microscopy
CTAB	Cetyltrimethylammoniumbromid (cationic surfactant)
DATM	Diacteyltartaric esters of monoglycerides
ESC	Saponin-rich extract from <i>Aesculus hippocastanum</i>
ESI	Electron spray ionization
FAB	Fast atom bombardment (ionization method)
FTIR	Fourier transform infrared spectroscopy
GA	Glycyrrhizic Acid Ammonium Salt from <i>Glycyrrhiza glabra</i>
GRAS	Generally regarded as safe
GS	Saponin-rich extract from <i>Panax ginseng</i>
GYP	Saponin-rich extract from <i>Gypsophia</i> species
HPLC	High performance liquid chromatography
HPTLC	High performance thin layer chromatography
IFT	Interfacial tension
ITC	Isothermal titration calorimetry
LC-MS	Liquid chromatography coupled with mass spectrometry
MALDI	Matrix-assisted laser desorption/ionization
MCT	Medium-chain triglyceride
NMR	Nuclear magnetic resonance spectroscopy
O/W	Oil/water-interface
O/W/A	Oil/water/air-interface
QS	Saponin-rich extract from <i>Quillaja saponaria</i> Molina
SDS	Sodium dodecyl sulfate (anionic surfactant)
SLS	Sodium laureth sulfate (anionic surfactant)
TOF	Time of flight detector
Triton X-100	Polyethylene oxide with aromatic hydrocarbon or hydrophobic group (non-ionic surfactant)
Trp	Tryptophan
TS	Saponin-rich extract from <i>Camellia oleifera</i> Abel

TT	Saponin-rich extract from <i>Tribulus terrestris</i>
Tween 80	Polysorbate 80 (non-ionic surfactant)
USDA	U.S. Department of Agriculture
β -LG	Beta-lactoglobulin
a	Interaction parameter
A	Area per molecule
A_{em}	Absorption value at the emission wavelength
A_{exc}	Absorption value at the excitation wavelength
b	Adsorption equilibrium constant
$BD_{m,n}$	Median of brightness distribution of foam profiles at time point n
$BD_{w,n}$	width of brightness distribution of foam profiles at time point n
c	Bulk concentration
c_0	Concentration of surfactant in the bulk solution
d	Diameter
D_{calc}	Calculated diffusion coefficient
D_{exp}	Experimental diffusion coefficient
d_x	Diameter at x-percentile
E^*	Interfacial/Complex dilational modulus
E'	Elastic (storage) dilational modulus
E''	Viscous (loss) dilational modulus
F_0	Fluorescence intensity of the initial β -LG-concentration
F_{corr}	Recalculated fluorescence value
$f_{Den,f-max}$	Percentage of incorporated liquid in the foam
$f_{Den,n}$	Foam density and foam density at f-max
F_{max}	Fluorescence intensity upon saturation
f_n	Remaining foam height at time point n
F_{obs}	Measured fluorescence value
G^*	Interfacial/Complex shear modulus
G'	Elastic (storage) shear modulus
G''	Viscous (loss) shear modulus
K	Adsorption parameter
$K'a$	Apparent affinity constant

$K'd$	Apparent dissociation constant
k_B	Boltzmann constant
k_f	Foaming speed (start of foaming until maximum foam height (f-max))
L_t	QS concentration in fluorescence experiments
n	Maximum number of binding sites
n	Specific time point in foam analysis
P	β -LG concentration in fluorescence experiments
R	General gas constant
r	Hydrodynamic radius of a spherical molecule
S	Strain stiffening ratio
S_{com}	Strain stiffening during compression
S_{ext}	Strain stiffening ratio during expansion
T	Absolute temperature
t	Time
$\tan \delta$	Dissipation factor (G''/G')
β	Interaction parameter
$\Delta A/A$	Area change
ε	Compressibility of the interfacial monolayer
ζ	Zeta-potential
η	Dynamic viscosity
θ	Surface coverage
Π	Surface pressure
Π_{2s}	Surface pressure 2 s after interfacial tension drop
σ	Interfacial tension
σ_0	Interfacial tension of water
Φ	Phase angle
ω	Molar surface area
ω_0	Molar area at $\Pi=0$
Γ	Surface concentration of surfactant
Γ_∞	Maximum surface concentration of surfactant at $c_0 \rightarrow \infty$

Publications

Manuscript I

Böttcher, S. and Drusch, S., 2016, “Interfacial Properties of Saponin Extracts and Their Impact on Foam Characteristics”, *Food Biophysics*, V. 11, No. 1, pp. 91–100.

The final publication is available at Springer via <http://dx.doi.org/10.1007/s11483-015-9420-5>.

Manuscript II

Böttcher, S.; Scampicchio, M.; and Drusch, S., 2016, “Mixtures of saponins and beta-lactoglobulin differ from classical protein/surfactant-systems at the air-water interface”, *Colloids and Surfaces A: Physicochemical and Engineering Aspects*, V. 506, pp. 765–773. doi: <http://dx.doi.org/10.1016/j.colsurfa.2016.07.057>.

Manuscript III

Böttcher, S.; Keppler, J.; and Drusch, S., 2017, “Mixtures of Quillaja saponin and beta-lactoglobulin at the oil/water-interface: adsorption, interfacial rheology and emulsion properties,” *Colloids and Surfaces A: Physicochemical and Engineering Aspects*, V. 518, pp. 46–56. doi: <http://dx.doi.org/10.1016/j.colsurfa.2016.12.041>.

Manuscript IV

Böttcher, S.*; Eichhorn, M.*; and Drusch, S., 2017, “Factors affecting foamed emulsions prepared with an extract from *Quillaja saponaria* Molina: oil droplet size, pH and presence of beta-lactoglobulin”, *Food Biophysics*, V. 12, No. 2, pp. 250–260. doi: <http://dx.doi.org/10.1007/s11483-017-9481-8>.

Manuscript V

Böttcher, S. and Drusch, S., 2016, “Saponins – self-assembly and behavior at aqueous interfaces”, *Advances in Colloids and Interface Science*, V. 243, pp. 105–113.

The final publication is available at Springer via <http://dx.doi.org/10.1016/j.cis.2017.02.008>.

*Co-first authorship

Conference contributions

- **Böttcher, S. and S. Drusch**, presentation at National ISEKI-Workshop on “hot topics” in the Field of Food Science and Technology: *Substitution von niedermolekularen Emulgatoren in dispersen Lebensmittelsystemen durch Saponine*, 01.07.2014 in Berlin, Germany
- **Böttcher, S. and S. Drusch**, presentation at 2nd colloquium of the Institute of Food Science and Technology TU Berlin: *Einsatz von Saponinen zur Stabilisierung von dispersen Systemen*, 20.10.2014 in Berlin, Germany
- **Böttcher, S. and S. Drusch**, poster at 3rd colloquium of the Institute of Food Science and Technology TU Berlin: *Saponins as stabilizing agents in foams*, 20.04.2015, Berlin, Germany
- **Böttcher, S. and S. Drusch**, presentation at SOMATAI-conference: „*Quillaja saponin: An emulsifier unlike common low-molecular weight surfactants*“, 03.06.16 in Crete, Greece
- **Böttcher, S. and S. Drusch**, poster at 30th Conference of the European Colloid and Interface Society: *Quillaja saponin – a promising natural surfactant*, 05.09.16 in Rome, Italy

1. Introduction¹

Saponins are natural phytochemicals, which occur in an estimated three out of four plants species (Hänsel and Sticher 2010). The broad occurrence of saponins in the plant kingdom can be attributed to their bitter taste, which protects the plant from being eaten by animals. For a long time, saponins in plant materials were considered undesirable ingredients in human and animal nutrition because of their bitter taste and undesired side-effects on the gastro-intestinal system when consumed at high concentrations (Fenwick *et al.* 1991). As a phytochemical, saponin content in plants is usually around 1 % or lower (Fenwick and Oakenfull 1983) but the bark of the Chilean soap bark tree (*Quillaja saponaria* Molina) has an exceptionally high saponin content of up to 5 % (Kuznesof and Soares 2005). The composition of saponin extracts and their saponin concentration does not only depend on the plant species but also on the part of the plant, seasonal changes and extraction parameters (Fenwick *et al.* 1991; Cheok *et al.* 2014). When saponins are extracted from plant material, the resulting extracts are always a mixture of different saponin derivatives. For instance extracts from *Quillaja saponaria* Molina may contain more than 100 different saponins (Kite *et al.* 2004) as well as other anionic residual plant substances (Maier *et al.* 2015a; Tippel *et al.* 2017).

The growing interest on saponins from *Quillaja saponaria* Molina as adjuvants (Sun *et al.* 2009) led to an increasing amount of studies investigating membranolytic and haemolytic properties (Oda *et al.* 2000; Sparg *et al.* 2004; Reim and Rohn 2015). For this purpose interactions of saponins with membrane lipids like DPPC and cholesterol (Demana *et al.* 2004; Wojciechowski *et al.* 2014c; Wojciechowski *et al.* 2016a) and lecithin bilayers (Wojciechowski *et al.* 2016b) were studied. Saponins may interact with the membrane cholesterol, which may have adverse effects on cells. The interactions are assumed to originate from hydrogen bonds formed between sugar residues of saponins and the polar head groups of the DPPC and cholesterol (Wojciechowski *et al.* 2016a).

Mixed systems play an important role in foods, but also in many other fields like cosmetics and especially dispersed systems are of high interest in research and industry. In dispersed food systems two or more immiscible phases are mixed, which may be of gaseous, liquid and/or solid state. When air is dispersed in a continuous liquid phase or liquid is dispersed in a continuous liquid phase these systems are referred to as ‘foam’ and

¹ Parts of the introduction were published as Manuscript V

‘emulsion’, respectively. Foams and emulsions (excluding microemulsions) are thermodynamically unstable systems by definition but meta-stable states may be obtained. To form and stabilize dispersed systems, surface active constituents are essential. A molecule is referred to as surface active when hydrophilic and hydrophobic parts are present in the molecular structure. Low-molecular weight surfactants, various proteins and certain charged polysaccharides are examples of surface active molecules. Surface active molecules adsorb at interfaces and align their hydrophobic (apolar) and hydrophilic (polar) structural features according to the affinity of the dispersed and the continuous phase. In an emulsion, apolar parts of the molecule are moved from the aqueous liquid phase (polar) and into the apolar oil phase because this is thermodynamically favored. As a result of the adsorption at the interface, interfacial tension is decreased and free energy of the system is reduced as described by the Gibbs adsorption equation. Surface active molecules may slow down coalescence and aggregation of oil droplets in emulsions by electrostatic and steric repulsion. In foams, adsorbed surface active molecules form an interfacial layer that decelerates bubble coalescence, which may be caused by the rupture of the thin liquid film (liquid film between two adjacent bubbles). In addition, these thin films could be stabilized by the formation of a viscoelastic network, steric and electrostatic repulsion as well as the Gibbs-Marangoni mechanism. A detailed description of stabilizing mechanisms of surface active constituents in foams and emulsions would be beyond the scope of this introduction. The reader is referred to Sadoc and Rivier (1999), Schramm (2005) and Kralova and Sjöblom (2009) for more extensive information on stabilizing mechanisms in dispersed systems in general.

In recent years, researchers regained interest in using saponins in dispersed systems due to their interfacial activity and unique behavior. Saponins have shown interesting interfacial properties like formation of a viscoelastic network at aqueous interfaces (Stanimirova *et al.* 2011; Golemanov *et al.* 2012; Wojciechowski 2013), formation of micelles (Mitra and Dungan 1997; Mitra and Dungan 2000) as well as formation of stable foams (Jian *et al.* 2011; Chen *et al.* 2010) and emulsions (Yang *et al.* 2013; Yang and McClements 2013). Especially the formation of a viscoelastic network is very unusual for such small molecules. Saponins usually have a molecular weight between 800 to 2,500 Da (Dinda *et al.* 2010; Thalhamer and Himmelsbach 2014) and are larger than low molecular weight surfactants,

which have a molecular weight below 500 Da. Nevertheless, the molecular weight of saponins is lower compared to common proteins like β -lactoglobulin (18,400 Da), β -casein (24,000 Da) and lysozyme (14,300 Da).

Only few interfacial studies focused on the interfacial properties of saponins from botanical sources other than Quillaja saponins (extracted from *Quillaja saponaria* Molina, QS). Molecular structures of different saponins from various botanical origin were extensively reported and reviewed (Güçlü-Üstündağ and Mazza 2007; Vincken *et al.* 2007; Dinda *et al.* 2010). The structural diversity that may be found in one extract makes it challenging to work with saponins. Initial studies on the relationship between structural features (type of aglycone and amount of sugar residues) and interfacial properties e.g. shear and dilational properties were conducted (Golemanov *et al.* 2014; Pagureva *et al.* 2016). Saponins with a triterpenoid aglycone form high viscoelastic interfacial layers, which exhibit higher shear and dilational moduli in comparison to saponins with a steroidal aglycone. In contrast, differences in interfacial properties were not as easily connected to the amount of linked sugar residues. Although the formation of the viscoelastic network is mainly influenced by the type of aglycone Golemanov *et al.* (2012) concluded from detailed experiments on interfacial rheology of QS layers that intermolecular hydrogen bonds between adjacent sugar residues are responsible for the network formation. It may be summarized that initial studies revealed some structural features, which are associated with high shear and dilational moduli but little is known for saponins regarding the relationship between interfacial rheology and properties in dispersed systems like foams.

Kezwon and Wojciechowski (2014) recently reviewed present state of knowledge on interactions between Quillaja saponins with food proteins like β -lactoglobulin (β -LG), β -casein and lysozyme. It is well-known that β -LG forms a viscoelastic network at the air/water-interface (Petkov *et al.* 2000). But it is still controversially discussed whether β -LG unfolds upon adsorption at the air/water-interface as recently reviewed by Wierenga and Gruppen (2010). For a long time it was generally accepted that proteins adsorb at the air/water-interface and slowly unfold at the interface over time as it was first described by Graham and Phillips (1979). The unfolding was concluded from dynamic interfacial data because it takes several hours for β -LG-solutions to reach equilibrium. A rather new explanation is the ‘colloid approach’ described by Talbot *et al.* (2000) using the ‘Random Sequential Adsorption model’, which proposes that no or only little unfolding of the β -LG molecules occurs at the interface. It is assumed that the full adsorption takes very long time, because

the likeliness for a protein to find an unoccupied space at the interface decreases over time and slows adsorption. Since the protein molecules at the interface are immobile, a protein molecule that wants to adsorb at an already occupied space is rejected and diffuses into the bulk again.

However, it was shown that complexes between Quillaja saponins and proteins influence interfacial properties and may impact foam properties (Kezwon and Wojciechowski 2014). But the impact of interactions between QS and β -LG on foam stability as well as interfacial shear and dilational rheology remains unknown. It may be speculated that a joint interfacial network between QS and β -LG might be formed, which leads to high viscoelastic moduli and corresponding high foam stability. The high foam stability due to the formation of a viscoelastic network discriminates the QS/ β -LG-systems and other surfactant/protein-systems. Surfactants usually stabilize foams by the Gibbs-Marangoni mechanisms and proteins by a viscoelastic interfacial network. These two possible mechanisms are opposing each other and usually lead to reduced foam stability in mixed surfactant/protein-systems (Pradines *et al.* 2009; Lech *et al.* 2014).

Both QS and β -LG have differing properties at the oil/water-interface, which might influence interactions between both constituents leading to deviating interfacial and emulsion properties. In contrast to the air/water-interface the viscoelastic dilational and shear moduli of QS are distinctively lower at the oil/water-interface (Wojciechowski 2013; Golemanov *et al.* 2014). Therefore, interactions with β -LG might not lead to a strong viscoelastic film, which can withstand deformation and thoroughly stabilize oil droplets against coalescence. Researchers agree on the considerable unfolding of β -LG at the oil/water-interface and numerous studies characterized adsorption with sophisticated methods (Maldonado-Valderrama and Patino 2010; Zhai *et al.* 2013; Zare *et al.* 2016).

Fundamental studies on interfacial rheology and two-phase dispersed systems like emulsions and foams are important to understand mechanisms in more complex systems. The application of new surfactants in real food products can be challenging, because multiple variables influence properties of these systems and matrix effects may occur between surfactant and food ingredients. Until now there have been various studies on the application of QS in food systems (Yang and McClements 2013; Ozturk *et al.* 2014; Zhang *et al.* 2015; Zhang *et al.* 2016). In certain products like mousse and vegan milk foam high stability is desired. These products contain a mixture of emulsion and foam and may be referred to as ‘foamed emulsion’. The presence of dispersed oil droplets contradicts the stability of the

foamed emulsion. In numerous studies the destabilizing effect of dispersed oil droplets on thin films was studied (Zhang *et al.* 2003; Langevin 2008; Karakashev and Grozdanova 2012; Simjoo *et al.* 2013). It was shown that oil droplets ‘bridge’ foam lamellae, which consequently leads to bubble coalescence by thin film rupture (Denkov 2004). In emulsions with constant surfactant content, oil droplets should have a moderate size, because at a small size of the oil droplets a sufficiently higher interfacial area needs to be stabilized by surfactant and at a large size of the oil droplets bridging of thin film occurs. Stability of foamed emulsions may also be increased by mixtures of QS and β -LG, with β -LG stabilizing the oil/water-interface and QS stabilizing the air/water-interface. This stabilization occurs because viscoelastic shear and dilational moduli of β -LG are not as prone to a reduction caused by changes in the polarity of the non-aqueous phase. Due to the presence of negatively charged constituents in the QS extract (Maier *et al.* 2015a; Tippel *et al.* 2017) and the carboxylic group in the molecular structure it is expected that stability of foamed emulsions increases with increasing pH.

The aim of this thesis is to analyze and understand interfacial behavior of saponins as well as their mixture with β -lactoglobulin at aqueous interfaces. In addition, the knowledge on interfacial properties is applied to explain stabilization and destabilization phenomena in dispersed model systems like foams and emulsions. Furthermore the gained understanding of underlying stabilization mechanisms of Quillaja saponins in simple dispersed systems is used to maximize stability of more complex systems like foamed emulsions.

To accomplish this, the following hypotheses were defined:

- 1) Saponins from different botanical origin differ in type of aglycone and amount of linked sugar residues, which affects adsorption and foam properties. It is expected that triterpenoid saponins have the highest foam stability due to molecular interactions between sugar residues. In addition, it is hypothesized that the type of aglycone has the highest impact whereas the type and amount of sugar chains has a minor impact on foam properties. (manuscript I)
- 2) Similar to β -lactoglobulin (globular protein) Quillaja saponins stabilize foams by forming a viscoelastic network, which counteracts film rupture and imposed stress. In mixtures of Quillaja saponins and β -lactoglobulin foam stability may be increased by development of a joint interfacial network, which can withstand dilational and shear stress. (manuscript II)
- 3) Interactions between Quillaja saponins and β -lactoglobulin at the oil/water-interface may differ from those at the air/water-interface because oil penetrates between adsorbed Quillaja saponin molecules and β -lactoglobulin undergoes substantial unfolding. The interactions may affect not only interfacial rheology but also emulsion properties. (manuscript III)
- 4) Quillaja saponins are more efficient in stabilizing the air/water-interface than the oil/water-interface. To maximize stability of complex dispersed systems (foamed emulsions) a primary distribution of Quillaja saponins at the air/water-interface must be ensured. This may be obtained by sequential addition of β -lactoglobulin and Quillaja saponins to emulsions. It may furthermore be hypothesized that stability of the foamed emulsions is maximized at neutral pH due to high electrostatic repulsion and at moderate oil droplet size. Above and below the moderate oil droplet size, stability of the foamed emulsion is reduced due to low amount of free surfactant and bridging of thin films by oil droplets, respectively. (manuscript IV)

2. Literature review²

2.1. Composition and characterization of saponin extracts

In recent years a lot of effort was made to develop new and improve existing methods for faster and more reliable determination of saponins. A detailed overview over experimental protocols reported in recent years was published by Cheok *et al.* (2014). As for various plant substances the absence of an easy to fabricate standard, which can be used to quantify all saponins in an extract complicates matters even more.

For this reason usually fingerprint chromatograms of different saponin extracts are compared to each other (San Martín and Briones 2000). When aiming for identifying and quantifying unknown saponin molecules, highly sophisticated methods are needed. Various analytic options were reviewed by Scognamiglio *et al.* (2015) highlighting 2-D NMR-techniques as the method of choice to determine aglycone structure, sugars and binding sites of the sugar residues. The author additionally emphasized the role of mass spectrometric (MS) methods with and without subsequent NMR analysis. In the context of saponin analysis the use of soft ionization methods like ESI is favorable because of the fragmentation of molecules originating from hard ionization. Less common ionization methods include fast atom bombardment (FAB) and matrix-assisted laser desorption ionization (MALDI). Masses are typically determined with time of flight (TOF) analyzers.

Before structural elucidation, saponin extracts are separated into single compounds by high performance liquid chromatography (HPLC) (San Martín and Briones 2000). For qualitative analysis the HPLC column is connected to subsequent mass spectrometry (MS). Various analytic options were reviewed by Scognamiglio *et al.* (2015) highlighting 2-D NMR-techniques as the method of choice to determine aglycone structure, sugars and binding sites of the sugar residues. The author additionally emphasized the role of mass spectrometric methods with and without subsequent NMR analysis. In recent past, high-performance thin-layer chromatography (HPTLC) coupled with MALDI-TOF-MS was used to qualitatively characterize a Quillaja saponin extract (Tippel *et al.* 2016a). Phenolic impurities in a Quillaja saponins extract were determined by HPLC-PDA-MSn and NMR spectroscopy (Maier *et al.* 2015). Until now a huge variety of saponin derivatives were found in Quillaja saponin extracts: ranging from a molecular weight of 930 to 2,322 g/mol (Thalhamer and Himmelsbach 2014; Tippel *et al.* 2016a).

² Parts of the literature review were published as Manuscript V

In general, saponins consist of a hydrophobic aglycone structure with linked hydrophilic sugar residues. Most classifications of saponins either focus on differences in aglycone structure or amount of linked sugar residues. Two general aglycone structures occur: most saponins have either a triterpenoid or steroidal aglycone. In addition, various subcategories of triterpenoid and steroidal aglycone structures exist. For example, triterpenoid saponins may be oleanane or dammarane type and steroidal saponins may be furostanol or spirostanol type. For further information on structural differences between the mentioned aglycone structures please refer to Figure 1.

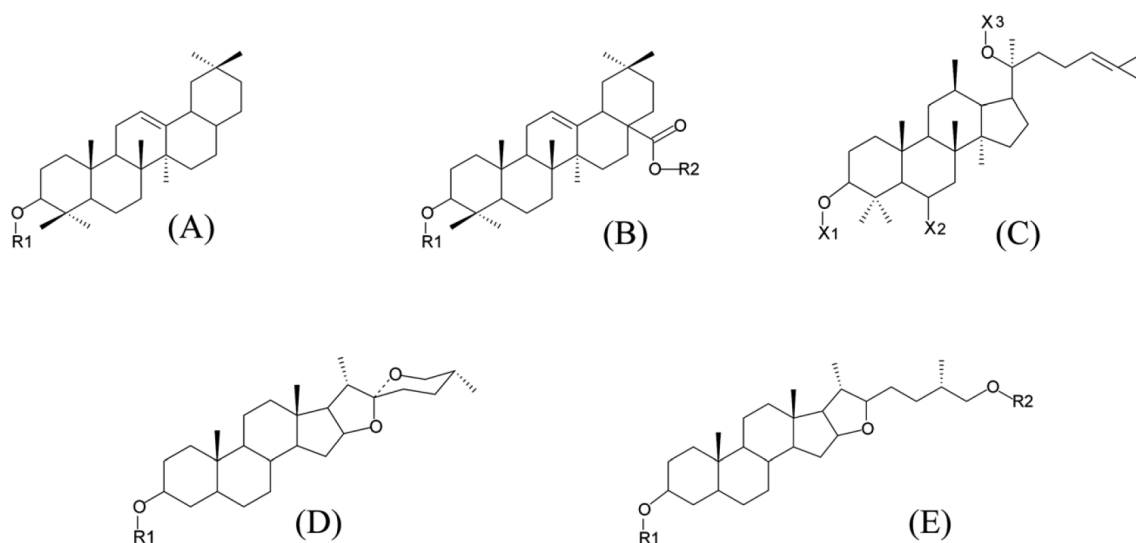


Figure 1 Molecular structure of triterpenoid saponins with A) one sugar chain (monodesmosidic) or B) two sugar chains (bidesmosidic) with oleanane aglycone structure, C) one or two linked sugar residues (Mono- and bidesmosidic) with dammarane aglycone structure and steroidal saponins of D) spirostanol and (E) furastanol type. Reproduced from Golemanov *et al.* 2013 with permission from The Royal Society of Chemistry.

When classifying saponins based on the amount of sugar residues: monodesmosidic, bidesmosidic or even tridesmosidic (very uncommon) saponins are known with one, two and tree sugar chains, respectively. The sugar chains of monodesmosidic saponins are usually attached at C-3 and the additional sugar chain of bidesmosidic saponins is normally attached at C-28 of the aglycone (Güçlü-Üstündağ and Mazza 2007). Saponins may also have acetylated groups like the fatty acyl group in some Quillaja saponins (Hänsel and Sticher 2010).

The general molecular structure of Quillaja saponins is illustrated in Figure 2.

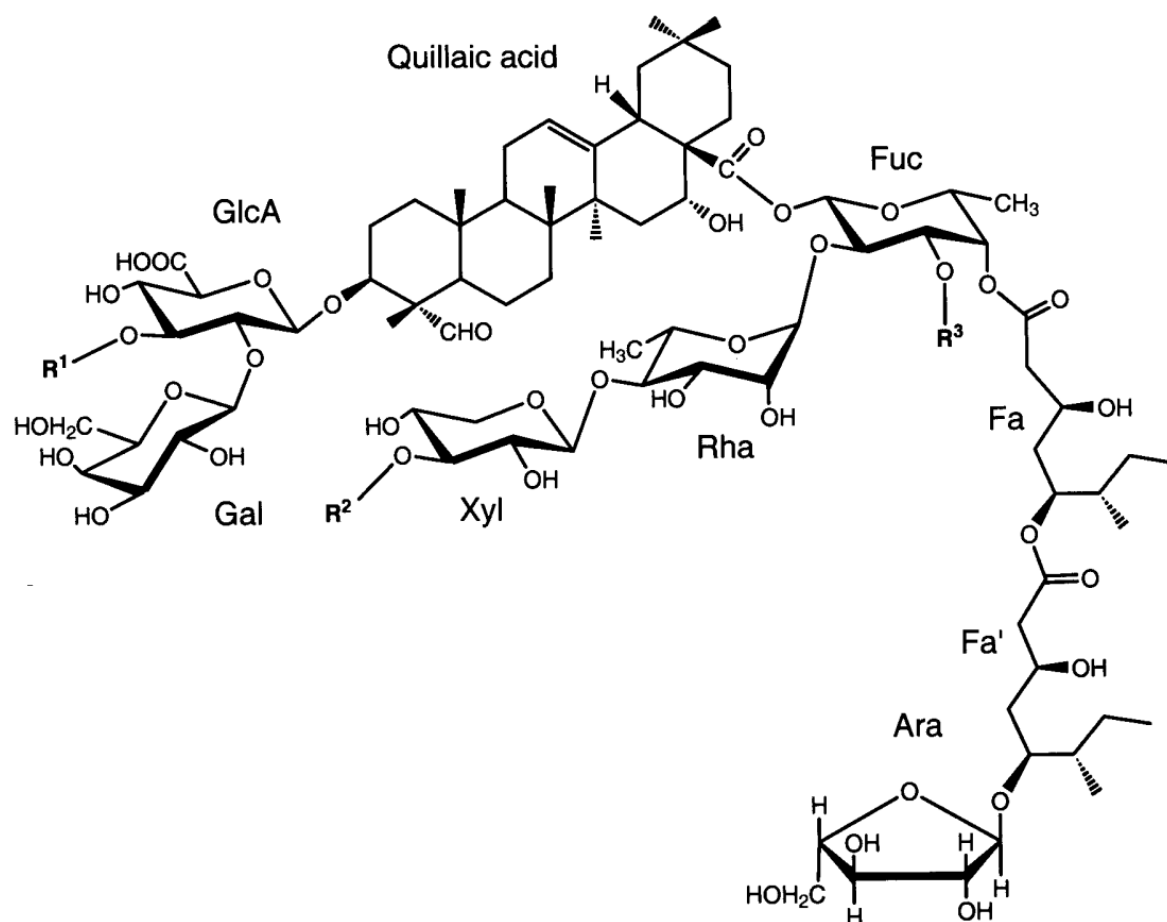


Figure 2 Molecular structure of bidesmosidic saponins extracted from *Quillaja saponaria* Molina with R¹⁻³ representing H, acetyl groups or sugar residues. Adapted from Nord and Kenne 2000 with permission from Elsevier.

There are commercially available saponin extracts from *Quillaja saponaria* Molina (San Martín and Briones 2000), *Yucca schidigera* (Sastre *et al.* 2016) and *Saponaria officinalis* (Oakenfull 1986). Quillaja saponins are the only saponin extracts to date, which are approved for application in food products in the EU (E 999) and have GRAS status in the US. There is a whole range of commercial Quillaja saponins extracts available. These extracts distinctly vary in purity, which ranges between 20 % (Resnik 2004) and >97 % (Wojciechowski *et al.* 2016a) and may contain various impurities like phenols, fats, tannins, proteins and sugars (Kuznesof and Soares 2005; Maier *et al.* 2015a; Tippel *et al.* 2017).

2.2. Self-assembly and micellar structure

Saponins are well soluble in aqueous solutions and when dissolved in aqueous solutions, the hydrophilic sugar residues are extensively hydrated. According to Sarnthein-Graf and La Mesa (2004) 30 water molecules hydrate one QS molecule and Wojciechowski *et al.* (2014a) reported 60 water molecules per QS molecule. Saponins are surface active and therefore adsorb at aqueous interfaces. When the interface is saturated with saponin molecules, micelles are formed in the bulk. Micellar properties may be affected by changes in pH, ionic strength and temperature (Mitra and Dungan 1997).

The concentration above, which micelles are formed is called ‘critical micelle concentration’ and may be obtained from a plot of the interfacial tension vs. concentration. The critical micelle concentration is very different between various saponins and saponin extracts. For example the critical micelle concentration for different Quillaja saponins ranged from 0.013 g/L (Wojciechowski 2013) up to 0.7 g/L (Mitra and Dungan 1997). Quillaja saponins can form spherical micelles in aqueous solutions with a diameter of 7.5 nm (Tippel *et al.* 2016a) (see Figure 3A) and can incorporate water-insoluble compounds. Quillaja saponins can also form micelles with various substances e.g. lutein esters (Tippel *et al.* 2016b), cholesterol+L- α -phosphatidylcholine (Demana *et al.* 2004). With about 130 nm, Quillaja saponin micelles loaded with lutein esters are distinctively larger compared to unloaded micelles. It is possible that elongated/worm-like micelles are formed between micelles consisting of QS and hydrophilic substances at low pH, see Figure 3B. The elongation was attributed to a decrease in electrostatic repulsion of the charged head-groups and thus, an increase in the critical packing parameter, which is responsible for the elongation of the micelles (Tippel *et al.* 2016a).

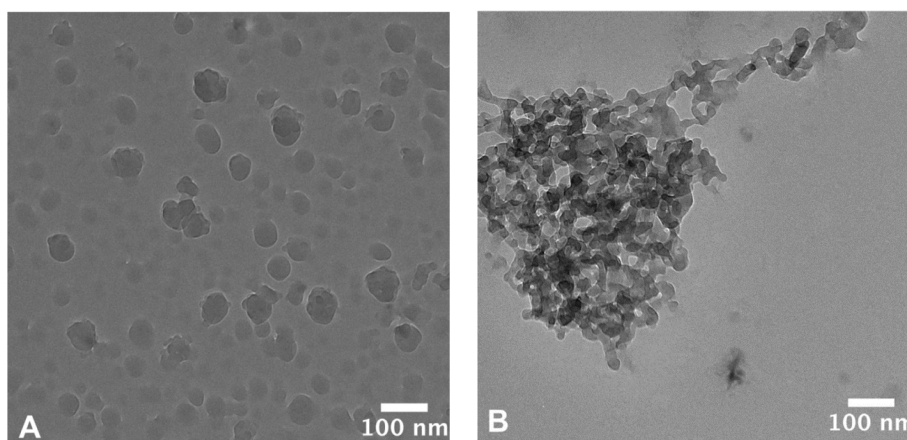


Figure 3 Cryo-TEM micrographs of Quillaja saponin/lutein ester micelles in (A) aqueous unbuffered solution (spherical) and B) in buffer at pH 3 (elongated). Reproduced from Tippel *et al.* 2016a with permission from Elsevier.

2.3. Linking molecular structure and behavior at aqueous interfaces

When trying to link molecular structure with interfacial behavior it has to be kept in mind, that extracts are prone to differences in saponin content and composition. A detailed collection of all reported saponins would be beyond the scope of this literature review. There are excellent reviews on the molecular structure of saponins found in different plants (Sparg *et al.* 2004; Vincken *et al.* 2007; Dinda *et al.* 2010). Usually saponin extracts also contain numerous plant residues, which may affect interfacial properties as shown by Pagureva *et al.* (2016). Figure 4 provides an overview over classification of the discussed saponins in this work with respect to aglycone structure and amount of sugar residues.

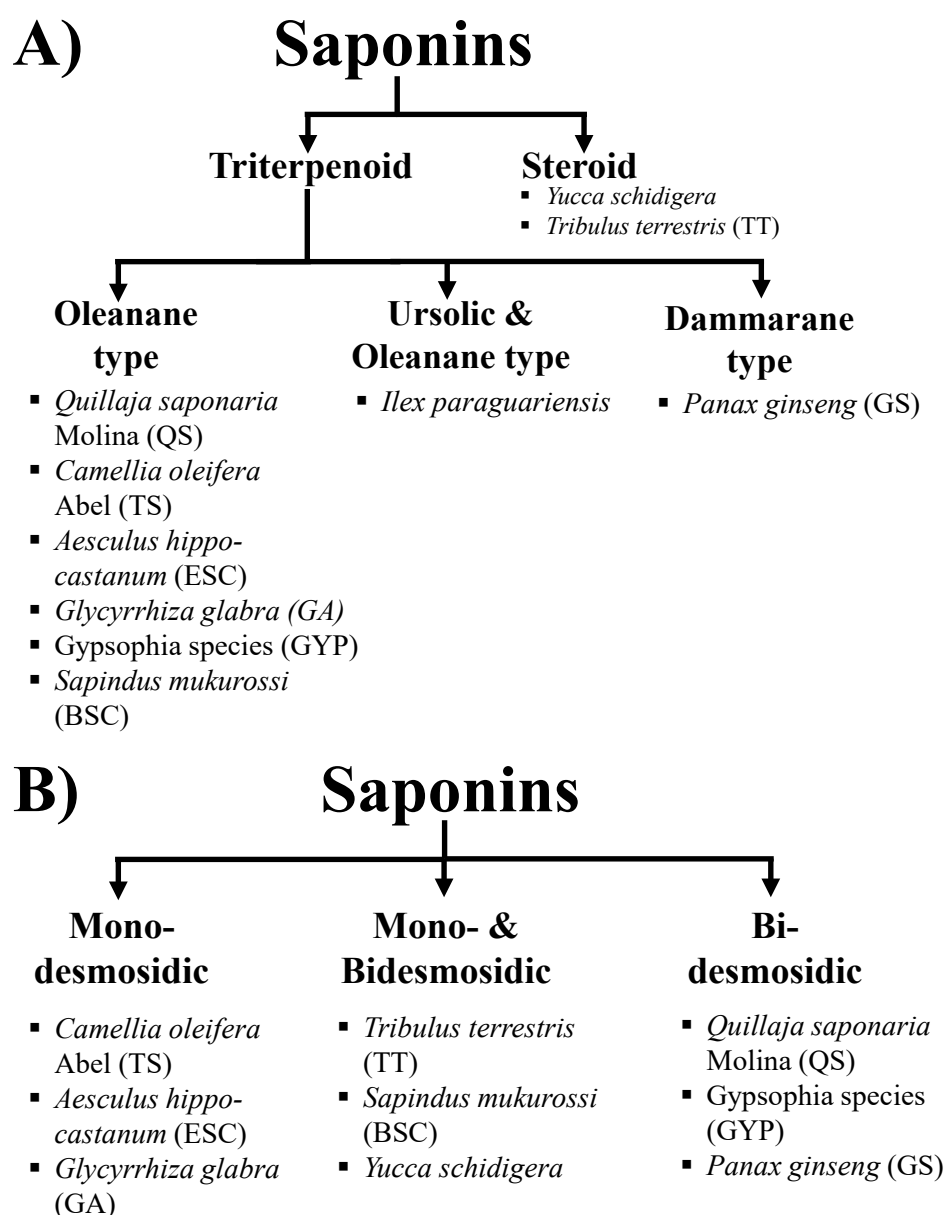


Figure 4 Structural classification of discussed saponin extracts in this thesis with respect to
A) aglycone structure B) amount of sugar residues

2.3.1. Interfacial configuration of saponins at the air/water-interface

For the determination of structure-function-relationship, information on the orientation and interfacial arrangement of the adsorbed molecules are needed. The adsorbed surfactant layer can be described with the equation of state and adsorption isotherm. The former equation describes the relationship of the surface pressure/surface tension as a function of surfactant concentration at the interface. In contrast the adsorption isotherm characterizes the dependence of the adsorbed amount of surfactant on the bulk concentration. There were different types of models used in studies on saponins so far, like the Langmuir or Volmer, which can be fitted to the experimental data. The Langmuir model (Eq. 1a+b) was derived for localized adsorption, which means that every molecule has a defined site at the interface and cannot freely diffuse in the interfacial layer.

Langmuir a) adsorption isotherm and b) equation of state

$$(1a) Kc_0 = \frac{\Gamma}{\Gamma_\infty - \Gamma}$$

$$(1b) \sigma = \sigma_0 + k_B T \Gamma_\infty \ln(1 - \Gamma/\Gamma_\infty)$$

where K is the adsorption parameter, c_0 the surfactant concentration in the bulk, Γ the surface concentration, Γ_∞ - maximum possible value of surface concentration at $c_0 \rightarrow \infty$, k_B the Boltzmann constant, T the absolute temperature, σ the surface tension and σ_0 surface tension of the pure solvent.

The Langmuir model can be expanded considering interactions between the molecules, which results in the Frumkin model (Eq. 2a+b).

Frumkin a) adsorption isotherm and b) equation of state

$$(2a) Kc_0 = \frac{\Gamma}{\Gamma_\infty - \Gamma} \exp\left(-\frac{2\beta\Gamma}{kT}\right)$$

$$(2b) \sigma = \sigma_0 + kT\Gamma_\infty \ln\left(1 - \frac{\Gamma}{\Gamma_\infty}\right) + \beta\Gamma^2$$

where β is the interaction parameter.

The Volmer (Eq. 3a+b) and van-der-Waals (Eq. 4a+b) model describe non-localized adsorption, with the assumption that molecules do not occupy a particular site and can freely diffuse in interfacial layer, where the latter takes molecular interactions into account (Kolev *et al.* 2002).

Volmer a) adsorption isotherm and b) equation of state

$$(3a) Kc_0 = \frac{\Gamma}{\Gamma_\infty - \Gamma} \exp\left(\frac{\Gamma}{\Gamma_\infty - \Gamma}\right)$$

$$(3b) \sigma = \sigma_0 + \frac{k_B T \Gamma_\infty \Gamma}{\Gamma_\infty - \Gamma}$$

Van der Waals a) adsorption isotherm and b) equation of state

$$(4a) Kc_0 = \frac{\Gamma}{\Gamma_\infty - \Gamma} \exp\left(\frac{\Gamma}{\Gamma_\infty - \Gamma} - \frac{2\beta\Gamma}{k_B T}\right)$$

$$(4b) \sigma = \sigma_0 + \frac{k_B T \Gamma_\infty \Gamma}{\Gamma_\infty - \Gamma} + \beta \Gamma^2$$

From the fitting of the interfacial tension data the area per molecule can be obtained. Combining the area per molecule with data on the molecular dimension, allows drawing conclusions on the orientation of the molecules at the interface.

In case of saponins, an interfacial area smaller than 0.75 nm² is related to the orientation of the molecules in the end-on/side-on configuration and over 0.75 nm² in the lay-on configuration (Pagureva *et al.* 2016). In the side-on configuration the aglycones of neighboring monodesmosidic saponin molecules are arranged parallel to each other in the hydrophobic phase and perpendicular to the interface (see Figure 5A). The end-on configuration is similar to the side-on configuration but describes the orientation of bidesmosidic saponins where one sugar residue is additionally facing into the hydrophobic phase besides the aglycone (see Figure 5B). Bidesmosidic saponins can also arrange in the lay-on configuration where both sugar chains are facing towards the water phase, leaving the aglycone orientated parallel to the interface (see Figure 5C).

Monodesmosidic saponins usually occupy an area of around 0.3 nm², which corresponds to the end-on configuration. Bidesmosidic triterpenoid saponins are more likely to arrange in a lay-on configuration, which corresponds to an interfacial area per molecule of 1 nm² (Stanimirova *et al.* 2011; Pagureva *et al.* 2016). However, it remains unclear if Quillaja saponins from different extracts always arrange in the lay-on configuration at the interface. In the past interfacial tension isotherms of various Quillaja saponin extracts were analyzed and data of 0.3 to 1 nm² for the area per molecule were reported by different research groups (Stanimirova *et al.* 2011; Kezwon and Wojciechowski 2014). The differences in area per molecule obtained at the air/water-interface were explained by the use of different Quillaja saponin extracts.

An exception is the extract from *Panax ginseng* (GS) with bidesmosidic saponins, which had an interfacial area per molecule of around 0.5 nm² (Pagureva *et al.* 2016). The end-on configuration observed for this bidesmosidic saponin may be justified because of the short sugar chains attached to the saponin, which make this configuration more advantageous. Steroidal saponins are often a mixture of mono- and bidesmosidic saponins and therefore interfacial area is between 0.3 and 1 nm² (Pagureva *et al.* 2016).

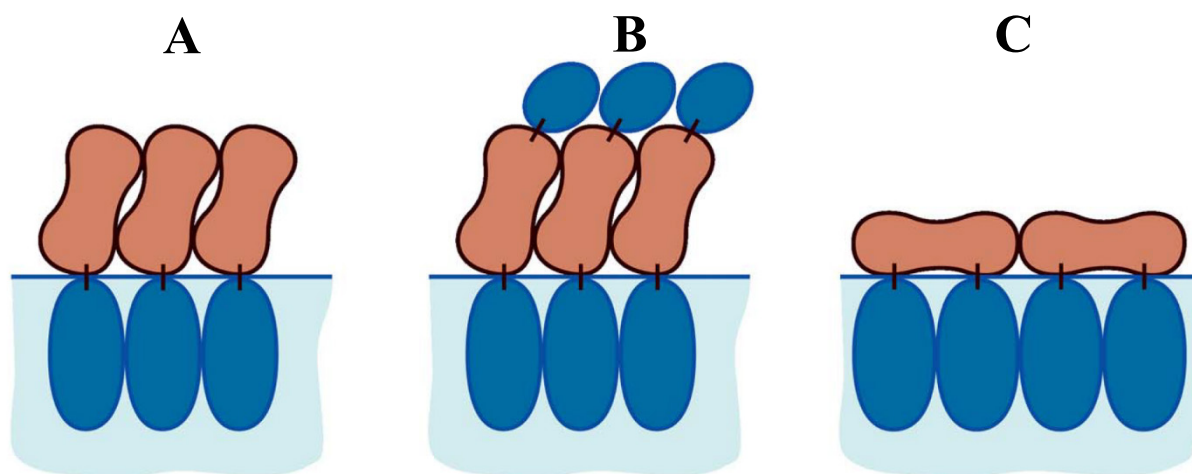


Figure 5 Interfacial configuration of saponins A) end-on configuration, B) side-on configuration and C) lay-on configuration. Blue parts of the schematic molecules indicate hydrophilic parts (sugar residues) and brown parts represent hydrophobic parts (aglycone). Adapted from Golemanov *et al.* 2013 with permission from The Royal Society of Chemistry.

In several studies (Pagureva *et al.* 2016; Golemanov *et al.* 2014; Golemanov *et al.* 2013) where 13 different saponins from different botanical origins were compared, a group of saponins with high dilational and shear viscoelastic properties was identified. This group consists of extracts from the plants *Camellia oleifera* Abel (TS), *Aesculus hippocastanum* (ESC), *Panax ginseng* (GS), *Sapindus mukurossi* (BSC) and *Quillaja saponaria* Molina (QS). All named saponins have an oleanane type aglycone but GS, which has a dammarane aglycone. Furthermore TS and ESC can be classified as monodesmosidic saponins and GS and QS as bidesmosidic saponins. BSC consists mainly of monodesmosidic saponins and a small portion of bidesmosidic saponins.

Pagureva *et al.* (2016) have shown using the van-der-Waals adsorption isotherm that some interfacial layers of monodesmosidic saponins (here: TS and ESC) and bidesmosidic saponin with short sugar chains (here: GS) can undergo phase transition, which means that the interaction parameter derived from the van der Waals isotherm is greater than 3.375. Phase transition was attributed on the one hand to strong hydrophobic interactions between aglycones and on the other hand on the hydrogen bonds between sugar residues. The observed phase transition seems to lead to high dilational and shear elasticity as well as high interfacial viscosity for these saponins (TS, ESC and GS). When subjecting the interfacial layers to increasing surface deformation a steep decline of the dilational elasticity was observed. Although the elastic modulus is still very high at increased amplitudes, it has to be

noted that intermolecular bonds of TS, ESC and GS are more fragile when dilational force is applied than for instance QS and BSC, which are less prone to reduction of dilational viscoelasticity imposed by surface deformation. High dilational and shear viscoelasticity is associated with intermolecular interactions (here: hydrogen bonds). The formation of hydrogen bonds was indirectly shown by the addition of the chaotropic reagent urea to an interfacial layer of TS. As a chaotropic agent, urea unlinks intermolecular hydrogen bonds thus, leading to a total loss of viscoelastic properties (Golemanov *et al.* 2014).

In contrast, until now all examined steroidal saponins (from *Yucca Schidigera*, *Tribulus terrestris* and *Trigonella foenum-graecum*) neither showed dilational nor shear elasticity or significant surface viscosity (Golemanov *et al.* 2013; Pagureva *et al.* 2016). It is supposed that interfacial layers are in a rather liquid condensed state with only weak intermolecular interactions.

The very small saponin glycyrrhizin from the root of *Glycyrrhiza glabra* was also not able to form a viscoelastic film at the air/water-interface, which was attributed to the low solubility because of only few hydrophilic sugar residues in the molecular structure (Golemanov *et al.* 2013). In addition, the amount of carboxylic groups is relatively high with respect to the size of the molecule in comparison to other saponins. The charged carboxylic groups may cause repulsion inside the interfacial layer and therefore prevent intermolecular interactions, which may lead to a viscoelastic film.

2.3.2. Supramolecular interfacial configuration of Quillaja saponins at the air/water-interface

Golemanov *et al.* (2012) analyzed the behavior (relaxation times) of a Quillaja saponin layer under shear and dilational stress and derived a reasonable model for the interfacial packaging of Quillaja saponin molecules. The authors hypothesized that molecules are packed in domains and strong intermolecular interactions exist between saponin molecules inside the domain as indicated by high dilational and shear moduli. Inside a domain, Quillaja saponin molecules orientate themselves similarly and exhibit strong intermolecular interactions (see Figure 6). At the boundaries of two neighboring domains weaker interactions and higher free energy occurs because boundary molecules of different domains may have divergent orientation.

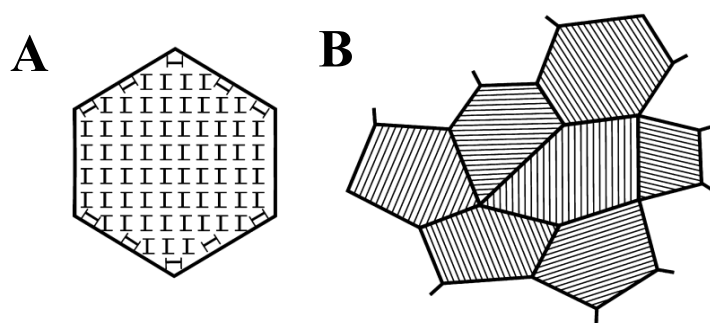


Figure 6 Supramolecular domain structure of Quillaja saponins at the air/water-interface. A) Inside a domain: Quillaja saponins (I) orientate themselves in the same direction, boundary molecules can have different orientations B) Neighboring domains can have different orientation of inside molecules. Adapted from Golemanov *et al.* 2012 with permission from The Royal Society of Chemistry.

When shear stress is applied Quillaja saponin molecules orientate in the direction of the applied stress and domain boundaries lengthen thereby increasing the energy of the interfacial layer (see Figure 7). Up to a certain level of shear stress the interfacial deformation is reversible and saponin molecules realign fast after the end of the shear stress (elastic response). When shear stress becomes too high, the domains laterally shift in the direction of shear stress, which is irreversible and results in a no longer elastic but viscous response. When the interfacial layer is subjected to expansion it is expected that the boundary region between the domains widen since these regions have relatively weak intermolecular bonds. Quillaja saponin molecules can diffuse from the subsurface to the widened boundary regions with subsequent re-orientation at the interface. Based on the differing interfacial configuration and interfacial rheology one has to assume that interfacial structure of Quillaja saponins is different from monodesmosidic saponins. Until now, there has been no proposed model on the supramolecular structure of monodesmosidic saponins.

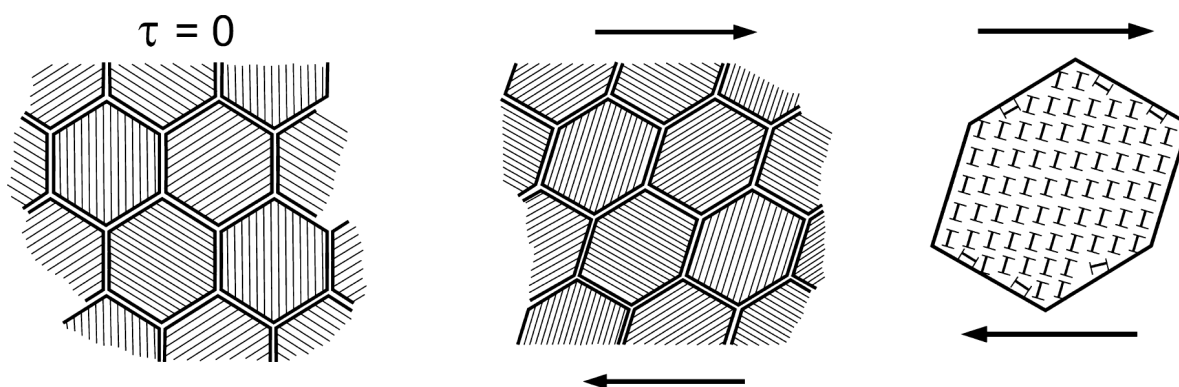


Figure 7 Elongation of the Quillaja saponin domains when shear stress is applied. Reproduced from Golemanov *et al.* 2012 with permission from The Royal Society of Chemistry.

2.3.3. Impact of the hydrophobic phase on interfacial properties of various saponins

Oil as a hydrophobic phase can influence interfacial properties by (1) penetrating between adsorbed surfactant molecules and (2) by solvation of surfactant molecules in the hydrophobic phase, thus reducing interfacial concentration and surface pressure. The first mechanism usually applies for tightly anchored surfactants and proteins that are non-soluble in the hydrophobic phase and the second mechanism for surfactants soluble in the hydrophobic phase like non-ionic low-molecular weight surfactants. The first mechanism applies for most saponins but for TS and BSC considerable solubility in the hydrophobic phase was reported. It is possible that solubility of TS and BSC in the hydrophobic phase additionally contributes to the reduction in viscoelasticity (Golemanov *et al.* 2014).

Triglycerides (tricaprylin and olive oil) tend to reduce dilational and shear viscoelasticity to a higher extend than linear alkanes (hexane or tetradecane). Golemanov *et al.* (2014) explained this with the bulky size of the triglyceride molecules and the tendency of their hydrophilic head groups to get in contact with the aqueous phase. As Figure 8 shows monodesmosidic saponins orientate differently at the interface in comparison to bidesmosidic saponins and are more affected by changes in the hydrophobic phase.

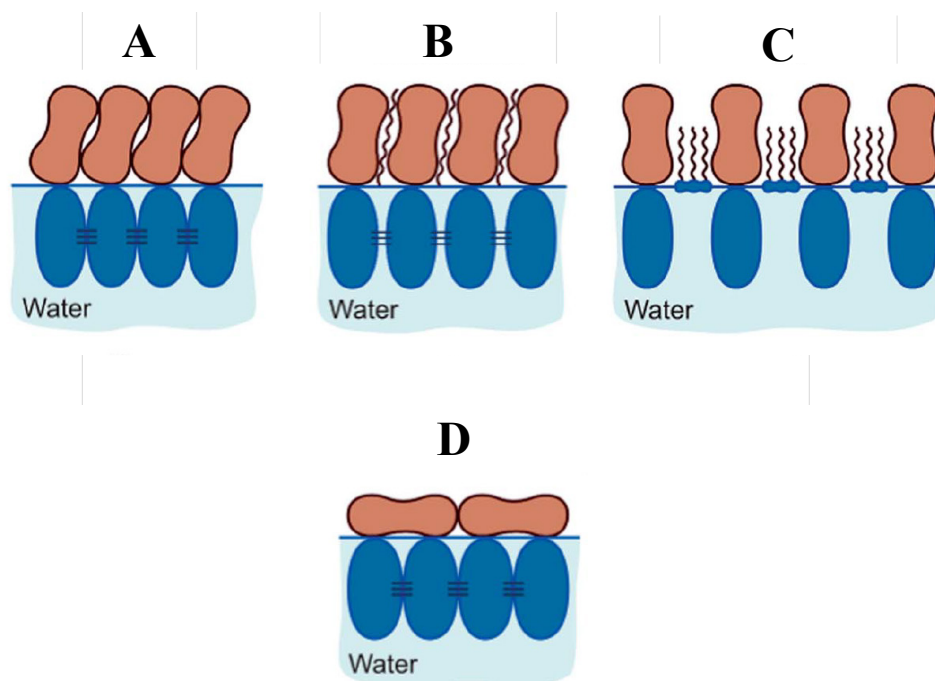


Figure 8 Orientation of monodesmosidic saponins at the (A) air (B) hexadecane (representing linear alkanes) and (C) Tricaprylin (representing triglycerides) as well as bidesmosidic saponins at (D) at different interfaces. Blue parts of the schematic molecules indicate hydrophilic parts (sugar residues), brown parts represent hydrophobic parts (aglycone) and dark blue lines show intermolecular hydrogen bonds. Adapted from Ref. (Golemanov *et al.* 2014) with permission from The Royal Society of Chemistry.

2.4. Interactions of saponins with other (food) components

Interactions of proteins and surfactants can result in deviating interfacial properties of mixtures (Lech *et al.* 2014; Mackie and Wilde 2005; Dan *et al.* 2013; Maldonado-Valderrama and Patino 2010). It is well known that low-molecular weight surfactants like SDS can interact with proteins (Pradines *et al.* 2009; Ulaganathan *et al.* 2012; Lech *et al.* 2014). As a food additive, interactions between Quillaja saponins and food proteins are relevant.

In the past, various studies examined the interactions of Quillaja saponin with food components like β -lactoglobulin (Kezwon and Wojciechowski 2014; Piotrowski *et al.* 2012), β -casein (Kezwon and Wojciechowski 2014; Wojciechowski *et al.* 2014b), lysozyme (Kezwon and Wojciechowski 2014; Wojciechowski *et al.* 2011) and gelatin (Sarnthein-Graf and La Mesa 2004).

Studying model Quillaja saponin/food components-systems is crucial in order to forecast interactions in real food products. Many publications determined protein-surfactant interactions, which is a topic far from trivial (Dan *et al.* 2013; Maldonado-Valderrama and Patino 2010; Krägel *et al.* 2008). Especially, protein-Quillaja saponin-systems are tremendously different from protein-surfactant-systems because of the unique interfacial properties of Quillaja saponins. To summarize previously mentioned studies, evidence for complex formation between Quillaja saponins and the random coil milk protein β -casein, globular protein β -lactoglobulin (β -LG) and hen egg lysozyme were found. It has to be noted that most assumptions on complex-formation were based on interfacial tension, interfacial rheology and fluorescence measurements.

By far most studies evaluated the interactions between QS and β -LG as well at the air/water (Piotrowski *et al.* 2012) and tetradecane/water-interface (Piotrowski *et al.* 2012). In contrast to β -LG, lysozyme is positively charged, which enables electrostatic attraction to Quillaja saponins. But, it has to be kept in mind that the negative charge of QS is only weak since only one carboxylic group is present in Quillaja saponins. In a different study on QS/gelatin interaction only minor interactions between QS and gelatin were found (Sarnthein-Graf and La Mesa 2004). In fact, in mixtures of QS/lysozyme adsorption rate in dynamic interfacial tension experiments at the air/water-interface increased compared to only QS. This increased adsorption rate was attributed to interfacial complex formation through electrostatic and hydrophobic interactions and additionally through sugar binding sites (Kezwon and Wojciechowski 2014).

When evaluating β -casein/QS interactions at various interfaces it has to be noted that β -casein is a random coil and not a globular protein like β -LG and lysozyme. As a consequence, no tertiary structures like a hydrophobic calyx are present in β -casein. At low QS/ β -casein concentrations, complex formation led to increased adsorption rate because the hydrophilic character was increased by electrostatic interaction of one or two QS molecules with the positively charged N-terminus of β -casein. At higher QS/ β -casein concentrations this effect was diminished and interfacial activity was reduced. This effect was attributed to additional QS molecules, which electrostatically interact with other positively charged parts of β -casein leading to reduced surface active properties. The described observations were valid for the air, tetradecane and olive-oil/water-interface (Wojciechowski *et al.* 2014b).

Another group focused their research on the miscibility of Quillaja in the presence of Na-caseinate, pea protein and different lecithins under heat and pH influence (Reichert *et al.* 2015; Reichert *et al.* 2016). As expected heat and pH affected miscibility in mixed systems tremendously. Mixtures of QS with Na-caseinate were miscible at pH 7 and different concentration ratios but when subjected to heat and reduction of the pH, sufficient aggregation was observed. Aggregation behavior because of pH reduction was on the one hand attributed to the self-aggregation of casein at the isoelectric point and due to electrostatic interactions at lower pH because of the opposite charge of both molecules. Aggregation of the QS/Na-caseinate mixture was associated with the behavior of each substance upon heating (turbidity increase of QS, phase transition of α s-casein or unfolding of β -casein) and possible hydrophobic interactions. It was further emphasized that impurities like phenols can also contribute to the aggregation behavior by forming protein-phenol-interactions.

The literature review showed that saponins are a diverse class of natural emulsifiers and that they may use to stabilize dispersed systems. In addition, the interaction between saponins and food proteins is highly relevant when applying saponins in food systems.

Manuscript I

Interfacial Properties of Saponin Extracts and Their Impact on Foam Characteristics

Food Biophysics, 2016, V. 11, No. 1, pp 91–100.

The final publication is available at Springer via <http://dx.doi.org/10.1007/s11483-015-9420-5>.

Authors

Sandra Böttcher^a

Stephan Drusch^a

^a Technische Universität Berlin, Institute for Food Technology and Food Chemistry
Department of Food Technology and Food Material Science
Königin-Luise-Str.22, 14195 Berlin

I-1 Abstract

Saponins from various botanical origins highly differ in molecular structure. Little is known of the influence of structural differences between the different saponins on interfacial tension, short-term adsorption and foam properties at the air-water interface (a/w). In this study five triterpenoid saponins, with three of these being monodesmosidic and two bidesmosidic as well as one steroid saponin, were analyzed. Interfacial tension isotherms were measured using a tensiometer with a Wilhelmy plate and were fitted using the modified Frumkin model. For characterization of the short-term adsorption at the a/w-interface, two-fluid needle experiments were performed. Foaming, foam stability and foam structure were analyzed using a foaming device. A new method for semi-quantitative analysis of different foam structures was established. In addition, the impact of pH and ionic strength (addition of NaCl) on interfacial tension and foam properties were determined. The short-term adsorption of all saponins was limited by an additional barrier and was not diffusion-limited. Extracts from *Quillaja saponaria* Molina (QS), *Gypsophila* (GYP), *Camellia oleifera* Abel (TS) and *Aesculus hippocastanum* (ESC) lowered the interfacial tension to 37-42 mN/m and produced stable foams. The steroid saponin from *Tribulus terrestris* (TT) and the monodesmosidic saponin from *Glycyrrhiza glabra* (GA) had only poor interfacial and foam properties. Foams made from QS and GYP were only little affected by changes in pH and ionic strength. A reduction of the pH from 5 to 3 increased stability of foams made from GA significantly. Foams made from ESC and TS were negatively affected by increasing ionic strength.

I-2 Introduction

Secondary plant metabolites like e.g. saponins are nowadays frequently standardized and used for nutritional or medical reasons in human nutrition. There has been an overwhelming amount of research on health related aspects of plant-derived food ingredients throughout the last two decades (Raskin *et al.* 2002; Schroeter *et al.* 2010; Pojer *et al.* 2013). In contrast scientific literature contributing to our understanding of plant extracts in foods and their technological functionality is scarce.

Saponins are a heterogenous amphiphilic class of substances, which consist of a hydrophobic aglycone and hydrophilic sugar residues. There are comprehensive studies on the distribution and structure of saponins in a variety of botanical sources (Haralampidis *et al.* 2002; Sparg *et al.* 2004; Vincken *et al.* 2007; Dinda *et al.* 2010). Numerous variations in the aglycone structure as well as the amount, type and location of the sugar residues are known until now. The quantitative determination of the various saponin types in a botanical extract remains a field of ongoing research, which requires specialized equipment, like LC-MS or HPTLC and which is limited by the availability of standard substances (Oleszek and Bialy 2006; Yao *et al.* 2008).

Due to the above mentioned structural properties of saponins from a technological point of view, research focused on the interfacial activity and their use in food applications (Kezwon and Wojciechowski 2014). The wide range of the botanical origin results in extracts with different saponin mixtures, which makes it challenging to identify structure-function relationships. Even saponin extracts from the same botanical origin may exhibit different interfacial properties (Mittra and Dungan 1997). Despite these aspects, the interest in saponins increases because saponins are natural surface active molecules and some saponin extracts exhibit a high interfacial activity. Saponins from the bark of *Quillaja saponaria* Molina are generally recognized as safe according to the USDA and they are approved for application in beverages in the EU as foam stabilizer.

Different studies analyzed basic aspects of the interfacial properties and orientation of the molecules of various *Quillaja* extracts at an interface (Stanimirova *et al.* 2011; Golemanov *et al.* 2012; Wojciechowski 2013). *Quillaja* saponins have a high molecular weight because of their fatty acyl and two sugar moieties, which influence the orientation/configuration (Golemanov *et al.* 2012). Recently, Yang *et al.* (2013) published data on the influence of temperature, pH change and ionic strength on the stability of emulsions containing *Quillaja* saponins. Apart from the research on *Quillaja* saponins, Golemanov *et*

al. (2013) published data on the surface elasticity and viscosity of 12 triterpenoid and steroid saponins. The authors observed a high elasticity and viscosity of the surface layers for triterpenoid saponins. In contrast, steroid saponins exhibited poor surface elasticity. With respect to food applications, only in a very limited number of studies specific aspects of the foam properties have been investigated (Chen *et al.* 2010; Wojciechowski *et al.* 2011; Piotrowski *et al.* 2012). To the best of our knowledge until now there has been no comprehensive approach on the characterization of saponin-based foams considering foaming, foam stability and foam structure for a range of saponin extracts from different botanical origin.

Aim of the present study was to collect data on the basic interfacial properties of saponin extracts from various botanical origins with their foam properties to contribute to our understanding how these parameters are interconnected. This study is a preliminary investigation, which requires more-in-depth mechanistic studies with chemically well-defined saponin extracts. To fulfill this aim the interfacial tension isotherms of saponin extracts were determined, fitted with the Frumkin model and the critical micelle concentration was calculated. For general characterization of the saponin extracts the foaming properties, interfacial tension and short-term adsorption at the air/water interface at pH 5 were determined. In a second step, the ionic properties of the saponins were determined and the influence of a pH reduction from 5 to 3 and increase of ionic strength from 0 mM to 100 and 500 mM on the foaming properties and interfacial tension was evaluated.

I-3 Materials and Methods

Six different saponin extracts were included in the present study based on their molecular structure, see Table I-1. The saponins comprised five triterpenoid and one steroidal saponin. Two of the triterpenoid saponins were bidesmosidic and the remaining three monodesmosidic. As indicated from the literature, saponins may additionally vary in molecular weight and the number of carboxylic groups.

Table I-1 Origin, purity and general chemical properties of the six saponin extracts

Botanical origin	Saponin	Abbreviation	Plant material	Saponin concentration* [%]	Aglycone	Sugar residues	Molecular weight [g/mol]
<i>Quillaja saponaria</i> Molina	Quillaja	QS	Bark	69.2	Triterpenoid	Bidesmosidic	1400-2300 ¹
Gypsophila	Gypsophila	GYP	n.s.	45.5**	Triterpenoid	Bidesmosidic	1400-1700 ²
<i>Camellia oleifera</i> Abel	Tea Saponin	TS	Seeds	95.3	Triterpenoid	Monodesmosidic	1200-1300 ³
<i>Aesculus hippocastanum</i>	Escin	ESC	n.s.	99.1	Triterpenoid	Monodesmosidic	1100 ⁴
<i>Glycyrrhiza glabra</i>	Glycyrrhizic Acid Ammonium Salt	GA	Root	95.1	Triterpenoid	Monodesmosidic	839
<i>Tribulus terrestris</i>	Tribulus terrestris	TT	Fruits	90.4	Steroid	Mono- and bidesmosidic	600-1100 ⁵

* calculated on dry matter, ** determined by vanillin-sulphuric acid assay, n.s.- not specified

¹ Bankefors *et al.* 2008; Thalhamer and Himmelsbach 2014

² Frechet *et al.* 1991; Chen *et al.* 2011; Yao *et al.* 2011; Voutquenne-Nazabadioko *et al.* 2013; Pertuit *et al.* 2014

³ Huang *et al.* 2007; Kuo *et al.* 2010; Zhang *et al.* 2012; Zhou *et al.* 2014

⁴ Wulff and Tschesche 1969

⁵ Dinchev *et al.* 2008

An extract from the bark of *Quillaja saponaria* Molina (QS) with a specified saponin content of 69.2 % (dry matter) was provided by Ingredion Germany GmbH (Hamburg, Germany). Gypsophila extract (GYP) was a kind gift of Dr. H. Schmittmann GmbH (Velbert, Germany). The saponin content as determined by the vanillin-sulphuric acid method amounted to 45.5 % (dry matter). A saponin extract from the seed of *Camellia oleifera* Abel (TS) with a saponin content of 95.1 % (dry matter) was provided by Changsha Nulant Chem. Co., Ltd. (Changsha City, Hunan, China). The extract of the fruits of *Tribulus terrestris* (TT) was kindly donated by Xi'An Union Pharmpro Co., Ltd (Xi'An, Shaanxi, China) and its saponin content was specified with 90.4 % (dry matter). Saponin-rich extract from *Aesculus hippocastanum* (ESC), 99.1 % (dry matter) and *Glycyrrhiza glabra* (GA), 95.1 % (dry matter) as well as the ionic surfactant sodium dodecyl sulfate (SDS), >99 %

were purchased from Sigma Aldrich Chemie GmbH (Steinheim, Germany). For all experiments mono-distilled water was used. Solutions made of GA were heated to 40°C to solve the surfactant. Vanillin (100 %), ethanol (99.5 %) and sulphuric acid (96 %) were purchased from Carl Roth GmbH & Co. KG (Karlsruhe, Germany).

No specific data on the quantitative composition of the saponin extracts were provided by the suppliers, but a range of literature dealing with the composition of the saponin fraction in different plants is available. In general, saponins of one botanical species only have slight differences in molecular structure. GA has a specific molecular structure and is not a mixture of various saponins. For QS, TT, TS and ESC the specific botanical origin is provided by the supplier, but not for GYP. A range of different studies identified common saponins in QS, TT, TS, ESC and GYP. General structural properties and the average molecular weight required to model the adsorption isotherms and to calculate the hydrodynamic radii were derived from the literature, see Table I-1.

I-3.1 Fourier transform infrared spectroscopy (FTIR)

For the analysis of the presence of different chemical bonds in the six different saponin extracts, the FTIR-spectra of all saponins were measured using a Bruker Tensor 27 (Bruker, Germany) with a diamond ATR. Prior to the measurements of the samples the instrument was calibrated against air. Spectra between 4000-400 cm^{-1} were obtained using 32 scans with a resolution of 4 cm^{-1} . Results were normalized to compare different spectra. A dried sample of the QS extract was used for the FTIR measurement. For the stretch of C-OH groups a broad peak around 3400 cm^{-1} occurs in the spectra. Peaks between 3200 and 2800 cm^{-1} represent the stretching of sp^2 and sp^3 -C-H bonds and C=C bonds can be identified at a wavenumber of around 1600 cm^{-1} . Most important in this study is the stretch of the carbonyl bonds (C=O) at 1730-1700 cm^{-1} . If there is no peak in this region, it can be concluded that no carboxylic groups are present in the saponin extract.

I-3.2 Conductivity measurements

To determine the ionic character of the different saponin extracts, a dilution test was conducted. The conductivity was measured with the Seven Easy by Mettler Toledo and an InLab 731 electrode. An aliquot of the diluted saponin extract was stirred and the conductivity was measured. Then a part of the sampled was removed and replaced with distilled water. Again the conductivity was recorded and the relation between conductivity and concentration was plotted. All dilution steps were equidistant. The dilution test is an option for fast determination of the CMC of ionic surfactants (Khan and Shah 2008). In solutions of non-ionic surfactants there is a linear dependency between the conductivity and the concentration of a substance. In contrast, in ionic extracts there is a breaking point at the CMC ($=\text{CMC}_{\text{cond}}$) with the slope of the curve being more flat above the CMC and more steep below the CMC. Above the breaking point the charged parts of the molecule are shielded because of micelle formation.

I-3.3 Interfacial tension measurements using Wilhelmy plate

The interfacial tension of the six different extracts was determined using a K11 tensiometer equipped with a Wilhelmy plate (KRÜSS GmbH, Hamburg, Germany). An aliquot of 80 mL of the diluted extracts was equilibrated to $20 \pm 1^\circ\text{C}$ and placed into the measurement glass vessel. Prior to the analysis the Wilhelmy plate was thoroughly rinsed with distilled water and acetone. Then the plate was heated above a lab burner to remove possible contaminants. The plate was cooled down and then again rinsed with distilled water. Finally the plate was wetted with the diluted extract for two times and then immersed with a speed of 100 mm/min into the solution before it reached its final position at the interface. The interfacial tension was measured for a period of 400 s. The vessel was equipped with a jacket to ensure a constant temperature throughout the measurement. Air circulation was eliminated by a plastic shield.

To determine the critical micelle concentration (CMC) a series of different concentrations of the extracts ranging from 0.0001 to 2 %wt were analyzed. The CMC was obtained by calculating the intersection between the flat curve above and the steep curve below the break in the interfacial tension isotherm. The interfacial tension isotherms were fitted with the modified Frumkin model using the Software “IsoFit”.

The following two equations describe the equation of state (Eq.I-1) and adsorption isotherm (Eq.I-2) of the modified Frumkin model:

$$-\frac{\pi\omega}{RT} = \ln(1 - \theta) + a\theta^2 \quad (\text{I-1})$$

$$bc = \frac{\theta}{1-\theta} \exp(-2a\theta) \quad (\text{I-2})$$

where Π is the surface pressure, ω the molar surface area, R the general gas constant, T the absolute temperature, θ the surface coverage, a the interaction parameter, b the adsorption equilibrium constant and c the bulk concentration. The Frumkin model assumes a monolayer of the surfactant at the interface and extends the Langmuir model by considering interactions between the molecules. In addition, the modified Frumkin model takes compressibility ε of the monolayer because of increasing surface pressure into account: $\omega = \omega_0(1 - \varepsilon\Pi)$. This changes ω into a dependent parameter. The parameter ω_0 is the molar area at $\Pi=0$.

I-3.4 Short-term adsorption of saponin extracts on the air-water interface

For experiments on short-term adsorption the drop shape analysis system OCA-20 (DataPhysics Instruments GmbH, Filderstadt, Germany) was used as described by Tamm *et al.* (2012). Briefly, a two-fluid needle composed of a large needle ($d=1.65$ mm) and a smaller needle ($d=0.51$ mm), which was placed inside the large needle, was used for droplet generation. Through the outer channel (large needle) a droplet of distilled water with a volume of 12 μL was generated manually. An aliquot of 3 μL of the saponin solution was dosed with the automatic dosing unit through the small needle inside the water droplet. A CCD camera recorded a high speed video with 200 fps of the drop shape for a maximum of 20 s. Interfacial tension was calculated from the shape of the droplet and based on these data the lag-time, surface pressure after 5 s after the start of the adsorption Π_{5s} and the experimental diffusion coefficient D_{exp} were derived. The lag-time is defined as the time period after the droplet volume is expanded by 1 % until an absolute change of >2.0 mN/m of the interfacial tension and describes the speed of a molecule to reach the blank surface. This speed depends on the generated current inside the molecule because of the injection, as well on diffusion based on concentration gradients.

The short-term approximation ($t \rightarrow 0$) for the Ward-Tordai equation (Ward and Tordai 1946) combined with the Henry Equation (Eq. I-3) was used to calculate D_{exp} :

$$\frac{d\sigma}{dt^{1/2}} = -2RT \cdot c_0 \sqrt{\frac{D_{exp}}{\pi}}, t \rightarrow 0 \quad (I-3)$$

where σ is the interfacial tension, t is the time and c_0 the concentration of the saponin in the bulk solution. For theoretical values for D_{calc} the maximum length of each molecule was estimated using bond lengths and angles. The maximum length of each molecule was defined as the diameter ($2r$) of a spherical shape although the saponins have a smaller width and height. The Stokes-Einstein Equation (Eq. I-4) was used to calculate the theoretical diffusion coefficient D_{calc} :

$$D_{calc} = \frac{k_B \cdot T}{6\pi \cdot \eta \cdot r} \quad (I-4)$$

where k_B is the Boltzmann constant, η is the dynamic viscosity and r is the hydrodynamic radius of the spherical molecule. The values for D_{exp} were compared to theoretical values D_{calc} . If experimental values for the diffusion coefficient are smaller than the calculated values, the adsorption is not diffusion limited but controlled by a further adsorption barrier.

I-3.5 Foaming and foam stability

To analyze the foaming properties of the saponin extracts a commercially available foaming device DFA 100 was used (KRÜSS GmbH, Hamburg, Germany) (Lunkenheimer *et al.* 2010). Instead of using an absolute concentration, which would neglect differences in the interfacial activity, a multiple of the CMC of the individual extracts was chosen for the experiments (0.5 and 2-fold). Following parameters were fixed in all experiments: A volume of 50 mL of the saponin solution was poured in a glass column with a diameter of 40 mm equipped with a porous glass frit with a pore size of 40-100 μm (FL 4502). Pressurized air was purged through the frit at a rate of 0.15 L/min and foaming was stopped at a total height of 180 mm (sum of liquid and foam). Foam generation and stability was monitored for 3600 s and the height of the foam and the remaining liquid as well as a brightness profile were measured and recorded by transmissibility measurement with a frame rate of 2/s. In addition, every 10 min an image of the foam was taken. To minimize external influences on the brightness profile and image all experiments were carried out under exclusion of light. In-between individual measurements the device was thoroughly rinsed with distilled water. All experiments were carried out at least in duplicate.

For comprehensive foam characterization multiple parameters were evaluated, see Figure A-2. Foaming was characterized by the foaming speed k_f from the start of the foaming until the maximum foam height (f-max). The remaining foam height f_n at time point n characterizes the percentaged amount of foam still present in relation to f-max. Small f_n values indicate high foam decay. The parameters foam density $f_{Den,n}$ and foam density at f-max $f_{Den,f-max}$ describe the percentage of incorporated liquid in the foam. The drainage is defined as the percentage of liquid draining from the foam in relation to the liquid height at the f-max. In dense foams the variation as determined from fivefold replicates, for all parameters calculated without the liquid height as a variable (like foam stability and foaming parameters) was below 3 % and about 15-20 % for parameters, which were calculated from the liquid height (like drainage and foam density). In less dense foams the variation for all parameters calculated without liquid height was between 5-12 % and about 30-40 % for parameters derived from the liquid height.

I-3.6 Determination of foam structure with analysis of brightness profiles and foam pictures

In order to characterize the foams in more detail and to overcome the high variation in parameters based on liquid height detection, a new method was established. Therefore, the brightness profile generated by the foaming device was analyzed, see Figure A-3. The brightness profile records the average transmissibility of the foam and liquid. Each pixel on the vertical axis displays the average transmissibility at a certain height of measurement and each pixel on the horizontal axis represents the average transmissibility at a specific time point. At different time points the brightness distribution within the foam in the column was measured in an area of 1 px width, which corresponds to a specific time point, using Adobe Photoshop CS6 Extended. The brightness distribution ranges from 0-255. 0 represents black and 255 represents white. In this study, data points between 0 and 253 were used to eliminate the background color. From the brightness distribution the median ($BD_{m,n}$) as well as the width ($BD_{w,n}$) between the d_{10} (10 % of the brightness values are beneath this value) and d_{90} were calculated for individual time points n . The higher the BD_m is, the more light is transmitted through the foam indicating that the foam is less dense. An increase of BD_w indicates that the foam structure is less homogeneous.

I-4 Results and discussion

I-4.1 CMC determination and fitting of interfacial tension isotherms using the modified Frumkin model

QS, GYP, ESC and GA showed a low CMC ranging from 0.008 to 0.015 wt%, see Table I-5. In contrast, high CMC values were analyzed for TS and TT with 0.5 %wt and 0.1 %wt, respectively. QS is well known for its low CMC, previous studies reported varying CMC values of 0.025 wt% (Stanimirova *et al.* 2011), 0.013 and 0.198 g/L (Wojciechowski 2013) and 0.5-0.7 g/L (Mitra and Dungan 1997). The differences were explained by the purity and variation in the saponin composition. There is no literature on the surface activity of *Gypsophila* saponins available, but studies on the molecular structure show that QS and GYP consist of a similar aglycone structure (see Table I-1). The CMC for ESC is in good agreement with Golemanov *et al.* (2013), who used an extract from the same supplier, botanical origin and purity. In contrast, Golemanov *et al.* (2013) reported lower CMC values for TS and TT of 0.017 wt% and 0.048 wt%, respectively. The difference can be explained by the botanical origin. Although extracts were obtained from the same plant, Golemanov

et al. (2013) used extracts from other parts of the plants, which may result in a different saponin composition and therefore different CMC values.

Table I-2 Fitting parameters of the experimental data using the Frumkin model

	Average MW*	ω_0 [10 ⁵ m ² /mol]	<i>a</i>	<i>A</i> [nm ²]	target	<i>b</i> [m ³ /mol]
QS	1850	2.6	1.5	0.43	0.23	7.8E+02
GYP	1550	4.7	2.0	0.77	0.14	5.1E+04
TS	1250	2.8	-1.2	0.47	0.37	3.2E+04
ESC	1100	3.5	0.3	0.58	0.17	4.6E+04
GA	839	3.5	1.5	0.58	0.10	2.5E+03
TT	850	4.0	-2.1	0.66	0.40	3.5E+04

* based on literature review in Table I-1

In Table I-2 the fitting parameter of the interfacial adsorption isotherms for the six saponins are displayed. The calculated molecular area *A*, derived from ω_0 , of the different saponins at the interface ranged from 0.43 to 0.77 nm² for QS and GYP, respectively. Although QS consists of saponins with the highest molecular weight, the packaging is more dense compared to all other saponins. For QS the determined area per molecule *A* is in agreement with previous studies, which reported 0.30 nm² and 1 nm² for other QS extracts (Stanimirova *et al.* 2011; Wojciechowski *et al.* 2011). The parameter ϵ was for saponin extracts below 0.005 m/mN, thus the surface coverage θ of the saponin interfaces does not depend on the surface pressure Π . For the interaction parameter *a* the saponins TS and TT have a negative value and QS, GYP and GA a positive value. In the literature there are different interpretations of the interaction parameter *a*. Some authors interpret a positive value as a sign for attraction between the molecules and a negative value as a sign for repulsion (Kolev *et al.* 2002; Karakashev *et al.* 2004). However, Fainerman *et al.* (1998) clarified that the interaction parameter is rather a modeling parameter and cannot be interpreted in that way.

I-4.2 Short-term adsorption using two-fluid needle experiments

Interfacial tension as determined by the Wilhelmy plate characterizes the interface in a quasi-static state. Kinetics of interfacial adsorption can be determined by dynamic interfacial tension measurement. However, in the classical approach in a pendant drop tensiometer, the interface is already partly covered by adsorbed molecules at the time a sufficiently high droplet volume is generated to start the calculation (Rodriguez *et al.* 2005). Tamm *et al.* (2012) recently described a two-fluid needle system to investigate the

adsorption behaviour of proteins at the interface, in which a protein solution is injected into an existing droplet of water. Thus, the two-fluid needle experiments give more insight on the short-term adsorption characteristics, which may be correlated to the foaming process. The lag-time and the diffusion coefficient can be derived from the development of the surface pressure after the injection of saponins (see Figure I-1 and Table I-3). TT, GA and TS occupied the interface very fast with lag-times of 0.6 s, 1.7 s and 2.9 s, respectively. In contrast, QS had a long lag-time of 12.4 s, which is at least two times higher compared to all other saponins. The differences in the varying lag-time may be explained by the different molecular weights of the saponins. Although no detailed information on the composition of the extracts were available in the present study, general data on the molecular weight can be derived from the literature (see Table I-1). QS and GYP contain saponins with high molecular weight of 1300-2300 g/mol. TS and ESC contain saponins with an intermediate molecular weight (~ 1200 g/mol) and GA contains a saponin with a molecular weight of 839 g/mol. TT extract has a high and low molecular fraction with 1100 g/mol and 600 g/mol, respectively. Saponins with a high molecular weight may need more time to reach the interface in comparison to saponins with low molecular weight.

Table I-3 Short- and midterm adsorption parameters of six saponin extracts at twofold CMC pH 5

	Lag time [s]	Π_{5s} [mN/m]	σ_{1800s} [mN/m]	Π_{5s}/Π_{1800s} [%]	r [nm]	D_{calc} [m ² /s]	D_{exp} [m ² /s]
QS	12.4 \pm 1.5	15.4 \pm 0.7	38.2 \pm 0.7	47.8 \pm 2.1	1.5	1.41E-10	2.5E-11 \pm 0.9E-11
GYP	6.1 \pm 0.5	15.0 \pm 0.9	40.4 \pm 0.7	50.9 \pm 3.8	1.3	1.61E-10	5.8E-11 \pm 1.5E-11
TS	2.9 \pm 1.5	23.1 \pm 0.8	37.0 \pm 1.0	67.8 \pm 2.0	1.9	1.11E-10	1.1E-11 \pm 0.2E-11
ESC	6.0 \pm 0.8	18.4 \pm 0.3	42.0 \pm 1.4	60.2 \pm 1.9	1.7	1.23E-10	3.4E-11 \pm 1.3E-11
GA	1.7 \pm 0.8	9.6 \pm 1.2	61.3 \pm 0.3	69.1 \pm 7.7	1.3	1.59E-10	1.0E-12 \pm 0.3E-12
TT	0.6 \pm 0.2	15.7 \pm 0.5	51.8 \pm 1.9	76.7 \pm 2.3	2.0	1.08E-10	5.4E-15 \pm 2.0E-15

In addition, it is interesting to compare the surface pressure 5 s after the start of its increase in relation to the surface pressure after 1800 s (Π_{5s}/Π_{1800s} , Table I-3). At a high ratio, the equilibrium interfacial tension is reached very fast. In contrast, a low ratio indicates that rearrangements at the interface slow down the incorporation of additional surfactant molecules and more time is required to reach equilibrium interfacial tension. 5 s after the start of the increase of the surface pressure the monodesmosidic saponins TS, ESC, TT and GA reached at minimum 60 % of the equilibrium value. In contrast, the bidesmosidic saponins QS and GYP reached less than 50 % of the equilibrium value, indicating that it takes longer for the bidesmosidic saponins to arrange at the interface because the additional sugar residue negatively affects the kinetics of the adsorption at the interface.

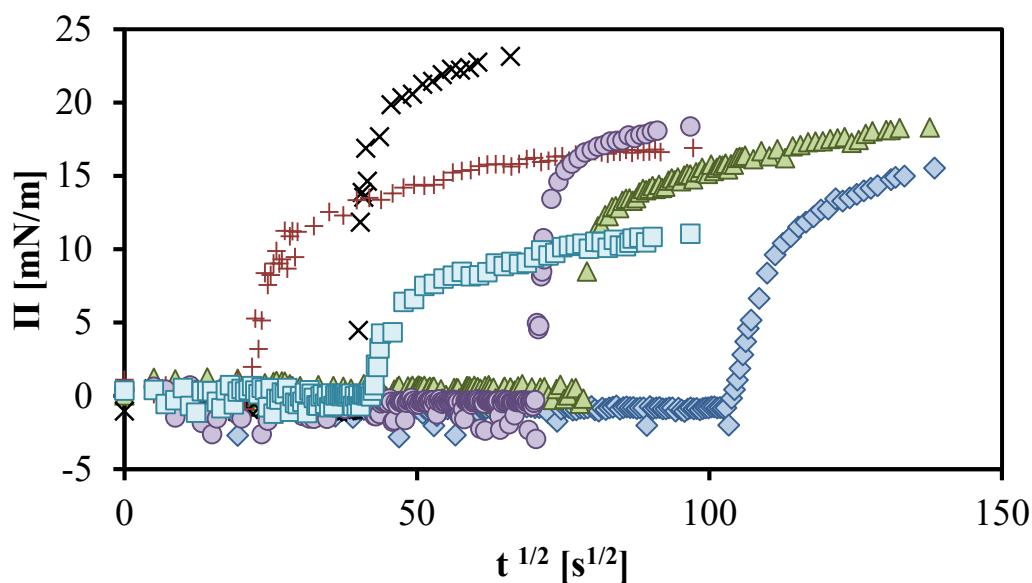


Figure I-1 Surface pressure Π versus square root of the drop age $t^{1/2}$ at the air/water interface of QS (◆), GYP (▲), TS (×), ESC (●), GA (■) and TT (+) from different botanical origins at pH 5, twofold CMC

A theoretical value for the diffusion coefficient from the subsurface to the surface of all six saponins was calculated based on the estimated maximum length of the molecules. Table I-3 shows that the roughly estimated radii of the different spherical shapes ranged from 1.3 to 2.0 nm resulting in calculated diffusion coefficients D_{calc} between $1.11\text{E-}11 \text{ m}^2/\text{s}$ and $1.61\text{E-}11 \text{ m}^2/\text{s}$. These coefficients imply a rather similar adsorption behavior for the saponin extracts. All experimentally derived diffusion coefficients were lower than the calculated values indicating that the diffusion at a short-term scale is not only diffusion-limited but an additional adsorption barrier exists. The difference between D_{calc} and D_{exp} was smallest for GYP and highest for GA and TT. The presence of an additional adsorption-barrier was reported for QS extracts before (Wojciechowski *et al.* 2011).

I-4.3 Foaming, foam stability and foam structure

As expected, with respect to formation of the foams the saponins with a high diffusion coefficient (QS, GYP, TS and ESC) had a high foaming speed k_f and immobilized larger amounts of liquid indicated by $f_{\text{den},f\text{-max}}$ (see Table I-4). TT was not foamable at twofold CMC and was not considered in all further experiments. GYP had the highest foaming speed with 1.81 mm/s, see Figure I-2A, but in general the foaming speed was in a similar range for all samples. However, the resulting foam structure was very different for GA compared with all other foams (Figure I-2C). In Figure I-2B, it can be seen that the saponins TS, GYP, QS and ESC incorporated 10 to 12 % of liquid. GA only incorporated 6.8 % of liquid. The difference in foam structure was also reflected in the data on transmissibility ($BD_{m,80s}$), see Table I-4. QS, GYP, TS and ESC all had similar values for transmissibility and a low value for $BD_{w,80s}$ at the end of foaming, which indicates a homogeneous and dense bubble distribution.

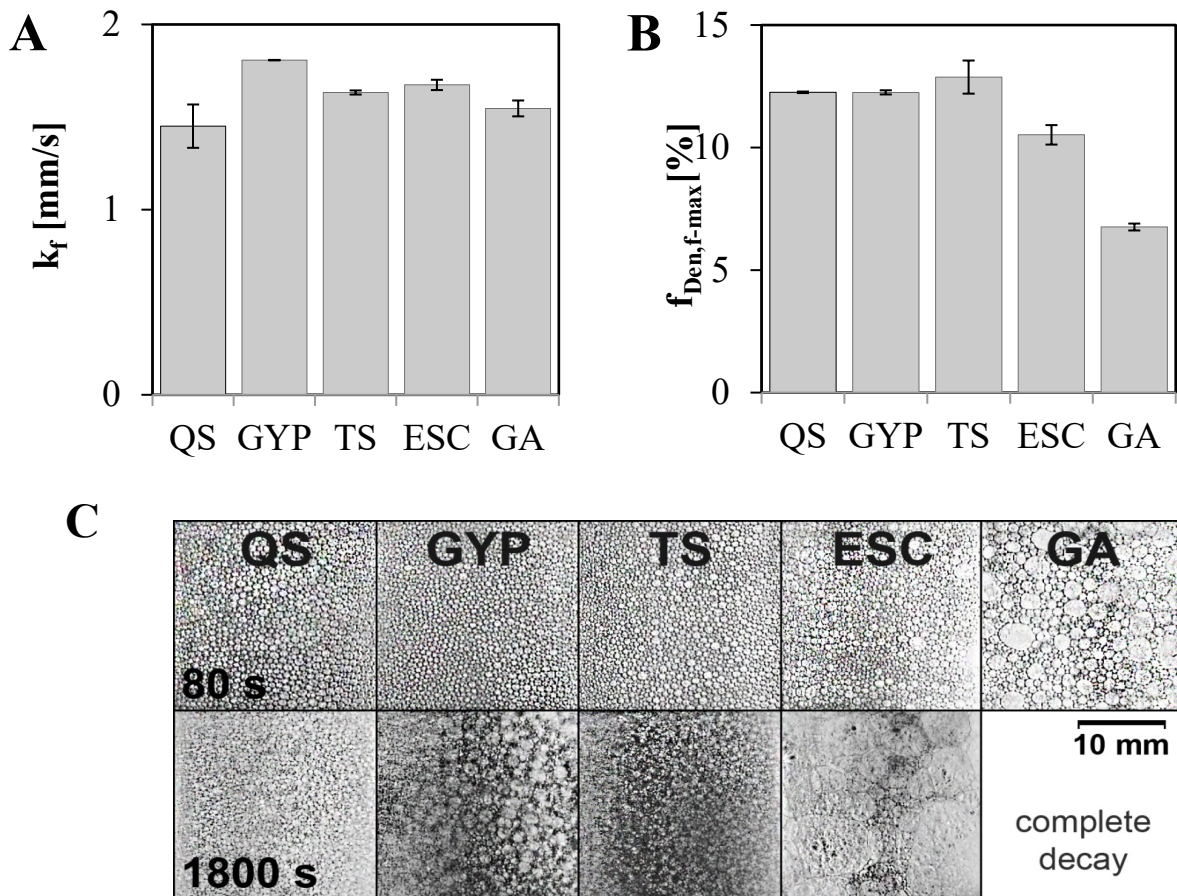


Figure I-2 Foam characterization with the parameters a) foaming speed (k_f) and b) foam density at $f\text{-max}$ ($f_{\text{Den},f\text{-max}}$) and (c) foaming pictures after 80 and 1800 s of foaming of QS, GYP, TS, ESC and GA at twofold CMC

In terms of foam stability, foams made from QS, GYP, TS and ESC were more stable and dense than foams made from GA. Foams made from QS, GYP and TS were most stable and after 3600 s over 85 % of the initial foaming height was still present. Foam stability of an extract of *Camellia oleifera* (here TS) was compared to the conventional foaming agents Tween 80 and SLS by Chen *et al.* (2011). Foams made from ESC were also stable, but only 77.2 % of the initial foam height was present after 3600 s, see Table I-4. A possible explanation is the more heterogenic bubble distribution of ESC foams at the beginning of the experiment compared to QS, GYP and TS based foams, see Figure I-2C.

In ESC-based foams, therefore in addition to coalescence, disproportionation occurred over time, where large bubbles grow and small bubbles disappear by diffusion of dissolved gas through the foam films. The comparison of foam density values does not show any differences though the foams vary tremendously, see Table I-4. The differences in homogeneity of the foam were visible when comparing the values for BD_w throughout the measurement, see Table I-4. The BD_w values of foams made from ESC increased from 20.0 at 80 s up to 124.5 at 3600 s. In comparison: the BD_w values of foams made from GYP only increased from 20.5 at 80 s to 34 at 3600 s. These factors account for the higher foam decay observed for ESC. The difference in homogeneity can only be quantified in the current experimental setup, when analyzing the brightness distribution.

Table I-4 Results from foam experiments of QS, GYP, TS, ESC and GA at twofold CMC, pH 5

	Parameter	QS	GYP	TS	ESC	GA
Foam stability	f_{1800s} [%]	94.2 ± 0.4	93.1 ± 0.8	92.8 ± 0.1	89.9 ± 0.5	0.0 ± 0.0
	f_{3600s} [%]	93.9 ± 0.2	92.6 ± 0.7	86.4 ± 0.1	77.2 ± 2.5	0.0 ± 0.0
Foam structure	$BD_{m,80s}$ [-]	62.5 ± 0.7	60.0 ± 0.0	61.5 ± 0.7	59.0 ± 0.0	58.0 ± 0.0
	$BD_{m,1800s}$ [-]	70.5 ± 2.1	68.5 ± 0.7	66.5 ± 0.7	77.0 ± 2.8	136.0 ± 53
	$BD_{m,3600s}$ [-]	73.0 ± 4.2	71.0 ± 1.4	68.5 ± 0.7	99.0 ± 2.8	0.0 ± 0.0
	$BD_{w,80s}$ [-]	20.5 ± 0.7	20.5 ± 0.7	21.0 ± 0.0	20.0 ± 0.0	20.0 ± 1.4
	$BD_{w,1800s}$ [-]	30.5 ± 0.7	28.5 ± 0.7	26.5 ± 0.7	37.5 ± 9.2	151.0 ± 1.4
	$BD_{w,3600s}$ [-]	35.5 ± 3.5	34.0 ± 0.0	32.5 ± 0.7	124.5 ± 16	0.0 ± 0.0
	$f_{den,f-max}$ [%]	12.3 ± 0.0	12.3 ± 0.1	12.9 ± 0.7	10.5 ± 0.4	6.8 ± 0.1
	$f_{den,1800s}$ [%]	6.4 ± 0.1	5.7 ± 0.1	6.0 ± 0.7	5.9 ± 0.5	43.8 ± 5.0
	$f_{den,3600s}$ [%]	6.3 ± 0.2	5.6 ± 0.2	6.2 ± 0.7	6.5 ± 0.3	0.0 ± 0.0

Foams made from GA fully collapsed in less than 20 min. The low foam stability of foams made from GA can be explained by the low ability of GA to reduce the interfacial tension, the small amount of incorporated liquid inside the foam and the poor solubility due to the small hydrophilic part in the molecule.

It is tempting to draw conclusions from the two-fluid needle-experiments on the short term adsorption and the foaming experiments of the different saponin extracts. In both experiments an empty surface is occupied by a surfactant. The two-fluid needle experiment is a rather static experiment. In contrast, foaming is a dynamic process with foam development and simultaneous foam decay. In addition, wall adhesion and gravitational forces affect the results of the foaming experiments. These differences have to be kept in mind when comparing the two-fluid needle experiments with the foaming experiments. Tamm *et al.* (2012) found a high correlation between the slope of the $\Pi/t^{0.5}$ -graph and the foam weight for different degrees of hydrolysis and concentrations of whey proteins, but for complex mixtures like the saponin extracts in the present study no clear correlation was found. However, the calculated diffusion coefficient derived from the two-fluid needle experiments, were in line with the foaming results.

I-4.4 Influence of pH and salt on interfacial tension and foam properties

After basic characterization of the interfacial tension behavior and foam properties of the six saponin extracts, it is important to analyze the behavior under different environmental conditions like pH reduction and addition of NaCl. One important question we had to answer in this context is, whether the saponins with a limited number of carboxylic groups behave like an ionic or non-ionic surfactant. The main advantage of non-ionic surfactants is their insensitivity to changes in ionic strength, because there are no dissociable groups inside the molecule. In the past there have been several approaches to determine whether saponin extracts behave more like ionic or non-ionic surfactants, but results have been contradictory (Wojciechowski 2013).

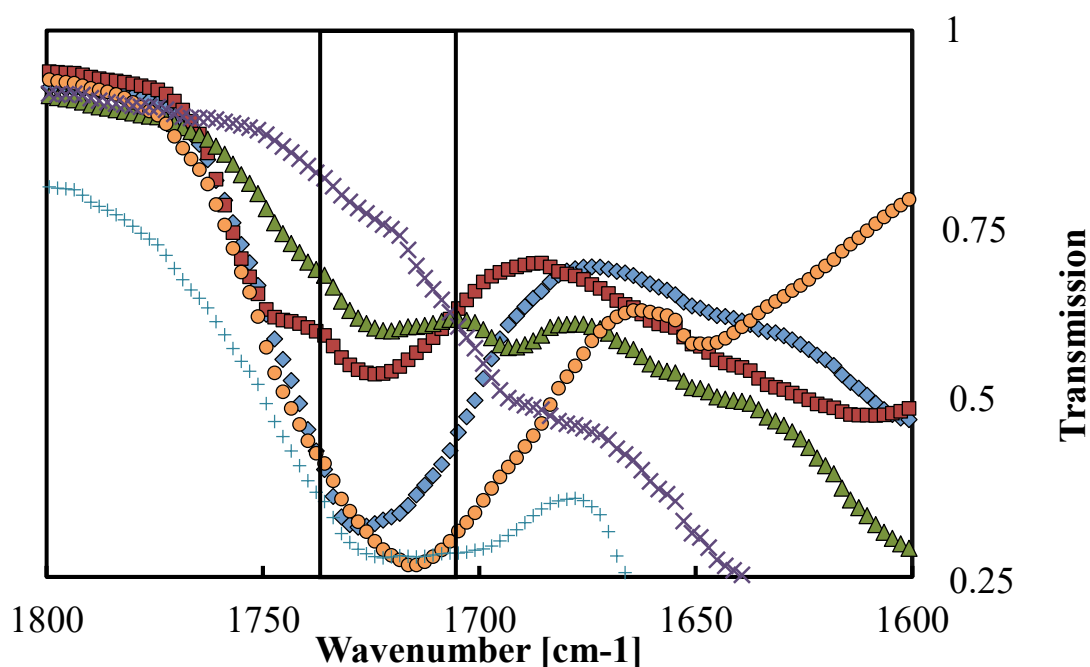
In the present study for the saponins QS, GYP, ESC and GA a breaking point was detected and therefore these extracts were classified as ionic surfactants, see Table I-5. The derived CMC values (CMC_{cond}) ranged between 0.011 and 0.023 %wt and were higher than the determined CMC values from interfacial tension measurements. For TS and TT there was no breaking point detectable.

Table I-5 CMC_{cond}, CMC_{SFT}, slope below (k_{below}), slope above (k_{above}) the CMC and ratio of both ($k_{\text{below}}/k_{\text{above}}$) for QS, GYP, ESC and GA; for TS and TT no breaking point was detected

	CMC _{SFT} [%wt]	CMC _{cond} [%w/v]	k_{below}	k_{above}	$k_{\text{below}}/k_{\text{above}}$
QS	0.008	0.012	2537	1905	1.3
GYP	0.014	0.011	2900	2582	1.1
TS	0.050	/	527	/	/
ESC	0.009	0.022	151	69	2.2
GA	0.015	0.023	2123	735	2.9
TT	0.106	/	2534	/	/
SDS	0.27*	0.24	1780	898	2.0

*%w/v (Khan and Shah 2008)

TS is described in the literature to behave like a non-ionic surfactant, although the literature on molecular structure reported several molecules in TS extracts with a carboxylic group (Feng *et al.* 2015), see references in Table 1. The literature on the structure of TT did not report a COOH-group in the different molecules. To confirm the absence of carboxylic groups in the extracts, FTIR spectra were recorded and analyzed concerning C=O-bonds. For both extracts no peak in the C=O binding region in the FTIR spectra was detectable, see Figure I-3.

**Figure I-3** FTIR spectra of C=O binding region (1718-1731 cm⁻¹) of QS (◆), GYP (■), TS (▲), ESC (●), GA (+) and TT (x)

The change in pH from pH 5 to 3 and the addition of NaCl decreased the interfacial tension of solutions made from QS, ESC and GA at 0.5-fold CMC, see Figure I-3. The interfacial tension of solutions made from GYP, TS and TT were less affected by the different environmental conditions. GYP was prior classified as an ionic surfactant for which the interfacial tension should be affected by changes in pH and ionic strength. But GYP had a much lower peak in the C=O region of about 1730 cm^{-1} in the FTIR spectra than QS, ESC and GA, which indicated a lower number of carbonyl or carboxylic groups inside the extract. FTIR-spectra with distinct peaks at around 1730 cm^{-1} were reported for different QS extracts by Almutairi and Ali (2015). It can be speculated that only a small amount of carboxylic groups is present in GYP and the peak in the C=O region is mainly due to carbonyl groups, see Figure I-3.

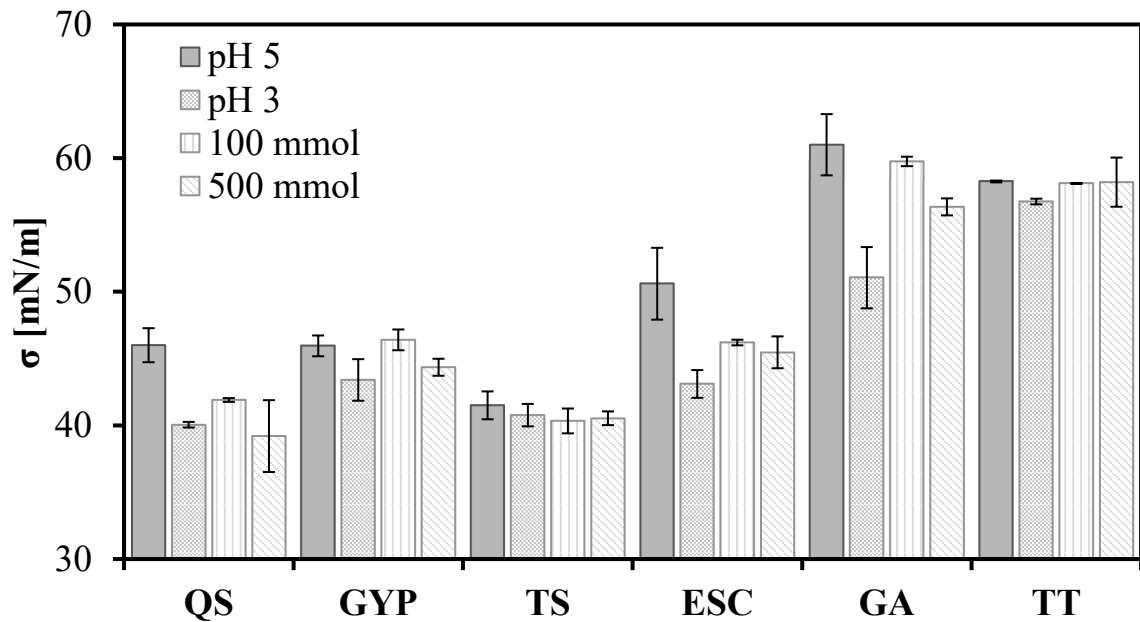


Figure I-4 Influence of pH and ionic strength on interfacial tension σ at 0.5-fold CMC

The influence of a change in pH and ionic strength were different when comparing foam results (see Figure I-4). To evaluate foam destabilization and foam stabilization all experiments were performed at a saponin concentration of 0.5-fold CMC. A low concentration of saponin was chosen to determine not only negative effects like fast foam destruction but also positive effects like foam stabilization. At higher concentrations, like twofold CMC, some foams were extremely stable and a positive effect would not be detectable. The values at pH 5 for foam decay after 3600 s (f_{3600s}), foaming speed (k_f) and the parameters describing foam structure ($BD_{m,600s}$; $BD_{w,600s}$ and $f_{den-fmax}$) were taken as reference value and set as 1. The values of the foam parameters at pH 3, 100 mM and 500 mM were calculated in

relation to the values obtained at pH 5, see Figure I-5. Foams made of QS were more stable at pH 3 and increased ionic strength but the foams were less dense and more heterogenic in structure. Foams made from GYP were less stable, less dense and more heterogenic under the same conditions. But the influence of the environmental conditions on the foam properties of QS and GYP were very small compared to foams made from TS, ESC and GA.

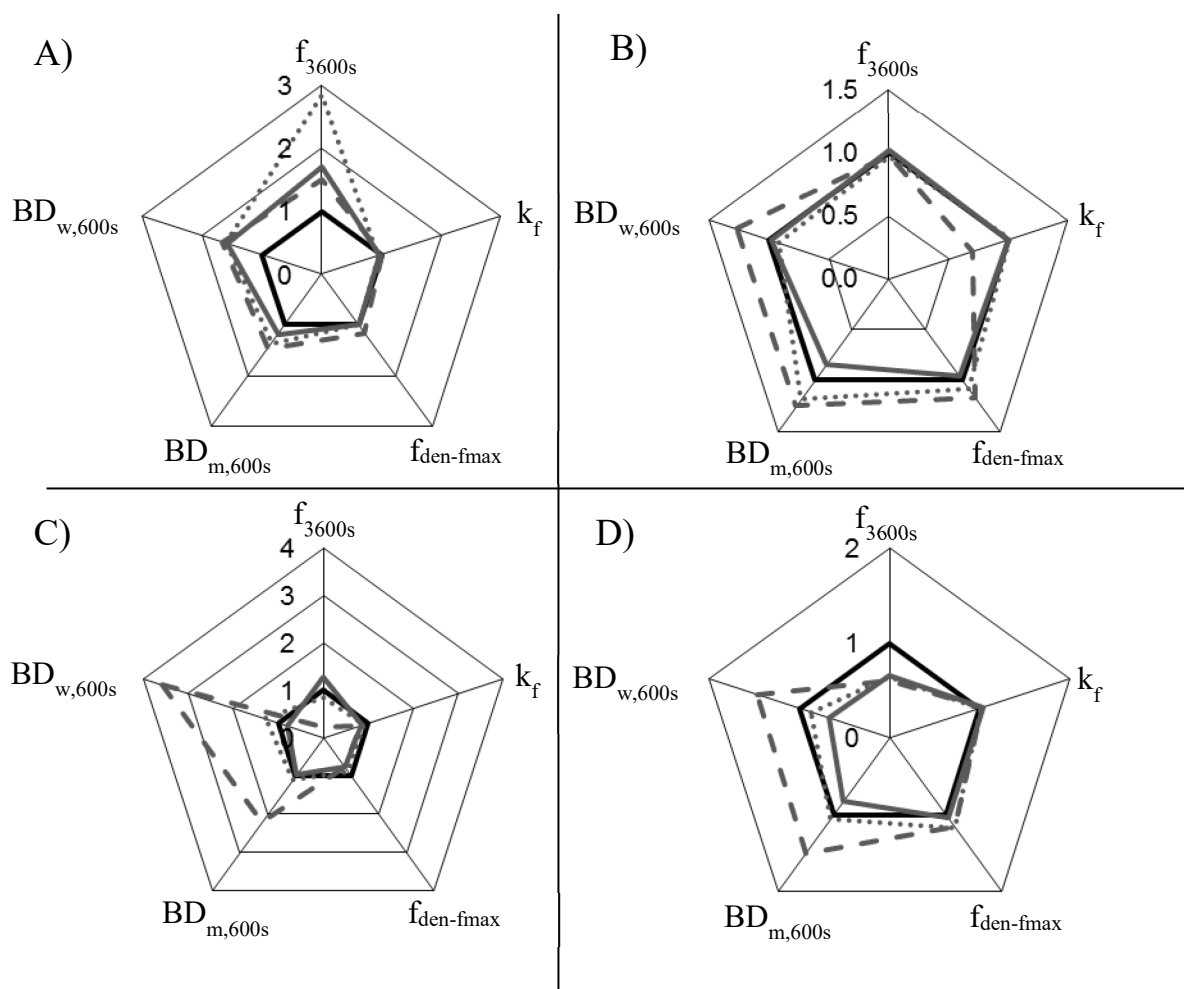


Figure I-5 Influence of decreased pH and increased ionic strength by the addition of NaCl on foaming speed (k_f), foam decay after 3600s (f_{3600s}) and foam structure ($BD_{m,600s}$, $BD_{w,600s}$ and $f_{den-fmax}$) of A) QS, B) GYP, C) TS and D) ESC at 0.5-fold CMC; pH 5 - black solid line (reference values set as 1), pH 3 - gray solid line, 100 mM - gray dotted line, 500 mM - gray dashed line

The reduction of pH 5 to pH 3 significantly stabilized the foams made of GA, see Figure I-6 upper panel. At pH 3 the majority of the carboxylic groups are non-dissociated and the electrostatic repulsion is significantly reduced. The effect of ionic strength on the stability of foams is rather complex and yet not fully understood. It is known, that the addition of neutral ions shields the charges inside the molecule, which reduces electrostatic repulsion

(Pavan *et al.* 1999). This could explain the positive influence of high ionic strength on GA (results not shown). The three carboxylic groups are negatively charged at pH 5 and the addition of ions can shield these groups and foam stability is increased. But this effect is only small compared to the impact of pH reduction on foams made from GA.

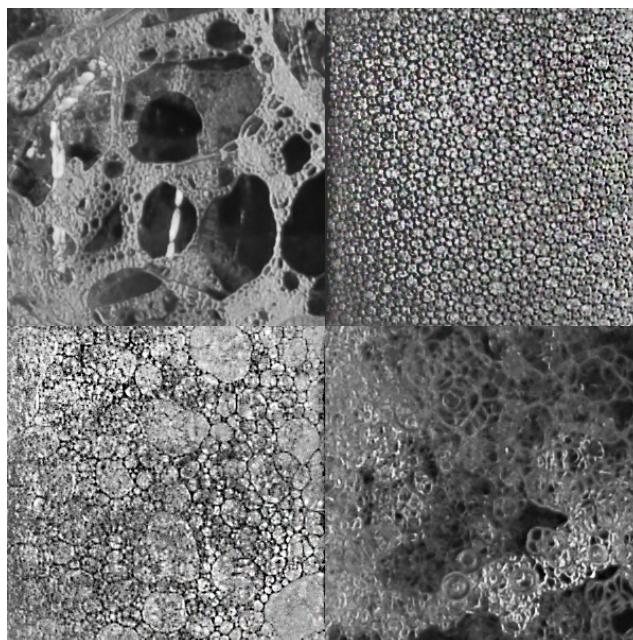


Figure I-6 Foam pictures of GA at 0.5-fold CMC after 80s of start of foaming at pH 5 (upper left) and pH 3 (upper right) and TS at 0.5-fold after 600 s of start of foaming at 0 mM (lower left) and 500 mM (lower right)

The presence of NaCl lead to a full decay of foams made from ESC and TS in less than 600 s, see Figure I-6 lower panel. The negative influence of the presence of electrolytes on saponin foams was reported before (do Canto *et al.* 2010). When comparing interfacial tension values, for the non-ionic TS there was no change when increasing ionic strength. In contrast, the increase of ionic strength lowered the interfacial tension of the ionic ESC. But foams made from TS and ESC were both tremendously influenced by changes in environmental conditions. However, the foams of the ionic saponins QS and GYP were less affected by increasing ionic strength. It can be speculated that the bidesmosidic saponins QS and GYP have an optimized packaging at the interface because of the additional sugar residue, compared to the monodesmosidic saponins TS and ESC, which prevents the foams from negative effects of environmental changes. In summary the results show, that the concept of classifying saponins in non-ionic and ionic surfactants is not practical in order to forecast foam properties in the presence of ionic molecules.

I-5 Conclusions

We showed that the botanical origin of six different saponins had a high impact on interfacial and foam properties. With respect to the methodology, the variables lag-time, Π_{5s}/Π_{1800s} and CMC, as well as the area per molecule and the interaction parameter from the Frumkin model had only limited ability to predict foaming properties. Foaming properties of saponins were more correlated to the experimental diffusion coefficient and its relation to the calculated values showed that adsorption was controlled by an additional adsorption barrier. However, other factors like simultaneous foam decay have to be taken into account and may limit the use of the experimental diffusion coefficient in more complex systems. Furthermore the concept of classifying saponins in ionic and non-ionic surfactants as the basis for characterization of foam properties seems to be questionable, since saponins classified as ionic surfactants are not necessarily sensitive to changes in ionic strength.

This study is another step to increase our understanding of the impact of botanical origin, and thus molecular structure and composition of saponins on the interfacial behavior. Comprehensive papers on this relationship are rare and future experiments should focus on investigating more botanical sources to perform statistically meaningful correlations between molecular structure and interfacial properties. For this purpose preparative techniques should be used to fractionate saponin extracts and with HPLC measurement the quantitative composition of saponin extracts should be analyzed. The analytical results can be correlated to interfacial tension measurements, oscillation results and short-term adsorption. These fundamental results can be used to predict foaming properties. Besides the analysis of basic interfacial phenomena of saponins, it is also important to increase research on the application of saponin in foods. Yet, saponins are only approved for some food products, however, for future applications it is necessary to understand interactions of saponins with other food ingredients like proteins.

Manuscript II

Mixtures of saponins and beta-lactoglobulin differ from classical protein/surfactant-sys- tems at the air-water interface

Colloids and Surfaces A: Physicochemical and Engineering Aspects, 2016, V. 506,
pp. 765-773. doi: <http://dx.doi.org/10.1016/j.colsurfa.2016.07.057>.

Authors

Sandra Böttcher^a

Matteo Scampicchio^b

Stephan Drusch^a

^a Technische Universität Berlin, Institute for Food Technology and Food Chemistry
Department of Food Technology and Food Material Science
Königin-Luise-Str.22, 14195 Berlin

^b Free University of Bolzano, Faculty of Science and Technology, Piazza Università 1,
39100 Bozen-Bolzano, Italy

II-1 Abstract

Interactions between surfactants and proteins have been intensively studied in the past because their interactions in food and cosmetic products can tremendously alter the product properties. Recent studies have shown that Quillaja saponins (QS) have very different interfacial properties in comparison to common low-molecular weight surfactants. It was reported that QS forms highly elastic interfacial films, adsorbs more slowly to the interface and cannot as easily be classified as an ionic or non-ionic surfactant. However, the mechanism of interaction between QS and proteins like beta-lactoglobulin (β -LG) is still to be understood. For this purpose the present study aimed to explore the interactions between Quillaja saponin and beta-lactoglobulin in the bulk and at the air/water-interface. At this purpose, interfacial properties were characterized with dynamic interfacial tension, short-term adsorption, shear and dilational oscillation experiments and the results were compared to foam properties. To study molecular interactions fluorescence quenching was analyzed and sequential two-fluid needle experiments were performed to get more insights on depletion of β -LG by QS.

The presence of β -LG lowered the dilational viscoelasticity of the mixed films. Although the interfacial film was weakened by β -LG the dilational elasticity was still very high and did not result in reduced foam stability. Interfacial shear results suggest that QS and β -LG can interact at the interface probably through hydrogen bonds and/or hydrophobic interactions. We determined 1.7 binding sites on β -LG in the bulk which are accessible for complex formation for QS by fluorescence quenching experiments. But these interactions did not affect interfacial properties at the analyzed concentrations. Results of the sequential two-fluid needle experiments indicated interactions between β -LG and QS at the interface. The findings of this work can contribute to a better understanding of the properties of complex systems with mixtures of natural surfactants and proteins.

II-2 Introduction

Quillaja saponins (QS) are surface active natural foaming agents, which consist of a hydrophobic triterpenoid aglycone with hydrophilic esterified sugar moieties. QS has a molecular weight of around 2000 Da and is smaller than most proteins but larger than low-molecular weight surfactants (<500 Da). The molecular structure of QS is more complex than the intensively studied common surfactants, like anionic SDS (Fainerman *et al.* 2010), cationic CTAB (Phan *et al.* 2012) or non-ionic C_nDMPO (Ivanov *et al.* 2010). Saponin extracts consist of a variety of derivatives, which differ in amount, position and type of sugar residues as well as the type of aglycone. Differences in saponin composition even between different QS extracts affect interfacial properties tremendously (Golemanov *et al.* 2013; Wojciechowski 2013). Although QS possess chargeable carboxylic groups, the amount is very small in relation to the molecular size of the QS molecule. The classification of QS as an ionic or non-ionic surfactant is therefore, not as straightforward as for other surface active molecules. But, as we reported before (Böttcher and Drusch 2016) Quillaja saponins behave more like ionic surfactants as determined by conductivity measurements. However, it has to be kept in mind that not all assumptions or explanations for ionic surfactants may be valid for QS because of the more complex and differing molecular structure. The high dilational (Stanimirova *et al.* 2011) and shear moduli (Golemanov *et al.* 2012) distinctively discriminate QS from common surfactants, which have rather poor dilational and shear viscoelastic properties (Mackie *et al.* 2000; Fainerman *et al.* 2010). Quillaja saponins are excellent foaming agents due to their high surface activity and QS foams exhibit a high stability over a long time because of the formation of viscoelastic interfacial films (Böttcher and Drusch 2016).

Beta-lactoglobulin (β -LG) is a well-studied surface active globular whey protein with a hydrophobic calyx in which small hydrophobic molecules can enter. At pH 7 (pH>isoelectric point), β -LG exists as a dimer with an overall negative charge (Creamer *et al.* 2011). Proteins in general and β -LG in particular can lower the interfacial tension, but adsorption is slower compared to common low-molecular weight surfactants (Wierenga and Gruppen 2010). β -LG can sufficiently stabilize foam lamellas by forming highly viscoelastic interfacial films (Petkov *et al.* 2000).

Interactions between low-molecular weight surfactants and proteins have been extensively studied in the past (Bos and van Vliet 2001). Complex formation in the bulk is

analyzed because complexation can influence interfacial properties like for example between diacetyltartaric esters of monoglycerides (DATEM) and whey proteins in bread dough. In mixtures, high foam stability of proteins is reduced by the addition of low-molecular weight surfactants. Experiments on the interaction between β -LG and the anionic surfactant SDS showed that SDS reduces the film viscoelasticity and leads to reduced foam stability (Pradines *et al.* 2009; Lech *et al.* 2014). The reduction in foam stability can be explained by the conflictive mechanisms of foam stabilization. Low-molecular weight surfactants stabilize foam lamellas by the Gibbs-Marangoni-mechanism (Wilde *et al.* 2004). When concentration gradients occur at the air/water-interface, surfactants will instantly move along the interface or diffuse from the bulk to areas of lower concentration. Simultaneously continuous phase is dragged along by the rapid movement of the surfactants. For this mechanism, the surfactant must have a high lateral mobility, which excludes the possibility of interactions between neighboring surfactant molecules at the interface. The surfactants disturb the linked protein network, which reduces essential intermolecular interactions between the proteins. Simultaneously, surfactants cannot level out interfacial tension gradients because the immobile protein molecules reduce the surfactants lateral mobility (Maldonado-Valderrama and Patino 2010).

The properties of the mixture of QS and β -LG differ from those of common surfactant/ β -LG-mixtures because of the unique interfacial properties of QS. In contrast to common surfactants QS molecules form a high viscoelastic network at the interface through interactions between the sugar moieties of neighboring QS molecules (Stanimirova *et al.* 2011). It is assumed that the sugar moieties of the QS and the side chains of the β -LG can interact as well through hydrogen bonds and form a high viscoelastic network at the interface. We therefore, hypothesize a synergistic effect in foam stability in β -LG/QS-mixtures because foam stabilization mechanisms of β -LG and QS are similar and not conflictive like in common surfactant and β -LG-systems. Until now foam stability of mixed β -LG/QS foams was not reported, but Kezwon and Wojciechowski (2014) showed that no synergistic effect in foaming can be detected. The authors also proposed, according to their interfacial tension results, that molecular complexes are formed between QS and β -LG. To the best of our knowledge no studies determined the interfacial rheology of mixed β -LG and QS-layers and linked these properties to foam experiments.

The main aim of this study is to investigate whether QS and β -LG can form a viscoelastic interfacial network, which results in increased foam stability as well as high shear and dilational moduli. Therefore, QS concentration was fixed at 0.005 % (below the CMC) and increasing concentrations of β -LG ranging from 0.005 to 0.1 % were added. General effects of the presence of β -LG in QS solutions on the dynamic interfacial tension, short-term adsorption, dilational viscoelasticity were evaluated using drop shape analysis. Shear viscoelasticity was analyzed using a rheometer equipped with a bicone tool. In addition, we wanted to find more evidences on whether and how saponins and β -LG interact and can form complexes. To better understand the interactions of QS and β -LG at the interface two-fluid needle experiments were performed. Molecular interactions in the bulk were further analyzed by fluorescence measurements.

II-3 Material and methods

An extract from the bark of *Quillaja saponaria* Molina (QS) was provided by Ingredion Germany GmbH (Hamburg, Germany). The QS extract in this study has been analyzed sufficiently considering interfacial properties and chemical structure (Tippel *et al.* 2016a). The extract was further purified by solid phase extraction (SPE) with a C-18 column (10 g/70 mL Thermo Fisher Scientific Germany BV & Co KG; Braunschweig, Germany) to a purity of 81 %. β -Lactoglobulin (β -LG) was isolated from whey protein isolate (Fonterra DSE 6668). Therefore, α -lactalbumin, bovine serum albumin and immunoglobulin were precipitated at pH 3.8 and the supernatant was freeze dried. The extracted β -LG had a purity of 89 %. For interfacial tension measurements, short-term adsorption, dilational and shear rheology as well as foam experiments a QS concentration of 0.005 % and increasing concentrations of β -LG: 0 (only QS), 0.005 (1:1), 0.01 (2:1), 0.05 (10:1) and 0.1 % (20:1) were analyzed. All solutions were prepared using 10 mM phosphate buffer (pH 7) and made at least 8 h before measurement and continuously stirred.

II-3.1 Purification of saponin extract

The saponin extract was purified and fractionated by a modified method using solid phase extraction as described before by Reim and Rohn (2015). At first methanol insoluble contents were separated to prevent sedimentation during solid phase extraction. Therefore, the extract was diluted with a sufficient amount of methanol and afterwards centrifuged at 5000 g. The clear supernatant was evaporated and diluted with distilled water to a saponin concentration of about 2 %. The column was conditioned with 70 mL of pure methanol and

equilibrated with 70 mL distilled water. 70 mL of diluted saponin solution was rinsed through the column and afterwards the column was washed with 35 mL of a mixture of water:methanol (95:5) and sucked dry with vacuum. Five elution steps were performed using 35 ml each of 40, 50, 60, 70 and 100 % alkali methanol. Fraction II-V were pooled, methanol was evaporated and samples were freeze-dried.

II-3.2 Fluorescence quenching of β -LG by the presence of QS

The fluorescence of proteins, more precisely the fluorescence of the tryptophan residues, can be altered by the presence of a quencher. Either static or dynamic quenching can occur. Dynamic or collisional quenching describes the interactions of protein and quencher only during the lifetime of the excited state. Static quenching occurs in the ground-state (non-excited state) when proteins and quencher form complexes, which are non-fluorescent. In this study QS is the quencher, which alters the fluorescence of β -LG. The main contributor to the emission intensity of native beta-lactoglobulin is Trp-19, which is situated inside the calyx in a rather hydrophobic environment. The second tryptophan residue Trp-61 is located at the binding site of the dimer and only minor contributes to the overall emission. (Viseu *et al.* 2007)

To distinguish between static and dynamic quenching the absorption spectra between 250-300 nm of QS, β -LG and their mixtures were analyzed (Shpigelman *et al.* 2010). If the adsorption spectrum of β -LG is not altered in the presence of QS then it is highly likely that dynamic quenching occurs, but if the adsorption of β -LG is reduced in the presence of QS it is highly likely that static quenching occurs and ground-state complexes are formed.

To determine the quenching of β -LG by QS fluorescence measurements were performed using a Cary Eclipse Fluorescence Spectrophotometer (Agilent Technologies Deutschland GmbH & Co. KG, Waldbronn Germany). The samples were excited at 295 nm (wavelength to excite tryptophan residues) and emission was recorded at 336 nm. 10 mM PBS buffer was used as blank. The self-fluorescence of QS and dilution of β -LG were determined by blank experiments. All experiments were conducted at 20°C, with excitation and emission slits of 5 nm and exited at 650 V. Samples were checked for inner filter effects and corrected according to the Eq. (I-1) stated by van der Weert (2010)

$$F_{corr} = F_{obs} \cdot 10^{\frac{A_{exc} + A_{em}}{2}} \quad (I-1)$$

where F_{corr} is the recalculated fluorescence value, F_{obs} is the measured fluorescence value and A_{exc} (here: 295 nm) and A_{em} (here: 336 nm) are the absorption values at the excitation and emission wavelength, respectively.

The adsorption values were determined using Helios Omega UV-VIS Spectrophotometer by Thermo Fisher Scientific Germany BV & Co KG (Braunschweig, Germany). Maximum binding sites were determined using the Cogan-plot. The quenching data can be analyzed using Eq. (I-2) and (I-3).

$$P \cdot \alpha = \frac{1 \cdot L_t \alpha}{n \cdot (1 - \alpha)} - \frac{K'd}{n} \quad (\text{I-2})$$

$$\alpha = \frac{F_{max} - F_{corr}}{F_{max} - F_0} \quad (\text{I-3})$$

where P is the β -LG concentration, L_t is the QS concentration, $K'd$ is the apparent dissociation constant, n the maximum number of binding sites, F_{max} and F_0 are the fluorescence intensities upon saturation and initial β -LG-concentration, respectively. Therefore, a plot with $L_t \cdot \alpha / (1 - \alpha)$ the x-axis and $P \cdot \alpha$ on the y-axis is created. The quantity of maximum binding sites is $1/\text{slope}$.

II-3.3 Dynamic interfacial tension measurements, dilational rheology, short-term adsorption and sequential two-fluid needle experiments

For dynamic interfacial tension measurements the pendant drop mode of drop shape analysis system OCA-20 from DataPhysics Instruments GmbH (Filderstadt, Germany) was used. A droplet with a volume of 15 μL was automatically dosed at the tip of a needle ($d=1.65$ mm) and the dynamic interfacial tension was recorded for 30 min. The system calculates the interfacial tension by fitting the Young-LaPlace-equation to the drop shape. Sinusoidal volume drop expansion and compression experiments were performed using the oscillation unit ODG-20 to analyze dilational rheology. A 15 μL drop was created at the tip of a needle and first oscillation cycle was started 30 s after drop creation. In each cycle the drop was oscillated six times at a frequency of 0.1 Hz with 2.8 % of volume amplitude, which resulted in an area change $\Delta A/A$. After a waiting time of 30 cycles (300 s) sequential oscillation was performed up to 20 times (Wan *et al.* 2014). From the data of each cycle the interfacial dilational modulus E^* was calculated with E' and E'' representing the elastic (storage) and viscous (loss) modulus, respectively.

To study short-term adsorption two-fluid needle experiments were performed (Tamm *et al.* 2012). For these experiments a needle with a diameter of 0.51 mm was placed inside a needle with a diameter of 1.65 mm. A droplet of 14 μL of distilled water was manually dosed and an aliquot of 1 μL of the surfactant solution was automatically dosed into the existing water droplet. Adsorption was monitored for 10 s at 130 fps with a CCD camera. QS and β -LG-concentrations were adjusted to achieve standard concentrations after injections into the droplet. Transport through the droplet was characterized by the lag-time,

which is the time between start of volume expansion (starting volume+1 % volume expansion) and the drop of the interfacial tension (surface pressure > 0.5 mN/m) and was discussed in several publications before (Tamm *et al.* 2012; Böttcher and Drusch 2016). The diffusion from the subsurface to the interface can be determined by plotting the surface pressure over square root of the time ($t^{1/2}$).

Sequential two-fluid needle experiments were performed by manually dosing a 14 μ L droplet of a 1 % β -LG-solution through the large needle of the two-fluid-needle. After 20 min 1 μ L of a 0.15 % QS-solution was automatically dosed into the existing droplet. After the injection the interfacial tension was recorded for an additional hour.

II-3.4 Shear rheology

For measurement of interfacial shear rheology the Rheometer Physica MCR301 from Anton Paar Germany GmbH (Ostfildern, Germany) was used, which is equipped with an interfacial rheology system cell (IRS) and a bicone tool. The diameter of the cell was 80 mm and was filled with 120 mL of liquid. The bicone tool had a diameter of 68.25 mm and an angle of 5.016° . Care was taken to remove all bubble from the solution prior to the measurement. Film formation was monitored for 9 h with a strain amplitude γ_0 of 0.1 % and frequency f of 1 Hz every 5 min. Samples were measured at 25°C .

Surfactant or protein loaded interfaces exhibit elastic and viscous properties when harmonic sinusoidal deformation (strain) is applied. The complex shear modulus $G^*(\omega)$ is defined as (Krägel *et al.* 2008): $G_i^*(\omega) = G_i'(\omega) + iG_i''(\omega)$, where ω is the straining frequency and G' and G'' are the elastic (storage modulus) and the viscous moduli (loss modulus), respectively.

II-3.5 Foaming, foam stability and foam structure

The foaming, foam decay and foam structure were monitored using DFA 100 (Krüss GmbH, Hamburg, Germany). The procedure is described elsewhere (Böttcher and Drusch 2016). Briefly, 50 mL saponin or protein solution was foamed using pressurized air flowing through a porous glass frit with a pore size of 40-100 μm . Foam and liquid height as well as a brightness profile were recorded twice a second for 3600 s by transmissibility measurement. All experiments were performed under light exclusion and repeated at least twice. Foam stability was characterized by relative remaining foam height $f_{\%,3600}$ after 3600 s and foam density was compared after end of foaming $f_{\text{den},\text{fmax}}$.

II-4 Results

II-4.1 Interactions in the bulk determined by fluorescence quenching

There is evidence that QS and β -LG form complexes in the bulk via static quenching. We observed a distinctive loss of absorption for β -LG when QS is present (Figure II-1A). As recently discussed by Keppler *et al.* (2014) for the quenching of β -LG, there are various models possible to analyze fluorescence data. The authors recommended to use the Cogan-Plot and showed that even though the calculated results for the ‘apparent affinity constant’ ($K'a$) and ‘apparent dissociation constant’ ($K'd$) showed high variation the ‘maximum number of binding sites’ (n) was relatively stable. The inverse slope of the graph of the Cogan-plot is the maximum number of binding sites. We determined a maximum of 1.7 binding sites (Figure II-1B).

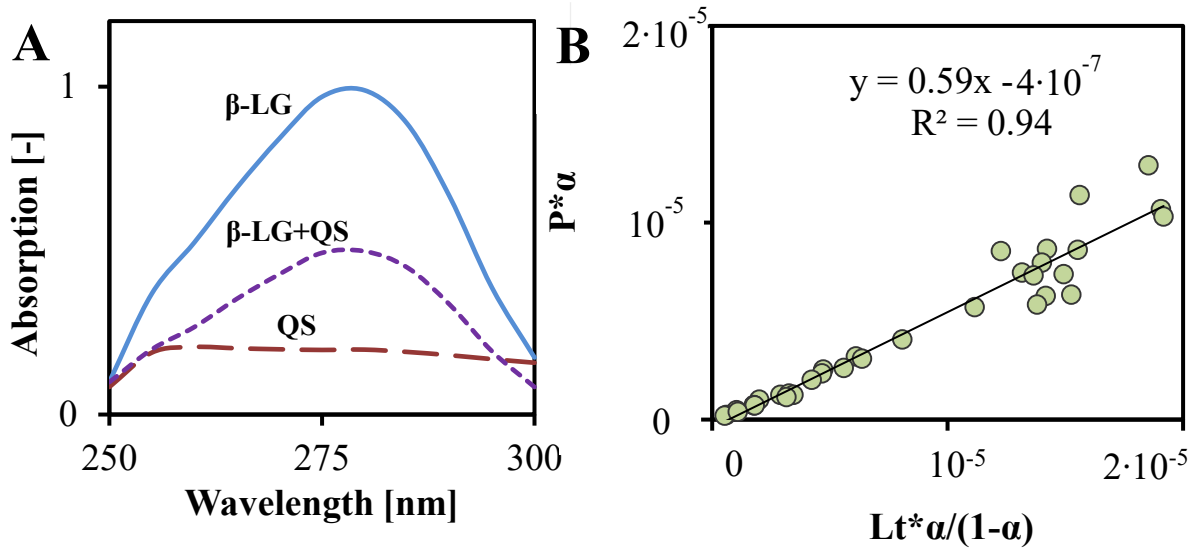


Figure II-1 Fluorescence measurements on the interactions of β -LG and QS, A) absorption spectra between 250-300 nm of pure β -LG (solid line), pure QS (dashed line) and mixture of β -LG+QS, which was corrected for QS adsorption (dotted line), B) Cogan-Plot of quenching of β -LG by QS with P = β -LG-concentration, α =fraction of free binding sites and L_t =QS-concentration

II-4.2 Interactions of QS and β -LG at the interface

An interfacial layer of β -LG can be penetrated by the addition of QS. In the experimental setup β -LG can adsorb at the air-water interface for 20 min. When QS is injected into the droplet, new interface is created (area expansion of about 5 %) for which QS and β -LG compete (Figure II-2, closed circles). A sharp decrease in interfacial tension after the injection is visible and reaches almost interfacial tension of pure QS. Afterwards the interfacial tension increases slightly by about 1 mN/m and after half an hour the interfacial tension decreases again. At the end of the measurement the interfacial tension value is between pure QS (Figure II-2, diamonds) and β -LG (Figure II-2, open circles).

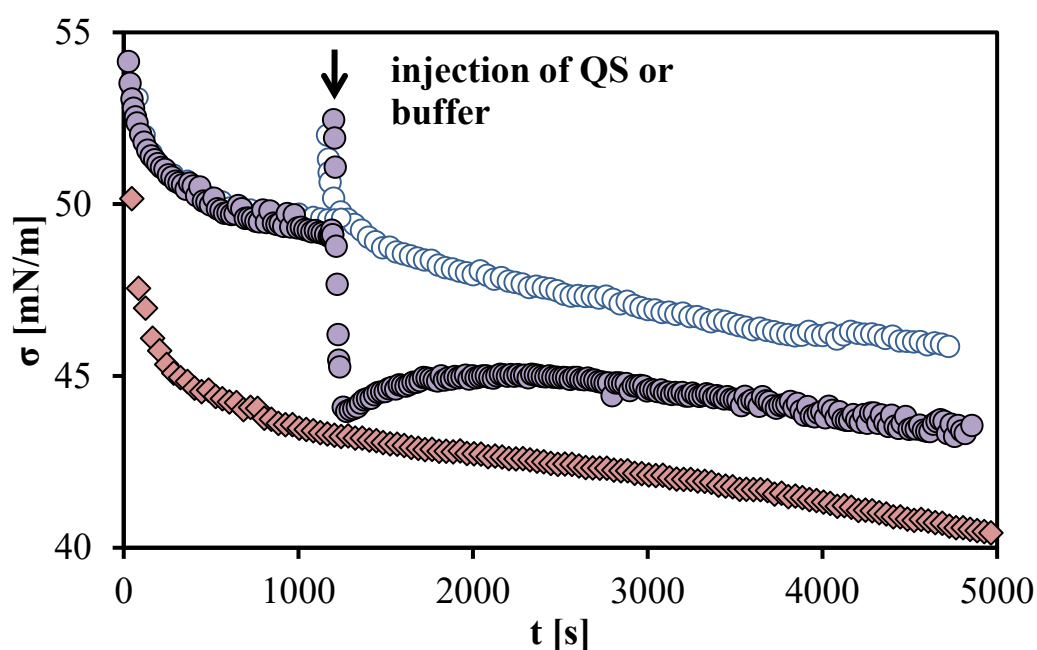


Figure II-2 Interfacial tension σ in relation to the drop age t for the injection of 0.15 % QS into a droplet of 10 mM phosphate buffer (\blacklozenge) and sequential adsorption of 1 % β -LG at the air water interface with injection indicated by the arrow of 0.15 % QS (\bullet) and injection of 10 mM phosphate buffer (\circ)

II-4.3 Short- and midterm adsorption of mixtures of QS and β -LG

The presence of β -LG cannot efficiently influence short- and midterm adsorption in mixtures of QS and β -LG. But still QS adsorbs more rapidly than β -LG, as shown in Figure II-3. The open symbols represent β -LG and it can be noted that with increasing concentration of β -LG the adsorption is faster and surface pressure Π is increasing. The presence of β -LG neither decreases nor increases the adsorption of the QS in the short time scale of 5 s. Lag-time of the different β -LG concentrations reduced with increasing β -LG concentration, but between mixtures of QS and β -LG and pure QS no differences were found (results not shown).

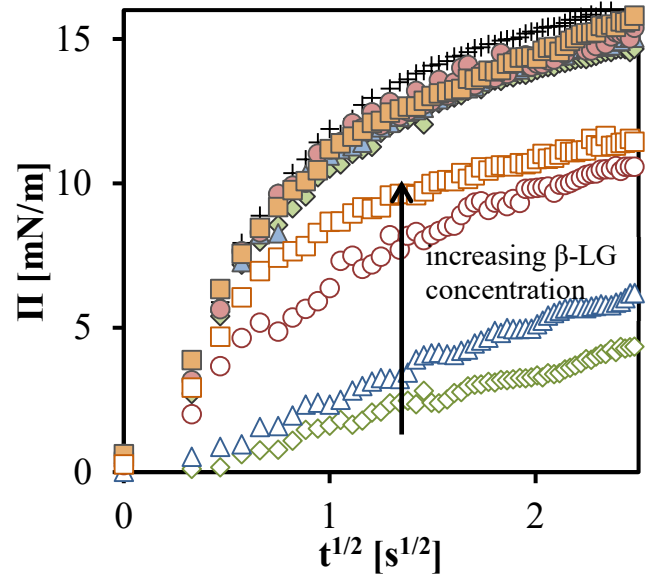


Figure II-3 Surface pressure Π versus square root of the drop age $t^{1/2}$ at the air/water interface of 0.005 % QS (+), 0.005 % β -LG (\diamond), 0.01 % β -LG (Δ), 0.05 % β -LG (\circ), 0.1 % β -LG (\square); filled symbols indicate β -LG is mixed with 0.005 % QS

At a timescale of several minutes (midterm adsorption) the dynamic interfacial tension is also governed by QS (see Table II-1). The interfacial tension of pure β -LG is distinctly higher than that of QS with 51.2 to 56 mN/m. In mixtures of QS and β -LG the interfacial tension was lowered similarly to QS to about 45 mN/m.

Table II-1 Dynamic interfacial tension σ of β -LG-solutions and β -LG/QS-mixtures measured for 20 min with pendant drop analysis

c_{QS} [%wt]	c_{BLG} [%wt]	β -LG/QS [%wt/%wt]	σ [mN/m]
0	0.005		56.0 ± 0.9
	0.01		55.0 ± 0.5
	0.05		51.7 ± 0.5
	0.1		51.2 ± 0.3
<hr/>			
0.005	0		45.7 ± 0.8
	0.005	1	44.7 ± 1.2
	0.01	2	44.8 ± 1.4
	0.05	10	45.0 ± 1.2
	0.1	20	45.4 ± 0.1

II-4.4 Dilational rheology of mixtures of β -LG/QS

Pure QS and β -LG interfacial layers as well as their mixtures build up strong viscoelastic interfacial layers. In Figure II-4A the complex dilational modulus E^* is displayed in relation to the drop age. Viscoelasticity was highest for QS with about 170-180 mN/m and lowest for all β -LG-concentrations, which had a viscoelasticity of around 110 mN/m. For mixtures of QS and β -LG the interfacial dilational modulus E^* modulus lies between the values for QS and β -LG. For all samples the viscous modulus E'' was below 10 mN/m, which indicates high elastic properties of the interfacial layers. In mixtures with the highest concentration of 0.1 % β -LG the complex dilational modulus (E^*) is close to the values of pure β -LG, which indicates that dilational rheology at this concentration is governed by β -LG.

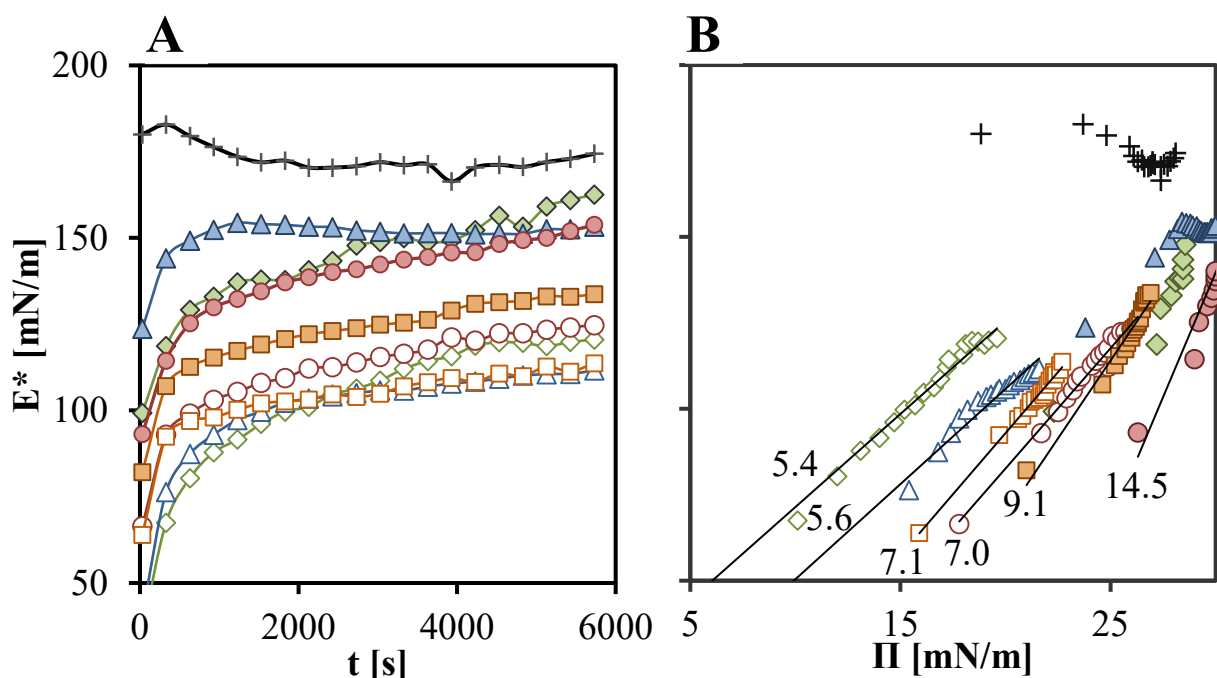


Figure II-4 Interfacial dilational modulus E^* in relation A) the drop age t and B) to the surface pressure Π of 0.005 % QS (+), 0.005 % β -LG (\diamond), 0.01 % β -LG (Δ), 0.05 % β -LG (\circ), 0.1 % β -LG (\square); filled symbols indicate β -LG is mixed with 0.005 % QS

The development of the complex dilational modulus E^* of a surface active substance over time is not independent from its concentration, therefore E^* should be normalized over the surface pressure Π (Patino *et al.* 2005). The resulting master curve eliminates concentration effects on the complex dilational modulus and therefore all β -LG curves should overlap. Normalization of all four β -LG concentrations was not possible, because E^* - Π -graphs were not similar and no master curve could be created (Figure II-4B). With increasing surface

pressure, the interactions and therefore E^* increased except for QS whose E^* was independent from the surface pressure. All protein concentrations had a slope greater than 1, which increased with increasing β -LG concentration from 5.4 to 7.0 for 0.005 and 0.1 % β -LG, respectively. In mixtures with the lowest β -LG concentrations 0.005 & 0.01 %, the slope could not be determined because after a steep ascent the slope became very flat similar to QS. Graph characteristics of the two highest β -LG concentrations 0.05 & 0.1 % were similar to pure β -LG and were without a plateau as described for the mixtures with lower β -LG concentration.

II-4.5 Shear rheology

Experiments on shear rheology give further insights on intermolecular interactions at the constant interface. High viscoelastic film properties indicate strong molecular interactions. We monitored film formation by applying low amplitude and frequency to the interface. As displayed in Figure II-5, QS builds up strong viscoelastic interfacial layers with $G^* \sim 70$ mN/m. Interfacial layers of β -LG take more time to develop but with increasing concentration of β -LG the complex shear modulus G^* increases and film formation is faster. In all samples G'' was below 10 mN/m and interfacial layers had pronounced elastic properties. In all QS/ β -LG-mixtures, apart from that containing 0.1% B-LG, the complex shear moduli G^* were sufficiently higher than pure QS and pure β -LG, which indicates additional interactions between QS and β -LG.

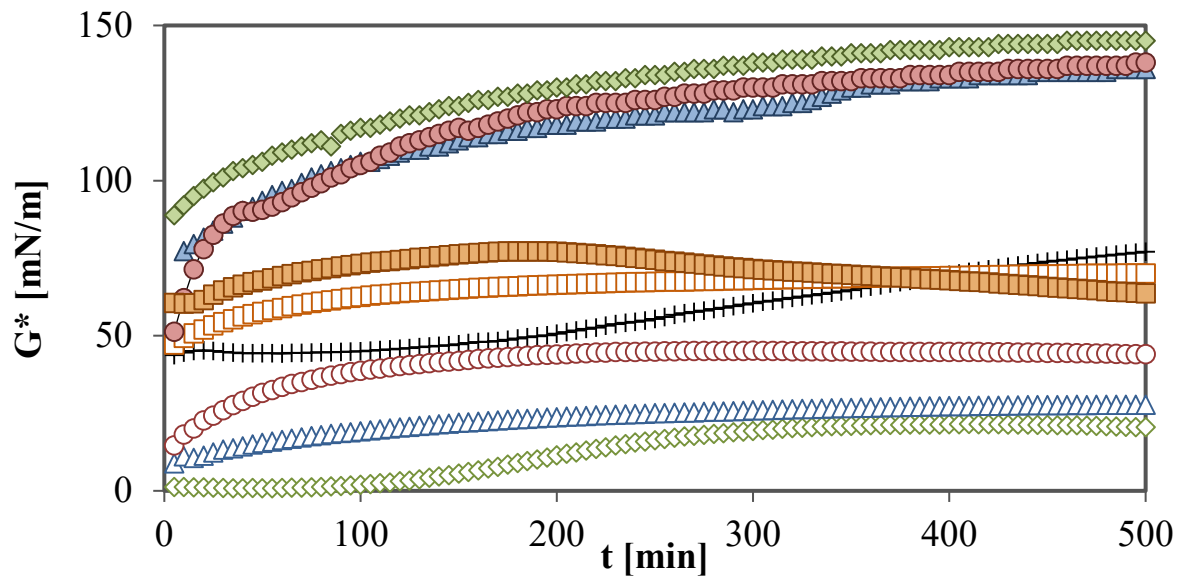


Figure II-5 Complex shear modulus G^* in relation the interface age t for of 0.005 % QS (+), 0.005 % β -LG (\diamond), 0.01 % β -LG (Δ), 0.05 % β -LG (\circ), 0.1 % β -LG (\square); filled symbols indicate β -LG is mixed with 0.005 % QS

II-4.6 Foam properties

Even low β -LG-concentrations can improve properties of QS foams. In mixtures with the highest β -LG concentration of 0.1 % a foaming speed of 1.745 ± 0.027 mm/s was determined, which is distinctively higher than the QS foaming speed of 1.671 ± 0.030 mm/s. In general, QS can form stable and long-lasting foams but in this study a very low concentration was chosen to obtain unstable foams over the measuring time of 3600 s. Foam stability of the mixtures was highly influenced by the addition of β -LG. In mixtures containing the lowest β -LG concentration of 0.005 % the remaining foam height after 3600 s increased to 71.1 % instead of only 21.3 % for pure QS, even though pure 0.005 % β -LG was already fully collapsed after 3600 s (Figure II-6A). In mixtures the presence of β -LG increased foam density and thereby the liquid content of the initial foam (Figure II-6B).

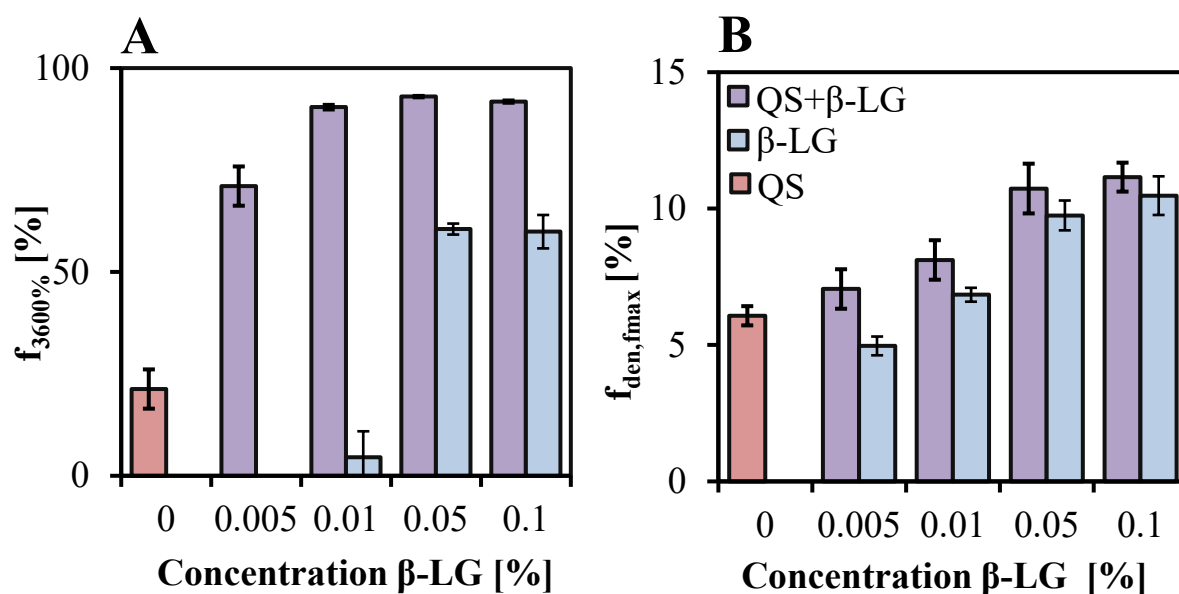


Figure II-6 Foam results of QS (red), β -LG (blue) and mixtures of QS and β -LG (violet) for A) remaining foam height after 3600 s and B) foam density at f_{\max} in relation to β -LG concentration

II-5 Discussion

At first we want to interpret fluorescence experiments on complex formation in the bulk and sequential adsorption experiments on the interactions at the interface. In the second part of the discussion we want to discuss results of foam experiments, adsorption and interfacial rheology.

Fluorescence quenching experiments showed that QS and β -LG can interact in the bulk via static quenching and a maximum of 1.7 binding sites at the β -LG are accessible for QS molecules (Figure II-1). Static quenching is most likely related to the formation of non-fluorescent complexes between QS and β -LG. In the past it was reported that β -LG can form complexes with naringenin (Gholami and Bordbar 2014) or resveratrol (Liang *et al.* 2008). Non-covalent binding to the two binding sites in β -LG can occur via hydrogen bonds, van der Waals forces or hydrophobic interactions (Keppler *et al.* 2013). The interactions in the bulk were predicted before by interfacial tension data (Piotrowski *et al.* 2012). The value of the maximum binding sites is between 1 and 2, which is very common for reactions of β -LG (Keppler *et al.* 2013). It also has to be kept in mind that the QS extract consists of a mixture of various saponins with different molecular structures. A clear stoichiometry is therefore not as straightforward as for a single well defined substance.

Two-fluid needle experiments were performed to determine whether QS can deplete β -LG from the interface. Fainerman *et al.* (2005) showed in their two-fluid needle experiments that common surfactants, i.e. C_{13} DMPO and Triton X-100 adsorb and desorb rapidly from the interface. Proteins, i.e. β -LG take a long time to adsorb and an even longer time to desorb from the interface, because high activation energy is necessary. But it is possible to accelerate desorption of proteins by the addition of surfactants (Fainerman *et al.* 2005). In the experiment of this study, β -LG was allowed to adsorb at the interface and QS was added into the droplet. It is clear that because of the addition of QS the interface of the droplet increases and QS and β -LG compete to adsorb at the unoccupied interface. After the injection of QS into the β -LG-droplet, a sharp decrease in interfacial tension was observed and, afterwards, the interfacial tension increased by about 1 mN/m reaching a plateau and decreasing after 30 min again. The results of this study indicate that QS and β -LG interact at the interface as well. But it is clear that QS cannot fully deplete β -LG from the interface during the measurement time since interfacial tension of the mixed layer is higher than pure QS. A possible explanation of these results is that QS and β -LG can either interact via the ‘complexation and competitive adsorption’ or via ‘orogenic displacement’.

The ‘orogenic displacement’ describes the adsorption of surfactants molecules at a protein covered interface (Mackie *et al.* 1999). First, surfactant molecules adsorb at defects in the interfacial protein film. Subsequently, additional surfactant molecules adsorb at these defects and, since proteins do not easily desorb, the protein network is compressed. At a certain point the protein network cannot be further compressed and protein molecules desorb and the protein network breaks down in favor of a lower interfacial tension obtained by surfactant molecules. Alternatively, the ‘competitive adsorption and complexation’ mechanism, which was proposed for ionic surfactants: surfactants adsorb at the interface and form via hydrophobic or electrostatic interactions (or both) complexes with the proteins (Kotsmar *et al.* 2009). The complexes are less surface active and are therefore, easier displaced from the interface. Free surfactant molecules and complexes compete for the newly created space. Over time more and more protein is displaced from the interface through the complexation and the interface is mainly covered by surfactant molecules.

We cannot verify, which of the two mechanisms takes place but we hypothesize, since QS behaved more like an ionic surfactant in conductivity measurements, that QS and β -LG interact by the mechanisms of ‘complexation and competitive adsorption’. After QS adsorbs at the newly created interface, QS molecules interact with β -LG forming less surface active complexes, which leads to an increase in interfacial tension. After a while the complexes desorb and free space at interface is created and additional QS and β -LG molecules from the bulk can compete for the newly created interface.

In the second part of the discussion we want to discuss and connect interfacial tension and rheology results with foam properties.

QS adsorbs faster at the interface than β -LG because of its lower molecular weight as shown by measurements on short-term adsorption (Figure II-3). This result is in line with the concept of slow adsorption of protein. Because of electrostatic hindrances and low hydrophobicity, it takes time for β -LG to diffuse from the subsurface to the interface (Wierenga and Gruppen 2010). However, recent studies have shown that QS also has a lower diffusion coefficient than regular surfactants as well and adsorption is not diffusion-controlled but an additional adsorption barrier exists (Piotrowski *et al.* 2012). Adsorption speeds of mixtures of QS and β -LG do not differ from pure QS showing that QS molecules clearly dominate the adsorption. Similar results were obtained in dynamic interfacial tension experiments: the interfacial tension of QS after 20 min was distinctively lower than β -LG. The interfacial tension of QS/ β -LG-mixtures did not differ from QS values (Table II-

1). In a previous study it was shown that the presence of β -LG can slightly reduce interfacial tension values (Kezwon and Wojciechowski 2014). We found the same reduction of interfacial tension at much lower QS/ β -LG-concentrations (results not shown). We attribute the differences to the use of a different QS extract because Kezwon and Wojciechowski (2014) also found differences in synergistic behavior between the two analyzed QS extracts in their study. It seems that the strength of synergistic effect between QS and β -LG depends on the kind of QS. In addition, Kezwon and Wojciechowski (2014) do not specify whether the used β -LG is mainly in native state. Partially denaturated proteins can adopt their structure more freely than native β -LG leading to a smaller area per molecule at the interface (Kim *et al.* 2005). In this study only native β -LG was used, which is less flexible and more rigid in its molecular structure. Therefore, native proteins cannot as easily interact with QS, forming complexes and optimize interfacial packing, which leads to synergistic effects in adsorption and interfacial tension.

Interfacial dilational rheology can give insights how an interfacial film can withstand expansion and compression. Viscoelastic response from the interfacial layer is influenced by interfacial rearrangements in the interfacial layer and exchange processes between the bulk and the interface (Miller *et al.* 1996; Freer *et al.* 2004).

Interfacial layers of pure QS and pure β -LG were highly viscoelastic $E^*_{QS} \sim 180$ mN/m and $E^*_{BLG} \sim 110$ mN/m with very low viscous moduli (<10 mN/m) (Figure II-4A). A high viscoelastic modulus E^* with a high elastic modulus of the interfacial layer may be attributed to intermolecular interactions and the inability of desorption from the interface when subjected to expansion and compression. The low viscous modulus E'' for all samples shows that only a small amount of the imposed energy is dissipated by relaxation processes like structural rearrangements in the interface (Ravera *et al.* 2009). For different QS extracts higher and lower values E^*_{QS} were reported with 280 mN/m (Stanimirova *et al.* 2011) and 80-100 mN/m (Golemanov *et al.* 2013; Wojciechowski 2013). Petkov *et al.* (2000) reported slightly smaller elastic moduli E' for β -LG-interfaces with $E' \sim 66$ -90 mN/m. For the sake of comparison typical viscoelasticity for common low-molecular weight surfactants like SDS are sufficiently lower with $E^*_{SDS} \sim 10$ mN/m as well as the elasticity of random coil proteins like β -casein with $E'_{\beta\text{-casein}} \sim 30$ mN/m (pH 7) (Fainerman *et al.* 2010; Wüstneck *et al.* 2012).

E^* in binary systems of β -LG/QS were lower than pure QS and higher than pure β -LG. The presence of a small amount of β -LG sufficiently decreased E^* , which may be attributed

to changes in interfacial molecular interactions or differing exchange characteristics between the interface and the bulk.

The E^* - Π -graph shows the dependency of the complex dilational modulus on the surface pressure (Figure II-4B). A steep slope indicates strong dependence of the E^* on the surface pressure, which means that with increasing surface pressure (because of higher interfacial surfactant concentration) the viscoelasticity increases. A slope greater than 1 in the E^* - Π -graph indicates non-ideal behavior of the film and high interaction between the molecules (Lucassen-Reynders *et al.* 1975). The fact, that it is not possible to achieve a master curve for β -LG may be attributed to different aggregation behavior at the air/water-interface at the chosen concentrations. Benjamins (2000) found about the same slope as in our experiments for similar β -LG concentration but in contrast a master curve was reported. This difference has to be attributed to divergent experimental conditions. The adsorption and formation of the viscoelastic network of QS is too fast to be determined in the timescale of our experiments. The same applies for the mixtures with the lowest β -LG concentrations, which show a fast structuration with an adjacent plateau at higher surface pressures. That means at low β -LG concentration the dilational interfacial properties are governed by QS. With increasing β -LG concentration in the mixtures the steepness of the slope decreases and approaches the steepness of pure β -LG interfacial layers. This indicates that the interfacial layers at higher β -LG concentrations are predominantly influenced by β -LG.

With interfacial shear rheology it is possible to determine interaction between molecules when shear stress is applied to the interface without the influence of relaxation processes imposed by diffusion to and from the interface (Freer *et al.* 2004). Similar to dilational rheology, QS interface was distinctively more viscoelastic ($G^*_{\text{QS}} \sim 70$ mN/m) than β -LG-interfaces ($G^*_{\text{BLG}} \sim 15 \dots 75$ mN/m), but in both cases elastic moduli G' were sufficiently higher than viscous moduli G'' (Figure II-5). In contrast to dilational rheology, it was possible to discriminate between the chosen β -LG-concentrations. Complex shear modulus G^* of QS and β -LG-layers in this study were higher than the reported values $G^*_{\text{QS}} \sim 30$ mN/m (Golemanov *et al.* 2012) and $G^*_{\text{BLG}} \sim 10 \dots 20$ mN/m (Petkov *et al.* 2000), which is attributed to deviating measuring conditions. In mixtures of QS and β -LG (up to a β -LG-concentration of 0.05 %) the G^* was higher than in pure QS and β -LG. At higher β -LG concentrations in the mixtures the interfacial shear properties are mostly influenced by β -LG and at lower concentrations by QS. Gunning *et al.* (2004) determined similar synergistic effects between the ionic surfactant LPC-L and β -LG. This effect was attributed to the strengthening of the

protein network by the presence of the surfactant, which increased shear viscoelasticity. It is assumed that β -LG and QS interact either through hydrogen bonds or hydrophobic interactions or a mixture of both. It is further hypothesized that β -LG can strengthen the firm QS network at low concentrations but with increasing β -LG concentration this effect is neglected. But it has to be kept in mind that the viscoelasticity is still very high compared to common surfactant/protein-systems.

Foam results showed a slightly increased foaming speed and tremendously increased foam stability and density in mixtures of QS and β -LG compared to pure QS (Figure II-6). Kezwon and Wojciechowski (2014) focused on analyzing foaming properties and found no synergistic effect of β -LG on foaming results of QS in the chosen (much lower) concentration range. Density and stability of the foams in this study were increased by the presence of β -LG in mixtures with QS. A higher foam density indicates a higher liquid content in the foam, which can increase foam stability.

Considering the discussed interfacial properties of QS, it is highly likely that QS is not primary stabilizing foams by the Gibbs-Marangoni mechanism because diffusion is too slow and lateral mobility not possible, as indicated by high shear and dilational viscoelasticity. We suppose that foam stability of QS foams is attributed to the formed viscoelastic network. But we also think that in contrast to proteins, QS can stabilize the interfacial films by diffusion of QS to areas of lower surfactant concentration. Although the QS molecules cannot laterally move to areas with lower concentration, the diffusion from the bulk to the interface is faster than β -LG and can additionally stabilize the interface by this mechanism. In mixtures of β -LG/QS the foam stabilizing mechanisms of both substances are not conflictive and therefore, the synergistic effect in foam properties can be explained.

In a last step, we want to compare the results of interfacial shear and dilational rheology with foam results. In mixtures with a low concentration of β -LG a sufficient increase in shear viscoelasticity was determined as well as a distinctive decrease in dilational viscoelasticity. This means the addition of a small amount of β -LG strengthened intermolecular interactions (shear rheology) but exchange characteristics between the interface and the bulk (dilational rheology) may have changed as well. In foam experiments especially at low concentrations, synergistic effects in foam stability were detectable. But it also has to be kept in mind that this effect probably is not solely because of increased shear viscoelasticity but also because more surface active molecules are present in the system to occupy

the interface. In addition, proteins are known to increase film thickness of foam lamellae and to increase liquid content, which are both connected with longer foam stability.

When the β -LG concentration in the mixtures is increased both shear and dilational viscoelasticity decreased and had values similar to pure β -LG. This can be interpreted as a reduction in intermolecular interactions (shear rheology) as well as may be attributed to varying exchange characteristics (dilational rheology). This effect was not detectable in foam experiments because foams of mixtures of QS and β -LG were still more stable than pure β -LG. It has to be kept in mind that interfacial shear and dilational rheology can only be indicators for the behavior of surface active molecules in real applications like foams. Increased foaming ability and foam stability are attributed to high interfacial shear and dilational moduli but small changes in viscoelasticity do not necessarily affect foam properties. Foams are complex and thermodynamically unstable systems and many factors have to be taken into account to predict foaming and decay properties.

II-6 Conclusion

In a binary system of Quillaja saponin and β -LG synergistic effects and interactions between both substances can occur. We analyzed various interfacial properties, like adsorption behavior and shear and dilational rheology of mixtures of QS and β -LG to draw conclusions to foam experiments. Fluorescence measurements on the interaction of QS and β -LG in the bulk showed that it is highly likely that ground-state complexes are formed. Whether or not these complexes change upon adsorption at the interface is subject to further investigations. QS, β -LG and their mixtures form highly viscoelastic interfaces, which can sufficiently resist dilational and shear deformation. Interfacial dilational and shear rheology can provide crucial information on interfacial interactions and underlying interfacial phenomena. It is assumed that intermolecular interactions between QS and β -LG at the interface are either formed through hydrogen bonds and/or hydrophobic interactions. In mixtures at low β -LG concentrations the interfacial properties are mainly governed by QS but at higher β -LG concentrations the interfacial properties approach pure β -LG layers. The ability of QS to build up and maintain stable foams is mainly caused by the strong viscoelastic interfacial network, unlike common low-molecular-weight surfactants, which stabilize by the Gibbs-Marangoni mechanism. Unlike in other surfactant/protein-systems QS is not able to easily deplete β -LG from the interface once β -LG adsorbed.

We have here discussed differences between common surfactant/protein-systems and the β -LG/QS-system. Although there have been studies on the interactions on Quillaja saponins and other food proteins like lysozyme and β -casein, general knowledge on the interactions of proteins and saponins is scarce. The combination of Quillaja saponins and proteins is promising and should be analyzed further to benefit from this knowledge in food products. Additional research on thin films for example with ellipsometry and Brewster-angle microscopy can give further insights in foam lamella thickness and black film formation. The formation of common and newton black films is attributed to very stable foam lamellas, which lead to increased foam stability. As is well known, β -LG properties at the oil/water-interface differ from those at the air/water-interface. It would therefore, be interesting to analyze the interactions of β -LG and Quillaja saponin at the oil/water-interface to correlate interfacial properties with emulsion stability. Furthermore, the finding of the interactions between β -LG and QS at the air/water and oil/water-interface can be a basis to analyze the properties of foams with oil content and their stability.

Manuscript III

Mixtures of Quillaja saponin and beta-lactoglobulin at the oil/water-interface: Adsorption, interfacial rheology and emulsion properties

Colloids and Surfaces A: Physicochemical and Engineering Aspects, 2017, V. 518, pp. 46–56. doi: <http://dx.doi.org/10.1016/j.colsurfa.2016.12.041>.

Authors

Sandra Böttcher^a

Julia K. Keppler^b

Stephan Drusch^a

^a Technische Universität Berlin, Institute for Food Technology and Food Chemistry
Department of Food Technology and Food Material Science
Königin-Luise-Str.22, 14195 Berlin

^b Christian-Albrechts-Universität zu Kiel, Division of Food Technology, Institute of Human Nutrition and Food Science, Heinrich-Hecht Platz 10, 24118 Kiel, Germany

III-1 Abstract

Aim of the present study was to investigate the interfacial properties of mixed films of Quillaja saponins (QS) and beta-lactoglobulin (β -LG) at the oil/water-interface. It was hypothesized that due to the differences in the physical characteristics of the dispersed phase molecular interactions and film characteristics at the oil/water interface substantially differ from the air/water-interface. Furthermore QS/ β -LG-interactions will affect stability of emulsions in a concentration-dependent manner.

Oscillating drop experiments were performed with subsequent analysis of raw data (Lissajous-plots) to discover non-linear behavior upon compression and expansion. Interfacial shear rheology as well as dynamic interfacial tension and two-fluid needle experiments were performed to comprehensively characterize interfacial properties of mixtures of QS/ β -LG. Finally, emulsions were prepared and their stability, oil droplet size and ζ -potential were determined.

It became obvious that QS dominates the interfacial film in a binary mixture as indicated by dynamic interfacial tension and dilational rheology. Strain stiffening was observed for mixed QS/ β -LG interfacial layers upon dilational expansion at an amplitude above 2.8 %. Intermolecular interactions increased in mixtures of QS/ β -LG as indicated by shear rheology. Emulsion experiments showed extensive aggregation of oil droplets in QS/ β -LG-emulsions with high content of β -LG. Aggregation of oil droplets increased velocity of creaming and after 7 days a distinct creaming layer was visible. Changes in dispersity were influenced by concentration and ratio of QS and β -LG.

III-2 Introduction

Quillaja saponins (QS) are natural amphiphilic emulsifiers approved as a food additive in the EU and US. Interfacial properties of saponins originate from the presence of hydrophilic and hydrophobic parts in the molecule (Vincken *et al.* 2007). Saponins consist of a hydrophobic aglycone with hydrophilic chains of sugar attached to the aglycone. They may be classified in two different groups depending on the number of chains. If a single sugar chain is linked to the aglycone, typically at C-3, the resulting saponin is called ‘monodesmosidic’. If an additional sugar chain is present, typically at C-28 (Güçlü-Üstündağ and Mazza 2007), the structure is referred to as ‘bidesmosidic’. Commercial available extracts from the Chilean soap bark tree *Quillaja saponaria* Molina mainly consist of a mixture of various bidesmosidic saponin derivatives (Thalhamer and Himmelsbach 2014; Bankefors *et al.* 2011; Bankefors *et al.* 2010).

Since QS is approved as a food additive, comprehensive studies on interfacial properties (Wojciechowski 2013) and chemical constitution (Maier *et al.* 2015a) were published in the past. The majority of studies on the interfacial properties of QS focused on the air/water-interface. Several studies (Wojciechowski 2013; Golemanov *et al.* 2012; Stanimirova *et al.* 2011) determined interfacial rheology and adsorption kinetics. In addition, in one study (the authors also proposed a model for interfacial arrangement of Quillaja saponin molecules at the air/water-interface (Golemanov *et al.* 2012). In this model, a domain structure was suggested, which explains the high elastic shear and dilational moduli of QS of ~ 80 mN/m and ~ 180 mN/m, respectively (Böttcher *et al.* 2016). High interfacial shear and dilational moduli are rather unique for such small molecules like the saponins. Usually low-molecular surfactants (< 500 Da) do not form strong interfacial films and cannot withstand shear and dilational deformation (Bos and van Vliet 2001). It was suggested that intermolecular hydrogen bonds between neighboring sugar residues account for the strong interfacial viscoelastic films (Golemanov *et al.* 2012).

However, it was also shown that the interfacial viscoelastic film of QS is much weaker at the oil/water-interface. As discussed by Golemanov *et al.* (2014) the general opinion is that interactions between the surface active molecules at the interface are reduced in the presence of oil. There are two possible mechanisms to explain this phenomenon: Firstly, oil may penetrate into the space between adsorbed surface active molecules or secondly, surface active molecules are solubilized in the oil phase. In both cases the result is a less dense packaging at the interface. It is assumed that the first mechanism occurs when using

surfactants, which are not soluble in oil, and proteins. The second mechanism is relevant for oil-soluble surfactants like non-ionic low-molecular weight surfactants. Golemanov *et al.* (2014) showed that Quillaja saponins are not soluble in triglyceride-based oils. The authors therefore concluded that the first mechanism applies and oil molecules penetrate between adsorbed QS molecules thereby reducing intermolecular interactions.

Apart from fundamental studies dealing with interfacial rheology and adsorption, several studies on practical aspects like formation and stability of QS-based emulsions were published in recent years (Yang *et al.* 2013; Zhang *et al.* 2015, Zhang *et al.* 2016). Emulsions are per definition thermodynamically unstable. However, if stabilizing mechanism sufficiently slow down thermodynamically driven changes in dispersity, emulsions are frequently described as kinetically stable (Dunkhin *et al.* 2001). Using a shift in the oil droplet size distribution as a marker, it was shown that QS-based emulsions are kinetically stable for one month even at high storage temperatures up to 55°C (Yang *et al.* 2013). Stability of QS emulsions was attributed to the highly negative ζ -potential at pH 7, which facilitates electrostatic repulsion between oil droplets.

With respect to the use in more complex food matrices, investigation of the interaction of QS with other food constituents is of utmost importance. The interaction between proteins and low molecular weight surfactants has been subject of various studies in the past and a summary goes beyond the scope of this introduction. In the bulk, complex formation between surfactants, like sodium dodecyl sulfate and proteins was reported (Hu *et al.* 2011; Kotsmar *et al.* 2009). Furthermore, it was shown that surfactants may penetrate into protein films at the interface (Morris and Gunning 2008) and consequently may cause replacement/desorption of proteins (Dan *et al.* 2015; Fainerman *et al.* 2006). The presence of surfactant may substantially reduce interfacial shear and dilational viscoelastic moduli (Dan *et al.* 2013, Ulaganathan *et al.* 2012; Maldonado-Valderrama and Patino 2010; Krägel *et al.* 2008). More specifically with respect to QS, Piotrowski *et al.* (2012) analyzed interactions of QS and β -lactoglobulin (β -LG) at the air/water-interface as well as at a water/tetradecane-interface. The authors reported that dynamic interfacial tension is lower in binary mixtures of QS and β -LG compared to only QS at the water/tetradecane-interface. Our group recently showed in fluorescence experiments that QS and β -LG form a complex in aqueous solution (Böttcher *et al.* 2016). Furthermore, synergistic effects with respect to the complex viscoelastic moduli of interfacial films at the air/water-interface and with respect to foam stability were found. It was hypothesized that intermolecular hydrogen bonds

between β -LG and sugar residues of QS are formed, which account for the increased viscoelasticity.

The question remains whether mixtures of QS and β -LG also form viscoelastic films at the oil/water-interface and how film properties affect the stability of emulsions. There are substantial differences in the adsorption of proteins at the oil/water-interface compared to the air/water-interface in general, and for β -LG in particular (Zare *et al.* 2016). As recently reviewed by Zhai *et al.* (2013) a significant increase in understanding of the unfolding and molecular mechanisms of adsorption of β -LG was achieved in the last couple of years but still the process is not fully understood, yet. The main driving force for the unfolding of β -LG at the interface is the re-orientation of the hydrophobic sites of the molecule towards the oil phase. To characterize the conformation of β -LG at the oil/water-interface, different techniques were used in the past, like Fourier transform infrared (FTIR) spectroscopy, far-UV circular dichroism (CD) spectroscopy and synchrotron radiation circular dichroism (SRCD). β -LG loses its tertiary structure upon adsorption, but the secondary structure including α -helices and β -sheets are preserved to a great extent depending on the hydrophobicity of the oil phase. It was concluded that structural rearrangements are more pronounced at the less polar interface n-alkane/water (e.g. tetradecane) than at more polar interface triglyceride/water.

Based on the considerations above it must be assumed that interactions between QS and β -LG at the oil/water-interface significantly differ from those at the air/water-interface (Maldonado-Valderrama and Patino 2010). Aim of the present study therefore was to characterize the interaction between QS and native β -LG at the MCT-oil/water-interface with respect to adsorption and interfacial rheology. In a second part, emulsions stabilized by blends of QS and native β -LG are prepared to evaluate the impact of interfacial interactions on emulsion properties. Interfacial properties of binary mixtures and the individual substances are determined using dynamic two-fluid needle analysis, dynamic interfacial tension measurement as well as dilational and shear rheology for characterization of the interfacial film. Interfacial microstructure in dilational experiments is qualitatively and quantitatively characterized by Lissajous-plots. In addition, emulsification trials are performed for the individual constituents and binary mixtures using high-pressure homogenization. Emulsions are characterized with respect to oil droplet size, ζ -potential and emulsion stability after seven days.

III-3 Material and methods

III-3.1 Materials

In the present study, a commercial saponin extract from the bark of the soap bark tree *Quilaja saponaria* Molina (QS) was used, which was kindly provided by Ingredion Germany GmbH (Hamburg, Germany). Solid phase extraction on a C-18 column (10 g/70 mL Thermo Scientific) was used to purify the saponin extract, as described in Böttcher *et al.* (2016). As Keppler *et al.* (2014a) described, native undenatured β -Lactoglobulin (β -LG) was isolated from whey protein isolate (Fonterra DSE 6668). Medium-chain triglyceride oil (MCT-oil) WITARIX® MCT 60/40 was purchased from CREMER OLEO GmbH & Co. KG (Hamburg, Germany). Surface active constituents in the MCT-oil were removed through adsorption onto magnesium silicate (Florisil®, Sigma-Aldrich GmbH, Seelze, Germany).

All aqueous solutions were prepared in 10 mM potassium phosphate buffer (pH 7) and continuously stirred at room temperature for at least 8 h. For all experiments QS concentration was fixed at 0.005 %wt. Four different concentrations of β -LG were chosen: 0.005, 0.01, 0.05 and 0.1 %wt. The low β -LG-concentration of 0.005 and 0.01 % as well as their mixtures with QS will be referred to as ' β -LG_{low}' and 'QS/ β -LG_{low}', respectively. In the same manner the high β -LG-concentration of 0.05 and 0.1 % will be referred to as ' β -LG_{high}' and the mixture with QS as 'QS/ β -LG_{high}' throughout the whole manuscript.

III-3.2 Drop shape analysis of adsorption, dynamic interfacial tension and dilational rheology

Dynamic interfacial tension was measured by pendant drop tensiometry (contact angle meter OCA-20, DataPhysics Instruments GmbH, Filderstadt, Germany). MCT-oil was poured in a glass cuvette and a droplet of surfactant solution (28 μ L) was generated through a needle immersed into the MCT-oil. Drop shape was recorded with a frame rate of five frames per minute for 20 min. Interfacial tension was calculated by fitting the Young-Laplace-equation to the drop shape according to Najmabadi *et al.* (2013).

Interfacial dilational rheology was studied using the above mentioned contact angle meter equipped with an oscillation unit ODG-20 and a slightly modified method as reported by Tamm & Drusch (2017). Briefly, a droplet of 32 μ L of the sample solution was manually generated in MCT-oil and allowed to equilibrate for 16 h. After equilibration an amplitude sweep ranging from 1.4 to 10 % deformation amplitude was performed at a frequency of 0.1 Hz. The interfacial dilational modulus E^* was calculated from the oscillation cycles.

The elastic modulus (storage modulus, E') and viscous modulus (loss modulus, E'') were derived from E^* . The phase angle Φ , which results from changes in interfacial tension due to area change, is calculated using $\tan \Phi = E''/E'$. At small Φ ($<45^\circ$) the interface is predominantly elastic ($E' > E''$), whereas at high Φ ($>45^\circ$) the interface shows more viscous ($E' < E''$) properties.

To get further insights in interfacial microstructure Lissajous-plots of the amplitude sweep were analyzed. Therefore, the change in interfacial tension described via the surface pressure $\Pi = \sigma - \sigma_0$ (stress) was plotted against the area change $\Delta A/A_0$ with $\Delta A = A - A_0$ (strain) for different amplitudes. A_0 represents the interfacial area at strain 0 and A the area at a certain strain. A Lissajous-plot is considered as a fingerprint of an interface, which shows the response of the interfacial layer to compression and expansion (Sagis and Fischer 2014). Data were quantified by calculating the strain-stiffening ratio S as defined by Ewoldt *et al.* (2008) and extended by van Kempen *et al.* (2013) for dilational experiments. Dilational extension is described by $S_{ext} = (E_{LE} - E_{ME})/E_{LE}$ and compression by $S_{com} = (E_{LC} - E_{MC})/E_{LC}$, where E_L is the large strain modulus and E_M is the minimum strain modulus. The subscripts 'E' and 'C' refer to extension and compression, respectively. All variables are slopes derived from the Lissajous-plot, where E_M is obtained at a strain of 0 and E_L at maximum strain. A detailed description and visualization of the method was published by van Kempen *et al.* (2013). Interpretation of S is as follows: at $S=0$ the interfacial layer shows either linear elastic or linear viscoelastic behavior. The latter is characterised by an elliptic shape of the Lissajous-plots (widening between compression and expansion curve). When $S \neq 0$ the interfacial layer has non-linear viscoelastic properties. Furthermore, $S < 0$ indicates non-linear behavior due to strain-softening and at $S > 0$ the reason is strain-stiffening of the interfacial layer upon compression or expansion.

For experiments on adsorption a two-fluid needle method developed in our group was used as it has previously been reported (Böttcher *et al.* 2016). Briefly, a droplet of buffer solution (28 μL) was generated at the tip of a needle with an inner diameter of 1.65 mm. A second needle with an inner diameter of 0.5 mm is inserted within the first needle and a drop of surfactant solution (2 μl) is injected into the buffer droplet using the dosing unit of the contact angle meter. Movement of the emulsifier through the droplet is characterized by the so-called lag-time, i.e. the time until surface pressure for the first time differs from zero. It must be emphasized that this movement must not be interpreted as diffusion. Adsorption from the subsurface (liquid layer adjacent to the interface, Fainerman *et al.* 2001) to the interface is described by Π_{2s} .

III-3.3 Interfacial shear rheology at the oil/water-interface

Shear experiments were performed using a Physica MCR301 rheometer (Anton Paar Germany GmbH, Ostfildern, Germany) equipped with a biconus for interfacial rheology. An aliquot of 120 mL of the individual sample solution was poured into a cell and bubbles were removed from the interface. Afterwards the biconus was placed directly at the interface and covered with 100 mL purified MCT-oil. Film formation was monitored by applying a strain amplitude γ_0 of 0.1 % and frequency f of 1 Hz to the interfacial film every 5 min. Samples were measured at 25°C. In a similar manner as described for the dilational rheology, viscoelastic properties of the interface may be described as complex shear modulus G^* , the elastic modulus (G') and viscous modulus (G'').

III-3.4 Emulsification and emulsion stability

Oil-in-water emulsions were prepared in two subsequent steps. At first, solutions of QS, β -LG and mixtures of both constituents were prepared 16 h prior to emulsification, 20 % purified MCT-oil containing 0.01 % oil red O (a hydrophobic dye) was added and a coarse emulsion was prepared by using a rotor-stator system (Ultra-Turrax T25 basic, IKA -Werke GmbH & CO. KG, Staufen, Germany) at 13,500 rpm for 30 s. In the second step, the coarse emulsion was homogenized in a high-pressure homogenizer (Panda 2K, Niro Soavi Deutschland, Lübeck, Germany) at 600 bar with 4 passes. An aliquot of the emulsions was transferred into graduated test tubes. Stability was checked after 7 days both, visually as well as via light microscopy at 400-fold magnification.

III-3.5 Determination of oil droplet size distribution and ζ -potential

The oil droplet size distribution was determined by static light scattering (Horiba LA-950, Retsch Technology GmbH, Haan, Germany). A droplet of the emulsion was diluted in mono-distilled water. The pump of the measuring device was set to 8 and the stirring unit to 3. A refractive index of 1.45 was used for the calculation for all samples. The oil droplet size distribution is reported based on the volume distribution. Different percentiles of the oil droplet size distribution (d_{10} , d_{25} , d_{50} , d_{75} and d_{90}) are displayed as a box plot to facilitate comparison between the samples. The ζ -potential was determined using a Nano Zetasizer ZS from Malvern Instruments GmbH (Herrenberg, Germany). Emulsions were diluted 1:100 and measured in clear disposable cells (DTS 1060 C, Malvern Instruments GmbH).

III-4 Results

III-4.1 Adsorption and dynamic interfacial tension at the oil/water-interface as determined by drop shape analysis

Movement of QS through the droplet was very fast as indicated by a short lag-time of 2.8 s. In addition, surface pressure increased fast as shown by the Π_{2s} -value of 12.9 mN/m (Figure III-1). In contrast, β -LG showed a rather long lag-time and surface pressure was comparably low after 2 s (low Π_{2s} -values). For β -LG, with increasing concentration lag-time decreased from 34.4 s to 6.3 s and surface pressure (Π_{2s}) increased from 2.7 to 7.8 mN/m. Adsorption from the subsurface to the oil-water interface of mixtures of QS/ β -LG (as indicated by the surface pressure Π_{2s}) was dominated by QS. In addition, movement of the binary mixture of QS/ β -LG through the droplet (described by the lag-time) was distinctively slowed down in the presence of β -LG compared to the lag-time of QS.

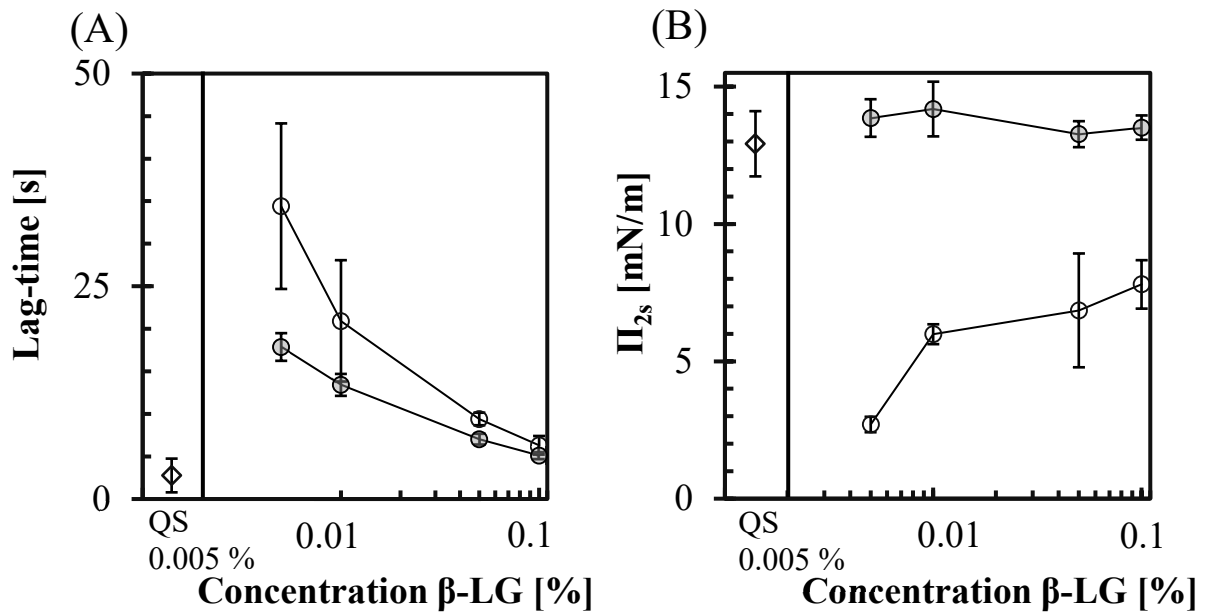


Figure III-1 Results of A) lag-time and B) surface pressure after 2 s of adsorption (Π_{2s}) in relation to the β -LG concentration of 0.005 % QS (◇), β -LG (○) and mixtures of 0.005 % QS and β -LG (●) at the MCT-oil/water-interface

As presented in Table III-1 QS efficiently lowered the dynamic interfacial tension after 20 min (12.6 mN/m) to a lower value than even the highest β -LG concentration (13.7 mN/m). In mixtures of QS/ β -LG interfacial tension was slightly lower than for individual QS or β -LG samples.

Table III-1 Dynamic interfacial tension (IFT) of β -LG-solutions and β -LG/QS-mixtures measured for 20 min with pendant drop analysis at the oil/water-interface

c_{QS} [%wt]	c_{BLG} [%wt]	β -LG/QS [%wt/%wt]	IFT [mN/m]
0	0.005		15.6 ± 0.1
	0.01		14.4 ± 0.1
	0.05		13.6 ± 0.0
	0.1		13.7 ± 0.0
0.005	0		12.6 ± 0.1
	0.005	1	12.7 ± 0.1
	0.01	2	12.4 ± 0.1
	0.05	10	12.1 ± 0.1
	0.1	20	12.0 ± 0.0

III-4.2 Dilational rheology determined by droplet oscillation and analysis of non-linear phenomena of interfacial layers

Via compression and expansion experiments (dilational rheology) it is possible to characterize the interfacial layer with respect to interfacial rearrangements and exchange processes between the bulk and the interface (Miller *et al.* 1996; Freer *et al.* 2004). The interfacial layer of QS showed a lower interfacial dilational modulus E^* and was more viscous than interfacial layers consisting of β -LG. Mixed interfacial layers of QS/ β -LG were rather viscous, which was similar to interfaces of QS, but E^* increased with increasing β -LG-concentration. When comparing the interfacial dilational modulus E^* (see Figure III-2) it becomes obvious that QS had a very low E^* of 15 mN/m. With increasing β -LG-concentration E^* increased from 51 to 68 mN/m. In mixtures of QS/ β -LG with up to 35 mN/m, E^* was lower than E^* of an interface solely occupied by β -LG.

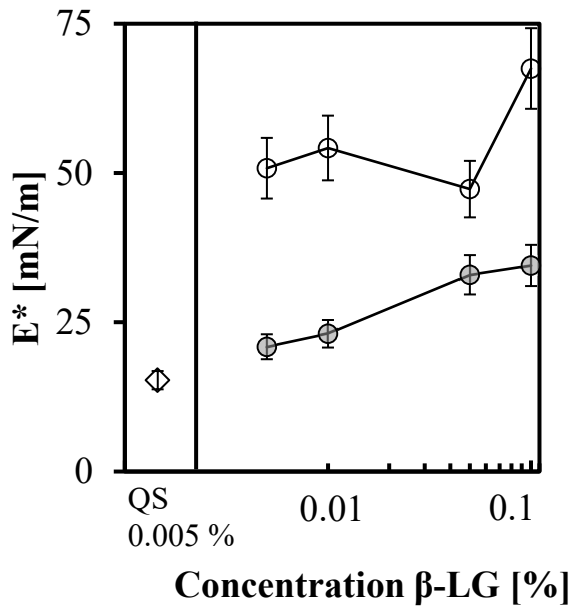


Figure III-2 Interfacial dilational modulus E^* in relation to β -LG-concentration determined by dilational oscillation at $f=0.1$ Hz, 2.8 % amplitude of 0.005 % QS (\diamond), β -LG (\circ) and mixtures of 0.005 % QS and β -LG (\bullet) at the MCT-oil/water interface. Error bars represent 10 % deviation, which was determined in previous experiments.

No distinctive reduction in E^* was found with increasing amplitude (data not shown) indicating that the interfacial layer was still intact and may only rupture at higher amplitudes as reported by Wan *et al.* (2016). In Figure III-3 the phase angle Φ is displayed versus the deformation amplitude $\Delta A/A_0$. The phase angle was very similar for all β -LG samples independent from the concentration. The low value of approximately 7° indicates a highly elastic interfacial film. In contrast with approximately 40° , the phase angle of QS was rather

high. The interfacial film still is predominantly elastic, but also has a high viscous modulus. Mixed interfacial films consisting of QS/ β -LG also showed a high phase angle, but with increasing β -LG concentration, Φ decreased (elastic properties were higher).

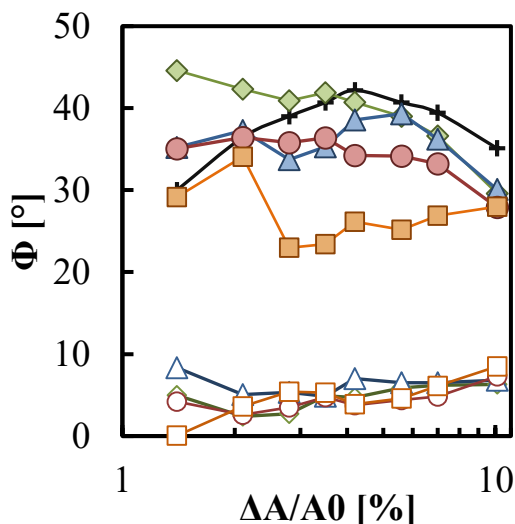


Figure III-3 Phase angle Φ in relation to area change $\Delta A/A_0$ determined by dilational oscillation at $f=0.1$ Hz at the MCT-oil/water interface of 0.005 % QS (+), 0.005 % β -LG (\diamond), 0.01 % β -LG (Δ), 0.05 % β -LG (\circ), 0.1 % β -LG (\square); filled symbols indicate β -LG is mixed with 0.005 % QS

In Figure III-4 the Lissajous-plots of QS, β -LG and mixtures of both are displayed at different amplitudes. Lissajous-plots were elliptic and thus showed a linear-viscoelastic behavior for QS and β -LG as well as their mixtures at low amplitude. Non-linear behavior in form of strain-stiffening, was detected in mixed interfacial films consisting of QS/ β -LG at a high amplitude. At the lowest amplitude (1.4 %) random scattering occurred and negatively affected the interpretation of the graphs for all samples. At an intermediate amplitude of 2.8 % the plots became more meaningful and all Lissajous plots showed an elliptic shape when oscillated. At a high amplitude (4.2 and 7.0 %) all graphs except β -LG revealed an asymmetric shape with strain-stiffening behavior upon expansion. There were marked differences between the sinusoidal response of β -LG, QS and the mixed interfacial layers. When interfacial layers with QS and mixtures of QS/ β -LG were oscillated a widening between compression and expansion curve occurred, which was absent in β -LG layers. In mixed interfacial films of QS/ β -LG non-linearity decreased with increasing β -LG-concentration and the shape of the Lissajous plot approached the form of the plot of β -LG.

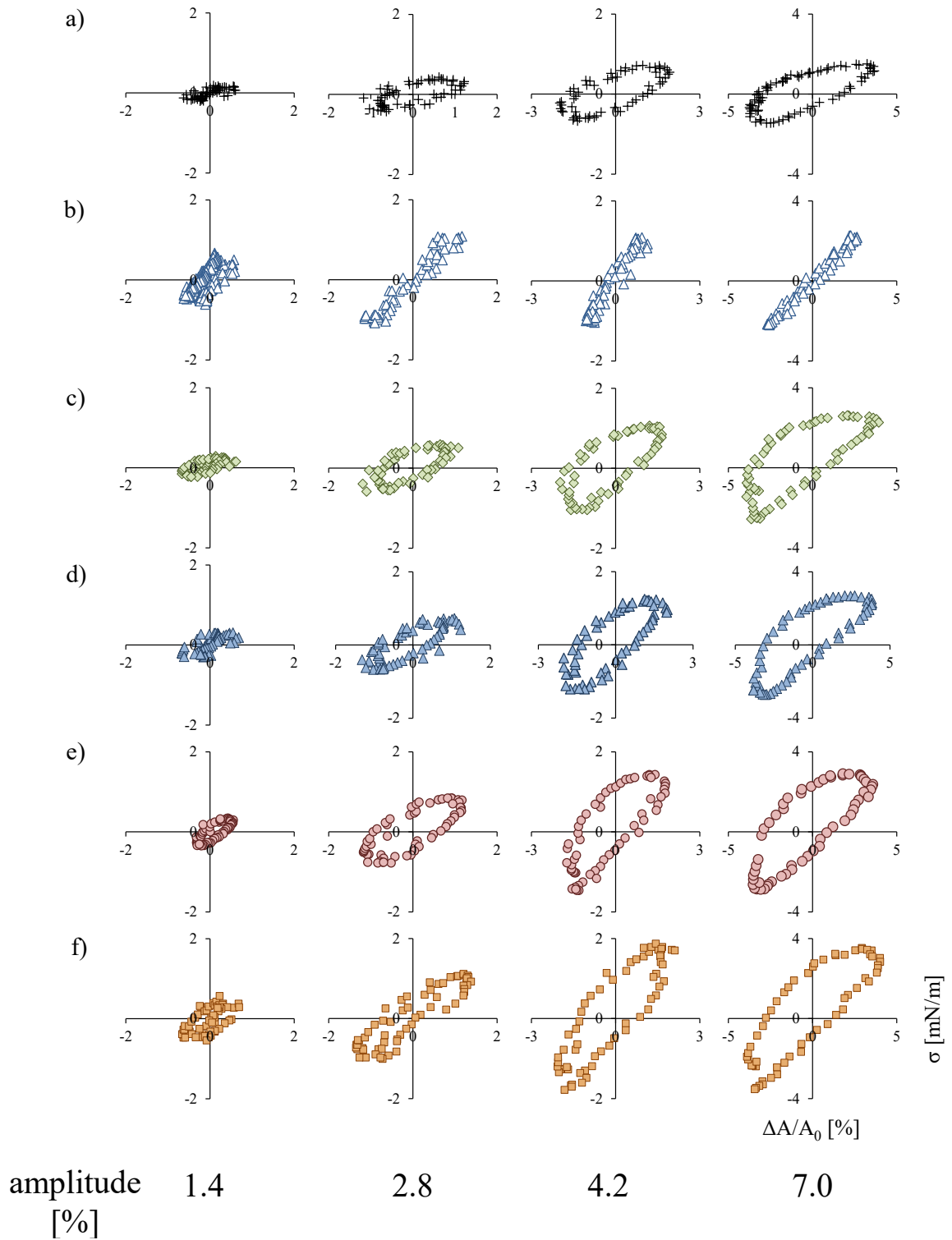


Figure III-4 Interfacial tension σ versus area change $\Delta A/A_0$ (Lissajous-plots) determined by dilational oscillation at $f=0.1$ Hz at different amplitudes 1.4, 2.8, 4.2 and 7.0 % at the MCT-oil/water interface of a) 0.005 % QS (+), b) 0.01 % β -LG (Δ), c) 0.005 % QS+0.005 % β -LG (\blacklozenge), d) 0.005 % QS+0.05 % β -LG (Δ), e) 0.005 % QS+0.05 % β -LG (\bullet), f) 0.005 % QS+0.1 % β -LG (\square)

In Figure III-5 the evolution of the S-factor versus the amplitude is shown. No difference of the S-factor was found upon compression but substantial differences occurred upon expansion. At an amplitude higher than 4.2 % the S-factor for QS and mixtures of QS/ β -LG distinctively increased. There was a concentration dependence of the S-factor in mixtures of QS/ β -LG: at low β -LG-concentration the increase of the S-factor at high amplitude was more pronounced than at high β -LG-concentration.

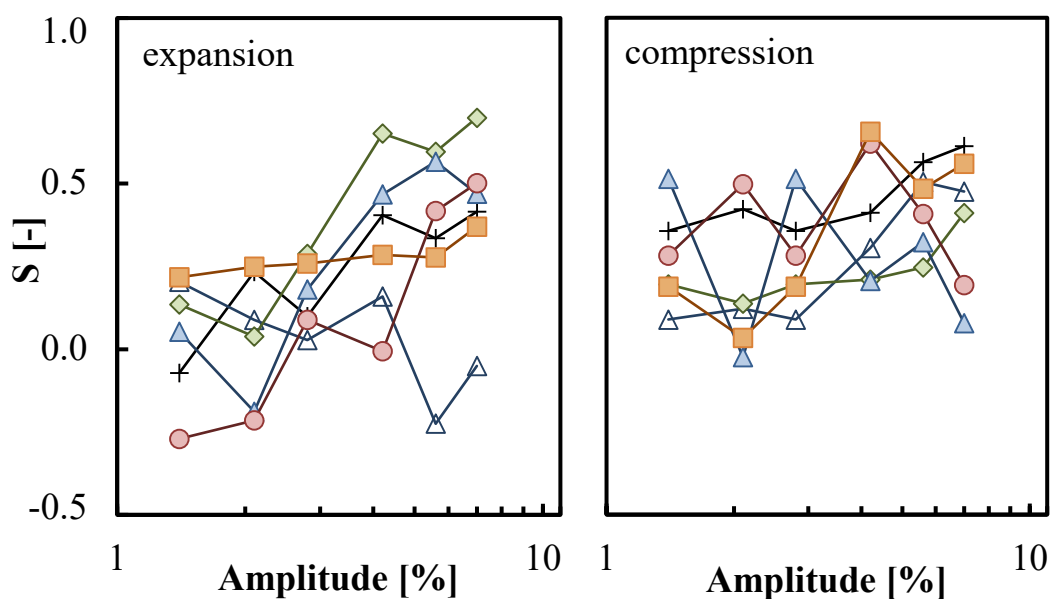


Figure III-5 S-factor versus amplitude during expansion (left panel) and compression (right panel) of a droplet at the oil/water-interface determined by dilational oscillation at $f=0.1$ Hz of 0.005 % QS (+), 0.005 % β -LG (\diamond), 0.01 % β -LG (Δ), 0.05 % β -LG (\circ), 0.1 % β -LG (\square); filled symbols indicate β -LG is mixed with 0.005 % QS

III-4.3 Shear rheology of interfacial layers

Experiments on shear rheology give insights in lateral intermolecular interactions between molecules. Results of shear rheological experiments supported the results from dilational rheological experiments. In Figure III-6 the complex (G^*), elastic (G') and viscous (G'') moduli of all samples are presented. The interfacial layer of QS showed a very small G^* of 7.4 mN/m with a high viscous modulus G'' of 4.9 mN/m. G^* of the interfacial layer of β -LG and binary mixtures of QS/ β -LG as well as the viscous contribution increased with increasing β -LG-concentration. For the highest β -LG-concentration in mixtures of QS/ β -LG ratio of G''/G' was 0.56 in contrast to interfacial layers solely prepared with β -LG, which had a ratio of G''/G' of 0.30.

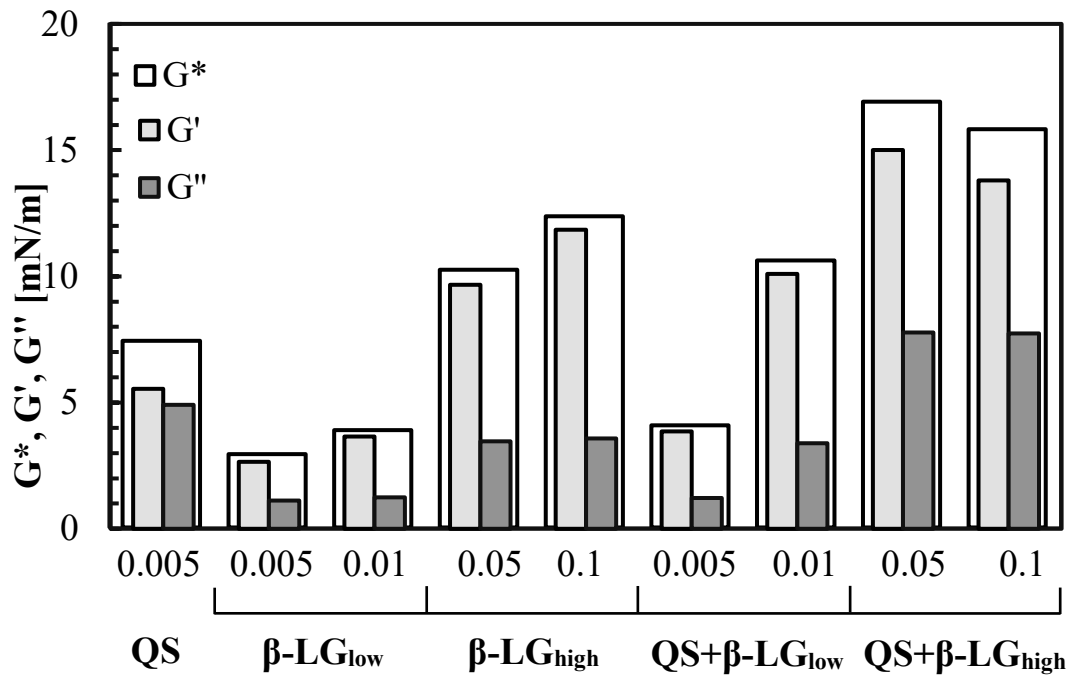


Figure III-6 Complex (G^*), elastic (G') and viscous (G'') shear moduli for 0.005 % QS; 0.005, 0.01, 0.05 & 0.1 % β -LG and 0.005 % QS mixed with 0.005, 0.01, 0.05 & 0.1 % β -LG (from left to right) at the MCT-oil/water-interface measured with $f=1$ Hz, deformation=0.1% after 9 h of film formation

III-4.4 Oil droplet size distribution of emulsions as determined by static light scattering

The emulsion prepared with QS exhibited a narrow oil droplet size distribution with a low median (d_{50}). In contrast, emulsions stabilized with β -LG had a comparably broad oil droplet size distribution and a high d_{50} . In mixtures of QS/ β -LG the d_{50} decreased with increasing β -LG-concentration and led to distinctively smaller oil droplets compared to emulsions made of QS. In Figure III-7 the oil droplet size distribution for all samples is summarized. The median of the oil droplet size distribution for β -LG-stabilized emulsions ranged from 21.3 to 9.0 μm for a β -LG concentration of 0.005 and 0.1 %, respectively. The median of the oil droplet size distribution of the QS-emulsion was markedly lower with a d_{50} of 4.1 μm . In binary mixtures of QS/ β -LG with a β -LG concentration of 0.005 % the median was 2.5 μm and in mixtures with 0.1 % β -LG the median was reduced to 0.6 μm .

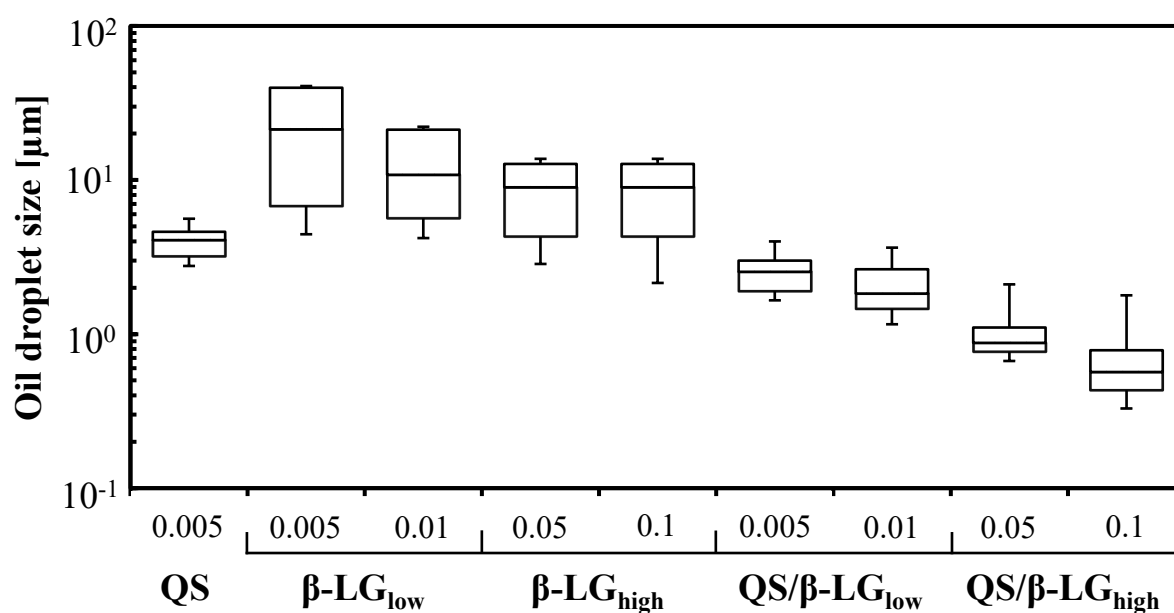


Figure III-7 Oil droplet size of emulsions prepared with 0.005 % QS (1st boxplot), 0.005...0.1 % β -LG (2nd to 5th boxplot) and mixtures of 0.005 % QS and 0.005...0.1 % β -LG (6th to 9th boxplot) with upper whisker representing d_{90} , upper box end d_{75} , dash in the box d_{50} , lower box end d_{25} and lower whisker d_{10}

III-4.5 ζ -potential of the emulsion droplets

In binary mixtures of the two emulsifiers at high β -LG-concentration ($\text{QS}/\beta\text{-LG}_{\text{high}}$) the ζ -potential was similar to emulsions stabilized with β -LG. In contrast, in emulsions stabilized with binary mixtures with low β -LG concentration ($\text{QS}/\beta\text{-LG}_{\text{low}}$) the ζ -potential was dominated by QS. In Figure III-8 the ζ -potential of emulsions with QS, β -LG and mixtures of QS/ β -LG are shown. The ζ -potential of all emulsions in the present study was lower than -30 mV. With increasing β -LG concentration the ζ -potential decreased from -51.1 to -67.1 mV for emulsions with 0.005 % to 0.1 % β -LG, respectively.

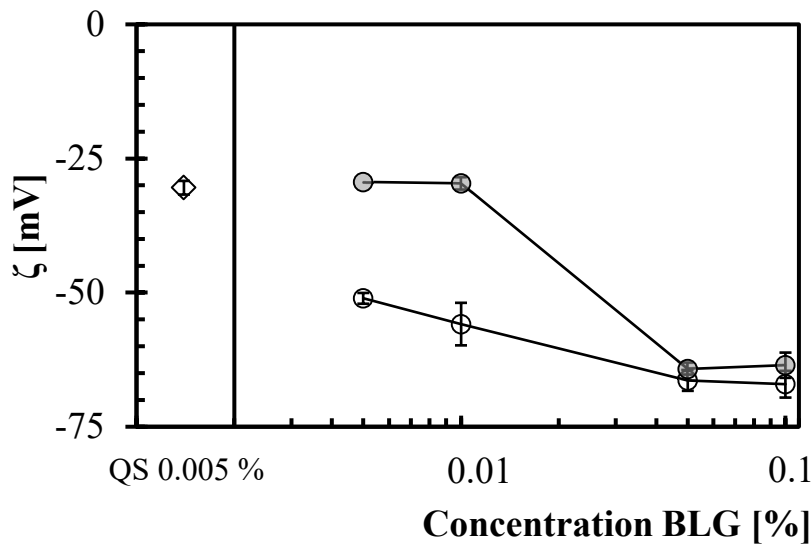


Figure III-8 ζ -potential in relation to the β -LG concentration of emulsions (600 bar, 4 passes, 5 % MCT-oil) with 0.005 % QS (◇), β -LG (○) and mixtures of 0.005 % QS and β -LG (●)

III-4.6 Visual analysis of emulsion stability after a storage time of 7 days

Emulsion stability was evaluated visually as presented in Figure III-9. Different kinds of destabilization mechanisms were observed in the analyzed emulsions. Coalescence is indicated by a continuous red oil layer on top of a serum layer. In contrast, creaming is characterized by color differences between upper and lower phase without clear phase separation and thus varying difference in color intensity. In the emulsion prepared with QS, destabilization was mainly due to creaming and to a small portion caused by coalescence. Similar phase separation by creaming was observed for β -LG_{high}-emulsions. In contrast, β -LG_{low} and QS/ β -LG_{low}-emulsions were mainly destabilized by coalescence.

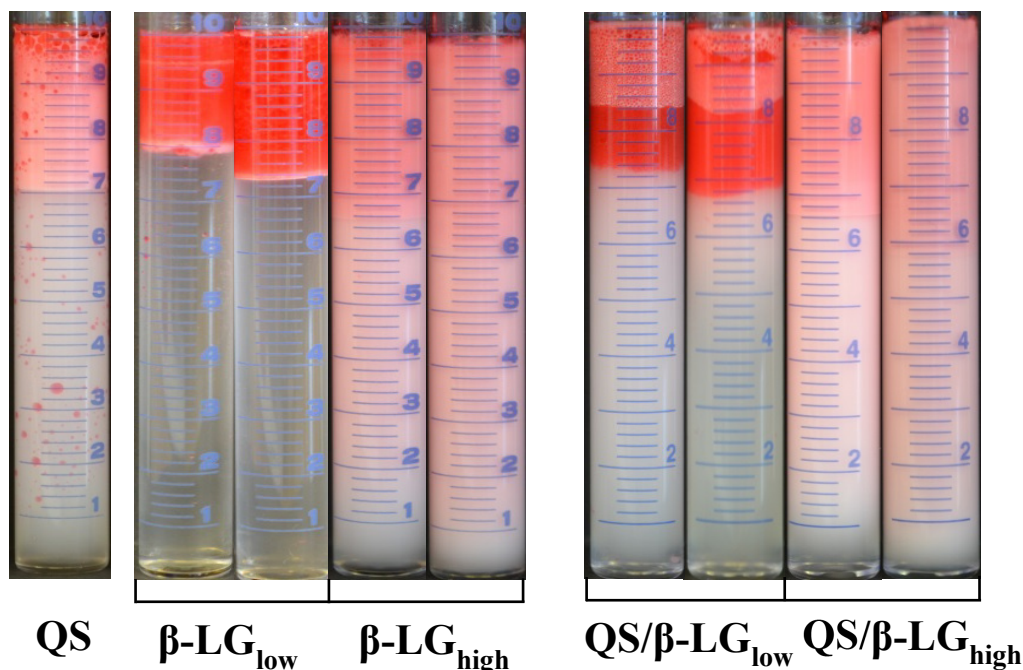


Figure III-9 Photographic images of emulsions prepared with 0.005 % QS; 0.005, 0.01, 0.05 & 0.1 % β -LG and 0.005 % QS mixed with 0.005, 0.01, 0.05 & 0.1 % β -LG (from left to right) after 7 days of storage

III-5 Discussion

In the first part of the discussion the interfacial properties of binary mixtures of QS and β -LG at the oil/water-interface are compared with the corresponding properties of the individual constituents. Afterwards, results of emulsion experiments are discussed with particular focus on emulsion stability.

Based on the model of Ward and Tordai (1946) the time dependence of the interfacial tension of solutions on a time-scale of a few seconds was analyzed in two-fluid needle experiments. Data are presented as time interval until surface pressure starts to increase (lag-time) and surface pressure after two seconds (Π_{2s}). The lag-time of QS was low and surface pressure after 2 s was high as it is generally expected for a low molecular weight emulsifier. QS (~2 kDa) is smaller than β -LG and therefore shows an increased mobility in the aqueous environment and adsorbs from the subsurface to the interface (see Figure III-1). In comparison, β -LG (18 kDa) exhibited a slower movement through the droplet and a lower surface pressure. These results reflect the typical behavior of globular proteins, where adsorption expressed as surface pressure is retarded due to slow adsorption kinetics and unfolding. The surface pressure after 2 s of mixtures of QS/ β -LG was similar to QS, but the lag-time was distinctively higher than the lag-time of QS. In a previous publication, we postulated (based on fluorescence experiments) a complex formation between β -LG and QS (Böttcher *et al.* 2016). By performing fluorescence experiments it is possible to determine non-covalent binding sites of β -LG. As Keppler *et al.* (2014b) reported it is advisable to use the Cogan-Plot for analyzing the fluorescence results because the parameter ‘maximum number of binding sites’ is relatively stable compared to other methods. As reported in the previous paper a maximum of 1.7 binding sites was determined between QS and β -LG, which can be derived from the inverse slope of the Cogan-Plot (see Figure III-10).

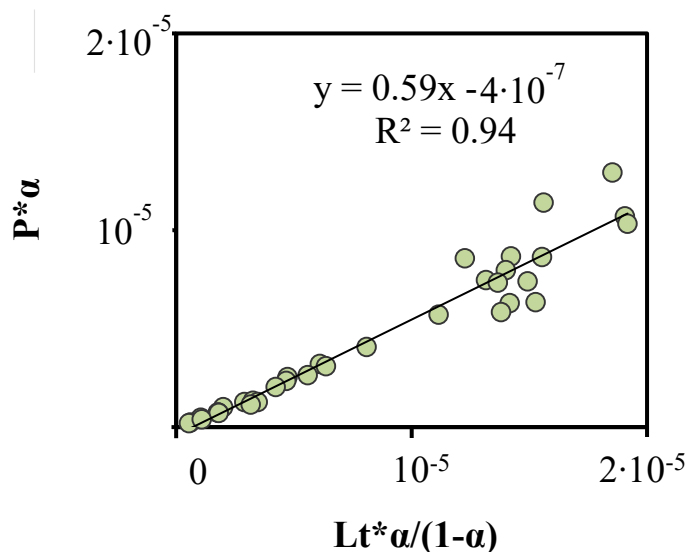


Figure III-10 Fluorescence measurements on the interactions of β -LG and QS showing results of the Cogan-Plot with $P=\beta$ -LG-concentration, α =fraction of free binding sites and L_t =QS-concentration. Adapted from Böttcher *et al.* (2015) with permission from Elsevier.

It is possible that movement through the droplet is slowed down by a size increase due to this complex formation. Although QS has only 10 % of the molecular mass of β -LG the hydrodynamic radii are quite similar. The hydrodynamic radii were reported before as 1.5 nm (Böttcher und Drusch 2016) and 2.5 nm (Taulier and Chalikian 2001) for QS and β -LG, respectively. It is more likely that the amount of free QS molecules is reduced because QS molecules reversibly bind to β -LG or movement is slowed down by steric hindrances. As shown before for the adsorption at the air-water interface (Böttcher *et al.* 2016), these complexes formed in the bulk do not influence the adsorption from the sub-surface as indicated by a similar surface pressure for QS and mixtures of QS/ β -LG in the present study.

In addition, it needs to be discussed why in two fluid needle experiments on interfacial adsorption differences in lag-time between QS and binary mixtures of QS/ β -LG at the oil/water-interface did not occur when analyzing the lag-time at the air/water-interface (Böttcher *et al.* 2016). Complex formation occurs in the bulk of the aqueous phase and therefore it is unlikely that the formation is affected by the type of hydrophobic phase. It is rather assumed that differences in lag-time were not large enough to unambiguously differentiate between QS and mixtures of QS/ β -LG in the experimental setup at the air/water-interface. Lag time was generally lower in the cited study and thus a “lower resolution” occurred, which may be attributed to a smaller droplet volume of 14 μ L in the study on the

adsorption behavior at the air/water-interface compared to 28 μL in the present study. A large droplet diameter in the experimental setup is only possible when the hydrophobic phase sufficiently increases buoyancy of the droplet. In contrast, a small droplet diameter results in a reduced distance from the inside of the droplet to the interface and thus a reduction in lag-time.

Upon prolonged measuring time, QS still dominated interfacial tension in mixtures of QS and β -LG as indicated by results of dynamic interfacial tension (see Table III-1). The results are in agreement with data from Piotrowski *et al.* (2012), who reported only slightly lower values for the dynamic interfacial tension in mixtures of QS/ β -LG in comparison to QS.

In dilational and shear experiments interfacial layers of β -LG showed more resistance against deformation (as indicated by high values for the complex moduli E^* and G^*) with a higher elastic modulus in comparison to an interfacial QS layer (see Figure III-2 & Figure III-6). Mixed interfacial layers of QS and β -LG were less viscoelastic (lower complex moduli) at the oil/water-interface compared to the air/water-interface (Böttcher *et al.* 2016). In the present study interfacial layers from binary mixtures of QS/ β -LG exhibited high viscous moduli (E'' and G'') resulting in relatively high Φ and $\tan \delta$ similar to QS.

Lissajous-plots were analyzed to get more insights into the rheological behavior of interfaces. The use of Lissajous-plots as an instrument for rheological characterization of interfacial films subjected to dilational stress is rather new in food-oriented disciplines. Lissajous-plots may be used to determine the viscoelastic regime (Sagis and Fischer 2014) and/or microstructure of interfacial films (Wan *et al.* 2016).

In general, Lissajous-plots illustrate the stress (interfacial tension) versus strain (area change) for the oscillation cycles. Within these plots viscoelastic behavior during expansion and compression is distinguished. In a linear regime, interfacial tension oscillates sinusoidal over time when low amplitudes/area changes are applied. A symmetrical diverge in the Lissajous-plot (widening between compression and expansion curve) indicates viscous properties of the interface (Sagis and Fischer 2014). When area changes become too high, non-linear behavior may occur. Non-linear behavior is reflected by non-elliptic curves upon compression and/or expansion. The response of the interface becomes irregular and varies distinctively from the sinusoidal form. However, dilational moduli are still calculated from raw data by Fourier transformation by most programs regardless of non-linear viscoelastic behavior.

All samples showed linear viscoelastic behavior upon compression even at high amplitude, which may be deduced from a linear decrease in the Lissajous-plots and an S-factor equal to zero (see Figure III-3 & Figure III-5). During expansion clear differences between samples were visible. Expansion of β -LG-interfaces at low and high amplitudes did not result in a change in the shape of the Lissajous-plot or the S-factor. When a QS-stabilized interface was subject of a sinusoidal deformation, beginning of strain stiffening was detectable upon expansion at higher amplitude as indicated by $S > 0$. For mixtures of QS/ β -LG a marked increase of the S-factor upon expansion was determined with increasing amplitude, which indicates strain stiffening like in QS-layers. Mixed interfacial layers of QS/ β -LG generally showed a similar widening between compression and expansion curves as QS (see Figure III-4), which indicates viscoelastic behavior. However, in contrast to QS the response of the mixed films was non-linear. At the beginning of the expansion a steep increase (lower left quadrant) of the interfacial tension with only small change in interfacial area was detected, which shows that the interfacial network initially restrains the area expansion (but not the volume expansion). The interfacial network opposes the area expansion but because additional solution is pumped into the droplet the droplet shape is changing into a more spherical shape. It can be hypothesized that the mixed film cannot rapidly react to the increase in volume (expansion) because of increase stiffness. This might be due to an increased cohesion/interaction between the molecules, which may be caused by prior compression. From this observation it can be concluded that the interfacial packaging of β -LG is distinctively changed by the presence of QS.

After discussing interfacial properties we focus on stability of emulsions prepared with QS, β -LG and their mixtures in the second part of the discussion. Emulsion stability is a complex matter where various destabilization phenomena, like creaming, Ostwald-Ripening, coalescence and aggregation may simultaneously happen (Walstra 2003). As described by Stokes' law, velocity of creaming of oil droplets increases with an increase in the difference in density between continuous and dispersed phase or oil droplet size, and decreases with increasing viscosity of the continuous phase. Intermolecular interactions resulting from attractive van der Waals forces and (in the case of two oil droplets in a macro-emulsion) repulsive electrostatic forces affect aggregation as well as steric hindrance (in the case of high molecular weight emulsifiers). Both may prevent aggregation and coalescence of oil droplets. As reviewed by Heurtault *et al.* (2003) with increasing ζ -potential electrostatic

repulsion between droplets increases, which is one factor preventing aggregation of oil droplets. In general, emulsions with an absolute ζ -potential below 30 mV may be prone to aggregation due to insufficient electrostatic repulsion. In contrast, an absolute ζ -potential higher than 60 mV is considered ideal and is associated with long-term kinetic stability as a result of high electrostatic repulsion. The ζ -potential of all emulsions in the present study was lower than -30 mV, indicating that electrostatic repulsion will support kinetic stability of the samples (see Figure III-8).

In general, use of QS as an emulsifier results in emulsions with sufficiently small oil droplets as shown in different studies on saponin-based nanoemulsions (Bai *et al.* 2016; Kaur *et al.* 2016). However, in the present study a concentration of QS was chosen, that did not yield emulsions with long-term kinetic stability. This was done on purpose to ensure that positive effects on droplet size reduction and/or kinetic stability by addition of β -LG become obvious. As a consequence, the mean oil droplet size of the QS-emulsion was rather large and emulsions were prone to creaming.

Net repulsion as indicated by the ζ -potential is usually considered to prevent aggregation. A negative ζ -potential (-30 mV) of QS emulsions was reported before by several authors and was attributed to the carboxylic group in the molecular structure of Quillaja saponin (Yang *et al.* 2013; Zhang *et al.* 2016; Maier *et al.* 2015b). Zhang *et al.* (2016) used a different Quillaja saponin extract but reported similar ζ -potential values of about -30 mV at pH 7. Using a similar QS extract like in the present study, Yang *et al.* (2013) reported an even lower ζ -potential for emulsions prepared with QS of -70 mV at pH 7. Differences in ζ -potential may be linked to the purification process applied in the present study. Emulsions prepared with crude, non-purified saponin extract had a ζ -potential of -50 mV at pH 7 (results not shown). It is clear that the ζ -potential of QS extracts is not only caused by saponin molecules but to a high extent by negatively charged organic compounds other than saponins in the extract. These compounds may adsorb at the interface, which influences net charge of the oil droplets. Phenols may be present at the droplet interface because of interactions between adsorbed phenolic compounds and saponins. As Toppel *et al.* (2017) showed, hydrophilic phenolic compounds are partially removed during purification, but a certain proportion is still present. These anionic residues are phenolic compounds like (+)-piscidic acid, syringic acid and p-coumaric acid (Maier *et al.* 2015a; Toppel *et al.* 2017).

However, since the QS content in the emulsions was below the CMC and not sufficient to completely cover the droplet surface, electrostatic repulsion did not prevent aggregation.

In general, a Weber number may be calculated by comparing external stress in the creaming layer against internal stress given as the Laplace pressure, and one may decide, whether drops remain unformed or if a flat film between them will be formed. Close proximity of oil droplets, i.e. a thin film between close droplets, generally facilitates film rupture and may lead to coalescence as partially observed in the present study. A gradient in interfacial tension occurs as a consequence of a liquid flow during film-thinning and film rupture may occur through hole formation in the interfacial film and development of capillary waves. The latter are damped through intermolecular electrostatic repulsion and slow down coalescence.

Oil droplet size of β -LG_{low}-emulsions was rather high and oil droplets showed a negative ζ -potential. A large oil droplet size increases velocity of creaming as stated by Stokes' law. Although oil droplets had a negative ζ -potential of approximately -60 mV, rapid coalescence and subsequently complete phase separation (indicated by red top layer in Figure III-9) was observed. The reason again is an insufficient concentration of the emulsifier (here: β -LG). Large oil droplets increase the effective film radius upon aggregation. In combination with an insufficient protein load at the interface coalescence may rapidly occur. At high protein concentration (β -LG_{high}) coalescence was reduced due to a higher interfacial concentration at the interface, but creaming still occurred due to the large oil droplet size. Microscopic images showed no aggregation of oil droplets after 7 days of storage, which would occur upon bridging flocculation.

QS/ β -LG_{low}-emulsions showed creaming and partial coalescence, but no complete phase separation occurred (see Figure III-9). Although a higher content of emulsifier was present, QS/ β -LG_{low}-emulsions were more prone to coalescence than the QS-emulsion. But at the same time coalescence was less pronounced compared to β -LG_{low}. Interactions between QS and β -LG in bulk and at the interface and displacement of β -LG by QS have been described before (Böttcher *et al.* 2016). Non-covalent interactions between β -LG and QS (as reported for other β -LG systems) may change the tertiary and quaternary structure of the protein, as well as its structural flexibility, thereby altering the surface activity of the complex (Staszewski *et al.* 2014). However, the kind of interaction was not determined yet and it has to be kept in mind that β -LG undergoes structural changes upon adsorption at the oil/water-interface, which may alter the interactions between QS and β -LG (Dan *et al.* 2013). It can therefore be concluded that changes in dispersity may be attributed to interactions between QS and β -LG, which increases coalescence.

Visual appearance and stability of QS/ β -LG_{high}-emulsions was similar to β -LG_{high}-emulsions although oil droplet size in QS/ β -LG_{high}-emulsions was sufficiently smaller (see Figure III-7) and ζ -potential was very low. We therefore took microscopic images of all emulsions after one week and detected a large number of aggregates in QS/ β -LG_{high} (see Figure III-11C+D), which were not observed in mixtures with a low concentration of β -LG (see Figure III-11A+B). In all other emulsion samples, also for β -LG_{high} no aggregates were found (results not shown). The presence of aggregates decreases kinetic stability because velocity of creaming increases with higher oil droplet size as stated by Stokes' law. In a recent study on interactions of QS and β -LG and the impact on emulsion stability no aggregation was reported (Piotrowski *et al.* 2012). However, it has to be kept in mind that in the previously mentioned study the emulsion stability was analyzed only up to 2 hours and with sufficiently smaller β -LG-concentrations.

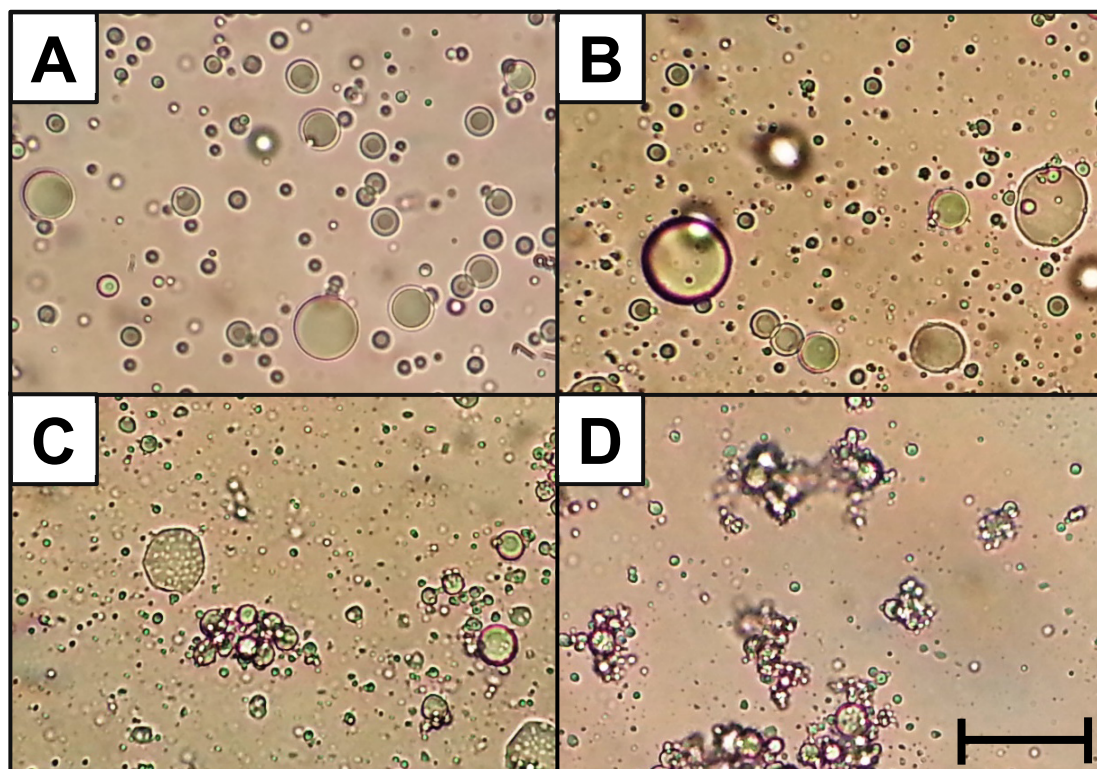


Figure III-11 Microscopic images of emulsions after 7 days of storage prepared with 0.005 % QS and A) 0.005 % β -LG, B) 0.01 % β -LG, C) 0.05 % β -LG and D) 0.1 % β -LG the black bar on the lower right represents 25 μ m

Different mechanisms may be responsible for aggregation in QS/ β -LG_{high}-emulsions. In general, the addition of a surfactant solution may increase the ionic strength by shielding of charged groups and thus weakening of electrostatic repulsion, which leads to aggregation. β -LG-stabilized emulsions can be prone to aggregation at moderate ionic strength of 150 mM due to electrostatic screening (McClements 2004). However, in the present study the increase in ionic strength and amount of di- or multivalent counter ions by the addition of QS extracts is negligible. Solutions prepared with 0.005 % QS in 10 mM phosphate buffer revealed the same conductivity as pure 10 mM phosphate buffer. As indicated by a low conductivity value for the QS-solution, electrostatic screening as a cause for aggregation can be excluded since ions were removed to a great extent during solid phase extraction. A second mechanism is aggregation due to depletion flocculation. Depletion flocculation describes a reversible phenomenon caused by excess protein in the aqueous phase. However, depletion flocculation at high protein concentration is considered very uncommon for β -LG (Dickinson 2010).

A third possible mechanism includes local electrostatic attraction. At neutral pH, QS and β -LG are both negatively charged similar to a system containing an anionic surfactant and β -LG. As it was emphasized before, QS has only a weak negative functional group (-COOH) and additional anionic residues in the QS extract lead to the highly negative ζ -potential. Interactions between two negatively charged surfactants/proteins can still occur, although interactions between counter charged surfactants/proteins are much more common (Hansted *et al.* 2011). β -LG has an overall negative charge at pH 7, but individual parts of the molecule are positively charged (Majhi *et al.* 2006) and offer reactive sites for the negative functional group of QS. Aggregation behavior between QS and the negatively charged egg lecithin was reported before presumably through hydrophobic attractive forces (Reichert *et al.* 2015).

In an additional experiment, we checked whether QS or β -LG facilitate aggregation between oil droplets. Therefore, an emulsion with a fixed concentration of 0.1 % β -LG was prepared and QS was added after emulsification to obtain a QS-concentration of 0.005/0.01/0.05 and 0.1 %. After few days of storage, substantial creaming was observed in all emulsions and the top layer of each emulsion sample was analyzed using light microscopy (results not shown). There were few aggregates in all β -LG-emulsions with added QS but there was no clear increase of the amount of aggregates with increasing QS concentration. It can be concluded that aggregation mainly occurs when both QS and β -LG are

present at the interface (homogenization of mixtures rather than adding QS after emulsification). The formation of aggregates upon addition of QS to a β -LG-emulsion may be attributed to slow displacement and structural changes of β -LG by QS, which leads to a mixed film. Protein displacement by surfactants is well described (Dan *et al.* 2012; Dan *et al.* 2015) and for QS and β -LG evidence was found at the air/water-interface (Böttcher *et al.* 2016).

III-6 Conclusions

The present study showed that interfacial and emulsion properties of QS may distinctively altered by the presence of beta-lactoglobulin (β -LG). Adsorption data (surface pressure after 2 s) indicate that interfacial adsorption of QS is not influenced by the presence of β -LG. When increasing concentration of β -LG in the binary mixture, data from the dynamic interfacial tension measurements confirm that the interfacial tension and thus interfacial composition is governed by QS. Interfacial layers of mixtures of QS and β -LG show a different rheological behavior compared to the air/water-interface, but still exhibit high dilational and shear moduli at the oil/water-interface. When mixed interfacial layers of QS/ β -LG were subjected to expansion, Lissajous-plots showed non-linear behavior and from the initial steep increase after start of expansion it can be concluded that a viscoelastic network is formed, which counteracts area expansion. This strengthens the lateral network as indicated by an increase in G^* , but weakens the film stability against stress upon interfacial expansion as it occurs in dilational rheology. Shear experiments also showed that mixed interfacial layers of QS/ β -LG had rather high viscous moduli. This strengthened the hypothesis that interfacial packaging is not ideal and upon shear and dilational deformation molecules cannot orientate as ideally, which leads to high loss of imposed energy. In emulsion experiments aggregation behavior was observed for mixtures of QS/ β -LG at high β -LG-concentrations, while the protein-based emulsions were stable. Aggregation therefore may be attributed to intermolecular interactions between QS and β -LG, which lead to structural changes of β -LG. The altered structure of β -LG may interact with native β -LG, which consequently leads to aggregation. QS/ β -LG-interactions in the bulk were detected before by fluorescence quenching. Aggregation of the emulsion droplets led to a decrease in the kinetic stability of the emulsions.

To get a better understanding of the behavior of QS at the interface, future studies should focus on *in situ* measurements like ellipsometry. With this method, the thickness of the

interfacial layer and kinetics of adsorption can be monitored and conclusions can be drawn on the arrangement of the molecules at the interface. To visualize interfacial structures Brewster angle microscopy would be appropriate. Although not in focus of the present study, it has to be kept in mind that there are noteworthy differences between interfacial properties of various QS extracts. It would be interesting to perform a systematic study on chemical composition of the various QS extracts and the resulting interfacial properties. With this setup it would be possible to unravel structure-function-relationships.

Manuscript IV

Factors affecting foamed emulsions prepared with an extract from Quillaja saponaria Molina: oil droplet size, pH and presence of beta-lactoglobulin

Food Biophysics, V. 12, No. 2, pp. 250–260. The final publication is available at Springer via <http://dx.doi.org/10.1016/j.cis.2017.02.008>.

Authors

Sandra Böttcher^{a*}

Marina Eichhorn^{a*}

Stephan Drusch^a

^a Technische Universität Berlin, Institute for Food Technology and Food Chemistry
Department of Food Technology and Food Material Science
Königin-Luise-Str.22, 14195 Berlin

*Co-first authorship

IV-1 Abstract

Oil is well-known to act as antifoam and destabilize foam lamellae by bridging between two adjacent foam bubbles. It was hypothesized that an optimal oil droplet size exists with respect to the stability of the foamed emulsions, where oil droplets are sufficiently small to postpone bridging and amount of free surfactant is sufficient to stabilize the oil/water-interface and air/water-interface. Emulsions with 0.3 % Quillaja saponin and a median oil drop-let size between 0.2 and 2.0 μm were prepared under varying homogenization conditions and characterized in a dynamic foam analyzer. Results confirmed the above-mentioned hypothesis. Stability of the foamed emulsions increased considerably with increasing pH, which was attributed to higher electrostatic repulsion between oil droplets and the effect on the balance between disjoining pressure and capillary pressure. Stability of foamed emulsions can be further increased when emulsifiers are added sequentially. The emulsion may solely be stabilized by β -LG, when QS is added after emulsification stability of the foamed emulsion is distinctly higher compared to systems with simultaneous addition of QS and β -LG. Future studies should deepen our understanding of these complex dispersed systems by investigating other proteins and food constituents.

IV-2 Introduction

Saponins are phytochemicals, which are widely spread in various plant species (Dinda *et al.* 2010; Hänsel and Sticher 2010; Negi *et al.* 2013; Vincken *et al.* 2007). The molecular structure of saponins is characterized by a hydrophobic aglycone and hydrophilic sugar residues resulting in an amphiphilic character of the molecule. Botanical sources for saponins include different vegetables like asparagus or spinach, but the majority of studies focused on extracts of the Chilean soap bark tree *Quillaja saponaria* Molina (QS) (Güçlü-Üstündağ and Mazza 2007). In the past five years numerous studies investigated the interfacial properties of Quillaja saponins at the air/water-interface (Stanimirova *et al.* 2011; Wojciechowski 2013; Golemanov *et al.* 2013), at the oil/water-interface (Wojciechowski 2013; Golemanov *et al.* 2014) as well as their use in dispersed systems like emulsions (Yang *et al.* 2013; Yang and McClements 2013; Bai *et al.* 2016) and foams (Böttcher and Drusch 2016). Quillaja saponins have a molecular weight of about 2 kDa and are therefore larger than common low molecular weight surfactants (<0.5 kDa) but distinctively smaller than proteins like β -lactoglobulin (18.4 kDa).

Adsorption of low molecular weight surfactants is diffusion-limited, whereas protein adsorption is distinctively slowed by an additional barrier resulting from steric hindrances (Wilde *et al.* 2004; Wierenga and Gruppen 2010). As a consequence of its structure and molecular weight QS has unique interfacial properties and its adsorption was described as mixed diffusion barrier controlled (Wojciechowski *et al.* 2011). This implies that adsorption in comparison to low molecular weight surfactants is rather slow, but faster compared to most proteins. At the air/water-interface high values for complex shear and dilational moduli (with high elastic moduli) were reported, which were explained by the formation of hydrogen bonds between neighboring QS molecules (Stanimirova *et al.* 2011). The formation of a firm viscoelastic network is very unusual for such a small molecule, but is much more common for proteins (Mackie *et al.* 2000; Petkov *et al.* 2000; Fainerman *et al.* 2010). Due to the viscoelastic interfacial QS-film, foam lamellae are sufficiently stabilized and counteract rapid foam collapse. In contrast, interfacial layers of QS at the oil/water-interface exhibited low complex dilational (15 mN/m) and shear moduli (7 mN/m) with high viscous proportion as indicated by a phase angle of around 45° for low concentrations of QS (Böttcher *et al.* 2017). Golemanov *et al.* (2014) suggested that penetration of oil inbetween QS molecules reduces viscoelasticity of the interfacial film.

Food products often represent dispersed systems with multiple phases (oil, water and air bubbles) and thus differ in complexity from previously examined model systems. When discussing a system with dispersed air and oil droplets in a continuous liquid phase, different terms were used by various research groups. A dispersion of air bubbles in a continuous liquid phase with a relatively small gas volume fraction may be described as ‘aerated’ (Langevin 2008) or ‘bubbly’ (Kichatov *et al.* 2016). In many publications ‘aerated emulsion’ is associated with systems similar to whipped cream, in which air bubbles are stabilized by shear-induced fat bridges (Bee *et al.* 1986; Leser and Michel 1999; Arboleya *et al.* 2009; Kim *et al.* 2013). The term ‘three phase foam’ may be used when the influence of oil droplets on stability of thin liquid films is determined (Lee *et al.* 2012) but was also used to describe the effect of solid particles in a foam (Mbama *et al.* 1998). The readers attention is drawn to the term ‘oil-based foam’. This term describes an aerated mixture of oil and surfactant (non-aqueous mixtures) and is usually used in the literature on petroleum (Sherif *et al.* 2015). Brun *et al.* (2015) used the term ‘air-in-oil-in-water emulsions’ to describe an oil-based foam (dispersed air bubble in oil), which was afterwards dispersed in an aqueous solution. In the present study the term ‘foamed emulsion’ is used to describe an emulsion, in which a gaseous phase is dispersed (Kichatov *et al.* 2016).

The presence of oil significantly affects foamability and foam stability of an aqueous system. Denkov (2004) reviewed two destabilization mechanisms of foams by oil droplets (‘antifoams’): *bridging-stretching* und *bridging-dewetting*. Both mechanisms require an oil bridge formed by an oil droplet between two adjacent foam bubbles. In the former mechanism the oil bridge is stretched due differences in the Laplace pressure in the aqueous phase and drainage, which leads to the formation of a biconcave oil bridge. Upon stretching of the film the oil bridge thins and film rupture may occur. Thinning of the oil bridge cannot be slowed down by usual processes of film stabilization like the Gibbs-Marangoni mechanism. When considering the *bridging-dewetting* mechanism, the bridging oil droplet is dewetted by the surrounding aqueous phase due to the hydrophobicity of the oil. The joint interface between aqueous solution and oil droplets decreases due to the dewetting, which subsequently leads to film rupture. In general, larger oil droplets tend to bridge foam lamellae faster than smaller oil droplets, because bridging of oil droplets happens when lamella thickness is similar to the size of the oil droplet.

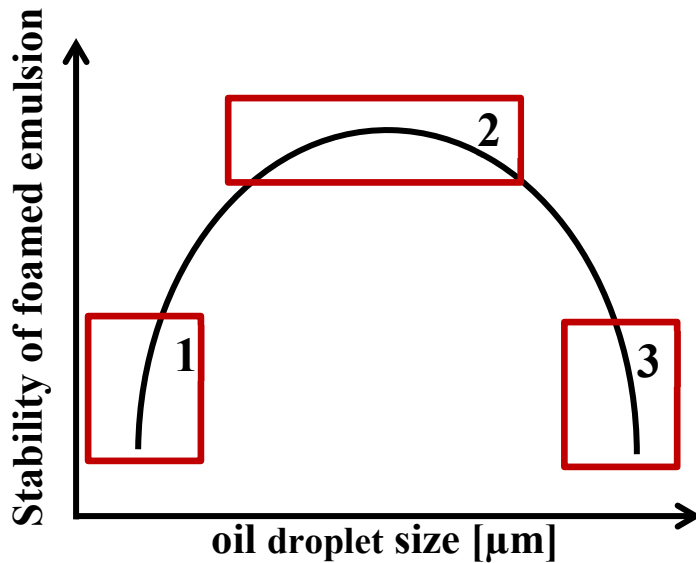


Figure IV-1 Schematic illustration of the relationship between the stability of foamed emulsions and their oil droplet size. Please refer to the text for appropriate explanation of the different ranges.

In addition, to the oil drop size the content of the emulsifier is another factor, which may affect the stability of the foamed emulsion. At a fixed content of the emulsifier, a higher proportion is required for the stabilization of the oil/water-interface at a small oil droplet size compared to a large oil droplet size. The interfacial area is distinctively larger in emulsions with small oil droplet size because the area-to-volume-ratio is higher. As a consequence, free surfactant content may be insufficient to stabilize the air/water-interface of air bubbles, which reduces stability of the foamed emulsion. It must therefore be hypothesized that there is an optimal oil droplet size of emulsions with maximum stability of a foamed emulsion (see range 2 in Figure IV-1). Below the optimal oil droplet size, in range 1 in Figure IV-1, the concentration of non-adsorbed emulsifier is too small to stabilize the air/water-interface in addition to the oil/water-interface. Above the optimal oil droplet size (see range 3 in Figure IV-1) stability of the foamed emulsions is reduced by bridging of the oil droplets, which leads to rupture of the foam lamella.

As reported in a previous studies the stability of QS-based foams and emulsions is distinctly affected by changes in pH (Böttcher and Drusch 2016; Yang *et al.* 2013), thus representing a third factor affecting foam properties. Quillaja saponins possess a free carboxylic group and since it's an aqueous plant-derived extract contains other constituents, which may carry ionic residues. At neutral pH anionic residues and the carboxylic group of QS are negatively charged, which leads to electrostatic repulsion in thin liquid films and between oil droplets.

It may therefore be hypothesized that stability of foamed emulsions at increased at a higher pH.

Due to the fact that QS is approved for some food products in the EU and US, various studies investigated the interactions with typical food ingredients e.g. β -lactoglobulin in model systems (Kezwon and Wojciechowski 2014; Böttcher *et al.* 2016). In previous publications mixtures of QS and β -LG showed synergistic and antagonistic effects with respect to the stability of dispersed systems. In general, QS and β -LG form complexes in bulk as demonstrated by fluorescence experiments (Böttcher *et al.* 2016). In foam experiments it was shown that foaming speed, foam stability and liquid content of the foam increase when using mixtures of QS and β -LG (Böttcher *et al.* 2016). The observed synergistic behavior in foams at low concentrations of QS and β -LG was explained by the formation of a joint interfacial network. Interfacial shear and dilational rheology supported this as indicated by an increase of the complex shear and dilational moduli. However, for emulsions an antagonistic effect on the kinetic stability due to extensive oil droplet aggregation was reported for binary mixtures of QS and β -LG (Böttcher *et al.* 2017). It was hypothesized that QS may prompt structural changes or partial displacement of β -LG which caused aggregation. The situation in foamed emulsions is different, since two different interfaces exist, which are formed in two subsequent steps of the process. As a consequence, physical stability will depend on the fact, whether proteins and saponins are already present during emulsion preparation or not. Depending on desorption and re-adsorption phenomena as well as the specific behavior of an emulsifier at these interfaces, it may be necessary to provide a specific emulsifier for each step of the formation of this more complex dispersed system.

Aim of the present study therefore is to identify key factors increasing the stability of foamed emulsions prepared with Quillaja saponins. In a first step the influence of oil droplet size (d_{50} 0.2 to 2 μm) and amount of free emulsifier on the stability of foamed emulsions is investigated. Emulsions are characterized with respect to oil droplet size distribution, ζ -potential and interfacial tension. Stability of foamed emulsions is evaluated with an automatic foam device. In a second step, the impact of pH within a range of pH 2 to 8 on stability of foamed emulsions is determined. Finally, the effect of the presence of β -lactoglobulin in a QS-based system is investigated by performing experiments with sequential addition of both constituents.

IV-3 Material and methods

A crude saponin extract from *Quillaja saponaria* Molina (QS) with a purity of 15.5 % was kindly provided by Ingredion Germany GmbH (Hamburg, Germany). Beta-Lactoglobulin (β -LG) with a purity of 85 % was purchased from Davisco Foods International, Inc. (Geneva, Switzerland). Medium-chain triglyceride oil (MCT-oil) WITARIX® MCT 60/40 containing a mixture of C:8 and C:10 triglycerides, was chosen as oil phase and was purchased from CREMER OLEO GmbH & Co. KG (Hamburg, Germany). Surface-active residues present in the MCT-oil were removed through adsorption onto magnesium silicate (Florisil®, Sigma-Aldrich GmbH, Seelze, Germany). For coloring the oil phase 0.017 % Oil Red O was used. All solutions of QS and β -LG were prepared in potassium phosphate buffer (10 mM, pH 7). For the experiment with variation of the pH, emulsions were homogenized using distilled water as aqueous phase and pH was adjusted afterwards within a range of 2 to 8 using hydrochloric acid and sodium hydroxide with a concentration of 0.01 M.

IV-3.1 Preparation of emulsions

Emulsions (o/w) were produced in two steps: first, a coarse emulsion was prepared using a rotor-stator system (Ultra-Turrax T25 basic, IKA -Werke GmbH & CO. KG, Staufen, Germany) with an adjusted speed of 13,500 rpm, which was applied for 30 s. Aqueous solutions containing QS, β -LG and mixtures of both were emulsified with 5 % of purified and dye-containing MCT-oil. Afterwards, the coarse emulsion was homogenized to obtain smaller oil droplets by using a high-pressure homogenizer (Panda 2K, GEA Niro Soavi Deutschland, Lübeck, Germany). In the first experiment on the impact of oil droplet size, pressure regime ranged between 50-600 bar and number of passes was varied between one and four in order to identify suitable conditions to produce emulsions with a median of the oil droplet size distribution between 0.2 and 2 μm (Table IV-1). In all other experiments emulsions with a d_{50} of 0.5 μm were prepared applying 200 bar and three passes.

In all emulsion experiments, QS concentration was fixed at 0.3 %. In emulsions containing β -LG, the β -LG concentration was varied between 0.1, 0.2 and 0.3 %. Throughout the whole manuscript Mix_{pre} describes the process, when QS and β -LG are co-dissolved prior to emulsification and Mix_{post} indicates that a β -LG emulsion was produced first and QS is added after emulsification.

Table IV-1 d_{50} of 0.3 % QS-emulsions (5 % MCT-oil) in relation to number of passes and homogenization pressure; bold numbers refer to chosen parameters for experiment on foaming of emulsions

pressure [bar]	1 pass	2 passes	3 passes	4 passes
50	3.7	2.2	2.1	1.8
100	2.3	1.2	1.0	0.8
200	1.4	0.6	0.5	0.4
300	0.8	0.4	0.3	0.3
400	0.6	0.3	0.3	0.3
500	0.4	0.3	0.3	0.2
600	0.4	0.2	0.2	0.2

IV-3.2 Oil droplet size distribution, ζ -potential and interfacial tension of the emulsions

A static light scattering device (Horiba LA-950, Retsch Technology GmbH, Haan, Germany) was used to analyze the oil droplet size distribution of emulsions. Based on the scattering patterns the volume distribution of the oil droplets is calculated and reported. Emulsions need to be diluted to obtain an optimal scattering pattern. Circulation and stirring speed were set to 8 and 3, respectively. For all calculations, a refractive index of 1.45 was used. Box plots comprising different quantiles (d_{10} , d_{25} , d_{50} , d_{75} and d_{90}) are used to describe differences in the oil droplet size distribution.

The ζ -potential of dispersed oil droplets was determined via the electrophoretic mobility using a Nano Zetasizer ZS from Malvern Instruments GmbH (Herrenberg, Germany). Experiments were carried out in clear disposable cells (DTS 1060 C, Malvern Instruments GmbH) and emulsions were diluted 1:10 using 10 mM phosphate buffer prior to measurement.

Drop shape analysis is a convenient possibility to determine dynamic interfacial tension. In this study contact angle meter in pendant drop mode was used (OCA-20, DataPhysics Instruments GmbH, Filderstadt, Germany). A droplet of emulsion ($15 \mu\text{L} \pm 0.3$) was automatically generated through a needle. Droplets were measured at 22 °C in a closed cuvette filled with a small amount of water to prevent extensive evaporation. The device calculates interfacial tension in real-time by fitting the Young-LaPlace-equation to the drop shape every 3 s for 20 mins (Najmabadi *et al.* 2013).

IV-3.3 Preparation and characterization of foamed emulsions

Dynamic foam properties (foaming and foam stability) of the emulsions were analyzed using a DFA 100 (Krüss GmbH, Hamburg, Germany) as described in Böttcher and Drusch (2016). For each measurement, an aliquot of 50 ml of emulsions was foamed to a maximum height of 180 mm by purging pressurized air (0.2 L/min) through a porous glass frit (FL 4504, Porosity 4, 10-16 μm , DURAN[®]) at the bottom of a cylinder. In this experimental setup foam and liquid height are typically differentiated by differences by their transmissibility. Due to opacity of the emulsions, discrimination between foam and liquid height was not possible. Therefore, stability was evaluated by comparing the total height, which is the sum of foam height and liquid height. All experiments were carried out in darkness over a period of 3600 s. Transmission was recorded every 0.5 s for layers of a height of 0.1 mm covering the whole foam column to generate the foam profile. The foam profile is thus composed of grey pixels and brightness values vary between 0 and 255, which refers to black and white, respectively.

Based on this foam profile the median of the brightness distribution (BD_m) was derived at 3600 s (for detailed explanation refer to Böttcher and Drusch (2016)). The BD_m may be interpreted as an indicator for density of the foamed emulsion. The amount of transmitted light is reduced at high foam density, which results in a low BD_m . In contrast, a high value for BD_m indicates a porous foam.

IV-4 Results and discussion

IV-4.1 Impact of homogenization parameters on oil droplet size distribution of emulsions

With increasing homogenization pressure and number of passes, the median (d_{50}) of the oil droplet size distribution decreased and width of the oil droplet size distribution decreased. Figure IV-2 shows the dependence of the oil droplet size on the number of passes (see Panel A) and homogenization pressure (see Panel B). At a pressure of 200 bar after one pass the width of the oil droplet size distribution (d_{10} to d_{90}) amounted to 1.6 μm . With increasing number of passes the width of the oil droplet size distribution steadily decreased to 0.7 μm at four passes. A similar trend was observed when comparing the oil droplet size distributions at 2 passes at varying pressure. The width of the oil droplet size distribution decreased from 2.4 μm at 50 bar to 0.3 μm at 600 bar. As expected, median of the oil droplet size distribution was highest at 50 bar (2.2 μm) and decreased with increasing pressure. Above 300 bar the median of all samples were in a similar range between 0.2 to 0.4 μm .

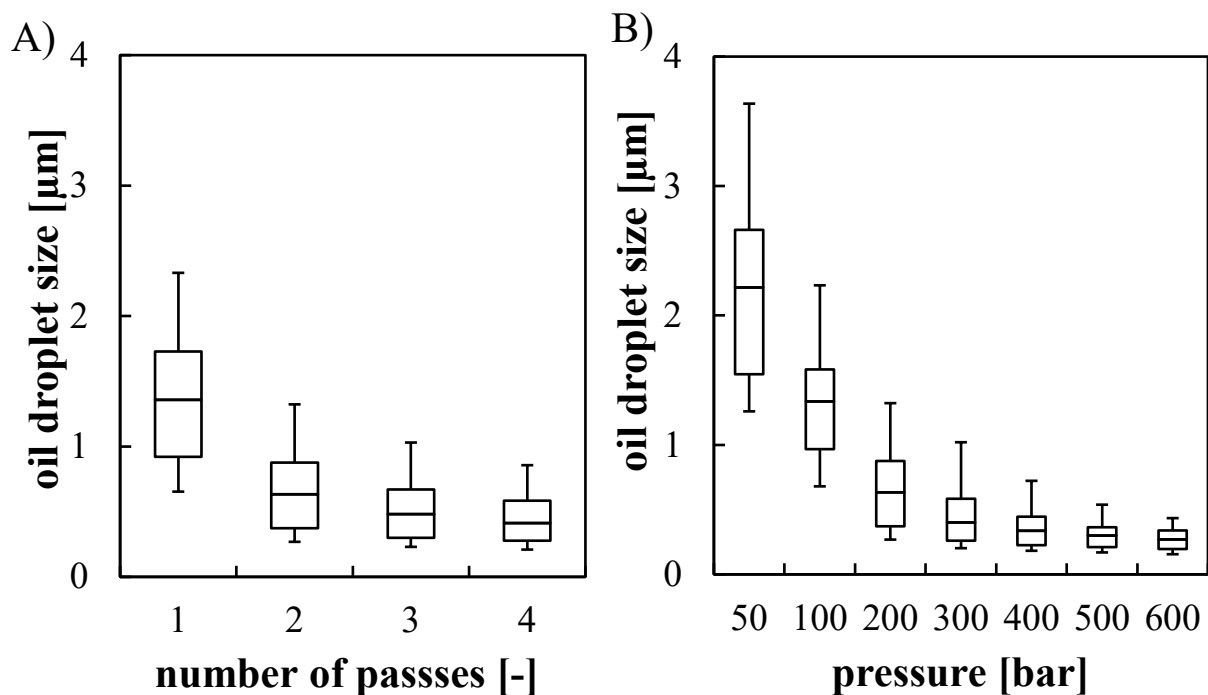


Figure IV-2 Influence of (A) number of on the oil droplet size distribution of 0.3 % QS-emulsion (200 bar, 5 % MCT-oil) with upper whisker representing d_{90} , upper box end d_{75} , dash in the box d_{50} , lower box end d_{25} and lower whisker d_{10} and (B) influence of homogenization pressure on the oil droplet size distribution of 0.3 % QS-emulsion (2 passes, 5 % MCT-oil)

The impact of the number of passes and homogenization pressure on oil droplet size is well known and has been described before for QS-emulsions by some authors. In the present study QS content and oil content differed from the experimental setup described in the literature. Therefore, it was important to identify homogenization parameters, which result in specific values for the d_{50} between 0.2 and 2 μm . At increasing homogenization pressure and number of passes stress increases and oil droplet size is reduced. Reduction in oil droplet size goes along with an increase of the area-to-volume-ratio and an increase of the total interfacial area. A linear relationship between the logarithm of the d_{50} of the volume distribution and the logarithm of the homogenization pressure was observed (see Figure IV-3) and is in agreement with the literature (Yang et al. 2013). It is generally known that an inverse linear relationship between the logarithm of the diameter of the oil droplets and the logarithm of the energy density exists as long as sufficient emulsifier is present in a system. The latter results from the general definition of the interfacial tension as amount of work required to create a specific new interfacial area.

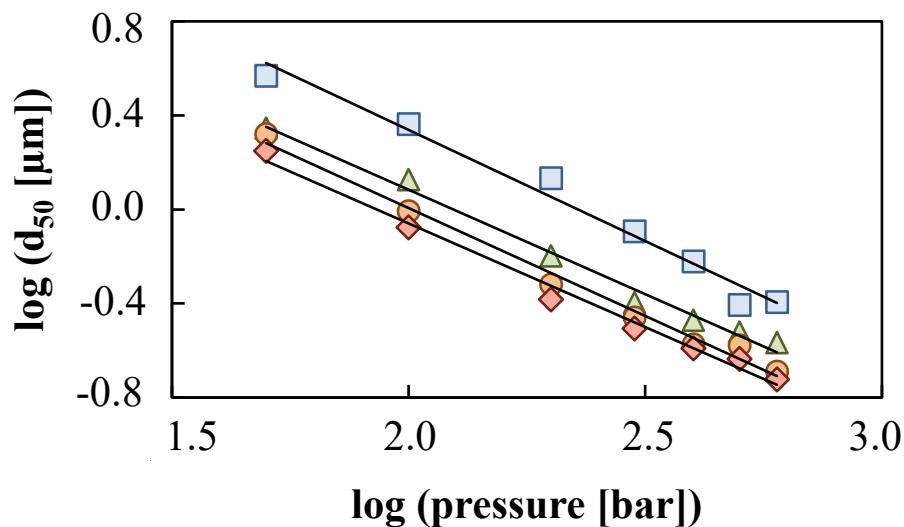


Figure IV-3 Double logarithmic plot of the relationship between d_{50} and homogenization pressure of a 0.3% QS-emulsion (5 % MCT-oil) for 1 pass (■), 2 (▲), 3 (●) and 4 passes (◆)

IV-4.2 Emulsion properties and stability of foamed QS-emulsions affected by the oil droplet size

The interfacial tension of an emulsion droplet against air provides information on the amount of free surfactant, which is not adsorbed to the oil/water-interface and is available to stabilize the air/water-interface. As outlined above with decreasing oil droplet size of an emulsion the total interfacial area increases and vice versa. Therefore, interfacial tension of the emulsions decreased with increasing d_{50} from 56 to 49 mN/m between 0.2 and 0.4 μm , respectively (see Figure IV-4A). Above a d_{50} of 0.5 μm interfacial tension did not change upon further increase of d_{50} . High values of the interfacial tension indicate a low concentration of QS at the air/water-interface and thus a low content of free emulsifier.

The amount of free QS affects the foaming speed of an emulsion. Free QS adsorbs at the air/water-interface to stabilize newly formed air bubbles and prevents rapid coalescence. As a consequence, foaming speed of the emulsions increased to a maximum of 2.85 mm/s at a d_{50} of 0.6 μm (Figure IV-4A). Thereafter foaming speed remained constant and slightly decreased above a d_{50} of 1 μm . Low foaming speed originates from low amount of free surfactant as it is indicated by high values for the interfacial tension.

Before discussing the impact of the oil droplet size on foam stability, general mechanisms responsible for changes in dispersity of foams need to be summarized. Foams and their stability have been a topic of extensive research (Langevin 2008; Aveyard *et al.* 1999; Stubenrauch and von Klitzing 2003; Fauser and von Klitzing 2014; Schramm 2005). Foams are thermodynamically instable and may be classified based on the relative content of the dispersed phase. Foams with a low content of dispersed phase may be referred to as wet foam ('kugelschaum') and foams with high content as dry foams (polyhedral). In polyhedral foams two adjacent air bubbles are separated by a thin liquid film (foam lamella). Three lamellae are joined by a Plateau border and four Plateau borders will form a so-called node in a three dimensional arrangement.

Different destabilizing mechanisms resulting in a change of dispersity may occur in foams: 1) evaporation of gas, 2) disproportionation of bubbles, 3) drainage, followed by 4) thin liquid film rupture and coalescence of adjacent bubbles (Aveyard *et al.* 1999; Langevin 2008). We expect that disproportionation, drainage and coalescence have the highest impact on foam stability in the present study. Evaporation of gas plays a minor role in this study because the surface of the foam in the column of the foam apparatus only amounts to 12.5 cm². Disproportionation originates from differences in the Laplace pressure in bubbles

in polydisperse foams. Small bubbles have a high Laplace pressure, which increases solubility of gas in the adjacent liquid phase. In the vicinity of a large bubble (with a low Laplace pressure) solubility of the gas in the continuous phase is reduced. The excess gas is released into the large bubble until equilibrium is achieved. Disproportionation results in shrinkage of small bubbles in favor of larger bubbles and is the dominating mechanism in foams.

Drainage (process 3) through the Plateau borders is caused by gravitational forces and differences in capillary pressure between the lamellae and the plateau border region pull out liquid from the lamellae. Immediately after their formation, liquid films between bubbles are thick but draining leads to the development of thin liquid films. In polyhedral foams, adjacent foam bubbles form a planar thin liquid film in the center, but in the Plateau border region foam bubbles are curved. Curvature of the bubbles leads to a reduction in pressure in the Plateau borders (as described by Young-Laplace equation). The pressure difference between the Plateau border regions and the center of the thin liquid film leads to drainage of the continuous phase, which reduces thin liquid film thickness and increase tendency of film rupture due to holes in the interfacial film (process 4). The Gibbs Marangoni mechanism may counteract thinning by a countercurrent liquid flow due to interfacial tension gradients. Disjoining forces are contradicting the thinning process of thin liquid films at small thickness (10-100 nm) of thin liquid films (Aveyard *et al.* 1999; Langevin 2008). As described in the introduction of the manuscript oil droplets may decrease foam stability by bridging of air bubbles followed by coalescence due to stretching and film rupture and or dewetting.

In the present study decay of the foamed emulsions was not necessarily indicated by a decrease in the height of the foam column. Also density of the foamed emulsions distinctly changed over the course of the measurement. Therefore, the brightness of the foam profiles was analyzed and the median of the brightness distribution (BD_m) was chosen. Generally spoken, a low value for the BD_m indicates a denser foam. The BD_m after 1 h showed a minimum value of approximately 100 for foamed emulsions with an oil droplet size between 0.6 to 1 μm (see Figure IV-4B). At a d_{50} above 0.5 μm the BD_m values were approximately 115. At a d_{50} below 0.5 μm foamed emulsions were unstable and rapidly collapsed after the end of foaming. Therefore, no values for BD_m are reported.

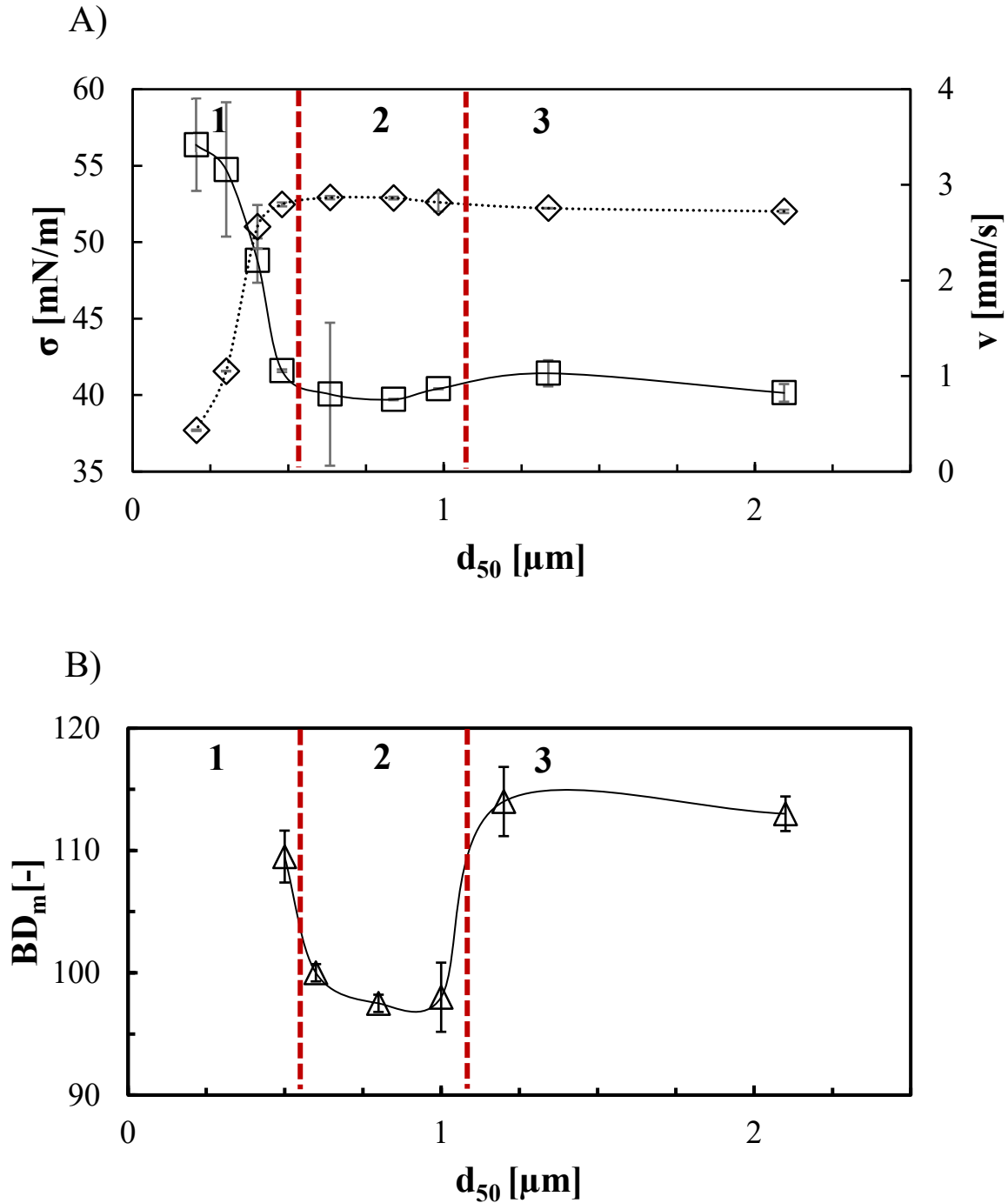


Figure IV-4 Emulsion properties with respect to (A) interfacial tension σ (\square) and foaming speed v (\diamond) and (B) properties of the foamed emulsions described by the median of the brightness distribution BD_m after 1 h measurement (Δ) in relation to the median (d_{50}) of 0.3 % QS-emulsions with range 1, 2 and 3. Lines are only guide to the eye. Please refer to the text for appropriate explanation of the different ranges.

The results of the interfacial tension, foaming speed and stability of the foamed emulsions confirmed the hypothesis that there is an optimal oil droplet size at which stability of the foamed emulsions is maximized. Thus, three ranges of the oil droplet size with differing stability may be described (see Figure IV-4, Figure IV-5).

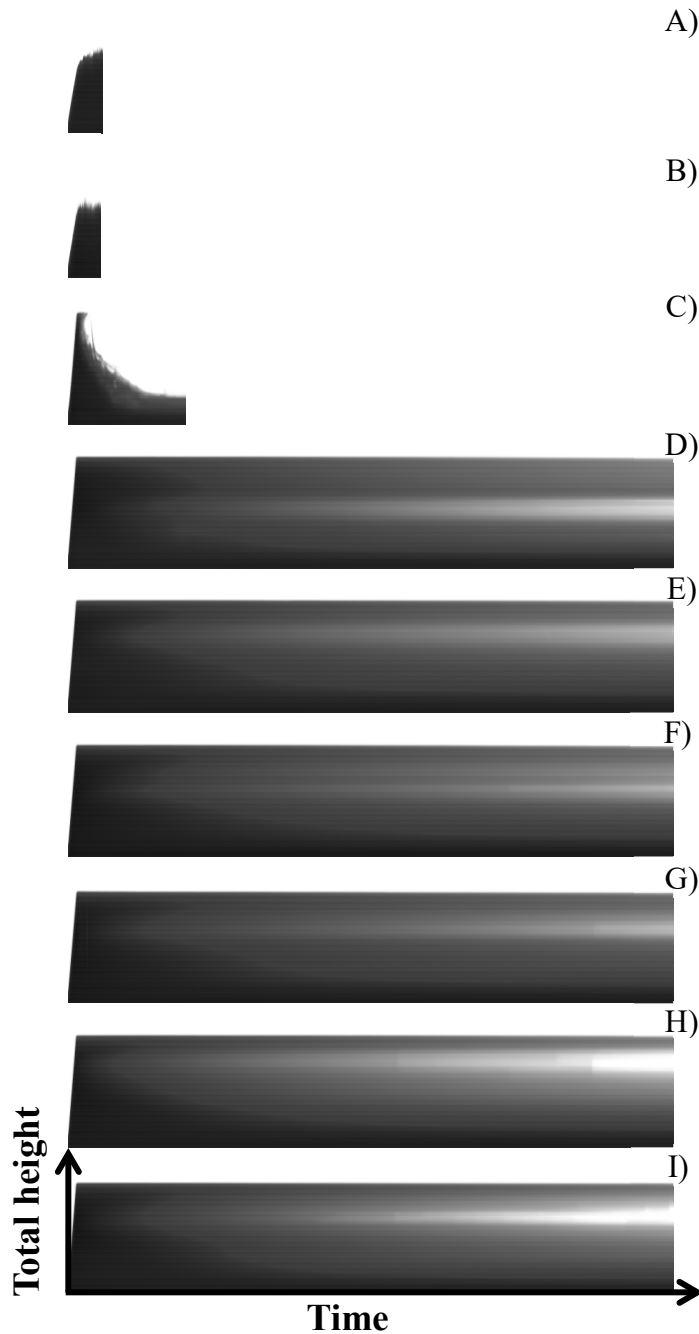


Figure IV-5 Foam profiles of foamed emulsions of 0.3 % QS with d_{50} of

A) 0.2 μm , 600 bar, 3 passes; B) 0.3 μm , 500 bar, 2 passes; C) 0.4 μm , 300 bar, 2 passes; D) 0.5 μm , 100 bar, 3 passes; E) 0.6 μm , 200 bar, 2 passes; F) 0.8 μm , 100 bar, 4 passes; G) 1 μm , 100 bar, 3 passes; H) 1.2 μm , 100 bar, 2 passes; I) 2.1 μm , 50 bar, 3 passes

In the first range up to a d_{50} of 0.4 μm a large proportion of QS is adsorbed to the oil/water-interface. The amount of free surfactant is too low to stabilize the air/water- after stabilizing the oil/water-interface, as indicated by high interfacial tension values. Rapid bubble coalescence during foaming and after the end of foaming occurred and hence foaming speed and

stability of the foamed emulsions were low. Characteristic properties of emulsions belonging to the first range are a high specific interfacial area of the oil droplets (o/w-interface). E.g. at a d_{50} of 0.2 μm the interfacial area amounts to 326,000 cm^2/cm^3 (see Figure IV-6). In the second range sufficient amount of QS-molecules is available to stabilize the oil/water-interface as well as the air/water-interface during foaming. Bridging of foam lamellae by oil droplets still occurs but is low due the relatively small size of the oil droplets (Denkov 2004). Emulsions with a d_{50} between 0.6 to 1 μm represent this range and may be considered as the optimum range of oil droplet size with respect to stability of foamed emulsions in the present system at a concentration of 0.3 % QS and 5 % MCT-oil.

In the third, range covers emulsions with a d_{50} above 1 μm . In this range enough free QS-molecules are present to stabilize both interfaces: oil/water and air/water. The specific interfacial area of an emulsion with a d_{50} of 2.1 μm (31,000 cm^2/cm^3 , see Figure IV-6) in the present study was 10-times smaller in comparison to an emulsion with a d_{50} of 0.2 μm . Foaming speed and interfacial tension are similar compared to the second range but stability of the foamed emulsion was lower. With increasing measurement time the formation of light areas along the brightness profile of the foam column were observed, which indicate foam decay in this area.

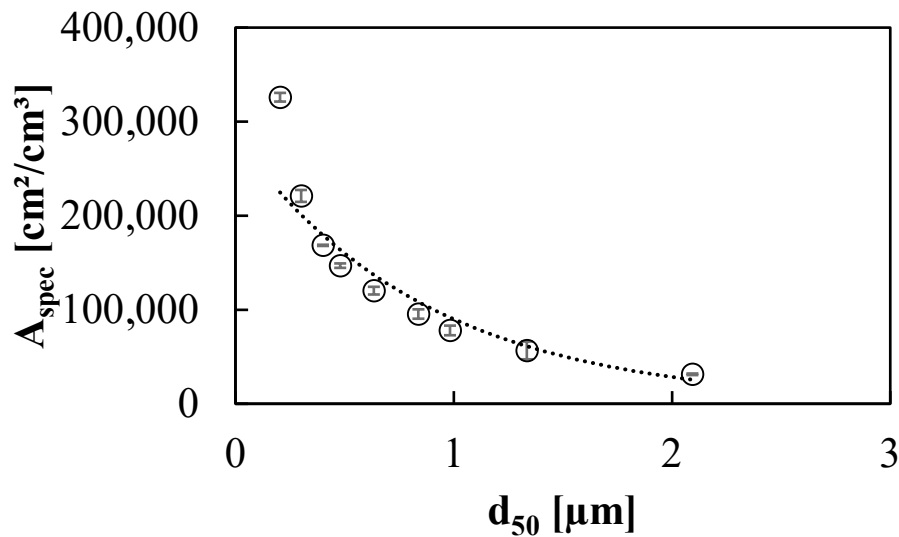


Figure IV-6 Specific interfacial area A_{spec} in relation to d_{50} of 0.3% QS-emulsions

As discussed by Karakashev and Grozdanova (2012) and Denkov (2004) the antifoam properties of oil may be classified based on the speed of foam destruction. Oil may act as slow or fast antifoam, which means that foams are either destroyed in seconds or minutes to hours by the presence of the oil, respectively. Fast antifoams have a low entry barrier, which may be determined with the film trapping technique (FTT) and destroy thin liquid films in

an early stadium. The destruction of the thin liquid films occurs only seconds after thin liquid film formation thereby preventing foam generation. However, slow antifoams have a high entry barrier and are trapped in the Plateau borders, because they are not able to enter the foam film. Drainage of the liquid phase increases compression of slow antifoam in the Plateau borders consequently leading to the rupture of Plateau borders. In the present system, it is assumed that dispersed MCT-oil acts as a slow antifoam, because foam destruction is relatively slow.

All trials described in the following subchapter were conducted with emulsions, which had a d_{50} of 0.5 μm . The oil droplet size is lower in comparison to the optimal oil droplet size (range 2), which results in reduced stability of the foamed emulsions (see Figure IV-5D+H). This oil droplet size was chosen on purpose to enable the determination of factors that positively influence stability of foamed emulsions.

IV-4.3 Influence of pH on ζ -potential and stability of foamed QS-emulsions

A pH-series of QS-emulsions with pH ranging from 2 to 8 were prepared and foamed. In Figure IV-7 foam profiles are displayed, which show the total height in relation to the measuring time of QS-emulsions with a pH 3, 5 and 7. A was

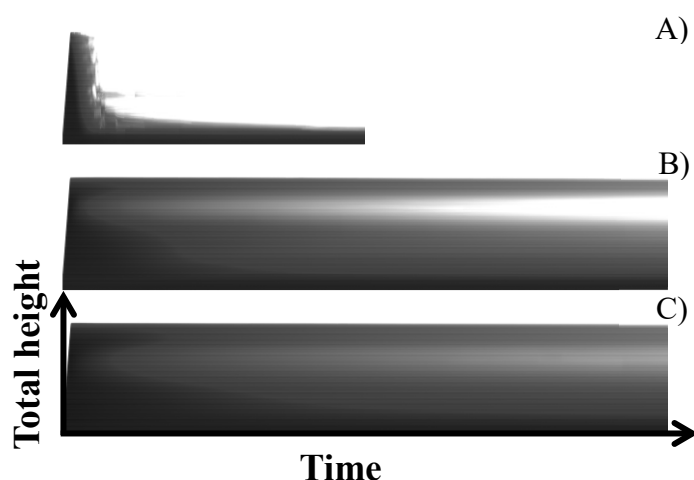


Figure IV-7 Foam profile showing total height in relation to measuring time for foamed emulsions (5 % MCT-oil, $d_{50}=0.5 \mu\text{m}$) prepared at A) pH 3 B) pH 5 and C) pH 7. A was analyzed for 1800 s, B and C for 3600 s

At low pH of 2 and 3 foamed emulsions rapidly collapsed after the end of foaming within less than 10 minutes. At pH 5, foamed emulsions were distinctly more stable and did not show any decay, but with increasing time, light regions developed in the foam profile. Foamed QS-emulsions with a pH above 5 showed no decay and almost no light regions during the course of the measurement. With increasing pH, ζ -potential decreased from -11 mV at pH 2 to -58 mV at pH 8 (see Figure IV-8).

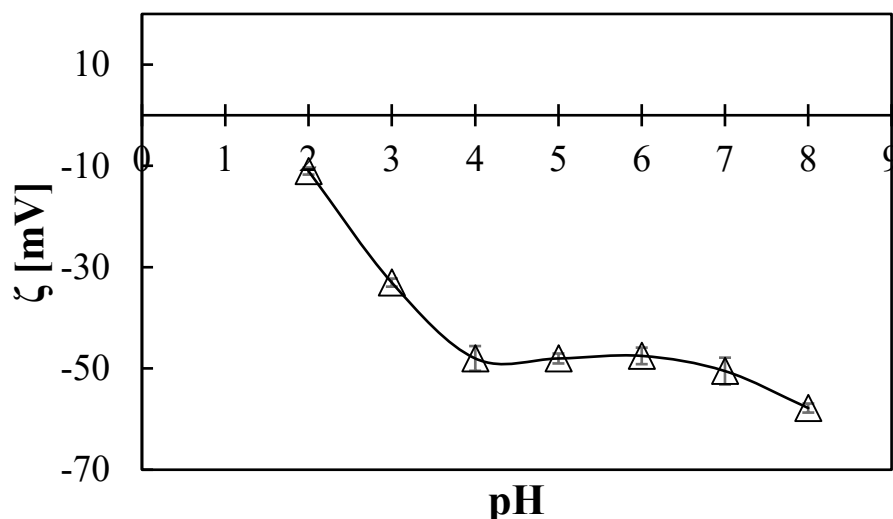


Figure IV-8 ζ -potential in relation to pH of 0.3 % QS-emulsions (5 % MCT-oil, $d_{50}=0.5 \mu\text{m}$)

Increased aggregation tendency of oil droplets in QS-emulsions at pH 2 was shown before (Yang *et al.* 2013) and was observed as well in the present study. In Figure IV-9 rapid aggregation of a foamed QS-emulsion at pH 2 at the end of the foam measurement is shown. With a decrease of the absolute value of the ζ -potential, electrostatic repulsion between oil droplets is reduced, which facilitates aggregation of oil droplets. In non-foamed emulsions, a ζ -potential with an absolute value above 30 mV is considered to slow down aggregation (Heurtault *et al.* 2003). Aggregates of oil droplets may bridge foam lamellae because of the increased diameter, which leads to film rupture and rapid foam decay. A highly negative ζ -potential of QS-emulsions at increasing pH may be attributed to the carboxylic group of QS and other constituents with ionic residues in the crude extract and enforces repulsion between oil droplets.

As it was discussed before, that in the present study, MCT-oil is considered to act as a slow antifoam and oil droplets at low pH accumulate in the Plateau borders. The electrostatic repulsion of oil droplets opposes compression of oil droplets in the Plateau borders due to drainage, which decelerates rupture.

However, the increasing foam stability with increasing pH cannot fully be explained by ζ -potential. At pH 5 ζ -potential amounted to -48 mV, which indicates increased electrostatic repulsion between oil droplets, but still, lighter regions in the foam profile appeared. Foams at pH 5 and 6 were less stable compared to pH 7 and 8, but ζ -potential between pH 5 to 8 did not distinctively change.



Figure IV-9 Foamed emulsion of 0.3 % QS (5 % MCT-Oil, $d_{50}=0.5\ \mu\text{m}$) after 1800 s with macroscopic aggregation of oil droplets

An additional factor explaining the increase in foam stability with increasing pH is a difference in disjoining pressure, and thus the behavior of the thin liquid films. Disjoining pressure Π is described as a function of film thickness h_t , and depends on the interaction forces, e.g. long-range repulsive electrostatic (Π_{el}), short-range attractive van der Waals (Π_{vw}) and short-range repulsive steric (Π_{steric}). The former two forces are described by the DLVO-theory developed from Derjaguin, Landau, Verwey and Overbeek. The disjoining pressure depends on the thickness of the thin liquid film and the relationship between the two is expressed in disjoining pressure isotherms. In some thin liquid films metastable states like *common black films* (10-100 nm) and *Newton black films* ($\sim 1\ \text{nm}$) may arise at a specific film thickness. The former is more thick and stabilized by electrostatic repulsion and the latter is sterically (entropically) stabilized. At these metastable states disjoining pressure is equal to capillary pressure, which prevents further film thinning. (Stubenrauch and von Klitzing 2003; Fauser and von Klitzing 2014; Schramm 2005)

It may be hypothesized that pH adjustment influences electrostatic properties of surface-active residues from the QS-extract, which are adsorbed at the air/water-interface and contribute together with non-electrostatic interactions to stabilization. Furthermore difference in the physicochemical properties of the dispersed phase (air vs. MCT oil) may result in an inhomogeneous distribution of anionic constituents at the air/water and oil/water-interface. Finally it is well described in the literature that disjoining pressure is affected by ionic strength of the medium, which is slightly altered because of pH adjustment. All these factors may affect the balance between disjoining pressure and capillary pressure in thin films and contribute to increased foam stability at higher pH although ζ -potential does not change at pH higher than 5.

IV-4.4 Emulsification of a binary mix of QS and β -lactoglobulin and the influence on the stability of foamed emulsions

As outlined in the introduction, food products often represent complex dispersed systems with a multitude of different constituents. Proteins may affect interfacial properties of dispersed systems by adsorbing onto aqueous interfaces and their interaction with other surface active constituents in the bulk and at the interface. Therefore, molecular interactions and the presence of more than one surface active constituent during processing need to be considered. In this chapter Mix_{pre} refers to samples in which QS and β -LG were mixed prior to emulsification and Mix_{post} specifies β -LG emulsions to which QS was added after emulsification.

Distribution of QS and β -lactoglobulin at the air/water- and oil/water-interface

ζ -potential of QS-, β -LG-, Mix_{pre} - and Mix_{post} -emulsions was measured to characterize electrostatic at the shear plane close to the interface of the dispersed oil droplets (oil/water-interface). ζ -potential of Mix_{post} was distinctly different from Mix_{pre} , however ζ -potential was in both cases independent from the β -LG concentration (see Figure IV-10). For Mix_{pre} -emulsions a ζ -potential of -62 to -56 mV was determined at β -LG concentrations of 0.1 and 0.3 %, respectively. The absolute values of the ζ -potential of Mix_{pre} -emulsions were higher than the ζ -potential of emulsions solely prepared with QS or β -LG. In contrast, with approximately 40 mV, the absolute value of the ζ -potential of Mix_{post} -emulsions was considerably lower and similar to emulsions solely prepared with β -LG.

In addition to the ζ -potential the interfacial tension of QS-, β -LG-, Mix_{pre} - and Mix_{post} -emulsions was used to describe interfacial characteristics at the air/water-interface. It should be noted that interfacial tension values were compared after 150 s because shortly after this time period in Mix_{post} -emulsions the droplet detached from the tip of the needle of the device (results not shown).

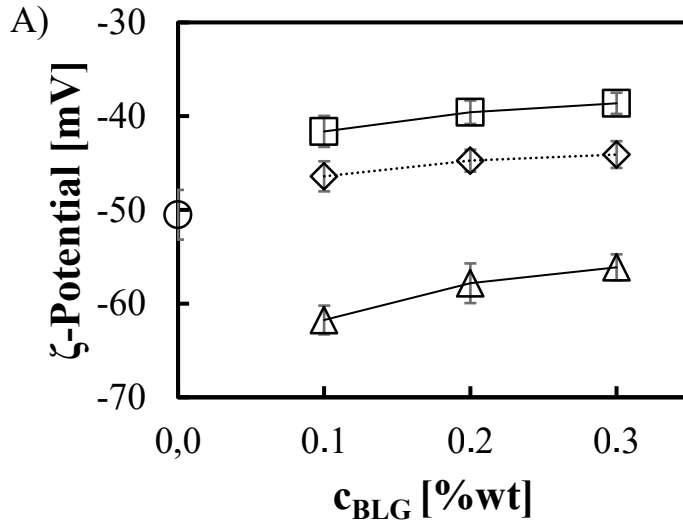


Figure IV-10 ζ -potential of emulsions (0.3 % QS, 5 % MCT-oil, $d_{50}=0.5 \mu\text{m}$) in relation to β -LG-concentration for QS (○), β -LG (◇), Mix_{pre} (Δ) and Mix_{post} (□)

From the results of the ζ -potential it can be hypothesized, see illustration in Figure IV-11A on the left, that in Mix_{pre}-emulsions a mixed film containing QS and β -LG is formed at the oil/water-interface, which is dominated by QS. It was discussed in previous publications (Böttcher *et al.* 2016, Böttcher *et al.* 2017) that QS is a small molecule, which adsorption at aqueous interfaces is slower than for common low molecular weight surfactants but faster in comparison to β -LG. However it is very likely at both interfaces (air/water- and oil/water) a mixed film of QS and β -LG is formed. The high absolute values of the ζ -potential may be explained by interactions between QS and β -LG. In Mix_{pre} a co-adsorption of QS and β -LG may take place (due to interactions of both), which increases overall surface coverage at the oil/water-interface, which increased the absolute value of the ζ -potential.

In contrast in Mix_{post}-emulsions oil droplets were predominantly covered by β -LG, which can be deduced from the similarity of the ζ -potential to β -LG (see Figure IV-11C). That means when QS is added after the emulsification QS is available to primarily stabilize the air/water-interface. Once the oil/water-interface is covered by β -LG co-adsorption with QS cannot take place, which results in ζ -potential similar to β -LG. It is yet unclear whether sequentially added QS may fully desorb β -LG from the oil/water-interface. The desorption of β -LG by QS was shown in experiments at the air/water-interface. But it has to be noted that β -LG considerably unfolds at the oil/water-interface (Zare *et al.* 2016, Zhai *et al.* 2017) thus it may be hypothesized that desorption is less likely at the oil/water-interface.

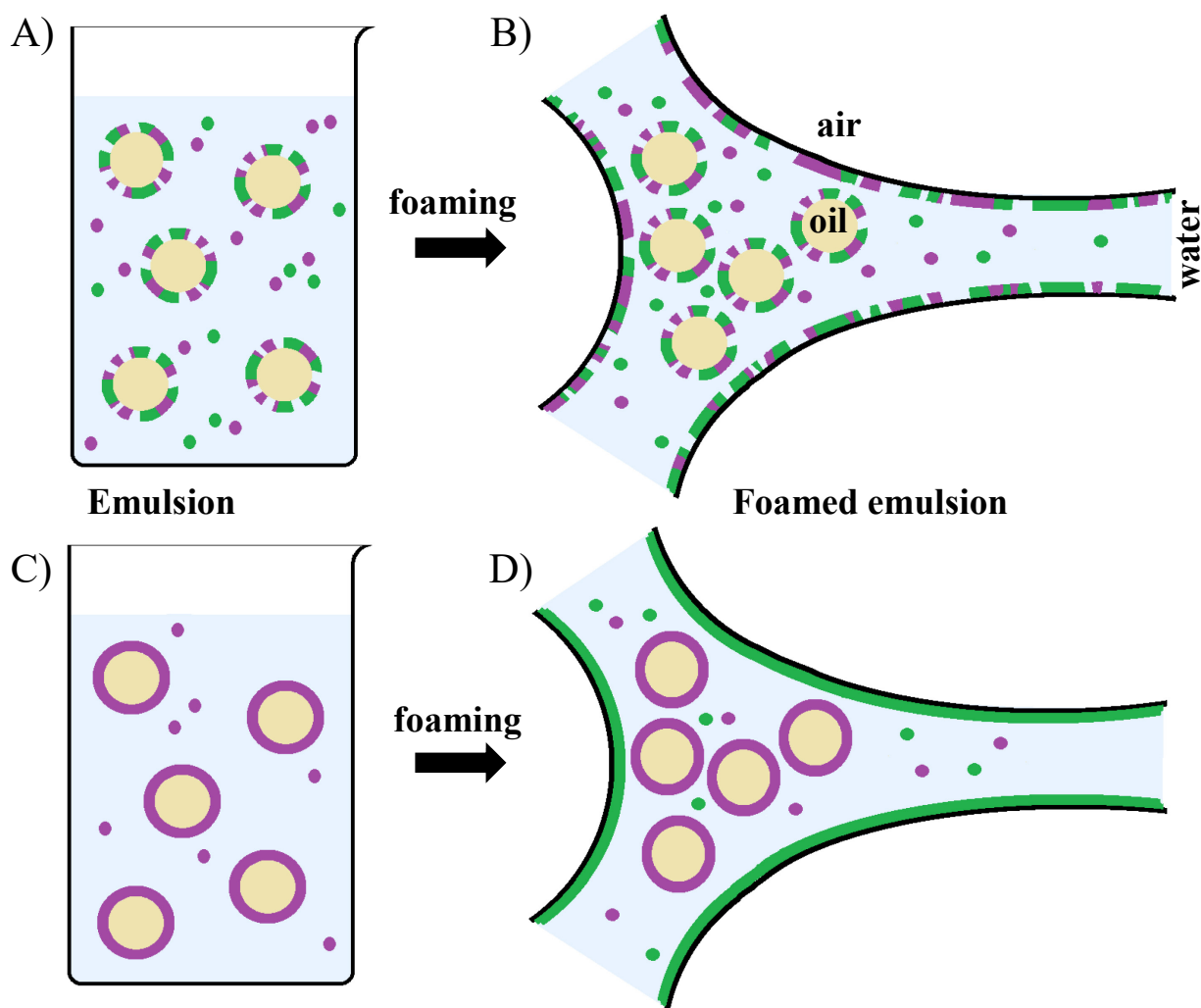


Figure IV-11 Schematic illustration of location of QS (green) and β -LG (violet) in emulsions (A+C) and foamed emulsions (B+D) whereas Mix_{pre} is illustrated in A+B and Mix_{post} in C+D

Influence of distribution of QS and β -lactoglobulin on foaming and stability of foamed emulsions

As discussed in the previous chapter, it is hypothesized that in Mix_{pre} -emulsions a mixed film of QS and β -LG is present at the air/water- as well as oil/water-interface. In Mix_{post} -emulsions ζ -potential and interfacial tension data indicated that the oil/water-interface is primarily stabilized by β -LG and that sequentially added QS is available to stabilize the air/water-interface.

Foam experiments were performed to determine the impact of the inhomogeneous distribution of QS and β -LG at the air/water- and oil/water-interface on foaming properties and foam stability. Figure IV-12 presents results of the foaming speed of QS-, β -LG-, Mix_{pre} - and Mix_{post} -emulsions. The highest values for the foaming speed with approximately 3

mm/s were obtained for β -LG-emulsions (with a concentration above 0.2 %) and all Mix_{pre}-emulsions. In contrast with 2.8 mm/s, foaming speed of QS was slightly lower. Lowest foaming speed was measured for Mix_{post} samples, ranging from 2.5 to 2.94 mm/s with increasing β -LG concentration.

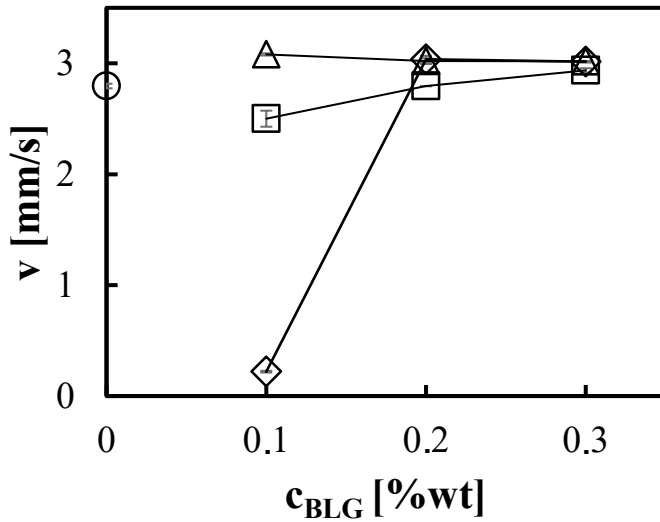


Figure IV-12 Foaming speed of emulsions (0.3 % QS, 5 % MCT-oil, $d_{50}=0.5 \mu\text{m}$) in relation to β -LG-concentration for QS (\circ), β -LG (\diamond), Mix_{pre} (Δ) and Mix_{post} (\square)

In Figure IV-13 foam profiles of foamed emulsions containing QS (A), β -LG (B-D), Mix_{pre} (E-G) and Mix_{post} (E-J) are displayed. Light patches appeared in the middle of the column of the foamed QS-emulsions after half of the measurement time, but total height of the foam column did not decrease. In contrast, total height of the foamed β -LG-emulsions rapidly decreased after end of foaming, but decay was slowed down at higher β -LG-concentrations. When foaming Mix_{pre}-emulsions light regions appeared after 30 mins and with increasing β -LG concentration the size of the light patches increased. In contrast, foam profile of Mix_{post}-emulsion neither exhibited any decay in total height nor light patches during the course of the measurement.

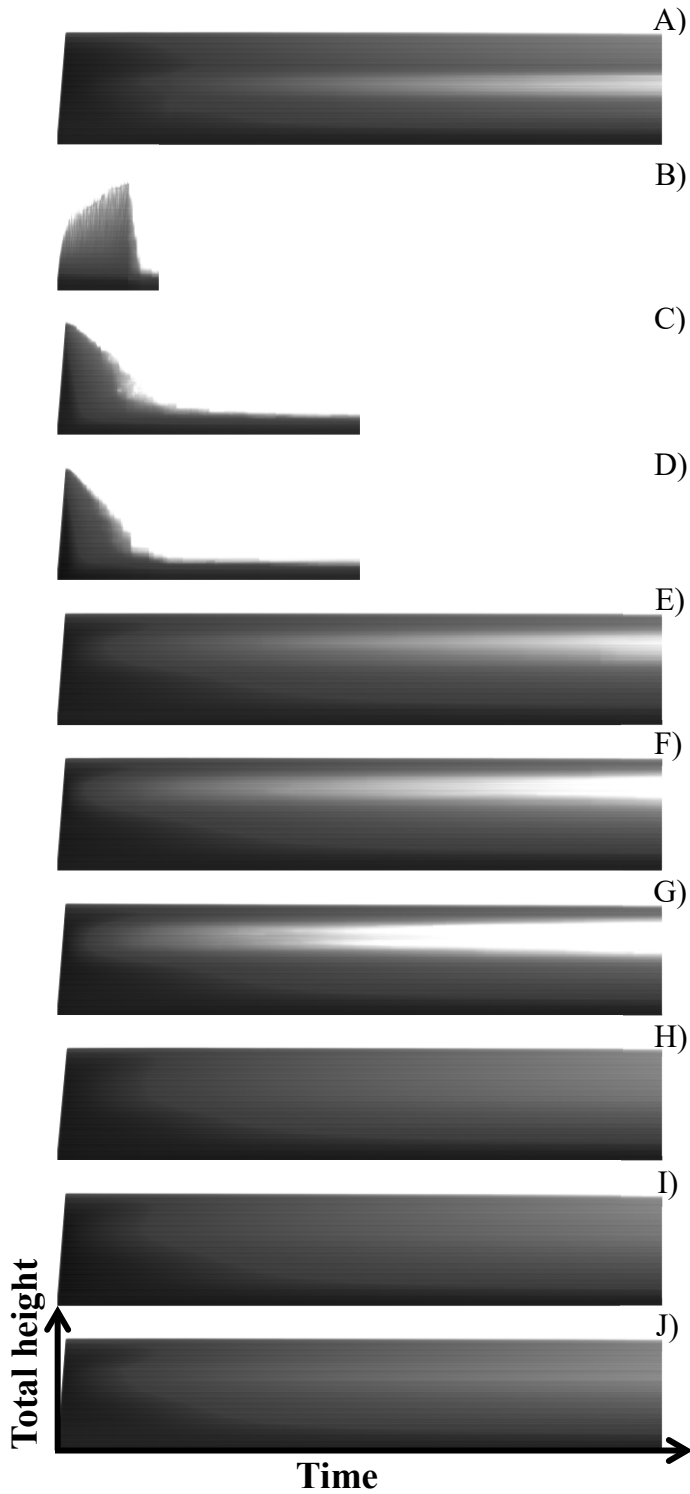


Figure IV-13 Foam profiles showing total height in relation to measuring time for a foamed emulsion ($d_{50}=0.5\ \mu\text{m}$) prepared with 5 % MCT-oil and (A) 0.3 % QS; (B) 0.1 % β -LG; (C) 0.2 % β -LG; (D) 0.3 % β -LG; (E) 0.3 % QS+0.1% β -LG (Mix_{pre}); (F) 0.3 % QS+0.2 % β -LG (Mix_{pre}); (G) 0.3 % QS+0.3% β -LG (Mix_{pre}); (H) 0.3 % QS+0.1% β -LG (Mix_{post}); (I) 0.3 % QS+0.2 % β -LG (Mix_{post}); (J) 0.3 % QS+0.3% β -LG (Mix_{post})

Summarizing results of the foam experiments it can be stated that foaming speed of Mix_{pre}-emulsions was faster in comparison to Mix_{post} but that stability of the Mix_{post}-emulsion was distinctly higher. Foaming speed and stability of the foamed emulsions are tremendously affected by the decision on the process step, during which QS is added, although the total emulsifier concentration is similar in both experimental setups.

As discussed above in Mix_{pre}-emulsions QS and β -LG form a mixed film at both interfaces: air/water and oil/water (see Figure IV-11B+D). Foaming speed of Mix_{pre}-emulsion was higher than QS and Mix_{post}, which supports previously, reported synergistic effect of QS/ β -LG on foaming properties (Böttcher *et al.* 2016). As stated in the previous chapter, a co-adsorption of QS and β -LG may not only occur at the oil/water-interface but also at the air/water-interface. Thus, foaming speed increases due to higher surface coverage at the air/water-interface. But the antagonistic effect of QS and β -LG in emulsions led to a decrease in stability of the foamed emulsion. Stability of foamed emulsions of Mix_{pre} reduced with increasing β -LG concentration as indicated by the formation of light patches in the foam profile. This behavior is unusual because the overall concentration of surface-active constituents increased. We therefore took microscopic images of the Mix_{pre}-emulsions (results not shown) and distinct coalescence of oil droplets was observed. As discussed before in this manuscript, large oil droplets lead to bridging of thin liquid films and subsequently to film rupture.

However, it was shown that stability of the foamed emulsion can be increased by sequentially adding QS to a β -LG-emulsion (Mix_{post}). In this experimental setup the presence of QS at the air/water-interface and the stabilization of the oil/water-interface by β -LG led to a considerably higher stability of the foamed emulsions (see Figure IV-13D).

IV-5 Conclusion

The present study clearly showed that oil droplet size and pH as well as the presence of β -LG and its use as an emulsifier for the oil/water-interface are key factors for foamability and foam stability of foamed QS-emulsions. At a constant QS-concentration there is an optimal range of the oil droplet size of emulsions, at which the stability of the foamed emulsion is maximized. Above the optimal oil droplet size, emulsions are easily foamed, but stability is limited due to fast occurrence of bridging induced by large oil droplets. Below the optimal oil droplet size, amount of free surfactant is too low to stabilize the air/water- and oil/water-interface, which results in low foamability and poor stability. It was further concluded that dispersed MCT-oil in the system studied acts as a slow antifoam. Slow antifoams may not enter the thin liquid film between two adjacent bubbles, but rather accumulate in the Plateau border regions and induce film rupture with increasing drainage. Stability of the foamed emulsions increased considerably with increasing pH, which was attributed to higher electrostatic repulsion between oil droplets and the effect on the balance between disjoining pressure and capillary pressure. The pH sensitivity originates from the carboxylic group of QS and constituents carrying ionic groups which are present in the QS-extract. Stability of foamed emulsions further increased when emulsifiers are added sequentially. The emulsion may solely be stabilized by β -LG. When QS is added after emulsification it is available to stabilize the air/water-interface. As shown in previous publications, β -LG efficiently stabilizes an oil/water-interface and QS forms a strong viscoelastic network to stabilize the air/water-interface. In this sequential approach the optimal properties of QS and β -LG are beneficially used to maximize stability.

Complex systems like foamed emulsions, which contain more than two phases, are challenging systems and various factors may influence stability. Although this study revealed important factors that influence stability of foamed emulsions, in future studies the impact of other (food) constituents like inorganic salts and hydrocolloids should be investigated. Charged groups may influence electrostatic conditions and hydrocolloids increase viscosity of the liquid phase, which may increase stability of the foamed emulsions. Their general impact on foams can be described from the literature, but their specific contribution and interrelations in these more complex systems need to be characterized in more detail. Future studies should also focus on other proteins like random coil proteins with different interfacial properties in comparison to globular proteins.

6. General discussion

This dissertation aimed to deepen understanding of the behavior of saponins at air/water- and oil/water-interfaces by combining interfacial rheology with experiments in dispersed model systems. Many studies focused on the characterization of interfacial properties but did not attempt to connect these with the stability of emulsions and/or foams. It is well-known that these systems are considerably more complicated than the idealized experimental setup in interfacial measurements. Therefore, interfacial properties can only be indicator for behavior in dispersed systems.

One part of this dissertation was to characterize interfacial properties, like adsorption and interfacial rheology of various saponins from different botanical origins and link these properties to foam properties (**manuscript I**). The second part of the dissertation focused on the interactions of Quillaja saponin (QS) and β -lactoglobulin (β -LG) in bulk (**manuscript II**). Afterwards interactions of QS and β -LG were characterized at the air/water- (**manuscript II**) and oil/water-interface (**manuscript III**) and these results were connected to foam and emulsion properties, respectively. In the last part of the dissertation the properties of foamed emulsions were characterized, which contained oil, water and air (**manuscript IV**). In these experiments, key factors were determined, which affected stability of foamed emulsions. Oil droplet size, pH and presence β -LG were identified as such key factors.

In the following chapters the results of this thesis are discussed in a general way and the light of new research findings. All subsections start with a short summary of the experimental findings.

6.1. The impact of structural features on interfacial properties of saponins from different botanical sources

In manuscript I, six different saponin-rich extracts from various botanical origin were analyzed with respect to adsorption as well as foaming, foam stability and foam structure (summarized as foam properties). Saponin extracts were chosen based on a previous study (Golemanov *et al.* 2013), which examined interfacial shear rheology of 13 saponin extracts. In Figure 1 differences in molecular structure of the discussed saponins are visualized. In the cited study, the authors grouped the saponin extracts based on their interfacial behavior. For experiments in manuscript I, three extracts from group EV, which formed strong viscoelastic interfacial layers, were chosen: *Quillaja saponaria* Molina (QS), *Camellia oleifera* Abel (TS) and *Aesculus hippocastanum* (ESC). To characterize the properties of saponins, which showed no viscoelastic properties (group LV) two extracts from *Tribulus terrestris* (TT) and *Glycyrrhiza glabra* (GA) were chosen as well as a previously not characterized extract from *Gypsophia* (GYP). From the six saponin extracts five had a triterpenoid aglycone and from these five QS and GYP mainly contain bidesmosidic saponins (two linked sugar residues) while TS, GA and ESC consist of monodesmoside saponins (one linked sugar residue). In contrast, TT is a mixture of mono- and bidesmosidic saponins, which have a steroidal aglycone. In addition, conductivity and FTIR measurements were performed to support results on foam stability due variation of pH and ionic strength. Although the number of samples in this thesis was relatively small, it can be concluded that usually, high dilational and shear viscoelasticity of saponin films at the air/water-interface led to a considerably high foamability and foam stability. But it was also shown that saponins with the highest dilational and shear moduli not necessarily yield the highest foam stability. However, adsorption and interfacial configuration of saponins did not correlate with foaming and foam stability. In addition, the classification of saponins as ionic or non-ionic surfactants is not useful with respect to forecast sensitivity to changes in pH and ionic strength.

It was shown that adsorption of all analyzed saponins is mixed-barrier controlled, which is in agreement with a previous study (Wojciechowski *et al.* 2011). The calculated diffusion coefficients were based on assumed hydrodynamic radii of the saponins. Calculated diffusion coefficients were distinctly lower than experimental diffusion coefficients (see Table I-3). This discrepancy led to the conclusion that adsorption is slowed down by an additional

barrier, which may be caused by steric hindrances and rearrangements of the saponin molecules upon adsorption. The amount of linked sugar residues may be an additional factor, which influences adsorption. As illustrated by the parameter Π_{5s}/Π_{1800s} (see Table I-3) the maximum surface pressure is reached faster by monodesmosidic saponins in comparison to bidesmosidic saponins. It may be hypothesized that the additional sugar residue in bidesmosidic saponins slows down adsorption.

As discussed in greater detail in chapter 2.3.1 and visualized in Figure 5 saponins may obtain two different interfacial configurations: lay-on and end-on configuration indicated by an area per molecule above and below 0.75 nm^2 , respectively (Pagureva *et al.* 2016). The area per molecule may be calculated by fitting the Frumkin-model to the concentration-dependent interfacial tension values. In manuscript I, the determined interfacial area for GYP indicated a lay-on configuration as expected for bidesmosidic saponins. For all other saponins with the exception of TT the obtained interfacial area indicated an end-on configuration. Results from the adsorption isotherm for TT were ambiguous and did not clearly indicate a certain type of interfacial configuration. As mentioned before, TT is a mixture of mono- and bidesmosidic saponins, which may explain the ambiguous results. However, interfacial configuration of saponins neither influenced adsorption nor foam properties.

When comparing the interfacial shear and dilational results of Golemanov *et al.* (2013) and Pagureva *et al.* (2016) with the foam properties presented in Figure I-2 of manuscript I it can be concluded that saponins with high dilational and shear viscoelasticity can form stable foams. Thereby it was possible to produce a foam of all aqueous solutions containing triterpenoid saponins. Bidesmosidic saponins (GYP and QS) yielded foams with highest stability. In contrast, foam properties are especially low for steroid saponins (here: TT) and saponins with only few sugar residues (here: GA), which also only showed a viscous response in shear experiments of Golemanov *et al.* (2013).

It was shown by Pagureva *et al.* (2016) that monodesmosidic saponins (TS and ESC) can undergo phase transition (indicated by high interaction values) and can form very high elastic interfacial films, which are somewhat sensitive to dilational stress but rather insensitive to shear stress. The authors additionally demonstrated that Quillaja saponins (bidesmosidic with long sugar chains and fatty acyl residue) can also form a strong viscoelastic network, which is less shear viscoelastic but is less affected by dilational stress. The reported phase transition may additionally contribute to the high foam stability of the analyzed saponin extracts TS and ESC.

Relatively high instability of foams from GA can be attributed to the proportional low amount of sugar residues in this saponin. The saponin is poorly soluble and only few intermolecular hydrogen bonds are formed between sugar residues, which consequentially lead to a weak interfacial network as shown by creep-recovery experiments (Golemanov *et al.* 2013).

Although differences between triterpenoid and steroidal aglycone structure are relatively small, these discrepancies tremendously impact interfacial rheology and foam properties. The exact reason or structural feature of steroidal saponins, which leads to poor foam properties and viscous films, is yet to be determined. The low ability of TT to form an interfacial viscoelastic network resulted in highly instable foams even at large concentrations of about 2 %. The very low ability to stabilize foams even at high concentrations, further supports the hypothesis that interfacial packaging of steroidal saponins is disadvantageous and the resulting interfacial film cannot withstand dilational and shear stress.

In colloidal science, low-molecular weight surfactants are usually classified as ‘ionic’ or ‘non-ionic’ based on their molecular structure. The former term is used when chargeable groups are present in the molecular structure of the surfactant. The latter term refers to surfactants with no chargeable groups and which interfacial properties are therefore insensitive to changes in ionic strength and changes in pH. In the past it was debated whether saponins may be classified as ionic or non-ionic surfactants (Wojciechowski 2013, Feng *et al.* 2015). In experiments of the present study the variation of pH and ionic strength showed that classifying saponins as ionic or non-ionic is not useful. FTIR and conductivity experiments revealed that QS, GYP, ESC and GA probably possessed chargeable groups or/and ionic residues in the extract. But interfacial tension and foam stability of these extracts were not always affected by changes in pH and ionic strength (see Figure I-3, Figure I-5 and chapter I-4.4). On the other hand, interfacial tension and foam stability of TS, which was classified as ‘non-ionic’, were tremendously influenced by changes in pH and ionic strength (see Figure I-6).

Manuscript I was an important step to increase knowledge on the link between interfacial rheology, adsorption and foam properties of saponins. However, due to diversity of saponins the impact of structural features, like subcategory of aglycone structure (e.g. oleanane, dammarane, ursolic to name a few), length of sugar residues and type of sugars on interfacial properties is yet to be determined.

6.2. Synergistic and antagonistic effects of QS/ β -LG-mixtures on stability of dispersed systems

As discussed in manuscript I and chapter 6.1, QS can thoroughly stabilize foams and is to-date the best characterized saponin extract. Therefore, all following experiments (manuscript II-IV) were performed with QS. The characterization of interfacial properties of an aqueous solution of QS was the first step to understand the relationship between interfacial properties, molecular structure and foam properties. In these relatively simple systems it is possible to study correlations between interfacial properties and foam and/or emulsion properties. Matrix effects occur when various constituents are mixed (proteins, lipids, carbohydrates, phenols and surfactants) and are a common phenomenon in food, animal nutrition or pharmaceutical products. Interactions between surfactants and proteins are well-known and were extensively researched in the past (Bos and van Vliet 2001; Pradines *et al.* 2009; Lech *et al.* 2014). As there have been evidences supporting the hypothesis that QS and β -LG form complexes, which influence interfacial properties (Kezwon and Wojciechowski 2014), additional experiments are carried out in this thesis on the binary system of QS and β -LG. In the next two subsections the interactions of QS with common food protein β -lactoglobulin in foams (see chapter 6.2.1), emulsions (see chapter 6.2.1) and foamed emulsions (see chapter 6.2.3) are discussed. All chapters start with a brief summary of the results from each manuscript and afterwards interfacial behavior and corresponding properties in dispersed systems are discussed.

6.2.1. Synergistic effect of QS/ β -LG-mixtures on foam properties

In manuscript II the interactions between QS and β -LG at the air/water-interface were characterized with respect to interfacial shear and dilational rheology, adsorption, complex formation and foam properties. The results of the experiments supported the hypothesis on molecular interaction of QS and β -LG in the bulk as well at the air/water-interface. Due to similar foam stabilizing mechanisms, a synergistic effect on foam stability was observed when QS and β -LG were mixed.

Interactions between QS and β -LG in the bulk were observed in an experiment on fluorescence quenching. Results indicated the formation of a ground-state complex (static quenching) and the inverse slope of the Cogan-plot revealed that QS interacts with 1.7 binding sites of β -LG (see Figure II-1). The interactions between QS and β -LG might be hydrogen bonds, electrostatic or hydrophobic interactions. In an additional experiment, it was shown that QS may slowly displace β -LG from the air/water-interface (Figure II-2). Whether displacement originated from the ‘orogenic displacement’ or the ‘competitive adsorption and complexation’ mechanism is unclear. But as QS was classified as an ionic surfactant (see Table I-5, Figure I-3 and chapter 6.1) it may be hypothesized that the ‘competitive adsorption and complexation’ mechanism is more likely to occur (Kotsmar *et al.* 2009).

Experimental results on short-term adsorption (Figure II-3) and dynamic interfacial tension (Table II-1) of mixtures of QS and β -LG were similar to QS, which imply that the interfacial film properties are dominated by QS. Interfacial interactions between QS and β -LG were characterized using dilational and shear experiments. High values of the complex viscoelastic moduli ($E^* > 100$ mN/m) were obtained when mixed interfacial films of QS and β -LG were subjected to dilational stress (see Figure II-4). As reported before (Stanimirova *et al.* 2011), QS film was highly viscoelastic with a high elastic proportion. All mixed interfacial films exhibited a primary elastic response and viscous moduli were very low. The high values for E^* are a sign for intermolecular interactions between adsorbed molecules. As all samples, QS, β -LG and their mixtures, exhibited high E^* it can be concluded that intermolecular interactions can be found in all interfacial films. These results were further supported by interfacial shear experiments (see Figure II-5). High values for the complex shear modulus (G^*) up to 70 mN/m were determined for QS and β -LG-interfacial films. Mixtures of QS and β -LG yielded even higher values for G^* , which imply an increase in intermolecular interaction. It was hypothesized that small concentrations of β -LG

strengthen the QS network, in accordance to hypothesis 2, which was reported before for another ionic surfactant and β -LG (Gunning *et al.* 2004). At higher β -LG concentration ($>0.05\%$) this effect is neglected.

As presented in manuscript I, stables foams are formed by QS due to the viscoelastic network. The stabilization of foam lamellae by a viscoelastic film is very unusual for such a small surfactant ($\sim 2\text{kDa}$) and is much more common for globular proteins. Usually low-molecular weight surfactants ($<0.5\text{ kDa}$) stabilize foam films by the Gibbs-Marangoni mechanism (Wilde *et al.* 2004) and are not able to form a viscoelastic network at the interface. Viscoelastic moduli for low-molecular surfactants are usually low with E^* around 10 mN/m as reported for SDS (Fainerman *et al.* 2010). For the Gibbs-Marangoni mechanism lateral mobility of the adsorbed surfactant molecules is necessary. Gravitational forces cause steady drainage of foam lamellae, thus decreasing their thickness. Concentration and interfacial tension gradients in the foam lamella, cause molecules from surfactant-enriched regions move along the interface to level out differences in concentration and interfacial tension. Hereby bulk solution is dragged along simultaneously and thereby restoring thickness of the foam lamellae. Quillaja saponins cannot stabilize foam lamellae by the Gibbs-Marangoni mechanism because intermolecular bonds fix saponin molecules inside the viscoelastic network.

Confirming hypothesis 2, in foam experiments it was shown that mixing QS and β -LG had a beneficial effect on foam density and foam stability. Even a small β -LG concentration tremendously increased foam stability (see Figure II-6). Foam stability distinctively increased in mixed QS/ β -LG-system because both substances form a strong joint viscoelastic network, which stabilizes foam lamellae (see Figure 9D). This is different from other protein-surfactant systems: usually foam stability in mixed systems is reduced because surfactants stabilize foam lamellae by the Gibbs-Marangoni mechanism, which requires high lateral mobility (Maldonado-Valderrama and Patino 2010). On the one hand, in protein-surfactant systems the lateral movement of the surfactant molecules is blocked by adsorbed protein molecules (see Figure 9A-C). On the other hand, the viscoelastic network of proteins is weakened by surfactants molecules.

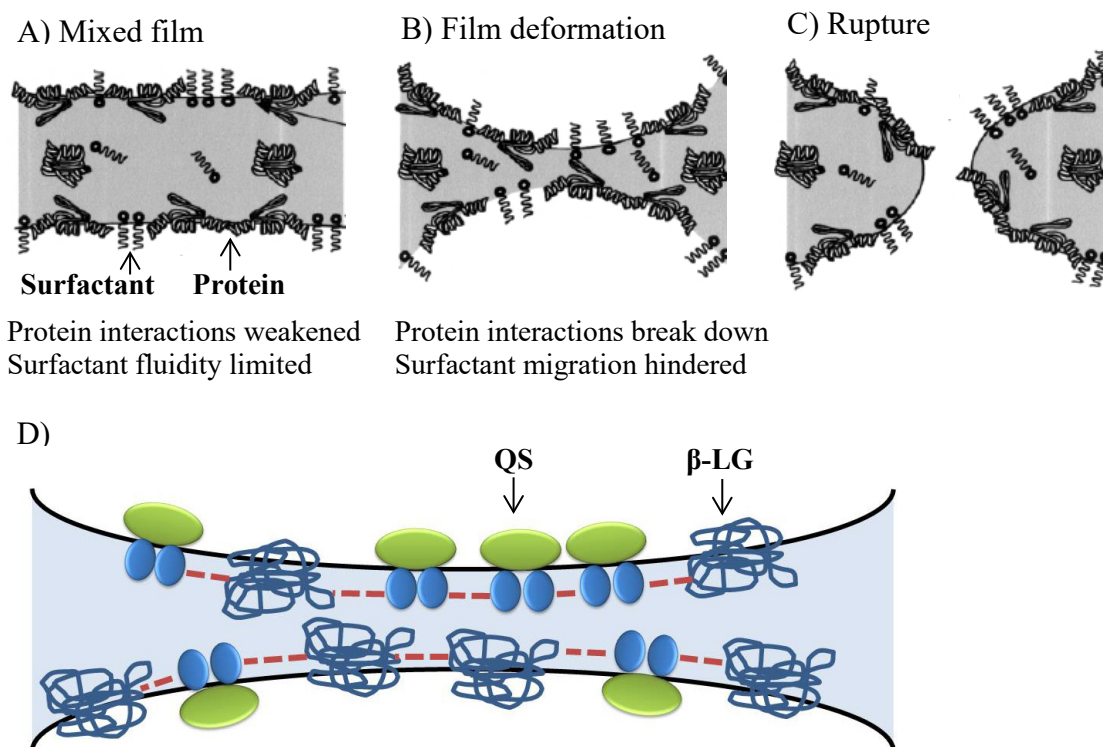


Figure 9 A-C) Vulnerability of thin films stabilized with a mixture of surfactant and protein (Adapted from Wilde *et al.* 2004 with permission from Elsevier) and D) joint interfacial network of QS and β -LG with intermolecular interactions (red dotted lines)

In manuscript II, results were presented supporting the hypothesis that complexes and interactions between QS and β -LG may occur both in the bulk and at the air/water-interface. These interactions did not only increase viscoelastic moduli in interfacial experiments but also foam stability was considerably increased in mixtures of QS and β -LG. Synergistic properties in surfactant/protein-systems are unusual and may open new opportunities in applications.

6.2.2. Antagonistic effect of QS/ β -LG-mixtures on emulsion stability

In manuscript II interactions of QS and β -LG in aqueous bulk as well as synergistic properties at the air/water-interface and in foams were determined. In contrast, experimental work in manuscript III was performed to investigate QS/ β -LG-interaction at a hydrophobic phase containing triglycerides (here: MCT-oil). It was shown, using similar experimental methods like in manuscript II that interactions between QS and β -LG lead to a viscous film that was prone to non-linear behavior upon imposed stress. In emulsions, mixtures of QS and β -LG led to extensive aggregation, which reduced kinetic stability.

The interfacial film containing QS was distinctly less viscoelastic and had a higher viscous proportion compared to the air/water-interface as visualized in Figure III-2,3,4 and 5. The reduction of viscoelastic properties of QS-films was described before by several authors (Wojciechowski 2013; Golemanov *et al.* 2014). In contrast, interfacial layers of β -LG were less affected by changes of the hydrophobic phase and remained primary elastic (indicated by low Φ in Figure III-3).

However, it remains unclear whether configuration of QS molecules adjusts when the hydrophobic phase is changed from air to oil. Several studies reported data, which showed that the area per molecule of a QS extract increased from 0.43 nm² at the air/water-interface (Böttcher and Drusch 2016) to \sim 1 nm² at the MCT-oil (Yang *et al.* 2013; Tippel *et al.* 2016b) and corn oil/water-interface water (Bai *et al.* 2016). But Wojciechowski (2013) presented results on the area per molecule for a Quillaja saponin extract, which did not differ at the air/water and tetradecane/water-interface. The increase in interfacial area per molecule from the air/water- to the triglyceride/water-interface may be associated with a change in configuration from end-on to lay-on configuration (see chapter 2.3.1) or may simply be attributed to the penetration of oil between adsorbed QS molecules (see chapter 2.3.3).

As discussed in further detail in chapter 2.3.3 linear alkanes and triglycerides may penetrate between adsorbed saponin molecules. Especially bulky triglycerides enter between adsorbed saponin molecules to hydrate the polar head groups and decreases intermolecular interactions between neighboring saponin molecules (see Figure 8). It may be therefore possible that the linear alkane tetradecane did lead to an increase in area per molecule as observed at the corn oil and MCT oil/water-interface in comparison to the air/water-interface, because tetradecane is less bulky.

Another reason may be a difference in adsorbed interfacial active residues of the saponin extract. It was characterized by Tippel *et al.* (2017) that phenols in the QS extract differ in hydrophilicity. Thus, with differing hydrophobicity of the non-aqueous phase other non-saponin constituents may adsorb at the interface and lead to differences in molecular arrangement at the interface.

Similar to manuscript II, experimental results of manuscript III showed that properties of mixed interfacial films containing QS and β -LG at the oil/water-interface were dominated by QS. Mixed interfacial layers of QS/ β -LG showed a non-linear response when subjected to dilational stress as indicated by Lissajous-plots (see Figure III-4). From Lissajous-plots it may be derived that the interfacial network between QS and β -LG is relatively stiff and is not able to rapidly adjust to increase of droplet volume (see Figure III-5). Stiffness of the interfacial network of mixed QS/ β -LG films decreased with increasing β -LG-concentration. Shear experiments supported the hypothesis on lateral interactions between QS and β -LG at the interface due to high shear moduli.

The divergent interfacial behavior of mixtures of QS and β -LG at the oil/water-interface in comparison to the air/water-interface may be attributed to differing properties of the individual substances. It is well-known that β -LG exhibits different adsorption kinetics at the oil/water-interface in comparison to the air/water-interface (Zhai *et al.* 2013; Zare *et al.* 2016). It is believed that unfolding is more pronounced at the oil/water-interface and therefore interfacial properties vary distinctly.

In further experiments in which emulsion properties were characterized it was shown that mixed QS and β -LG-emulsions were stabilized by electrostatic repulsion (see Figure III-8). The high negative charge of oil droplets covered by QS was reported before and attributed to the carboxylic group of QS and anionic residues like (+)-piscidic acid, syringic acid and *p*-coumaric acid, which can be found in the crude extract (Maier *et al.* 2015a; Tippel *et al.* 2017). It was shown that purification and thereby removing anionic non-saponin residues, can increase absolute values of ζ -potential from -70 mV to -50 mV (pH 7). β -LG is negatively charged at pH 7 because this pH is above the isoelectric point, which is around 5.1 (Schwenke 1998).

In mixed QS/ β -LG-emulsions with high β -LG-concentrations considerable aggregation was observed, which led to intense creaming after storage time of 7 days. Aggregation was attributed to partial displacement and/or structural changes of β -LG induced by QS. It is

possible that QS induces changes in the tertiary or quaternary structure of β -LG when complexes are formed. Prompted structural changes of β -LG by a phenol were described before for green tea polyphenol/ β -LG-systems (Staszewski *et al.* 2014). It may also be possible that, as reported in manuscript II, QS partially desorbs β -LG and that the detached β -LG parts cause the aggregation.

In summary, manuscript III revealed that properties of mixed interfacial films of QS and β -LG at the oil/water-interface are considerably different from the air/water-interface. Results indicate that interfacial interactions lead to a stiff network which is prone to non-linear behavior upon imposed stress. Furthermore, QS induced changes of β -LG, which prompted aggregation of oil droplets, thus reducing kinetic stability of emulsions.

6.2.3. Maximizing stability of foamed emulsions

Aim of manuscript IV was to evaluate important factors that affect stability of the foamed emulsions by using knowledge on destabilizing mechanism of foams and emulsions as well as finding from previous studies of this thesis (manuscript II+III). Foamed emulsions are a more complex dispersed system in comparison to foam and emulsion, which were described in manuscript II and III, respectively. It was hypothesized and shown that emulsions with a moderate oil droplet size yielded foamed emulsions with the highest stability. Furthermore, with increasing pH, electrostatic charge of oil droplets and in thin liquid films increased, which contributed to increased stability of the foamed emulsions. Another tool for increasing the stability of foamed QS emulsions is the use of β -LG to stabilize the oil/water-interface while QS stabilizes the air/water-interface.

Dispersed oil droplets in foams may be referred to as antifoams and either lead to a fast or slow foam destruction depending on the distribution of the oil droplets in the foam. The thermodynamic conditions, which determine the location of the oil droplets either in the Plateau borders (slow antifoam) or the thin liquid film (fast antifoam) may be determined using the film trapping technique (FTT). With the FTT the critical pressure of rupturing of an A/W/O-pseudoemulsion film is measured, which is also called 'entry-barrier'. Fast antifoams have a low entry-barrier and slow antifoams a high entry-barrier (Denkov 2004; Miller 2008). It was concluded that dispersed MCT-oil may be classified as a slow antifoam (see Figure 10) because foam decay was relatively slow (see Figure IV-5). Therefore, it was hypothesized that oil droplets accumulate in Plateau borders because slow antifoams cannot enter the thin liquid film due to thermodynamic conditions (Karakashev and Grozdanova 2012). Foam destruction in this case originates from liquid drainage, which reduced size of the Plateau borders and localized oil droplets subsequently lead to film rupture by spreading and bridging the Plateau borders. In contrast, fast antifoams may enter the thin liquid film between two adjacent bubbles and lead to bridging of foam lamella within seconds.

The influence of the oil droplet size on the stability of the foamed emulsion was shown by preparing emulsions with a constant QS-concentration and varying oil droplet size with a d_{50} ranging from 0.2 to 2 μm . At the optimal oil droplet size (0.6-1 μm), stability of the foamed emulsion was maximized (see Figure IV-4 and Figure IV-5). When oil droplets were smaller than the optimal size the amount of free QS was not sufficient to cover the oil/water- and air/water-interface at the same time and as a result foamed emulsions were

highly instable. Due to the insufficient coverage of the freshly formed bubble surface by QS rapid bubble coalescence occurred. The bubble coalescence during foaming led to a very low foaming speed. In contrast, large oil droplets have a proportionally smaller interfacial area and QS can stabilize both interfaces, which led to high foamability of emulsions. Free QS, which is not adsorbed at the oil/water-interface, adsorbs at the air/water-interface. The adsorption lowers the interfacial tension and a viscoelastic film is formed, which slows down thin liquid film rupture and coalescence. But the increased size of the oil droplets simultaneously accelerated bridging thin liquid films, which decreased foam stability.

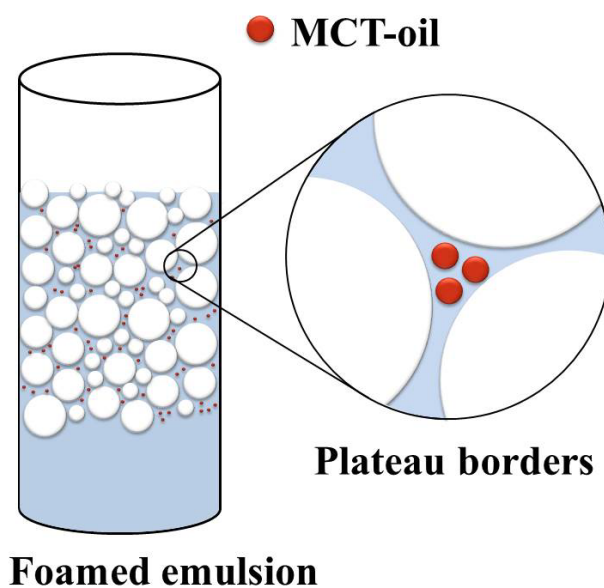


Figure 10 Dispersed droplets of MCT-oil presumably accumulate in Plateau borders as it is characteristic for slow antifoam

In experiments with varying pH it was shown that stability of the foamed emulsions was pH dependent and was maximized at pH 7 (Figure IV-7). The pH dependency of the stability of the foamed emulsions may be attributed to anionic residues present in the QS extract as well as the carboxylic group in the molecular structure of QS. Various anionic residues were reported before (Maier *et al.* 2015; Toppel *et al.* 2017), which affect the electrostatic conditions in the thin liquid film and on the surface of oil droplets. At very low pH (here: pH 2) electrostatic charge of the dispersed oil droplets was low (indicated by ζ -potential close to zero, see Figure IV-8). Therefore, electrostatic repulsion was too low to prevent coalescence of oil droplets, which caused distinct size enhancement of the oil droplets. Thus, foamed emulsions at pH 2 were highly instable due to the size of the aggregates, which accelerated bridging of foam lamellae. With increasing pH the electrostatic repulsion

between oil droplets increased (as indicated by ζ -potential), which prevented aggregation of oil droplets, thus increasing stability of the foamed emulsions. Stability of the foamed emulsions increased above pH 5 although ζ -potential did not change. It was therefore hypothesized that anionic residues may adsorb at the air/water-interface and that further increase of pH led to further deprotonation of the anionic groups. Thus electrostatic repulsion in the thin liquid films increased. At increasing pH electrostatic repulsion in the thin liquid film opposes further thinning, which increases foam stability.

In thin liquid films (<100 nm) attractive and repulsive forces determine the stability of the film. These forces may be repulsive electrostatic, attractive van der Waals and repulsive steric forces. The disjoining pressure Π thereby sums up the condition in the thin liquid film. When the disjoining pressure is smaller than the capillary pressure (which originates from pressure differences between the dispersed and continuous phase), the thin liquid film is thinning. With decreasing thickness of the thin liquid film the disjoining pressure changes and meta-stable states like *common black films* and *Newton black films* may be obtained. (Stubenrauch and von Klitzing 2003; Fauser and von Klitzing 2014; Schramm 2005)

In food products, proteins are commonly present and it was shown before in manuscript II and III that QS and β -LG interact in the bulk and at the interface. In manuscript IV the impact of β -LG on the stability of foamed QS-emulsions was characterized. Based on previously reported results on interfacial rheology it was hypothesized that QS is most suitable to stabilize the air/water-interface and β -LG is best in stabilizing the oil/water-interface. Results of interfacial tension, ζ -potential and foaming speed showed that this distribution of QS and β -LG can be obtained by sequentially adding QS to a β -LG emulsion (see Figure IV-10). As hypothesized it was shown that the stability of a foamed QS/ β -LG emulsion distinctly increased by sequential addition of QS to a previously homogenized β -LG emulsion (Mix_{post}). In contrast, when QS and β -LG were simultaneously homogenized stability of a QS/ β -LG emulsion was considerably lower. Mixed films of QS and β -LG are on the one hand beneficial at the air/water-interface and mixed films showed higher viscoelasticity, which resulted in higher foam stability (as shown in manuscript II). On the other hand mixtures of QS and β -LG at the oil/water-interface led to interfacial layers, which responded to interfacial stress (dilatational experiments) with non-linear behavior and had a high viscous proportion (manuscript III). Apart from that QS/ β -LG-emulsions were prone to aggregation, which decreased emulsion stability. In foamed emulsions (Mix_{pre}) mixed interfacial layers of QS and β -LG at the air/water- and oil/water-interface did not increase

stability of the foamed emulsions in comparison to a foamed QS-emulsion. It was expected that stability of foamed emulsions would increase when β -LG is added, because the amount of surface active molecules was increased.

In manuscript IV findings of the previous manuscripts were applied to determine major factors, which impact stability of a food product-like system (foamed emulsions). Oil droplet size was a crucial factor to control stability of the foamed emulsions. It was shown that a moderate oil droplet size should be applied to minimize bridging foam lamella by oil droplets and to maximize amount of free surfactant. Stability of the foamed emulsion may also be increased by adjusting a high pH, which increased electrostatic repulsion in thin liquid films and between oil droplets. Furthermore the oil/water-interface should be stabilized by another surface active constituent (here: β -LG) in order for QS to solely stabilize the air/water-interface.

7. Concluding remarks and outlook

The comprehensive experimental methodology of the present thesis led to a significant contribution in understanding of the structure-function relationship in saponin-based dispersed systems. This thesis aimed to connect behavior of saponins at aqueous interfaces with foam and emulsion properties. It was further aimed to explain underlying stabilizing or destabilizing phenomena of dispersed systems containing Quillaja saponin (QS) and β -lactoglobulin (β -LG).

The present work showed that there are several structural features of saponins, which are associated with good foam properties (high foaming speed, liquid content and foam stability). Saponins should have a triterpenoid aglycone structure of oleanane type. The amount of sugar residues seems to play a minor role on interfacial properties, but as discussed, sugar chains should have a certain length to provide sufficient hydrophilicity. The good foam properties of triterpenoid saponins were attributed to the formation of a highly viscoelastic network at the air/water-interface through intermolecular hydrogen bonds between neighboring sugar residues. It was therefore concluded that saponin foams are not stabilized by the Gibbs-Marangoni mechanisms, which usually applies for low-molecular weight surfactants.

It was shown that QS has unique properties at aqueous interfaces and in dispersed systems. QS is suitable to stabilize foams and emulsions by the formation of a viscoelastic network and electrostatic repulsion, respectively. High foam stability was supported by data on interfacial rheology from previous publications, which revealed unusually high viscoelastic moduli.

In mixtures of QS and β -LG, complex formation in the bulk and interactions at aqueous interfaces (here: air/water and MCT-oil/water) were shown by fluorescence experiments and pendant drop experiments as well as shear rheology, respectively. It was further discussed that QS desorbs β -LG from the air/water-interface and it was assumed that this was due to the competitive adsorption and complexation mechanism. Foam stability distinctly increased in mixed QS/ β -LG-systems due to the joint viscoelastic network formed by both constituents. The usual antagonistic effect (competitive stabilization by Gibbs Marangoni mechanism vs. the viscoelastic network) of mixing of a low-molecular weight surfactant and protein on foam properties was not observed.

Results furthermore showed that interfacial properties of mixed QS/ β -LG-systems were distinctly affected by the type of the hydrophobic phase. In contrast to the air/water-interface interfacial layers at the oil/water-interface were distinctly less viscoelastic and had a high viscous proportion. These differences were attributed to changes in interfacial arrangement of QS and β -LG due to changes of hydrophobicity of the non-aqueous phase. The aggregation of oil droplets in emulsions containing QS and β -LG presumably originated from structural changes of β -LG (tertiary or quaternary structure) induced by QS and/or partial displacement of β -LG from the oil/water-interface.

This thesis showed that stability of complex systems like foamed emulsion may be controlled by a few key factors. The oil droplet size and the pH of an emulsion are crucial factors that affect stability of the foamed emulsion. Oil droplets should be in a medium size to postpone bridging of oil droplets and to provide sufficient amount of free surfactant that can stabilize the air/water-interface. At high pH the stability of the foamed emulsions is highest due to electrostatic repulsion of oil droplets, which slows down shrinkage of Plateau borders. In addition, the higher electrostatic repulsion in foam lamellae also reduces drainage of the aqueous phase from the thin liquid film and therefore postpones rupture of foam lamellae. Based on the speed of defoaming it was concluded that the dispersed MCT-oil may be classified as a slow antifoam and may therefore be located in the Plateau borders of the foam.

From an academic point of view it would be interesting in future studies to deepen understanding on the relationship between molecular features of saponins and their interfacial properties by performing experiments with a larger samples size including plants without commercially available extracts. Preparative HPLC methods can help to obtain purified saponin extracts. These studies should especially include saponins with aglycone structures different from oleanane type like ursolic and dammarane type. In addition, the role of the length of sugar residues and other structural features like fatty acyl group should be examined. It would be expected (as stated in this thesis) that with increasing length of the sugar residues (regardless of mono- or bidesmosidic) the hydrophilicity increases, which leads to higher stability of foams. Future project should involve close cooperation of analytical chemists and research groups focusing on interfacial properties. When reliable information on chemical composition of saponin extracts are available and are directly connected to

interfacial properties, even more distinct and meaningful correlations on structure-function-relationship can be obtained.

Further research should also examine the supramolecular structure of monodesmosidic saponins and observed phase transition of some monodesmosidic saponins. More fundamental studies may address the inability of steroid saponins to form viscoelastic layers in more detail to identify the responsible molecular feature. One major question is whether and how the level of viscoelasticity is connected to foam properties. Besides that, comprehensive data are still necessary to also connect interfacial properties with emulsifying and emulsion stabilizing properties as viscoelasticity of the interfacial layers may distinctly affect emulsion properties.

The knowledge on mixtures of QS and β -LG distinctly increased in the last years and the analysis of other proteins, like random coil proteins would be an interesting opportunity due to the absence of tertiary and quarternary structure. Another scope of future research project may be the mechanism by which QS desorbs β -LG and other proteins. Therefore, sequential adsorption of QS to a loaded β -LG interface may be studied using Brewster angle microscopy or atomic force microscopy (AFM). These methods were successfully applied in previous studies for other surfactant/protein-systems. To better understand stabilizing mechanisms in QS/ β -LG foams model experiments of thin liquid films should be performed by thin film pressure balance experiments. In this context, it would be interesting to determine whether QS and its mixtures with β -LG are able to form *common black films* or *Newton black films*. These terms refer to thermodynamically meta-stable states of thin liquid films and are associated with high stability. The interfacial arrangement of QS and β -LG (or other proteins) at aqueous interfaces may be analyzed by further studies by ellipsometry, which gives insights in thickness of the interfacial layer. To determine the underlying mechanism that is responsible for the aggregation of oil droplets in mixed QS/ β -LG emulsions, Fourier transform infrared spectroscopy may be used to determine structural change of β -LG.

From an industrial point of view, the interactions between QS and other (food) constituents, like inorganic salts and hydrocolloids need to be determined to control properties of dispersed systems. Salts are well-known to affect electrostatic charge of functional groups and a screening of these groups may reduce stability of dispersed systems because electrostatic repulsion between oil droplets and in thin liquid films may be reduced. To enhance knowledge on the underlying mechanisms that are responsible for the stability of foamed

emulsions fundamental studies may be connected to stability tests. One option for a fundamental approach is the film trapping technique, which may be used to determine the entry barrier of dispersed MCT-oil droplets and to derive the location of the oil droplets in the foam. For visual conformation of the location of the oil droplets light microscopy may also be used.

With respect to sustainability and ecological responsibility, research projects should focus on saponins from sustainable resources like legumes. Saponins are undesired constituents in animal nutrition due to adverse gastro-intestinal effects. By extracting saponins and using them in food products the added value of legumes increases and financial incentive may increase popularity of legumes for agricultural businesses. Saponins from legumes are usually monodesmosidic saponins and in the case of pea saponins an additional heat-sensitive group is linked to the aglycone structure. It is yet unclear how the functional group affects interfacial properties and if these saponins may be used in dispersed systems.

It can be summarized, that saponins, despite of some drawback, are a promising class of natural surfactants to be used in dispersed systems. The haemolytic activity of saponins is an issue when using saponins as adjuvants in vaccines, but low dosage of saponins in food should not cause adverse effects on human health. Molecular structure of saponins is neither similar to low-molecular weight surfactants nor globular proteins and the same holds true for interfacial properties and stabilization mechanisms in foams. But a generalization of the properties of saponins is difficult due to the immense structural diversity. A vision for the future may be the customization of interfacial properties by mixing various saponin derivates. In addition, the use of sustainable resources is an excellent option to increase added value of low-price products like legumes.

References

- Almutairi, M. S. and Ali, M., 2015**, “Direct detection of saponins in crude extracts of soapnuts by FTIR,” *Natural Product Research*, V. 29, No. 13, pp. 1271–1275. doi: 10.1080/14786419.2014.992345.
- Andreuccetti, C.; Carvalho, R. A.; and Grosso, C. R., 2010**, “Gelatin-based films containing hydrophobic plasticizers and saponin from *Yucca schidigera* as the surfactant,” *Food Research International*, V. 43, No. 6, pp. 1710–1718. doi: 10.1016/j.foodres.2010.05.013.
- Andreuccetti, C.; Carvalho, R. A.; Galicia-García, T.; Martínez-Bustos, F.; and Grosso, C. R., 2011**, “Effect of surfactants on the functional properties of gelatin-based edible films,” *Journal of Food Engineering*, V. 103, No. 2, pp. 129–136. doi: 10.1016/j.jfoodeng.2010.10.007.
- Aveyard, R.; Binks, B. P.; Clint, J. H.; and Fletcher, P., 1999**, “Foams and emulsions: their stability and breakdown by solid particles and liquid droplets,” J. F. Sadoc and N. Rivier, eds., *Foams and Emulsions*, pp. 21–44.
- Bai, L.; Huan, S.; Gu, J.; and McClements, D. J., 2016**, “Fabrication of oil-in-water nanoemulsions by dual-channel microfluidization using natural emulsifiers: Saponins, phospholipids, proteins, and polysaccharides,” *Food Hydrocolloids*, V. 61, pp. 703–711. doi:10.1016/j.foodhyd.2016.06.035.
- Bankefors, J.; Nord, L. I.; and Kenne, L., 2008**, “Structural classification of Quillaja saponins by electrospray ionization ion trap multiple-stage mass spectrometry in combination with multivariate analysis, proof of concept,” *Chemometrics and Intelligent Laboratory Systems*, V. 90, No. 2, pp. 178–187. doi: 10.1016/j.chemolab.2007.09.008.
- Bankefors, J.; Nord, L. I.; and Kenne, L., 2010**, “Multidimensional profiling of components in complex mixtures of natural products for metabolic analysis, proof of concept: Application to Quillaja saponins,” *Journal of Chromatography B*, V. 878, No. 3-4, pp. 471–476. doi: 10.1016/j.jchromb.2009.11.034.
- Bankefors, J.; Broberg, S.; Nord, L. I.; and Kenne, L., 2011**, “Electrospray ionization ion-trap multiple-stage mass spectrometry of Quillaja saponins,” *J. Mass Spectrom.*, V. 46, No. 7, pp. 658–665. doi: 10.1002/jms.1935.
- Bee, R. D.; Clement, A.; and Prins, A., 1987**, “Behaviour of an Aerated Food Model,” E. Dickinson, ed., *Food Emulsions and Foams: Based on the proceedings of an International Symposium organised by the Food Chemistry Group of The Royal Society of Chemistry at Leeds from 24th to 26th March 1986*, pp. 128–143.
- Benjamins, J., 2000**, “Static and dynamic properties of protein adsorbed at liquid interfaces.” Ph.D. Thesis, Wageningen University.
- Bos, M. and van Vliet, T., 2001**, “Interfacial rheological properties of adsorbed protein layers and surfactants: a review,” *Advances in Colloid and Interface Science*, V. 91, No. 3, pp. 437–471. doi: 10.1016/S0001-8686(00)00077-4.
- Böttcher, S. and Drusch, S., 2016**, “Interfacial Properties of Saponin Extracts and Their Impact on Foam Characteristics,” *Food Biophysics*. V.11, No. 1, pp.91-100. doi: 10.1007/s11483-015-9420-5.

- Böttcher, S.; Scampicchio, M.; and Drusch, S., 2016**, “Mixtures of saponins and beta-lactoglobulin differ from classical protein/surfactant-systems at the air-water interface,” *Colloids and Surfaces A: Physicochemical and Engineering Aspects*, V. 506, pp. 765–773. doi: 10.1016/j.colsurfa.2016.07.057.
- Böttcher, S.; Keppler, J.; and Drusch, S., 2017**, “Mixtures of Quillaja saponin and beta-lactoglobulin at the oil/water-interface: Adsorption, interfacial rheology and emulsion properties”, *Colloids and Surfaces A: Physicochemical and Engineering Aspects*, V. 518, pp. 46–56. doi: 10.1016/j.colsurfa.2016.12.041.
- Brun, M.; Delample, M.; Harte, E.; Lecomte, S.; and Leal-Calderon, F., 2015**, “Stabilization of air bubbles in oil by surfactant crystals: A route to produce air-in-oil foams and air-in-oil-in-water emulsions,” *Food Research International*, V. 67, pp. 366–375. doi: 10.1016/j.foodres.2014.11.044.
- Canto, Gizele Scotti do; Treter, J.; Yang, S.; Borré, G. L.; Peixoto, Maria Paula Garofo; and Ortega, G. G., 2010**, “Evaluation of foam properties of saponin from *Ilex paraguariensis* A. St. Hil. (Aquifoliaceae) fruits,” *Braz. J. Pharm. Sci.*, V. 46. doi: 10.1590/S1984-82502010000200010.
- Carpiné, D.; Dagostin, João Luiz Andreotti; de Andrade, Eriel Forville; Bertan, L. C.; and Mafra, M. R., 2016**, “Effect of the natural surfactant *Yucca schidigera* extract on the properties of biodegradable emulsified films produced from soy protein isolate and coconut oil,” *Industrial Crops and Products*, V. 83, pp. 364–371. doi: 10.1016/j.indcrop.2016.01.014.
- Chen, Q.; Luo, J.-G.; and Kong, L.-Y., 2011**, “New triterpenoid saponins from the roots of *Gypsophila perfoliata* Linn,” *Carbohydrate Research*, V. 346, No. 14, pp. 2206–2212. doi: 10.1016/j.carres.2011.07.027.
- Chen, Y.-F.; Yang, C.-H.; Chang, M.-S.; Ciou, Y.-P.; and Huang, Y.-C., 2010**, “Foam Properties and Detergent Abilities of the Saponins from *Camellia oleifera*,” *IJMS*, V. 11, No. 11, pp. 4417–4425. doi: 10.3390/ijms11114417.
- Cheok, C. Y.; Salman, Hanaa Abdel Karim; and Sulaiman, R., 2014**, “Extraction and quantification of saponins: A review,” *Food Research International*, V. 59, pp. 16–40. doi: 10.1016/j.foodres.2014.01.057.
- Creamer, L. K.; Loveday, S. M.; and Sawyer, L., 2011**, “Milk Proteins | β -Lactoglobulin,” J. W. Fuquay, ed., *Encyclopedia of Dairy Sciences*, pp. 787–794. doi: 10.1016/B978-0-12-374407-4.00433-7.
- Dan, A.; Kotsmar, C.; Ferri, J. K.; Javadi, A.; Karbaschi, M.; Krägel, J.; Wüstneck, R.; and Miller, R., 2012**, “Mixed protein–surfactant adsorption layers formed in a sequential and simultaneous way at water–air and water–oil interfaces,” *Soft Matter*, V. 8, No. 22, p. 6057.
- Dan, A.; Gochev, G.; Krägel, J.; Aksenenko, E. V.; Fainerman, V. B.; and Miller, R., 2013**, “Interfacial rheology of mixed layers of food proteins and surfactants,” *Current Opinion in Colloid & Interface Science*, V. 18, No. 4, pp. 302–310. doi: 10.1016/j.cocis.2013.04.002.

- Dan, A.; Gochev, G.; and Miller, R., 2015**, “Tensiometry and dilational rheology of mixed β -lactoglobulin/ionic surfactant adsorption layers at water/air and water/hexane interfaces,” *Journal of Colloid and Interface Science*, V. 449, pp. 383–391. doi: 10.1016/j.jcis.2015.01.035.
- Demana, P. H.; Davies, N. M.; Vosgerau, U.; and Rades, T., 2004**, “Pseudo-ternary phase diagrams of aqueous mixtures of Quil A, cholesterol and phospholipid prepared by the lipid-film hydration method,” *International Journal of Pharmaceutics*, V. 270, No. 1-2, pp. 229–239.
- Denkov, N. D., 2004**, “Mechanisms of Foam Destruction by Oil-Based Antifoams,” *Langmuir*, V. 20, No. 22, pp. 9463–9505.
- Dickinson, E., 2010**, “Flocculation of protein-stabilized oil-in-water emulsions,” *Colloids and Surfaces B: Biointerfaces*, V. 81, No. 1, pp. 130–140.
- Dickinson, E., 2015**, “Structuring of colloidal particles at interfaces and the relationship to food emulsion and foam stability,” *Journal of Colloid and Interface Science*, V. 449, pp. 38–45. doi: 10.1016/j.jcis.2014.09.080.
- Dinchev, D.; Janda, B.; Evstatieva, L.; Oleszek, W.; Aslani, M. R.; and Kostova, I., 2008**, “Distribution of steroidal saponins in *Tribulus terrestris* from different geographical regions,” *Phytochemistry*, V. 69, No. 1, pp. 176–186. doi: 10.1016/j.phytochem.2007.07.003.
- Dinda, B.; Debnath, S.; Mohanta, B.C.; Harigaya, Y., 2010** “Naturally Occurring Triterpenoid Saponins”, *Chemistry & Biodiversity*, V. 7, No.10, pp. 2327–2580. doi: 10.1002/cbdv.200800070
- Dukhin, S.; Saezther, O.; and Sjöblom, J., 2001**, “Coupling of Coalescence and Flocculation in Dilute O/W Emulsions,” J. Sjöblom, ed., *Encyclopedic handbook of emulsion technology*. Marc Dekker, New York, Basel.
- Ewoldt, R. H.; Hosoi, A. E.; and McKinley, G. H., 2008**, “New measures for characterizing nonlinear viscoelasticity in large amplitude oscillatory shear,” *J. Rheol.*, V. 52, No. 6, p. 1427. doi: 10.1122/1.2970095.
- Fainerman, V.; Lucassen-Reynders, E.; and Miller, R., 1998**, “Adsorption of surfactants and proteins at fluid interfaces,” *Colloids and Surfaces A: Physicochemical and Engineering Aspects*, V. 143, 2-3, pp. 141–165. doi: 10.1016/S0927-7757(98)00585-8.
- Fainerman, V. B.; Möbius, D. and Miller, R., 2001**, “Surfactants. Chemistry, interfacial properties, applications”, *Elsevier Science*, Amsterdam, New York, 1st edn., V. 13. ISBN: 0444509623.
- Fainerman, V. B.; Leser, M. E.; Michel, M.; Lucassen-Reynders, E. H.; and Miller, R., 2005**, “Kinetics of the Desorption of Surfactants and Proteins from Adsorption Layers at the Solution/Air Interface,” *J. Phys. Chem. B*, V. 109, No. 19, pp. 9672–9677. doi: 10.1021/jp050212o.
- Fainerman, V. B.; Miller, R.; Ferri, J. K.; Watzke, H.; Leser, M. E.; and Michel, M., 2006**, “Reversibility and irreversibility of adsorption of surfactants and proteins at liquid interfaces,” *Advances in Colloid and Interface Science*, 123-126, pp. 163–171. doi: 10.1016/j.cis.2006.05.023.

- Fainerman, V. B.; Lylyk, S. V.; Aksenenko, E. V.; Petkov, J. T.; Yorke, J.; and Miller, R., 2010**, “Surface tension isotherms, adsorption dynamics and dilational viscoelasticity of sodium dodecyl sulphate solutions,” *Colloids and Surfaces A: Physicochemical and Engineering Aspects*, V. 354, No. 1-3, pp. 8–15. doi: 10.1016/j.colsurfa.2009.02.022.
- Fausser, H. and Klitzing, R. v., 2014**, “Effect of polyelectrolytes on (de)stability of liquid foam films,” *Soft Matter*, V. 10, No. 36, pp. 6903–6916.
- Feng, J.; Chen, Y.; Liu, X.; and Liu, S., 2015**, “Efficient improvement of surface activity of tea saponin through Gemini-like modification by straightforward esterification,” *Food Chemistry*, V. 171, pp. 272–279. doi: 10.1016/j.foodchem.2014.08.125.
- Fenwick, D. E. and Oakenfull, D., 1983**, “Saponin Content of Food Plants and Some Prepared Foods,” *Journal of the Science of Food and Agriculture*, V. 34, pp. 186–191. doi: 10.1002/jsfa.2740340212.
- Fenwick, G. R.; Price, K. R.; Tsukamoto, C.; and Okubo, K., 1991**, “Saponins,” in: D’Mello, J. P. Felix; C. M. Duffus; J. H. Duffus; D. G. Allen, eds., *Toxic substances in crop plants*, pp. 285–328.
- Frechet, D.; Christ, B.; du Sorbier, Bertrand Monegier; Fischer, H.; and Vuilhorgne, M., 1991**, “Four triterpenoid saponins from dried roots of *Gypsophila* species,” *Phytochemistry*, V. 30, No. 3, pp. 927–931. doi: 10.1016/0031-9422(91)85281-4.
- Freer, E. M.; Yim, K. S.; Fuller, G. G.; and Radke, C. J., 2004**, “Shear and Dilational Relaxation Mechanisms of Globular and Flexible Proteins at the Hexadecane/Water Interface,” *Langmuir*, V. 20, No. 23, pp. 10159–10167. doi: 10.1021/la0485226.
- Gholami, S. and Bordbar, A.-K., 2014**, “Exploring binding properties of naringenin with bovine β -lactoglobulin: A fluorescence, molecular docking and molecular dynamics simulation study,” *Biophysical Chemistry*, V. 187-188, pp. 33–42. doi: 10.1016/j.bpc.2014.01.003.
- Golemanov, K.; Tcholakova, S.; Denkov, N.; Pelan, E.; and Stoyanov, S. D., 2012**, “Surface Shear Rheology of Saponin Adsorption Layers,” *Langmuir*, V. 28, No. 33, pp. 12071–12084. doi: 10.1021/la302150j.
- Golemanov, K.; Tcholakova, S.; Denkov, N.; Pelan, E.; and Stoyanov, S. D., 2013**, “Remarkably high surface visco-elasticity of adsorption layers of triterpenoid saponins,” *Soft Matter*, V. 9, No. 24, p. 5738. doi: 10.1039/c3sm27950b.
- Golemanov, K.; Tcholakova, S.; Denkov, N.; Pelan, E.; and Stoyanov, S. D., 2014**, “The role of the hydrophobic phase in the unique rheological properties of saponin adsorption layers,” *Soft Matter*, V. 10, No. 36, pp. 7034–7044. doi: 10.1039/c4sm00406j.
- Graham, D. and Phillips, M., 1979**, “Proteins at liquid interfaces: I. Kinetics of Adsorption and Surface Denaturation,” *Journal of Colloid and Interface Science*, V. 70, No. 3, pp. 403–414. doi: 10.1016/0021-9797(79)90048-1.

- Güçlü-Üstündağ, Ö. and Mazza, G., 2007**, “Saponins: Properties, Applications and Processing,” *Critical Reviews in Food Science and Nutrition*, V. 47, No. 3, pp. 231–258. doi: 10.1080/10408390600698197.
- Gunning, P. A.; Mackie, A. R.; Gunning, A. P.; Woodward, N. C.; Wilde, P. J.; and Morris, V. J., 2004**, “Effect of Surfactant Type on Surfactant–Protein Interactions at the Air–Water Interface,” *Biomacromolecules*, V. 5, No. 3, pp. 984–991.
- Hänsel, R. and Sticher, O., 2010**, *Pharmakognosie – Phytopharmazie*, Springer Medizin Verlag, Heidelberg. ISBN: 978-3-642-00962-4.
- Hansted, J. G.; Wejse, P. L.; Bertelsen, H.; and Otzen, D. E., 2011**, “Effect of protein–surfactant interactions on aggregation of β -lactoglobulin,” *Biochimica et Biophysica Acta (BBA) - Proteins and Proteomics*, V. 1814, No. 5, pp. 713–723. doi: 10.1016/j.bbapap.2011.03.011.
- Haralampidis, K.; Trojanowska, M.; Osbourn, A.E., 2002**, “Biosynthesis of Triterpenoid Saponins in Plants,” *Advances in Biochemical Engineering/Biotechnology*, V. 75, 31–49. doi: 10.1007/3-540-44604-4_2.
- Heurtault, B.; Saulnier, P.; Pech, B.; Proust, J.-E.; and Benoit, J.-P., 2003**, “Physico-chemical stability of colloidal lipid particles,” *Biomaterials*, V. 24, No. 23, pp. 4283–4300. doi: 10.1016/S0142-9612(03)00331-4.
- Hu, W.; Liu, J.; Luo, Q.; Han, Y.; Wu, K.; Lv, S.; Xiong, S.; and Wang, F., 2011**, “Elucidation of the binding sites of sodium dodecyl sulfate to β -lactoglobulin using hydrogen/deuterium exchange mass spectrometry combined with docking simulation,” *Rapid Commun. Mass Spectrom.*, V. 25, No. 10, pp. 1429–1436. doi: 10.1002/rcm.5012.
- Huang, Q.; He, M.; Chen, H.; Shao, L.; Liu, D.; Luo, Y.; and Dai, Y., 2007**, “Protective Effects of Sasanquasaponin on Injury of Endothelial Cells Induced by Anoxia and Reoxygenation in vitro,” *Basic Clin Pharmacol Toxicol*, V. 101, No. 5, pp. 301–308. doi: 10.1111/j.1742-7843.2007.00119.x.
- Ibanoglu, E., 2000**, “Foaming behaviour of liquorice (*Glycyrrhiza glabra*) extract,” *Food Chemistry*, V. 70, No. 3, pp. 333–336. doi: 10.1016/S0308-8146(00)00098-4.
- Ivanov, I. B.; Danov, K. D.; Dimitrova, D.; Boyanov, M.; Ananthapadmanabhan, K. P.; and Lips, A., 2010**, “Equations of state and adsorption isotherms of low molecular non-ionic surfactants,” *Colloids and Surfaces A: Physicochemical and Engineering Aspects*, V. 354, 1-3, pp. 118–133. doi: 10.1016/j.colsurfa.2009.11.031.
- Jian, H.-l.; Liao, X.-x.; Zhu, L.-w.; Zhang, W.-m.; and Jiang, J.-x., 2011**, “Synergism and foaming properties in binary mixtures of a biosurfactant derived from *Camellia oleifera* Abel and synthetic surfactants,” *Journal of Colloid and Interface Science*, V. 359, No. 2, pp. 487–492. doi: 10.1016/j.jcis.2011.04.038.
- Karakashev, S.; Manev, E.; and Nguyen, A., 2004**, “Interpretation of negative values of the interaction parameter in the adsorption equation through the effects of surface layer heterogeneity,” *Advances in Colloid and Interface Science*, V. 112, 1-3, pp. 31–36. doi: 10.1016/j.cis.2004.06.002.
- Karakashev, S. I. and Grozdanova, M. V., 2012**, “Foams and antifoams,” *Advances in Colloid and Interface Science*, 176-177, pp. 1–17. doi: 10.1016/j.cis.2012.04.001.

- Kaur, K.; Kumar, R.; and Mehta, S. K., 2016**, “Formulation of saponin stabilized nanoemulsion by ultrasonic method and its role to protect the degradation of quercetin from UV light,” *Ultrasonics Sonochemistry*, V. 31, pp. 29–38. doi: 10.1016/j.ultsonch.2015.11.017.
- Keppler, J. K.; Koudelka, T.; Palani, K.; Stuhldreier, M. C.; Temps, F.; Tholey, A.; and Schwarz, K., 2013**, “Characterization of the covalent binding of allyl isothiocyanate to β -lactoglobulin by fluorescence quenching, equilibrium measurement, and mass spectrometry,” *Journal of Biomolecular Structure and Dynamics*, V. 32, No. 7, pp. 1103–1117. doi: 10.1080/07391102.2013.809605.
- Keppler, J. K.; Stuhldreier, M. C.; Temps, F.; and Schwarz, K., 2014**, “Influence of mathematical models and correction factors on binding results of polyphenols and retinol with β -lactoglobulin measured with fluorescence quenching,” *Food Biophysics*, V. 9, No. 2, pp. 158–168. doi: 10.1007/s11483-013-9328-x.
- Kezwon, A. and Wojciechowski, K., 2014**, “Interaction of Quillaja bark saponins with food-relevant proteins,” *Advances in Colloid and Interface Science*. V. 209, pp. 185–195. doi: 10.1016/j.cis.2014.04.005.
- Khan, A. M. and Shah, S. S., 2008**, “Determination of CMC of SDS and the Effect of Low Concentration of Pyrene on its CMC,” *J.Chem.Soc.Pak.*, V. 30, No. 2, pp. 186–191.
- Kichatov, B.; Korshunov, A.; Son, K.; and Son, E., 2016**, “Combustion of emulsion-based foam,” *Combustion and Flame*, V. 172, pp. 162–172. doi: 10.1016/j.combustflame.2016.07.017.
- Kim, D. A.; Cornec, M.; and Narsimhan, G., 2005**, “Effect of thermal treatment on interfacial properties of β -lactoglobulin,” *Journal of Colloid and Interface Science*, V. 285, No. 1, pp. 100–109. doi: 10.1016/j.jcis.2004.10.044.
- Kim, H.-J.; Bot, A.; de Vries, Isabel C.M.; Golding, M.; and Pelan, E. G., 2013**, “Effects of emulsifiers on vegetable-fat based aerated emulsions with interfacial rheological contributions,” *Food Research International*, V. 53, No. 1, pp. 342–351. doi: 10.1016/j.foodres.2013.04.027.
- Kite, G. C.; Howes, M.-J. R.; and Simmonds, Monique S. J., 2004**, “Metabolomic analysis of saponins in crude extracts of Quillaja saponaria by liquid chromatography/mass spectrometry for product authentication,” *Rapid Commun. Mass Spectrom.*, V. 18, No. 23, pp. 2859–2870. doi: 10.1002/rcm.1698.
- Kolev, V. L.; Danov, K. D.; Kralchevsky, P. A.; Broze, G.; and Mehreteab, A., 2002**, “Comparison of the van der Waals and Frumkin Adsorption Isotherms for Sodium Dodecyl Sulfate at Various Salt Concentrations,” *Langmuir*, V. 18, No. 23, pp. 9106–9109. doi: 10.1021/la0259858.
- Kotsmar, C.; Pradines, V.; Alahverdijeva, V. S.; Aksenenko, E. V.; Fainerman, V. B.; Kovalchuk, V. I.; Krägel, J.; Leser, M. E.; Noskov, B. A.; and Miller, R., 2009**, “Thermodynamics, adsorption kinetics and rheology of mixed protein–surfactant interfacial layers,” *Advances in Colloid and Interface Science*, V. 150, No. 1, pp. 41–54. doi: 10.1016/j.cis.2009.05.002.
- Krägel, J.; Derkatch, S. R.; and Miller, R., 2008**, “Interfacial shear rheology of protein–surfactant layers,” *Advances in Colloid and Interface Science*, V. 144, No. 1-2, pp. 38–53. doi: 10.1016/j.cis.2008.08.010.

- Kralova, I. and Sjöblom, J., 2009**, “Surfactants Used in Food Industry: A Review,” *Journal of Dispersion Science and Technology*, V. 30, No. 9, pp. 1363–1383. doi: 10.1080/01932690902735561.
- Kuo, P.-C.; Lin, T.-C.; Yang, C.-W.; Lin, C.-L.; Chen, G.-F.; and Huang, J.-W., 2010**, “Bioactive Saponin from Tea Seed Pomace with Inhibitory Effects against *Rhizoctonia solani*,” *J. Agric. Food Chem.*, V. 58, No. 15, pp. 8618–8622. doi: 10.1021/jf1017115.
- Kuznesof, P. M. and Soares, L. M. V., 2005**, *Quillaja Extracts Type 1 and Type 2 Chemical and Technical Assessment (CTA)*.
- Langevin, D., 2008**, “Aqueous Foams: A Field of Investigation at the Frontier Between Chemistry and Physics,” *ChemPhysChem*, V. 9, No. 4, pp. 510–522. doi: 10.1002/cphc.200700675.
- Lech, F. J.; Steltenpool, P.; Meinders, M. B.; Sforza, S.; Gruppen, H.; and Wierenga, P. A., 2014**, “Identifying changes in chemical, interfacial and foam properties of β -lactoglobulin–sodium dodecyl sulphate mixtures,” *Colloids and Surfaces A: Physicochemical and Engineering Aspects*, V. 462, pp. 34–44. doi: 10.1016/j.colsurfa.2014.08.019.
- Liang, L.; Tajmir-Riahi, H. A.; and Subirade, M., 2008**, “Interaction of β -Lactoglobulin with Resveratrol and its Biological Implications,” *Biomacromolecules*, V. 9, No. 1, pp. 50–56. doi: 10.1021/bm700728k.
- Lucassen-Reynders, E. H.; Lucassen, J.; Garrett, P. R.; Giles, D.; and Hollway, F., 1975**, “Dynamic Surface Measurements as a Tool to Obtain Equation-of-State Data for Soluble Monolayers,” E. D. Goddard, ed., *Monolayers*, pp. 272–285. doi: 10.1021/ba-1975-0144.ch021.
- Lunkenheimer, K.; Malysa, K.; Winsel, K.; Geggel, K.; and St. Siegel, 2010**, “Novel Method and Parameters for Testing and Characterization of Foam Stability,” *Langmuir*, V. 26, No. 6, pp. 3883–3888. doi: 10.1021/la9035002.
- Mackie, A. R.; Gunning, A.; Wilde, P. J.; and Morris, V. J., 1999**, “Orogenic Displacement of Protein from the Air/Water Interface by Competitive Adsorption,” *Journal of Colloid and Interface Science*, V. 210, No. 1, pp. 157–166. doi: 10.1006/jcis.1998.5941.
- Mackie, A. R.; Gunning, A. P.; Wilde, P. J.; and Morris, V. J., 2000**, “Competitive Displacement of β -Lactoglobulin from the Air/Water Interface by Sodium Dodecyl Sulfate,” *Langmuir*, V. 16, No. 21, pp. 8176–8181. doi: 10.1021/la0003950.
- Mackie, A. and Wilde, P., 2005**, “The role of interactions in defining the structure of mixed protein–surfactant interfaces,” *Advances in Colloid and Interface Science*, V. 117, No. 1-3, pp. 3–13. doi: 10.1016/j.cis.2005.04.002.
- Maier, C.; Conrad, J.; Carle, R.; Weiss, J.; and Schweiggert, R. M., 2015a**, “Phenolic Constituents in Commercial Aqueous Quillaja (*Quillaja saponaria* Molina) Wood Extracts,” *J. Agric. Food Chem.*, V. 63, No. 6, pp. 1756–1762. doi:10.1021/jf506277p.
- Maier, C.; Oechsle, A. M.; and Weiss, J., 2015b**, “Cross-linking oppositely charged oil-in-water emulsions to enhance heteroaggregate stability,” *Colloids and Surfaces B: Biointerfaces*, V. 135, pp. 525–532. doi: 10.1016/j.colsurfb.2015.08.009.

- Majhi, P. R.; Ganta, R. R.; Vanam, R. P.; Seyrek, E.; Giger, K.; and Dubin, P. L., 2006**, “Electrostatically Driven Protein Aggregation: β -Lactoglobulin at Low Ionic Strength,” *Langmuir*, V. 22, No. 22, pp. 9150–9159. doi: 10.1021/la053528w.
- Maldonado-Valderrama, J. and Patino, J., 2010**, “Interfacial rheology of protein–surfactant mixtures,” *Current Opinion in Colloid & Interface Science*, V. 15, No. 4, pp. 271–282. doi: 10.1016/j.cocis.2009.12.004.
- Mbama Gaporaud, B. M.; Sajet, P.; and Antonini, G., 1998**, “Three-phase foam equation of state,” *Chemical Engineering Science*, V. 53, No. 4, pp. 735–741. doi: 10.1016/S0009-2509(98)00332-7.
- McClements, D. J., 2004**, “Protein-stabilized emulsions,” *Current Opinion in Colloid & Interface Science*, V. 9, No. 5, pp. 305–313. doi: 10.1016/j.cocis.2004.09.003.
- Miller, R.; Wüstneck, R.; Krägel, J.; and Kretzschmar, G., 1996**, “Dilational and shear rheology of adsorption layers at liquid interfaces,” *Colloids and Surfaces A: Physicochemical and Engineering Aspects*, V. 111, No. 1-2, pp. 75–118. doi: 10.1016/0927-7757(95)03492-7.
- Miller, C., 2008**, “Antifoaming in aqueous foams,” *Current Opinion in Colloid & Interface Science*, V. 13, No. 3, pp. 177–182. doi: 10.1016/j.cocis.2007.11.007.
- Mitra, S. and Dungan, S. R., 1997**, “Micellar Properties of Quillaja Saponin. 1. Effects of Temperature, Salt, and pH on Solution Properties,” *Journal of Agriculture and Food Chemistry*, V. 45, pp. 1587–1595. doi: 10.1021/jf960349z.
- Mitra, S. and Dungan, S. R., 2000**, “Micellar properties of quillaja saponin. 2. Effect of solubilized cholesterol on solution properties,” *Colloids and Surfaces B: Biointerfaces*, V. 17, No. 2, pp. 117–133. doi: 10.1016/S0927-7765(99)00088-0.
- Morris, V. J. and Gunning, A. P., 2008**, “Microscopy, microstructure and displacement of proteins from interfaces: implications for food quality and digestion,” *Soft Matter*, V. 4, No. 5, p. 943. doi: 10.1039/B718904D.
- Najmabadi, M.; Tamm, T.; Klaiber, M.; Baroud, Y.; Drusch, S.; and Simon, S., 2013**, Real-time Determination of Interfacial Tension from the Shape of a Pendant Drop Based on Embedded Image Processing, Chania, Greece. ILASS – Europe 2013, 25th European Conference on Liquid Atomization and Spray Systems.
- Negi, J. S.; Negi, P. S.; Pant, G. J.; Rawat, M.; and Negi, S. K., 2013**, “Naturally occurring saponins: Chemistry and biology,” *Journal of Poisonous and Medicinal Plant Research*, V. 1, No. 1, pp. 6–11.
- Nord, L. I. and Kenne, L., 2000**, “Novel acetylated triterpenoid saponins in a chromatographic fraction from Quillaja saponaria Molina,” *Carbohydrate Research*, V. 329, No. 4, pp. 817–829. doi: 10.1016/S0008-6215(00)00248-2.
- Oakenfull, D., 1986**, “Aggregation of Saponins and Bile Acids in Aqueous Solution,” *Australian Journal of Chemistry*, V. 39, No. 10, pp. 1671–1683. doi: 10.1071/CH9861671.
- Oda, K.; Matsuda, H.; Murakami, T.; Katayama, S.; Ohgitani, T.; and Yoshikawa, M., 2000**, “Adjuvant and Haemolytic Activities of 47 Saponins,” *Biological Chemistry*, V. 381, pp. 66–74.

- Oleszek, W. and Bialy, Z., 2006, "Chromatographic determination of plant saponins—An update (2002–2005)," *Journal of Chromatography A*, V. 1112, No. 1-2, pp. 78–91. doi: 10.1016/j.chroma.2006.01.037.
- Ozturk, B.; Argin, S.; Ozilgen, M.; and McClements, D. J., 2014, "Formation and Stabilization of Nanoemulsion-Based Vitamin E Delivery Systems using Natural Surfactants: Quillaja Saponin and Lecithin," *Journal of Food Engineering*, V. 142, pp. 57–63. doi: 10.1016/j.jfoodeng.2014.06.015.
- Pagureva, N.; Tcholakova, S.; Golemanov, K.; Denkov, N.; Pelan, E.; and Stoyanov, S. D., 2016, "Surface properties of adsorption layers formed from triterpenoid and steroid saponins," *Colloids and Surfaces A: Physicochemical and Engineering Aspects*, V. 491, pp. 18–28. doi: 10.1016/j.colsurfa.2015.12.001.
- Patino, J., Rodriguez Niño, R.; Sánchez, C. C.; Molina Ortiz, S.; and Añón, M. C., 2005, "Dilatational properties of soy globulin adsorbed films at the air–water interface from acidic solutions," *Journal of Food Engineering*, V. 68, No. 4, pp. 429–437. doi: 10.1016/j.jfoodeng.2004.06.020.
- Pavan, P. C.; Crepaldi, E. L.; de A. Gomes, Gilmar; and Valim, J. B., 1999, "Adsorption of sodium dodecylsulfate on a hydrotalcite-like compound. Effect of temperature, pH and ionic strength," *Colloids and Surfaces A: Physicochemical and Engineering Aspects*, V. 154, No. 3, pp. 399–410. doi: 10.1016/S0927-7757(98)00847-4.
- Peixoto, Maria Paula G.; Treter, J.; de Resende, Pedro Ernesto; da Silveira, Nádyá Pesce; Ortega, G. G.; Lawrence, M. J.; and Dreiss, C. A., 2011, "Wormlike Micellar Aggregates of Saponins from *Ilex paraguariensis* A. St. Hil. (mate): A Characterisation by Cryo-TEM, Rheology, Light Scattering and Small-Angle Neutron Scattering," *Journal of Pharmaceutical Sciences*, V. 100, No. 2, pp. 536–546. doi: 10.1002/jps.22283
- Pertuit, D.; Avunduk, S.; Mitaine-Offer, A.-C.; Miyamoto, T.; Tanaka, C.; Paululat, T.; Delemasure, S.; Dutartre, P.; and Lacaille-Dubois, M.-A., 2014, "Triterpenoid saponins from the roots of two *Gypsophila* species," *Phytochemistry*, V. 102, pp. 182–188. doi: 10.1016/j.phytochem.2014.02.018
- Petkov, J. T.; Gurkov, T. D.; Campbell, B. E.; and Borwankar, R. P., 2000, "Dilatational and Shear Elasticity of Gel-like Protein Layers on Air/Water Interface," *Langmuir*, V. 16, No. 8, pp. 3703–3711. doi: 10.1021/la991287k.
- Phan, C. M.; Le, T. N.; and Yusa, S., 2012, "A new and consistent model for dynamic adsorption of CTAB at air/water interface," *Colloids and Surfaces A: Physicochemical and Engineering Aspects*, V. 406, pp. 24–30. doi: 10.1016/j.colsurfa.2012.04.044.
- Piotrowski, M.; Lewandowska, J.; and Wojciechowski, K., 2012, "Biosurfactant–Protein Mixtures: Quillaja Bark Saponin at Water/Air and Water/Oil Interfaces in Presence of β -Lactoglobulin," *The Journal of Physical Chemistry B*, V. 116, No. 16, pp. 4843–4850. doi: 10.1021/jp301174d.
- Pojer, E.; Mattivi, F.; Johnson, D.; Stockley, C.S., 2013, "The Case for Anthocyanin Consumption to Promote Human Health: A Review" *Comprehensive Reviews in Food Science and Food Safety*, V. 12, No. 5, pp. 483–508. doi: 10.1111/1541-4337.12024.

- Pradines, V.; Krägel, J.; Fainerman, V. B.; and Miller, R., 2009**, “Interfacial Properties of Mixed β -Lactoglobulin–SDS Layers at the Water/Air and Water/Oil Interface,” *J. Phys. Chem. B*, V. 113, No. 3, pp. 745–751. doi: 10.1021/jp8091573.
- Raskin, I.; Ribnicky, D.M.; Komarnytsky, S.; Ilic, N.; Poulev, A.; Borisjuk, N.; Brinker, A.; Moreno, D.A.; Ripoll, C.; Yakoby, N.; O'Neal, J.M.; Cornwell, T.; Pastor, I.; Fridlender, B., 2002**, “Plants and human health in the twenty-first century”, *Trends in Biotechnology*, V. 20, No. 12, pp. 522–531. doi: 10.1016/S0167-7799(02)02080-2.
- Ravera, F.; Liggieri, F.; Loglio, G., “Dilational rheology of adsorbed layers by oscillating drop bubbles”, in: Miller, R.; Liggieri, L.; and Krotov, V. V., (Eds.) 2009, *Interfacial rheology*, Brill, Leiden-Boston. pp 137-177. doi: 10.1016/j.cocis.2010.04.001.**
- Reichert, C. L.; Salminen, H.; Leuenberger, B. H.; Hinrichs, J.; and Weiss, J., 2015**, “Miscibility of Quillaja Saponins with other Co-surfactants under Different pH Values,” *Journal of Food Science*, V. 80, No. 11, pp. E2495-E2503. doi: 10.1111/1750-3841.13097
- Reichert, C. L.; Salminen, H.; Leuenberger, B. H.; and Weiss, J., 2016**, “Influence of heat on miscibility of Quillaja saponins in mixtures with a co-surfactant,” *Food Research International*, V. 88, Part A, pp. 16–23. doi: 10.1016/j.foodres.2016.03.034.
- Reim, V. and Rohn, S., 2015**, “Characterization of saponins in peas (*Pisum sativum* L.) by HPTLC coupled to mass spectrometry and a hemolysis assay,” *Food Research International*, V. 76, pp. 3–10. doi: 10.1016/j.foodres.2014.06.043.
- Rodriguez Nino, M.; Sanchez, C.; Ruizhenestrosa, V.; and Patino, J., 2005**, “Milk and soy protein films at the air/water interface,” *Food Hydrocolloids*, V. 19, No. 3, pp. 417–428. doi: 10.1016/j.foodhyd.2004.10.008.
- Sagis, L. M. and Fischer, P., 2014**, “Nonlinear rheology of complex fluid–fluid interfaces,” *Current Opinion in Colloid & Interface Science*, V. 19, No. 6, pp. 520–529. doi: 10.1016/j.cocis.2014.09.003.
- Salminen, H.; Aulbach, S.; Leuenberger, B. H.; Tedeschi, C.; and Weiss, J., 2014**, “Influence of surfactant composition on physical and oxidative stability of Quillaja saponin-stabilized lipid particles with encapsulated ω -3 fish oil,” *Colloids and Surfaces B: Biointerfaces*, V. 122, pp. 46–55. doi: 10.1016/j.colsurfb.2014.06.045.
- San Martín, R. and Briones, R., 2000**, “Quality control of commercial quillaja (*Quillaja saponaria* Molina) extracts by reverse phase HPLC,” *Journal of the Science of Food and Agriculture*, V. 80, No. 14, pp. 2063–2068.
- Sarnthein-Graf, C. and La Mesa, C., 2004**, “Association of saponins in water and water–gelatine mixtures,” *Thermochimica Acta*, V. 418, No. 1-2, pp. 79–84. doi: 10.1016/j.tca.2003.11.044.
- Sastre, F.; Ferreira, F.; and Pedreschi, F., 2016**, “MALDI-TOF mass spectrometry and reversed-phase HPLC-ELSD chromatography for structural and quantitative studies of major steroid saponins in commercial extracts of *Yucca schidigera* Roezl,” *Journal of Pharmaceutical and Biomedical Analysis*, V. 120, pp. 270–282. doi: 10.1016/j.jpba.2015.12.043

- Schroeter, H.; Heiss, C.; Spencer, J.P.; Keen, C.L.; Lupton, J.R.; Schmitz, H.H., 2010**, “Recommending flavanols and procyanidins for cardiovascular health: Current knowledge and future needs”, *Molecular Aspects of Medicine*, V. 31, No. 6, pp. 546–557. doi: 10.1016/j.mam.2010.09.008.
- Schwenke, K. D., 1998**, “Proteins: Some Principles of Classification and Structure,” in: D. Möbius and R. Miller, eds., *Proteins at liquid interfaces*, pp. 1–50.
- Scognamiglio, M.; Severino, V.; D’Abrosca, B.; Chambery, A.; and Fiorentino, A., 2015**, “Structural Elucidation of Saponins,” *Studies in Natural Products Chemistry*, pp. 85–120. doi: 10.1016/B978-0-444-63473-3.00004-6.
- Sherif, T.; Ahmed, R.; Shah, S.; and Amani, M., 2015**, “Rheological behavior of oil-based drilling foams,” *Journal of Natural Gas Science and Engineering*, V. 26, pp. 873–882. doi: 10.1016/j.jngse.2015.07.022.
- Shpigelman, A.; Israeli, G.; and Livney, Y. D., 2010**, “Thermally-induced protein–polyphenol co-assemblies: beta lactoglobulin-based nanocomplexes as protective nanovehicles for EGCG,” *Food Hydrocolloids*, V. 24, No. 8, pp. 735–743. doi: 10.1016/j.foodhyd.2010.03.015.
- Simjoo, M.; Rezaei, T.; Andrianov, A.; and Zitha, P., 2013**, “Foam stability in the presence of oil: Effect of surfactant concentration and oil type,” *Colloids and Surfaces A: Physicochemical and Engineering Aspects*, V. 438, pp. 148–158. doi: 10.1016/j.colsurfa.2013.05.062.
- Sparg, S.G.; Light, M.E.; van Staden, J., 2004**, “Biological activities and distribution of plant saponins”, *Journal of Ethnopharmacology*, V. 94, No. 2-3, pp. 219–243. doi: 10.1016/j.jep.2004.05.016.
- Stanimirova, R.; Marinova, K.; Tcholakova, S.; Denkov, N. D.; Stoyanov, S.; and Pelan, E., 2011**, “Surface Rheology of Saponin Adsorption Layers,” *Langmuir*, V. 27, No. 20, pp. 12486–12498. doi: 10.1021/la202860u.
- Staszewski, M. von; Pizones Ruiz-Henestrosa, Victor M.; and Pilosof, A. M., 2014**, “Green tea polyphenols- β -lactoglobulin nanocomplexes: Interfacial behavior, emulsification and oxidation stability of fish oil,” *Food Hydrocolloids*, V. 35, pp. 505–511.
- Stubenrauch, C. and Klitzing, R. v., 2003**, “Disjoining pressure in thin liquid foam and emulsion films—new concepts and perspectives,” *J. Phys.: Condens. Matter*, V. 15, No. 27, pp. R1197.
- Sun, H.-X.; Xie, Y.; and Ye, Y.-P., 2009**, “Advances in saponin-based adjuvants,” *Vaccine*, V. 27, No. 12, pp. 1787–1796. doi: 10.1016/j.vaccine.2009.01.091.
- Talbot, J.; Tarjus, G.; van Tassel, P. R.; and Viot, P., 2000**, “From car parking to protein adsorption: an overview of sequential adsorption processes,” *Colloids and Surfaces A: Physicochemical and Engineering Aspects*, V. 165, 1-3, pp. 287–324. doi: 10.1016/S0927-7757(99)00409-4.
- Tamm, F.; Sauer, G.; Scampicchio, M.; and Drusch, S., 2012**, “Pendant drop tensiometry for the evaluation of the foaming properties of milk-derived proteins,” *Food Hydrocolloids*, V. 27, No. 2, pp. 371–377. doi: 10.1016/j.foodhyd.2011.10.013.

- Taulier, N. and Chalikian, T. V., 2001**, “Characterization of pH-induced transitions of β -lactoglobulin: ultrasonic, densimetric, and spectroscopic studies,” *Journal of Molecular Biology*, V. 314, No. 4, pp. 873–889.
- Thalhamer, B. and Himmelsbach, M., 2014**, “Characterization of quillaja bark extracts and evaluation of their purity using liquid chromatography–high resolution mass spectrometry,” *Phytochemistry Letters*, V. 8, pp. 97–100.
doi: 10.1016/j.phytol.2014.02.009.
- Tippel, J.; Reim, V.; Rohn, S.; and Drusch, S., 2016a**, “Colour stability of lutein esters in liquid and spray dried delivery systems based on Quillaja saponins,” *Food Research International*. V. 87, pp.68-75. doi:10.1016/j.foodres.2016.06.014.
- Tippel, J.; Lehmann, M.; Klitzing, R. v.; and Drusch, S., 2016b**, “Interfacial properties of Quillaja saponins and its use for micellisation of lutein esters,” *Food Chemistry*, V. 212, pp. 35–42. doi: 10.1016/j.foodchem.2016.05.130.
- Tippel, J.; Gies, K.; Harbaum-Piayda, B.; Steffen-Heins, A.; and Drusch, S., 2017**, “Composition of Quillaja saponin extract affects lipid oxidation in oil-in-water emulsions,” *Food Chemistry*, V. 221, pp. 386–394.
- Treter, J.; Peixoto, Maria P. G.; Ortega, G. G.; and Canto, G. S., 2010**, “Foam-forming properties of *Ilex paraguariensis* (mate) saponin: foamability and foam lifetime analysis by Weibull equation,” *Quím. Nova*, V. 33, No. 7, pp. 1440–1443.
doi: 10.1590/S0100-40422010000700003.
- Ulaganathan, V.; Bergenstahl, B.; Krägel, J.; and Miller, R., 2012**, “Adsorption and shear rheology of β -lactoglobulin/SDS mixtures at water/hexane and water/MCT interfaces,” *Colloids and Surfaces A: Physicochemical and Engineering Aspects*, V. 413, pp. 136–141. doi: 10.1016/j.colsurfa.2012.02.027.
- van de Weert, Marco, 2010**, “Fluorescence Quenching to Study Protein-ligand Binding: Common Errors,” *J Fluoresc*, V. 20, No. 2, pp. 625–629.
doi:10.1007/s10895-009-0572-x.
- van Kempen, Silvia E. H. J.; Schols, H. A.; van der Linden, Erik; and Sagis, Leonard M. C., 2013**, “Non-linear surface dilatational rheology as a tool for understanding microstructures of air/water interfaces stabilized by oligofructose fatty acid esters,” *Soft Matter*, V. 9, No. 40, p. 9579. doi: 10.1039/C3SM51770E.
- Vincken, J.-P.; Heng, L.; de Groot, A.; Gruppen, H., 2007** “Saponins, classification and occurrence in the plant kingdom”, *Phytochemistry*, V. 68, No. 3, pp. 275–297.
doi: 10.1016/j.phytochem.2006.10.008.
- Viseu, M. I.; Melo, E. P.; Carvalho, T. I.; Correia, R. F.; and Costa, S. M., 2007**, “Unfolding Kinetics of β -Lactoglobulin Induced by Surfactant and Denaturant: A Stopped-Flow/Fluorescence Study,” *Biophysical Journal*, V. 93, No. 10, pp. 3601–3612. doi: 10.1529/biophysj.106.101667.
- Voutquenne-Nazabadioko, L.; Gevrenova, R.; Borie, N.; Harakat, D.; Sayagh, C.; Weng, A.; Thakur, M.; Zaharieva, M.; and Henry, M., 2013**, “Triterpenoid saponins from the roots of *Gypsophila trichotoma* Wender,” *Phytochemistry*, V. 90, pp. 114–127. doi: 10.1016/j.phytochem.2013.03.001.
- Walstra, P., 2003**, *Physical chemistry of foods*, Marcel Dekker, New York.

- Wan, Z.; Yang, X.; and Sagis, Leonard M. C., 2016**, “Nonlinear Surface Dilatational Rheology and Foaming Behavior of Protein and Protein Fibrillar Aggregates in the Presence of Natural Surfactant,” *Langmuir*, V. 32, No. 15, pp. 3679–3690. doi: 10.1021/acs.langmuir.6b00446.
- Wan, Z.-L.; Wang, L.-Y.; Wang, J.-M.; Yuan, Y.; and Yang, X.-Q., 2014**, “Synergistic Foaming and Surface Properties of a Weakly Interacting Mixture of Soy Glycinin and Biosurfactant Stevioside,” *J. Agric. Food Chem.*, V. 62, No. 28, pp. 6834–6843. doi: 10.1021/jf502027u.
- Ward, A. F. H. and Tordai, L., 1946**, “Time-Dependence of Boundary Tensions of Solutions I. The Role of Diffusion in Time-Effects,” *J. Chem. Phys.*, V. 14, No. 7, p. 453. doi: 10.1063/1.1724167.
- Wierenga, P. A. and Gruppen, H., 2010**, “New views on foams from protein solutions” *Current Opinion in Colloid & Interface Science*, V. 15, No. 5, pp. 365–373. doi: 10.1016/j.cocis.2010.05.017.
- Wilde, P.; Mackie, A.; Husband, F.; Gunning, P.; and Morris, V., 2004**, “Proteins and emulsifiers at liquid interfaces,” *Advances in Colloid and Interface Science*, V. 108–109, pp. 63–71. doi: 10.1016/j.cis.2003.10.011.
- Wojciechowski, K.; Piotrowski, M.; Popielarz, W.; and Sosnowski, T. R., 2011**, “Short- and mid-term adsorption behaviour of Quillaja Bark Saponin and its mixtures with lysozyme,” *Food Hydrocolloids*, V. 25, No. 4, pp. 687–693. doi: 10.1016/j.foodhyd.2010.07.007.
- Wojciechowski, K., 2013**, “Surface activity of saponin from Quillaja bark at the air/water and oil/water interfaces,” *Colloids and Surfaces B: Biointerfaces*, V. 108, pp. 95–102. doi: 10.1016/j.colsurfb.2013.02.008.
- Wojciechowski, K.; Orczyk, M.; Marcinkowski, K.; Kobiela, T.; Trapp, M.; Gutberlet, T.; and Geue, T., 2014a**, “Effect of hydration of sugar groups on adsorption of Quillaja bark saponin at air/water and Si/water interfaces,” *Colloids and Surfaces B: Biointerfaces*, V. 117, pp. 60–67. doi: 10.1016/j.colsurfb.2014.02.010.
- Wojciechowski, K.; Kezwon, A.; Lewandowska, J.; and Marcinkowski, K., 2014b**, “Effect of β -casein on surface activity of Quillaja bark saponin at fluid/fluid interfaces,” *Food Hydrocolloids*, V. 34, pp. 208–216. doi: 10.1016/j.foodhyd.2012.09.010.
- Wojciechowski, K.; Orczyk, M.; Gutberlet, T.; Trapp, M.; Marcinkowski, K.; Kobiela, T.; and Geue, T., 2014c**, “Unusual penetration of phospholipid mono- and bilayers by Quillaja bark saponin biosurfactant,” *Biochimica et Biophysica Acta (BBA) - Biomembranes*, V. 1838, No. 7, pp. 1931–1940. doi: 10.1016/j.bbamem.2014.04.008.
- Wojciechowski, K.; Orczyk, M.; Gutberlet, T.; and Geue, T., 2016a**, “Complexation of phospholipids and cholesterol by triterpenic saponins in bulk and in monolayers,” *Biochimica et Biophysica Acta (BBA) - Biomembranes*, V. 1858, No. 2, pp. 363–373. doi: 10.1016/j.bbamem.2015.12.001.
- Wojciechowski, K.; Orczyk, M.; Trapp, M.; and Gutberlet, T., 2016b**, “Effect of triterpene and steroid saponins on lecithin bilayers,” *Colloids and Surfaces A: Physicochemical and Engineering Aspects*. Vol. 510, pp. 150–158. doi: 10.1016/j.colsurfa.2016.04.065.

- Wulff, G. and Tschesche, R., 1969**, “Über Triterpene - XXVI: Über die Struktur der Roskastaniensaponine (Aescin) und die Aglykone verwandter Glykoside,” *Tetrahedron*, V. 25, pp. 415–436.
- Wüstneck, R.; Fainerman, V. B.; Aksenenko, E. V.; Kotsmar, C.; Pradines, V.; Krägel, J.; and Miller, R., 2012**, “Surface dilatational behavior of β -casein at the solution/air interface at different pH values,” *Colloids and Surfaces A: Physicochemical and Engineering Aspects*, V. 404, pp. 17–24. doi: 10.1016/j.colsurfa.2012.03.050.
- Yan, J.; Wu, Z.; Zhao, Y.; and Jiang, C., 2011**, “Separation of tea saponin by two-stage foam fractionation,” *Separation and Purification Technology*, V. 80, No. 2, pp. 300–305. doi: 10.1016/j.seppur.2011.05.010.
- Yang, Y. and McClements, D. J., 2013**, “Encapsulation of vitamin E in edible emulsions fabricated using a natural surfactant,” *Food Hydrocolloids*, V. 30, No. 2, pp. 712–720. doi: 10.1016/j.foodhyd.2012.09.003.
- Yang, Y.; Leser, M. E.; Sher, A. A.; and McClements, D. J., 2013**, “Formation and stability of emulsions using a natural small molecule surfactant: Quillaja saponin (Q-Naturale®),” *Food Hydrocolloids*, V. 30, No. 2, pp. 589–596. doi: 10.1016/j.foodhyd.2012.08.008.
- Yao, S.; Luo, J.; Huang, X.; and Kong, L., 2008**, “Application of preparative high-speed counter-current chromatography/preparative high-performance liquid chromatography mode in rapid separation of saponins,” *Journal of Chromatography B*, V. 864, No. 1-2, pp. 69–77. doi: 10.1016/j.jchromb.2008.01.047.
- Yao, S.; Luo, J.-G.; Ma, L.; and Kong, L.-Y., 2011**, “Two New Triterpenoid Saponins from the Roots of *Gypsophila paniculata* with Potent α -Glucosidase Inhibition Activity,” *Chinese Journal of Natural Medicines*, V. 9, No. 6, pp. 401–405. doi: 10.3724/SP.J.1009.2011.00401.
- Zare, D.; Allison, J. R.; and McGrath, K. M., 2016**, “Molecular Dynamics Simulation of β -Lactoglobulin at Different Oil/Water Interfaces,” *Biomacromolecules*, V. 17, No. 5, pp. 1572–1581. doi: 10.1021/acs.biomac.5b01709.
- Zhai, J. I.; Day, L.; Aguilar, M.-I.; and Wooster, T. J., 2013**, “Protein folding at emulsion oil/water interfaces,” *Current Opinion in Colloid & Interface Science*, V. 18, No. 4, pp. 257–271. doi: 10.1016/j.cocis.2013.03.002.
- Zhang, J.; Bing, L.; and Reineccius, G. A., 2015**, “Formation, optical property and stability of orange oil nanoemulsions stabilized by Quillaja saponins,” *LWT - Food Science and Technology*, V. 64, No. 2, pp. 1063–1070. doi: 10.1016/j.lwt.2015.07.034.
- Zhang, J.; Bing, L.; and Reineccius, G. A., 2016**, “Comparison of modified starch and Quillaja saponins in the formation and stabilization of flavor nanoemulsions,” *Food Chemistry*, V. 192, pp. 53–59. doi: 10.1016/j.foodchem.2015.06.078.
- Zhang, X.-F.; Han, Y.-Y.; Bao, G.-H.; Ling, T.-J.; Zhang, L.; Gao, L.-P.; and Xia, T., 2012**, “A New Saponin from Tea Seed Pomace (*Camellia oleifera* Abel) and Its Protective Effect on PC12 Cells,” *Molecules*, V. 17, No. 12, pp. 11721–11728. doi: 10.3390/molecules171011721.
- Zhou, H.; Wang, C. Z.; Ye, J. Z.; and Chen, H. X., 2014**, “New triterpene saponins from the seed cake of *Camellia Oleifera* and their cytotoxic activity,” *Phytochemistry Letters*, V. 8, pp. 46–51. doi: 10.1016/j.phytol.2014.01.006.

Annex

A-I Materials and devices

Table A-1 Origin, purity and general chemical properties of the used saponin extracts

Material	Supplier	Purity [%]
Extract from <i>Quillaja saponaria</i> Molina (QS)	Ingredion Germany GmbH	69.2
Extract from <i>Gypsophila</i> (GYP)	Dr. H. Schmittmann GmbH	45.5
Extract from <i>Camellia oleifera</i> Abel (TS)	Changsha Nulant Chem. Co., Ltd.	95.3
Extract from <i>Aesculus hippocastanum</i>	Sigma Aldrich Chemie GmbH	99.1
Extract from <i>Glycyrrhiza glabra</i>	Sigma Aldrich Chemie GmbH	95.1
Extract from <i>Tribulus terrestris</i>	Xi'An Union Pharmpro Co., Ltd	90.4
Sodium dodecyl sulfate (SDS)	Sigma Aldrich Chemie GmbH	>99
Vanillin	Carl Roth GmbH & Co. KG	100
Ethanol	Carl Roth GmbH & Co. KG	99.5
Sulphuric acid	Carl Roth GmbH & Co. KG	96
Whey protein isolate	Fonterra DSE	-
Native β -Lactoglobulin	Isolated from whey protein isolate	89
KH ₂ PO ₄	Carl Roth GmbH & Co. KG	>99
K ₂ HPO ₄	Carl Roth GmbH & Co. KG	>99
Methanol	VWR International GmbH	>99
Ammonia	Merck & Co.	32
Medium-chain triglyceride oil (MCT-oil) WITARIX® MCT 60/40	CREMER OLEO GmbH & Co. KG	C8: 57.5% C10: 41.8% C12: 0.6% MgO: 15.5 %
Florisil	Carl Roth GmbH & Co. KG	SiO ₂ : 84 % Na ₂ SO ₄ : 0.5 %
Oil red O	/	/

Table A-2 Devices

Device	Manufacturer	Tradename
Foam device	KRÜSS GmbH	DFA 100
Glass frit	DURAN Group GmbH	FL4502 Filter Plate G4
Glass column	/	CY4502 Glass Column
Tensiometer with Wilhelmy plate	KRÜSS GmbH	K11
Conductometer	Mettler-Toledo GmbH	Seven Easy
Electrode Conductometer	Mettler-Toledo GmbH	InLab 731
Membrane for Dialysis	SPECTRUM® LABORATORIES, INC	Spectra/Por 1 Dialysis Membrane
Drop shape analysis	DataPhysics Instruments GmbH	OCA-20
Two-fluid channel needle	Self-made	-
Oscillation unit	DataPhysics Instruments GmbH	ODG-20
Dosing unit	DataPhysics Instruments GmbH	ES 6
1 mL syringe	B.Braun Melsungen AG	Injekt F
C-18 column	Thermo Fisher Scientific Germany BV & Co KG	HyperSep C18 10g/75mL
FTIR	Bruker Corporation	Bruker Tensor 27
High pressure homogenizer	Niro Soavi Deutschland	Panda 2K
Particle Sizer	Retsch GmbH & Co. KG	LA-950 Horiba
Photometer	Thermo Fisher Scientific Germany BV & Co KG	Helios Omega UV-VIS
Digital single-lens reflex camera	Nikon GmbH	3100
Camera lens	Nikon GmbH	AF-S Nikkor 18-55 mm 1:3.5-5.6G
Fluorescence Spectrophotometer	Agilent Technologies Deutschland GmbH & Co. KG	Cary Eclipse
Rheometer	Anton Paar Germany GmbH	Physica MCR301
Interfacial rheology system cell	Anton Paar Germany GmbH	/
Bicone tool	Anton Paar Germany GmbH	/
Zetasizer	Malvern Instruments GmbH	Nano Zetasizer ZS
Zeta cells	Malvern Instruments GmbH	DTS 1060 C
Ultra-Turrax	IKA -Werke GmbH & CO. KG	T25 basic
Microscope		
Vacuum block	Carl Roth GmbH & Co. KG	16 slots

A-II Characterizing foaming, foam stability and foam structure

Foam experiments were conducted using the foaming device DFA 100 (KRÜSS GmbH, Hamburg, Germany). For all experiments the following parameters were chosen: 50 mL of a surfactant solution were filled in a glass column (Ø40 mm). Foam was generated by purging pressurized air (0.15 L/min) through a porous glass frit (pore size 40-100 µm). As soon as the sum of liquid and foam reached 180 mm, foaming was stopped. Foam profiles were recorded by transmissibility measurement every 0.5 s for 1 hour. During that time foam and liquid height as well as the average brightness profile were measured and recorded. Figure A-1 shows typical foam profiles of (A) a foam made from 0.01 % and (B) a foam made of 0.003 % saponin solution.

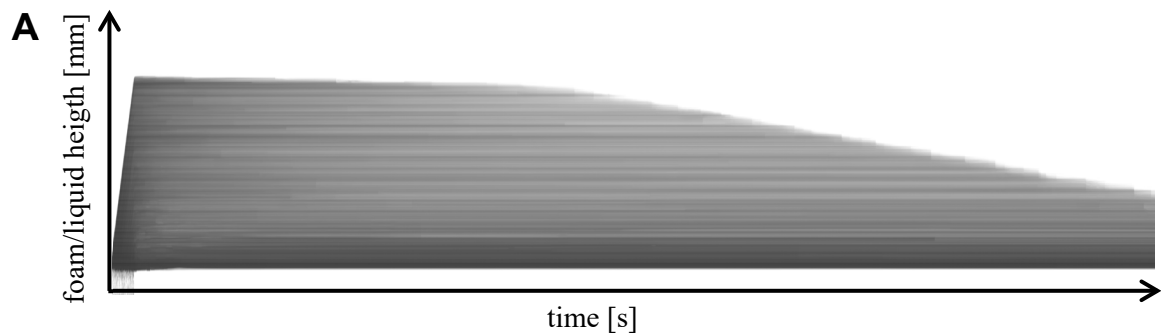


Figure A-1 Foam profile of a foam made from a (A) 0.003 % and (B) 0.01 % QS solution

In addition, photographs of the foam were taken every 10 min with a Nikon D3100 to have visual information on foam structure. All experiments were conducted under light exclusion to minimize external influences on the brightness profiles. The device was thoroughly rinsed with distilled water between experiments. All foaming experiments were conducted at least twice.

The foams were characterized using multiple parameters, see Figure A-2. All derived parameters were clustered in foaming, foam stability and foam structure.

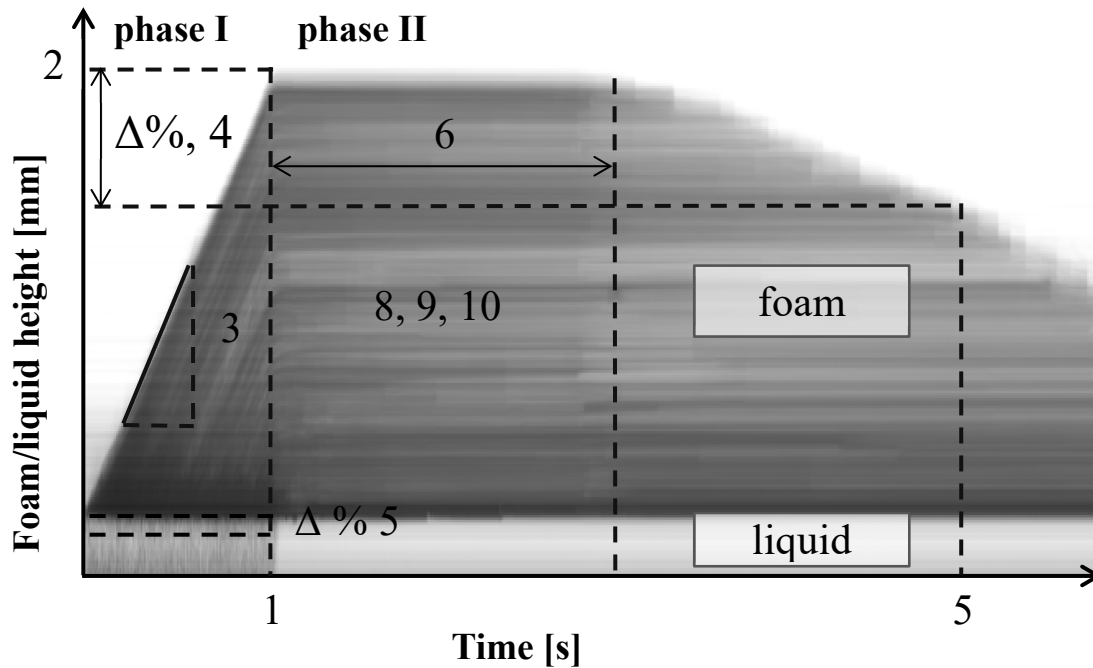


Figure A-2 Derived parameters from foam profile 1 - Time to maximum foaming level – t_{fmax} [s], 2 - Maximum foaming level – f_{max} [mm], 3 - Slope of foaming – k_f [mm/s], 4 – Relative remaining foam height– $f_n\%$ [%], 5 - Foam half-life time – $t_{f1/2}$ [s], 6 - Stability of maximum foam height – $t_{fmax-5\%}$ [s], 7 – relative drainage – $d_n\%$ [%], 8 - Foam density – $f_{den,n}$ [%], 9 - Foam density at f_{max} – $f_{den,fmax\%}$ [%], 10 - Analysis of image brightness distribution – median $BD_{m,n}$ and width $BD_{w,n}$

In Table A-3 all parameters, their abbreviation and measuring unit are displayed. If the parameters were calculated from other parameters the calculation is also specified. The subscript n represents variable time points. For example f_{1800s} is the relative remaining foam height after 1800 s. Foaming speed k_f was calculated from the deviation of foam height in relation to time from the start of the foaming until the maximum foam height (f_{max}). The parameters maximum foaming level f_{max} and time to maximum foaming level t_{fmax} were selected from the data. The relative foam remaining foam height $f_n\%$ characterizes the percentaged amount of foam still present in relation to f_{max} . A high foam decay is indicated by small $f_n\%$ values. The foam half-life time $t_{f1/2}$ is defined as the time when 50 % of the foam collapsed. The stability of the maximum foam height $t_{fmax-5\%}$ is defined as the time from reaching f_{max} until 95 % that height is still present. The relative drainage $d_n\%$ is defined as the percentage of liquid draining from the foam in relation to the liquid height at the f_{max} . The parameters relative foam density $f_{den,n}$ describe the percentage of incorporated liquid in the foam.

Table A-3 Parameters to characterize foaming, foam stability and foam structure; n - time point during the analysis; / - none

	Parameter	Abbreviation	Unit	Calculation/Definition
foaming	Time to maximum foaming level	t_{fmax}	s	$t(f_{max})$
	Maximum foaming level	f_{max}	mm	$f_n = max$
	Foaming speed	k_f	mm/s	$\frac{\Delta f}{\Delta t}; f \leq f_{max}; t \leq t(f_{max})$
foam stability	Relative remaining foam height	$f_{n\%}$	%	$\frac{f_n}{f_{max}} \cdot 100; t > t_{fmax}$
	Foam half-life time	$t_{f1/2}$	s	$t(0.5f_{max}) - t(f_{max}); t > t_{fmax}$
	Stability of maximum foam height	$t_{fmax-5\%}$	s	$t(0.95f_{max}) - t(f_{max}); t > t_{fmax}$
	Relative drainage	$d_{n\%}$	%	$abs\left(\frac{d_n}{d(f_{max})} \cdot 100\right); t > t_{f-max}$
foam structure	Relative foam density	$f_{den,n}$	%	$abs\left(\frac{(d_0 - d_n)}{f_n} \cdot 100\right)$
	Median of brightness distribution	$BD_{m,n}$	/	See Figure A-3
	Width of brightness distribution	$BD_{w,n}$	/	See Figure A-3

Determination of foam structure with analysis of brightness profiles and foam pictures

Since there was no device available to determine the bubble size distribution and variations in foam density were very high, a new semi-quantitative method was established. For this purpose the brightness profile generated by the foaming device was analyzed, see Figure A-3.

The brightness profile is generated from the transmissibility data of the column and the foam device can derive liquid and foam height from the foam profile. Zones filled with air or liquid have a high transmissibility and appear white in the brightness profile since light is not scattered. When light is sent through foam, the light is scattered at the bubbles, which leads to darker areas in the foam profile. That means, the smaller the bubble the more light is scattered and the less light transmits through the foam and the darker is the area on the foam profile. Each pixel on the Y-axis displays the average transmissibility at a certain height of measurement and each pixel on the X-axis represents the average transmissibility

at a specific time point. At different time points the brightness distribution within the foam in the column was measured in an area of 1 px width, which corresponds to a specific time point, using Adobe Photoshop CS6 Extended. The brightness distribution ranges from 0-255. 0 represents black and 255 represents white. In this study, data points between 1 and 253 were used to eliminate white background color. In Figure A-3 the procedure is displayed. From the brightness distribution the median ($BD_{m,n}$) as well as the width ($BD_{w,n}$) between the d_{10} (10 % of the brightness values are beneath this value) and d_{90} were calculated for individual time points n . The higher the BD_m is, the more light is transmitted through the foam indicating that the foam is less dense. An increase of BD_w indicates that the foam structure is less homogeneous.

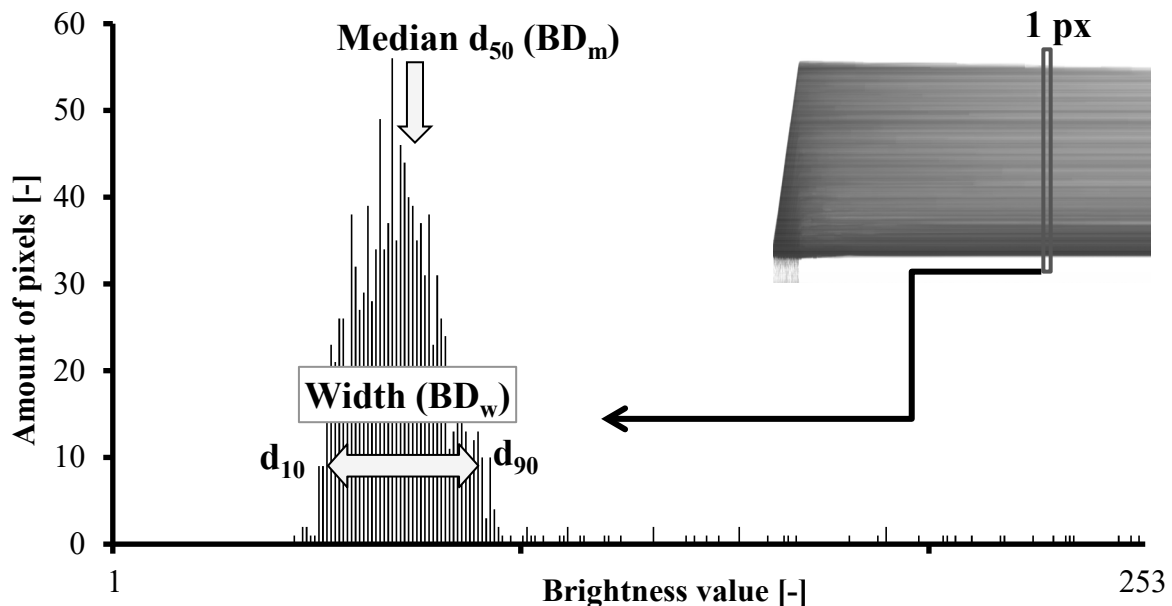


Figure A-3 Example for histogram of brightness distribution at a specific time point (rectangle of 1 px width) of a foam made from 0.01 % QS solution after 1800 s

A-III Validation of foam analysis

The used method for characterization of foaming, foam stability and foam structure had to be validated in order to evaluate the quality of the results. Therefore, the coefficients of variation of the different parameters of two different foam types were analyzed: foams with higher density and therefore higher content of liquid (Higher density foams) and foams with lower density with a smaller amount of incorporated liquid (Lower density foams). This discrimination was necessary because lower density foams had high and irregular foam decay. In addition, difference of the liquid height at the time points ‘maximum foam

height' and 'end of measurement' was less than 2 mm. In higher density foams the difference was still low with about 10 mm but normal variation of the device had considerably less impact on the results compared to low density foams.

In Table A-4 the coefficients of variation (CV) of all analyzed parameters are listed. Concentrations of 0.003 % (5 replicates) and 0.01 % (4 replicates) of QS were chosen as a representative of low and high density foams, respectively. For parameters with the subscript n the CVs of all measurement points (0, 10, 20 ... 60 min) were averaged.

Table A-4 Variation of parameters to characterize foaming, foam stability and foam structure depending on QS concentration; n - time point during the analysis

	Parameter	CV _{0.003%} [%]	CV _{0.01%} [%]
foaming	t_{fmax}	0.5	0.4
	f_{max}	5.6	0.1
	k_f	2.4	1.0
foam stability	$f_{n\%}$	5.2	0.6
	$t_{f1/2}$	11.1	n.a.
	$t_{fmax-5\%}$	31.6	n.a.
	$d_{n\%}$	42.6	18.3
foam structure	$f_{den,n}$	45.6	21.7
	$BD_{m,n}$	5.4	2.1
	$BD_{w,n}$	12.1	3.2

The parameters time to maximum foaming level t_{fmax} and foaming speed k_f are quite similar and had only small CVs below 5 %. With both parameters it is possible to compare different foaming behaviors, but it is not necessary to determine both parameters for each foam individually. In our further analysis only foaming speeds are compared. High values for the maximum foaming level f_{max} indicate a higher foam density since the higher f_{max} is, the more foam was produced and the more fluid was incorporated in the foam. However, more sophisticated parameters are used in this work to quantify foam density and the amount of liquid in the foam. For this reason we only compare foaming speeds of different foams to characterize the foaming.

To characterize foam stability it is possible to compare several parameters. As a standard parameter, the relative remaining foam height $f_{n\%}$ at different time point n can be characterized. It is also possible to compare the foam half-life time $t_{f1/2}$ but for this parameter foams have to collapse at least to 50 %, which is not applicable for most saponin foams

since they are very stable even at low concentrations, like 0.01 %. With the parameter stability of the maximum foam height $t_{\text{fmax-5\%}}$ different collapse profiles can be quantified. But as well as for the foam half-life time not all foams collapse by 5 %. A limit of less than 5 % was tested but yielded for $t_{\text{fmax-1\%}}$ CVs of 24 % and 41 % and $t_{\text{fmax-3\%}}$ CVs of 47 % and 22 % for concentrations of 0.01 and 0.003 % saponin, respectively. Because of the high variations and limitations for the required amount of foam decay this parameter is not further discussed in this work. The results for the relative drainage $d_n\%$ had high variations and therefore uncertainties. Even in higher density foams (0.01 % saponin) the variations were well above 10 %. These variations can be explained, especially in lower density foams, because the change in the fluid levels is very small for each of the analyzed saponin concentrations and at maximum only 10 mm. In this range even small measurement errors have a high impact on the relative drainage and high variations occur.

Very similar to the high uncertainties in the relative drainage, the variations in foam density $f_{\text{den},n}$ arise from the dependency on the liquid height. That is why CVs are similar between $f_{\text{den},n}$ and $d_n\%$. The foam density is not an appropriate parameter to reliably quantify foam structure. For this reason a new method using the differences in brightness of the foam profiles was developed, see Figure A-3. From the brightness distribution the two parameters $BD_{m,n}$ and $BD_{w,n}$ were derived. As in Table A-4 displayed, the variation using the new method are clearly below the variations using $f_{\text{den},n}$. For $BD_{m,n}$ and $BD_{w,n}$ the variations of the higher density foam were smaller and beneath 5 %. For the lower density foams the median $BD_{m,n}$ is around 5 % but the variation of the width $BD_{w,n}$ is at 12 %. Although 12 % is still a high variation, this value is considerably lower compared to the foam density values.

To summarize, for all further analysis $k_f, f_n\%, f_{\text{den},n}, BD_{m,n}, BD_{w,n}$ and foam picture were used to characterize foaming, foam stability and foam structure.

Curriculum Vitae

Sandra Böttcher



Education

Oct 13-Jan 17	<p>PhD (Dr. Ing.) Prof. Dr. Stephan Drusch Food Technology and Food Material Science Technische Universität Berlin <u>Dissertation:</u> <i>Saponins as natural foaming and emulsifying agents</i></p>
Oct 11-Sep 13	<p>Master of Science (1.3) with distinction Food Science and Technology Beuth University of Applied Sciences Berlin <u>Master thesis:</u> <i>Off-flavor masking of secondary lipid oxidation products by pea dextrin</i> <u>Project thesis:</u> <i>Determination of cancerous contaminants in home-made foods like toast and grilled meat using GC-MS</i></p>
Oct 08-Sep 11	<p>Bachelor of Science (1.3) Food Science and Technology Beuth University of Applied Sciences Berlin <u>Bachelor thesis (Symrise AG):</u> <i>Extraction and crystallization of active ingredients from the bark of ash tree</i> <u>Project thesis:</u> <i>Coazervation of alginates to form liquid-filled spheres for oral consumption</i></p>
July 08	<p>A-levels (1.5) Johann-Wolfgang-von-Goethe Gymnasium Chemnitz</p>

Awards and scholarships

Oct 13-Dez 16	Graduate scholarship of Friedrich Naumann Foundation for Freedom
Oct 09-Sep 13	Student scholarship of Friedrich Naumann Foundation for Freedom
Mar 15	Fellowship award of Harvard School of Public Health

International experience

Jun-Jul 15	Research visit, Free University Bolzano Research group of Prof. Dr. Matteo Scampicchio <i>Characterization of saponin/beta-lactoglobulin-interactions with isothermal titration calorimetry</i>
Sep-Oct 07	Student exchange, Fargo, North Dakota German American Partnership program (GAPP) Fargo North High School

Professional Experience

Okt 13-Jan 17	Teaching assistant, Technische Universität Berlin Lectures on design of experiments, molecular inclusion Supervision of several bachelor/master theses Organization of practical lab workshops for students
Apr 10-Apr 13	Teaching assistant, Beuth University of Applied Sciences Process Engineering, Food Chemistry
Feb-Aug 11	Symrise AG, Holzminden Internship and bachelor thesis at Competence Center for Health & Nutrition
Aug-Sep 09	Deutsche Extrakt Kaffee GmbH, Berlin Internship in Quality Management and Research
Feb-Mar 09	Ehrmann AG, Freiberg Internship in Research and Development
Jul-Sep 08	Ehrmann AG, Freiberg Internship in Research and Development